
Electronic Thesis and Dissertation Repository

8-5-2015 12:00 AM

Field Scale Application of Nanoscale Zero Valent Iron: Mobility, Contaminant Degradation, and Impact on Microbial Communities


Chris M.D. Kocur, *The University of Western Ontario*

Supervisor: Dr. Denis O'Carroll, *The University of Western Ontario*

A thesis submitted in partial fulfillment of the requirements for the Doctor of Philosophy degree in Civil and Environmental Engineering

© Chris M.D. Kocur 2015

Follow this and additional works at: <https://ir.lib.uwo.ca/etd>

 Part of the [Analytical Chemistry Commons](#), [Environmental Chemistry Commons](#), [Environmental Engineering Commons](#), [Environmental Microbiology and Microbial Ecology Commons](#), [Environmental Monitoring Commons](#), [Hydrology Commons](#), [Nanoscience and Nanotechnology Commons](#), and the [Water Resource Management Commons](#)

Recommended Citation

Kocur, Chris M.D., "Field Scale Application of Nanoscale Zero Valent Iron: Mobility, Contaminant Degradation, and Impact on Microbial Communities" (2015). *Electronic Thesis and Dissertation Repository*. 3068.

<https://ir.lib.uwo.ca/etd/3068>

This Dissertation/Thesis is brought to you for free and open access by Scholarship@Western. It has been accepted for inclusion in Electronic Thesis and Dissertation Repository by an authorized administrator of Scholarship@Western. For more information, please contact wlsadmin@uwo.ca.

FIELD SCALE APPLICATION OF NANOSCALE ZERO VALENT IRON: MOBILITY,
CONTAMINANT DEGRADATION, AND IMPACT ON MICROBIAL COMMUNITIES

(Thesis format: Integrated Article)

by

Christopher Michael Donald Kocur

Graduate Program in Civil & Environmental Engineering

A thesis submitted in partial fulfillment
of the requirements for the degree of
Doctor of Philosophy

The School of Graduate and Postdoctoral Studies
The University of Western Ontario
London, Ontario, Canada

© Chris Kocur 2015

Abstract

This thesis began by verifying that nanoscale zero valent iron (nZVI) synthesis methods could be scaled up and implemented at the field scale in a safe manner. This led to successful demonstration of nZVI injection and mobility under constant head gravity injection into a contaminated utility corridor in Sarnia, Ontario. Where field studies have fallen short in the past was linking the somewhat qualitative field geochemical parameters to other evidence of nZVI transport. Definitive nZVI detection was elusive in previous field studies due to the highly reactive nature of the particles caused by their high surface area. nZVI was detected and characterized in this study using UV/Vis spectrophotometry, Dynamic light scattering, zeta potential, Transmission Electron Microscopy, and energy dispersive x-ray spectroscopy, proving that field mobility was reliably achieved.

The second study provides the first insight into the interactions and reaction that occur on an active field site immediately following nZVI injection. A fine temporal resolution of samples was used to define chlorinated ethene, ethane, and methane (cVOC) degradation among nZVI impacted zones, showing that these zones were distinct from areas that were not affected by nZVI. Building upon previous indirect evidence that nZVI enhances organohalide-respiring microorganisms, this study set out to prove that microbiological communities on sites were enhanced following injection. Quantitative polymerase chain reaction (qPCR) was used to target *Dehalococcoides spp.* (*dhc*) and vinyl chloride reductase genes (*vcrA*). The distinct zones where nZVI treatment was applied subsequently had high abundances of *dhc* and *vcrA*. The qPCR methods presented in the second study can act as a template for future field investigation on nZVI.

Finally, the long-term effects of the injection amendments nZVI and Carboxymethyl-cellulose were monitoring on the microbial communities on site. It was hypothesized that the organohalide-respiring species on site would be enriched and cVOC degradation would be sustained due to the polymer amendments that accompany nZVI injection. Over a two year period next-generation pyrosequencing, qPCR, and cVOC degradation were monitored, providing the first ever phylum level microbiological evaluation at a field site undergoing remediation.

Keywords

nZVI, Nanoscale Zero Valent Iron, Fe^0 , nanoparticle mobility, groundwater remediation, insitu chemical reductants, chlorinated solvents, degradation, perchloroethylene (PCE), tetrachloroethylene, trichloroethylene (TCE), cis-Dichloroethene isomer (cis-1,2 DCE), vinyl chloride, enhanced bioremediation, *Dehalococcoides*, *Dehalogenimonas*, vinyl chloride reductase (*vcrA*), microbial ecology, microbial community, next-generation pyrosequencing, amplicon sequencing, pyrotag sequencing, non-metric multi-dimensional scaling (NMDS)

Co-Authorship Statement

This document was written in accordance with the guidelines and regulations for a manuscript format thesis as stipulated by the school of graduate and post-graduate studies at the University of Western Ontario. The candidate designed, performed and supervised all field work in this thesis in close guidance and supervision of Dr. Denis O'Carroll. The candidate also coordinated and performed laboratory analysis with several collaborators, leading the data analysis. The themes and development of this work were developed in discussions with Dr. Brent Sleep, Dr. Elizabeth Edwards, and Dr. Denis O'Carroll. The candidate wrote three manuscripts that are included as chapters of this thesis.

Chapter 2: Literature Review: Field Scale Evaluation of nZVI

Contributions:

Chris Kocur	developed outline, wrote manuscript and reviewed references.
Denis O'Carroll	invited to submit book chapter, reviewed/revised chapter.
Brent Sleep	reviewed/revised chapter

Chapter 3: Characterization of nZVI in a field scale test

Contributions:

Chris Kocur	wrote the manuscript draft, performed field work, developed field synthesis protocol, designed synthesis reactors, analyzed TEM samples, analyzed DLS samples, and performed sedimentation tests.
Ahmed Chowdhury	assistance in field work, analyzed iron and ion data,
Nataphan Sakulchaicharoen	developed synthesis protocol, analyzed TEM samples
Hardiljeet Boparai	analyzed iron data, reviewed/revised manuscript
Kela Weber	assistance in field work, reviewed/revised manuscript
Prabhakar Sharma	provided assistance in laboratory analysis.
Magdalena Krol	assistance in field work, reviewed/revised manuscript
Leanne Austrins	coordinated regulatory approvals and field activities.
Chris Peace	coordinated regulation and field activities, assisted in field methods and troubleshooting, equipment and apparatus
Brent Sleep	provided formative discussion, provided data interpretation, reviewed/revised manuscript
Denis O'Carroll	initiated work, planning and regulatory approval, awardee of funding, reviewed/revised manuscript.

Chapter 4: Contributions of abiotic and biotic dechlorination following carboxymethyl cellulose stabilized nanoscale zero valent iron injection

Contributions:

Chris Kocur	performed field work, coordinated sampling, interpreted data, led discussion of concepts and themes, coordinated reviews and submission, wrote manuscript
Line Lomheim	performed the analysis of the qPCR at UofT, provided methods sections regarding her work, assisted in interpretation of qPCR data.
Hardiljeet Boparai	performed the aqueous phase chlorinated solvent extractions and analysis, and thus provided details of her methods, assisted in interpretation of cVOC data. reviewed/revised manuscript.
Ahmed Chowdhury	helped with field work and sampling
Kela Weber	helped with field work, assisted in data interpretation and background, reviewed/revised manuscript
Leanne Austrins	coordinated regulatory approvals. contributed formative discussion
Elizabeth Edwards	contributed to methodology of microbial sampling methods, contributed discussion, assisted in development of concepts and themes of the manuscript, reviewed/revised manuscript
Brent Sleep	contributing ideas for data analysis, contributed to themes of paper, reviewed/revised manuscript
Denis O'Carroll	initiated work, led discussion, awardee of funding, contributed to review and revision of manuscript

Chapter 5: Long Term Dechlorination Following nZVI/CMC Injection and Impact on Microbial Communities, Including Organohalide-Respiring Microorganisms

Contributions:

Chris Kocur	performed field work, coordinated sampling, interpreted data, led discussion of concepts and themes, decided on pyrotag samples analysis, coordinated reviews and submission, wrote manuscript
Line Lomheim	performed the analysis of the qPCR at UofT, prepared pyrotag samples for sequencing, provided methods sections regarding her work, assisted in interpretation of qPCR data, developed NMDS figures
Elizabeth Edwards	contributed to methodology of microbial sampling methods, contributed discussion, assisted in development of concepts and themes of the manuscript, reviewed/revised manuscript
Hardiljeet Boparai	performed the aqueous phase chlorinated solvent extractions and analysis, and thus provided details of her methods, assisted in interpretation of cVOC data. reviewed/revised manuscript.
Kela Weber	helped with field work, assisted in data interpretation and background, reviewed/revised manuscript
Brent Sleep	contributing ideas for data analysis, contributed to themes of paper, reviewed/revised manuscript
Denis O'Carroll	initiated work, led discussion, awardee of funding, contributed to review and revision of manuscript

Appendix A: Nanoscale zero valent iron and bimetallic particles for contaminated site remediation.

Contributions:

Denis O'Carroll	initiated the review, coordinated and outlined the sub-sections, wrote introduction, edited, reviewed/revised all sections.
Brent Sleep	review/revised all sections, consulted on content and sections
Hardiljeet Boparai	wrote sections 2, 4, and subsections of 5, reviewed/revised all sections
Magdalena Krol	wrote sections 3, and subsections of 5, reviewed/revised all sections
Chris Kocur	wrote subsection 5.4, sections 6 through 8, reviewed/revised all sections

Acknowledgments

I would like to start by acknowledging the significant contribution that Dr. Denis O'Carroll has made to my work and my life at Western. Denis was an example of work life balance and was extremely supportive in the more difficult parts of my studies. Denis' enthusiasm has continually motivated me while challenging my goals in research. Thank you for your role in my development as a researcher, scientist, and engineer. I will sincerely miss your doors-open, red-pants, ice-cream-social style of mentorship and leadership.

Secondly, I would like to express my extreme gratitude to Dr. Brent Sleep at the University of Toronto for the many lengthy reviews and critiques of my work. Brent has played a critical role in improving my writing and analysis skills. In all of my work, Brent has provided the most difficult comments and reviews, speaking to his expertise in a wide number of fields. Thank you for your mentorship and sharing your expertise in academic reviews.

Thirdly, Thank you Dr. Elizabeth Edwards at the University of Toronto for our passionate collaborative discussions and formative critique of the work. The contribution of my work has been greatly elevated as a result of your analysis and assistance.

Leanne Austrins and the staff at CH2M HILL Canada Ltd. in Kitchener must be acknowledged. Thank you for allowing me to be a part of your work and for supporting my studies. This project would not have been successful without the assistance of Chris Peace, Matt Horlings, and Chris Kuron. Special thanks must be extended to Lisa Moffatt for her pivotal role in health and safety of field operations.

I must acknowledge those whom I have worked with on the project. Ahmed Chowdhury spent a considerable amount of time in the preparation, field implementation, and sample analysis portions of this project. Line Lomheim performed the qPCR analysis at UofT, and prepared samples for Pyrotag, providing analysis and processing results using NMDS. Hardiljeet Boparai provided significant laboratory support in metals and cVOC analysis. These individuals have gone to significant effort to support my work and I am grateful for their contributions. Without you I would have needed 6 more years.

Undertaking this large scale effort would not have be possible without the efforts of other supporting researchers, Dr. Kela Weber, for his expertise in field sampling and help with microbiological background, Dr. Nataphan Sakulchaichaoen for her work in scaling up nZVI synthesis and for standing outside all night. There were many other co-workers that I have forgotten and should have mentioned.

Thank you to the administrative staff in the Civil & Environmental Engineering department for their patient and committed support of myself and all students. Special thanks to Stephanie Lawrence for doing everything and with a smile on her face, Diana Lee for her assistance in scholarship applications, and Whitney Barrett for asking when I am going to finish, but not too often. Your support over my many years of undergrad and grad school has been greatly appreciated. Thank you.

To the technical staff in the department. I am sorry for flooding the basement labs more than once. Tim for his laboratory expertise and suggestions, it was a pleasure working with

you. To Melodie and Erol for all their geotechnical knowledge and random help. Wilbert, thank you for your cheerful demeanor and always having the tool or equipment that I needed to borrow. I hope we gave everything back.

The geotechnical research center at Western has been a continuing support network. Particularly, thanks to Cindy Quintus for your work behind the scenes. Thank you to the GRC for the financial support of my research through numerous awards. Also, thank you to Western, the Canadian Foundation for Geotechnique, NSERC, CH2M Hill for their generous financial support.

I would like to thank all of my colleagues and friends that have come and gone in Restore. From the inception of ice cream socials, to the parties, triumphant trivia victories, coffee runs, grad club afternoons, restore summer research songs, and conversations in the office, there have been uncountable individuals that have made my time at Western, and in Restore a great memory. I particularly appreciate the advice and friendship of my colleagues Drs Rory Hadden, Cjstmir de Boer, Kevin Mumford, Kela Weber, and Magda Krol, and the many others. To those that have contributed to my graduate experience at Western. Thank you.

Drs Clare Robinson, Jason Gerhard, Denis O'Carroll, I find it difficult to leave Western because you have created an environment that I love.

Ahmed Chowdhury and Hardiljeet Boparai have shared a laboratory with me for too many years, and they should be commended for putting up with my neglect of washing laboratory glass. I have the upmost gratitude for their co-authorship and friendship over the years. I wish you the best as you are both poised to leave Western. Know that you will be greatly missed.

Thank You,

To my great friends who have been there throughout. Brian Nourse, Halliday Pearson, Erin Cullen, Andrew Ross, Shawn Gettler, Goutom Datta, and Laura Molnar.

To Ian Molnar, with whom I have earned "Ten-year" and a few at Western. I sense that you will do truly great things and I am looking forward to seeing what they are. You are a great friend. I hope that we can always find a way to be brothers in research.

To my family, for their unending support, inspiration, and welcome distractions, I cannot even begin to thank you.

To Jess, You are my soulmate. Thank you for your patience and loving support in my asymptotic approach to completion. I look forward to the many adventures that we will share together in life. I love you with all my heart.

Tim, I love you

Dad, I miss you

Mom, Thanks for always believing in me

Dedication

This thesis is dedicated to the women in my family, particularly

Mary Kocur

Joan Bedford

Pat Aplevich

Carrol Dawkins

Linda Kocur

You may not be aware of your impact

Table of Contents

Abstract	ii
Co-Authorship Statement.....	iv
Acknowledgments.....	ix
Dedication	xii
List of Tables	xx
List of Figures	xxi
List of Appendices	xxiv
Chapter 1	1
1 Introduction	1
1.1 Background	1
1.2 Scope of Work	2
1.3 Research Objectives.....	3
1.4 Thesis Outline	3
1.5 References	5
Chapter 2.....	8
2 Field scale evaluation of nZVI.....	8
2.1 Contaminated site management and technology evaluation	8
2.1.1 Contamination and legislation	9
2.1.2 The cost and endpoints of remediation	9
2.1.3 Conceptual site model.....	11
2.1.4 Remediation timeline & performance objectives	13

2.1.5	nZVI alternatives for remediation.....	14
2.1.6	Role of nZVI.....	15
2.2	Site characterization.....	17
2.2.1	Conceptual model development for nZVI applications.....	17
2.2.2	Subsurface characterizing using well methods.....	21
2.2.3	Investigating the subsurface using alternative methods.....	21
2.2.4	Pre-screening porous media with nZVI.....	23
2.3	Evaluating injection and mobility.....	23
2.4	nZVI detection and evaluation methods.....	27
2.4.1	Techniques and approaches for evaluating nZVI in wells.....	27
2.4.2	Challenges in interpretation of well data.....	28
2.4.3	Methods of evaluating and characterizing particles.....	29
2.5	Geochemical methods.....	34
2.6	Determining Fe ⁰ content.....	35
2.7	Fe ⁰ in a complex matrix.....	35
2.7.1	Alternative and emerging methods of nZVI determination.....	36
2.7.2	Modelling field scale nZVI transport.....	37
2.8	Evaluating degradation.....	39
2.8.1	Reactivity in closed systems.....	39
2.8.2	Pathways of degradation.....	41
2.8.3	Considerations for field applications.....	43
2.8.4	Monitoring VOCs in the Field.....	45
2.9	Lessons learned from nZVI field applications.....	46
2.9.1	Occupational health and safety considerations.....	46
2.9.2	nZVI performance evaluation.....	48
2.9.3	Coupling technologies with nZVI.....	48

2.10	References	52
Chapter 3	70
3	Characterization of nZVI Mobility in a Field Scale Test	70
3.1	Abstract	71
3.2	Introduction	72
3.3	Site Background	74
3.3.1	Site Description	74
3.3.2	Site Characterization	74
3.4	Field Methods and Materials	75
3.4.1	nZVI Synthesis on Site	75
3.4.2	Injection Schedule and Sampling	76
3.5	Analytical Methods	77
3.6	Results	79
3.6.1	Pumping, Slug, and Tracer Testing	79
3.6.2	nZVI Synthesis, Injection, and Stability	80
3.6.3	nZVI Mobility	81
3.6.4	Characterization of nZVI before and after transport	84
3.7	Environmental Implications	87
3.8	Acknowledgments	88
3.9	References	88
Chapter 4	95
4	Contributions of Abiotic and Biotic Dechlorination Following Carboxymethyl Cellulose Stabilized Nanoscale Zero Valent Iron Injection	95
4.1	Abstract	96
4.2	Introduction	97
4.3	Methods	100

4.3.1	Site Description.....	100
4.3.2	Sampling and Analytical Methods.....	100
4.3.3	DNA extraction and quantitative PCR (qPCR) analyses.....	101
4.3.4	nZVI/CMC injection.....	102
4.3.5	Estimating abiotic and biotic dechlorination	103
4.4	Results and Discussion	103
4.4.1	Composition of cVOCs along nZVI flowpath.....	103
4.4.2	Short term microbiological response to nZVI	106
4.4.3	Estimating nZVI vs. Biotic Degradation	108
4.5	Environmental Implications.....	110
4.6	Acknowledgements.....	112
4.7	References.....	113
	Chapter 5.....	121
5	Long Term Dechlorination Following nZVI/CMC Injection and Impact on Microbial Communities, Including Organohalide-Respiring Microorganisms.....	121
5.1	Abstract.....	122
5.2	Introduction.....	122
5.3	Methods.....	126
5.3.1	Site Background, Injection, and Sampling	126
5.3.2	cVOCs.....	126
5.3.3	DNA extraction.....	127
5.3.4	Quantitative PCR (qPCR) analyses	127
5.3.5	Pyrotag Sequencing	128
5.3.6	Nonmetric Dimensional Scaling.....	129
5.4	Results.....	130
5.4.1	4.1 Degradation of cVOCs.....	130

5.4.2	Abundance of <i>Dehalococcoides spp.</i>	133
5.4.3	Effects of dilution on <i>Dehalococcoides spp.</i> in injection wells.....	134
5.4.4	Microbial Composition.....	135
5.4.5	Community evaluation using NMDS.....	138
5.5	Environmental Implications.....	141
5.6	References.....	143
Chapter 6	153
6	Conclusions and Recommendation.....	153
6.1	Summary.....	153
6.2	Conclusions.....	154
6.3	Implications.....	157
6.4	Future Outlook and Research Needs.....	157
Appendices	159
7	Appendix A: NANOSCALE ZERO VALENT IRON AND BIMETALLIC PARTICLES FOR CONTAMINATED SITE REMEDIATION	159
7.1	Abstract:.....	160
7.2	Introduction.....	160
7.3	Background.....	163
7.3.1	Development of Zero Valent Metals for Remediation	163
7.3.2	nZVI Particle Structure	164
7.4	Reaction of Chlorinated Solvents with Nanometals	166
7.5	Reaction of Heavy Metals with Nanometals	171
7.6	Factors Affecting Reactivity of nZVI with Metals and Chlorinated Solvents....	177
7.6.1	Surface Area.....	177
7.6.2	Aging.....	178
7.6.3	pH.....	180

7.6.4	Coatings/Stabilizers	182
7.6.5	Impact of Natural Groundwater Constituents and Initial Chlorinated Solvent Concentrations	183
7.6.6	Bimetallic Nanoparticles.....	186
7.7	Stability and Mobility of Unstabilized nZVI.....	188
7.7.1	Improved Colloidal Stability.....	190
7.7.2	Bench scale experiments investigating nZVI mobility.....	193
7.7.3	NAPL Targeting.....	196
7.8	Simulation of nZVI Transport	196
7.9	nZVI Field Applications	200
7.9.1	Early Studies of nZVI in the Field.....	200
7.9.2	Improvements to Field Scale nZVI Delivery.....	202
7.9.3	Tracking Remediation Following nZVI Injection	204
7.10	Summary and Outlook	207
7.11	References.....	208
8	Appendix B: Supporting Information for Chapter 3 Characterization of nZVI mobility in a field scale test.	235
8.1.1	Calculations of nanoparticle filtration in soil.....	246
	References.....	247
9	Appendix C: Supplemental Information for Chapter 4: Contributions of Abiotic and Biotic Dechlorination Following Carboxymethyl Cellulose Stabilized Nanoscale Zero Valent Iron Injection	248
9.1	Background.....	253
9.1.1	Electron Balance for the oxidation of nZVI	253
9.1.2	Electron balance for aqueous cVOC Sample data	255
9.1.3	Electron balance for chloride ion evolution.....	258
9.1.4	Electron Balance based on Microbial yield.	259
9.2	References.....	263

10 Appendix D: Supplemental Information for Chapter 5: Long Term Dechlorination Following nZVI/CMC Injection and Impact on Microbial Communities, Including Organohalide-Respiring Microorganisms	264
Curriculum Vitae	272

List of Tables

Table 2.1: Phases of contamination in the site conceptual model laid out in the 14 compartment model. The 14 compartment model is an example of a tool for evaluating chlorinated solvent sites.	13
Table 2.2: Comparative summary of ZVI remediation alternatives in wide use and in development.	15
Table 2.3: Impact of monitoring well design on conceptual model of the cVOC contamination on site (modified from Einerson 2005)	19
Table 2.4: Analytical electron spectroscopic and x-ray tools for characterizing nZVI	33
Table 3.1: Summary of the nZVI injection schedule	77
Table 4.1: Estimated electron equivalents (as a concentration, mol/L) from reaction following injection of nZVI/CMC.....	109

List of Figures

Figure 2.1: Contaminant Removal Level (concentration standard, MCL) vs Remediation Cost. The cost of remediating contaminated sites to strict concentrations can exponentially increase as the extent of remediation grows.	11
Figure 2.2: Site conceptual model of subsurface contamination showing all possible phases of contamination within the 14 compartment model: DNAPL, sorbed, aqueous, vapor. (from IRTC 2011)	12
Figure 2.3: Three cases where nZVI may be a suitable remediation alternative. a.) contamination in fractured bedrock b.) existing critical infrastructure is too expensive to dismantle prior to remediation. c.) contamination reaches depths unattainable by other remediation methods.	16
Figure 2.4: a.) Illustration of three different wells screen lengths (Long screened interval (L), Medium (M), and Multilevel (N)) and b.) an example of possible concentrations of solute measured with these different screened intervals. (Einerson 2005)	18
Figure 2.5: Transect of a groundwater plume with total cVOC concentrations shaded at different contour intervals. The transect was installed transverse to the direction of travel of a groundwater plume (Einerson and Cherry 2002).....	20
Figure 2.6: nZVI slurry synthesized at 1 g/L in 0.8 % wt CMC prior to injection (Left). nZVI sample collection at a monitoring well downstream of the injection (right)	29
Figure 2.7: Demonstration of 4 g/L nZVI stabilized with PAA moving through a heterogeneous sandbox (Kanel 2008).....	30
Figure 2.8: UV/Vis spectra of nZVI (black) and oxidized ZVI (yellow), showing the peaks used in two wavelength calibration. (Johnson et al 2013)	31
Figure 2.9: First order decay of TCE with nZVI (modified from He ES&T 2005).	40

Figure 2.10: Reductive dechlorination pathways of chlorinated methanes, ethanes, and ethenes. (Modified from Song and Carraway 2005, Arnold and Roberts 2000, Tratnyek et al 2014)	42
Figure 2.11: Photo of nZVI rapidly oxidizing as it is poured out of a beaker (www.nanoiron.cz)	47
Figure 3.1: Site layout showing the injection and monitoring wells in the study area.	75
Figure 3.2: Breakthrough data collected at MW1 including a) total Fe and Sulfate (tracer) and b) Fe ₀ content in nZVI particles. t = 0 for both plots is denoted by the start of injection at INJW.	82
Figure 3.3: TEM Images of nZVI nanoparticles a) freshly synthesized prior to injection and b) recovered from MW1 following transport through the subsurface (12 hrs after injection began).....	85
Figure 3.4: Energy dispersive spectroscopy (EDS) spectrum (right) for the nanoparticle (highlighted in left) collected from MW1 - 1hr following injection.	86
Figure 4.1: Composition of cVOCs shown as a pie chart with the total cVOC concentration represented as the radius for the monitoring wells. Flow path #1, shown in green, shows the path of nZVI travel from the primary injection well. The adjacent flow path #2, shown in purple, was not affected by the nZVI/CMC injection.....	104
Figure 4.2: qPCR was performed on aqueous samples prior to and two days following nZVI/CMC injection to determine the abundance of <i>Dehalococcoides spp (dhc)</i> . The wells are ordered by decreasing exposure to nZVI/CMC from left to right. Injection wells (INJW and MW2) and the well where nZVI/CMC travelled (MW1) were most affected, followed by downgradient wells (MW6 and MW5). The wells along the adjacent flow path (MW4 and MW9) were least affected by the nZVI/CMC injection.	107
Figure 5.1: Degradation of chlorinated ethenes in monitoring wells over the two-year monitoring period. Pie charts show the composition of chlorinated ethenes in each well. The radius of each pie illustrates the total concentration of all chlorinated ethenes in the well	

(mM). Three distinct groups of wells are shown; wells that were impacted by nZVI/CMC through injection or transport (Flow Path #1), wells that were less impacted by the injection (Flow Path #2), and injection wells. 132

Figure 5.2: Concentration of *Dehalococcoides* genes in each well (gene copies/L) over a two year monitoring period following CMC-nZVI injection, determined by qPCR analysis. Prior to CMC-nZVI injection the average of all monitoring wells yielded *dhc* levels of 7×10^6 gene copies/L, which is above the level at which dechlorination is expected to occur at contaminated sites (Wilson et al. 2007). Compared to pre-injection conditions, the average of post injection *dhc* levels in all nZVI/CMC impacted wells increased by an order of magnitude while the average of the less impacted wells stayed the same. 134

Figure 5.3: Phylogenetic composition of the microbial community in one monitoring well that was impacted (MW1), and one well that was less impacted (MW9) by the CMC-nZVI injection. Relative abundance of each phylum is represented for each monitoring well. Within the chloroflexi Phyla, more specific operational taxonomy units were identified for the dechlorinating species *Dehalococcoides spp.* and *Dehalogenimonas*. 136

Figure 5.4: Relative abundance (%) and absolute abundance (gene copies/L) of *dhc* measured by amplicon pyrosequencing and qPCR, respectively. Wells impacted by CMC-nZVI show higher relative and absolute abundance compared to non-impacted wells that remain unchanged following injection. 137

Figure 5.5: Phylogenetic distance matrices, minimized using non-metric dimensional scaling (NMDS) a.) shows the 95% confidence ellipses for sampling time groups (-2 days, 246 days, 448 days, 671 days), b.) shows the 95% confidence ellipses for samples grouped by nZVI/CMC impact (impacted, non-impacted/less impacted, pre-injection) c.) same as b.) but overlain with vectors representing the measured environmental parameters. The size and direction of the vectors express the correlation of each variable with the samples in the plot. d.) shows species/OTUs plotted within the ordination space according to their most dominant position. The plot identifies aerobic/facultative anaerobes (red), anaerobes (blue), and non-specified (black) microbial species overlaid by the ORP contour plot. 140

List of Appendices

Appendix A

Appendix A. 1: Core-shell structure of nZVI depicting various mechanisms for the removal of metals and chlorinated compounds. Adapted from Li et al [62].	165
Appendix A. 2: Standard redox potentials (E^0) in aqueous solution at 25 °C [80, 220]	170
Appendix A. 3: Conceptual Model of DLVO interaction forces for nZVI particles with different surface properties. a.) Bare nZVI b.) nZVI with strong electro-static repulsion c.) nZVI with both electro-static and steric repulsion. Points 1 and 2 refer to the primary and secondary minimum, respectively.	189

Appendix B

Appendix B. 1: 3-Dimensional conceptual model of the utility corridor showing the existing utilities (blue cylinders), as well as, the installed monitoring well field and a representation of the engineered hydraulic gradient used during nZVI injection.	235
Appendix B. 2: Stability curves for 1 g/L nZVI stabilized with 0.8% CMC polymer sampled from field synthesis drums prior to injection into the subsurface. Samples were diluted 10x in de-ionized de-oxygenated water prior to analysis using UV-vis spectrophotometry at $\lambda = 504\text{nm}$. $t = 0$ for the stability curve corresponds to $t = 16$ hr for the injection due to the sample travel time to the laboratory.....	236
Appendix B. 3: Flow rates measured during gravity feed (constant well head) injection of 1.0 g/L nZVI stabilized with 0.8% CMC into sandy media. Injection proceeded over a 24 hr period in the primary injection well (INJW) and over shorter periods in secondary injection wells. The well productivity was observed to decrease in all cases as the viscous fluid traveled from the injection well.	237
Appendix B. 4: a) Redox Potential (ORP), b) pH, c) Dissolved oxygen (DO) plotted for the primary injection well (INJW) and other significant monitoring wells cross gradient (MW9) and down gradient (MW6) of the nZVI detection and characterization area (MW1).	238

Appendix B. 5: Transmission electron micrographs of nZVI particles a.) freshly synthesized in suspension, b) retrieved from MW1 1 hr after injection began, c) 12 hr after injection began, d) 24 hr after injection began.	239
Appendix B. 6: Energy dispersive X-ray spectroscopy (EDS) results showing micrographs and corresponding elemental composition for nZVI particles a) freshly synthesized in Drum 1, b) collected from MW1 – 1 hr after injection, c) from MW1 isolated under high magnification, d) collected from MW1 – 12 hrs after injection began, e) collected from MW1 – 24 hrs after injection began. The results confirm that nanoparticles that traveled to MW1 are composed of Fe.	240
Appendix B. 7: Results of slug testing prior to nZVI injection for all monitoring wells and 10 days following nZVI injection for injection wells. Results show that there was a slight increase in the hydraulic conductivity of the injection wells following injection.	243
Appendix B. 8: Estimates of hydraulic conductivity (K), pore velocity (v_p), and arrival times were performed using theoretical, laboratory, and field methods. Laboratory analysis resulted in higher estimated K due to the specific targeting of sandy samples for analysis due to the assumption that nZVI will travel preferentially through these zones.	244
Appendix B. 9: Results of quantitative characterization of nZVI particles prior to injection and following transport through the subsurface.....	245
Appendix C	
Appendix C. 1: Schematic of the injection and monitoring wells on site showing the estimated spatial distribution of nZVI from each injected volume.....	248
Appendix C. 2: Geochemical data showing a.) total Fe, b.) ORP, c.) pH, d.) Chloride in the monitoring wells	249
Appendix C. 3: Example Calculation of electron balance for aqueous cVOCs at Monitoring Well 1.....	257
Appendix C. 4: Example Calculation of electron balance for Chloride concentrations at MW1	259

Appendix C. 5: Microbial electron reducing equivalents based on the yield of microorganism	261
Appendix C. 6: Raw data from analytical analysis.....	262
Appendix D	
Appendix D. 1: Bubble Pie charts similar to the Chlorinated Ethenes in Figure 1, showing the Chlorinated Ethanes and Methanes. Although these cVOCs are an order of magnitude lower than the Chlorinated Ethenes, they show distinct patterns of degradation over the monitoring period, and show the potential inhibition due to high concentrations of chloroform in MW4. MW6 provides a good comparison to MW4 as both contain high CF concentrations prior to injection. In MW6, CF concentrations declined and were accompanied by declining concentrations of all cVOCS, whereas in MW4 there were minimal changes in cVOCs overall, apart from the increased inhibitor concentrations (CF and 1,1,1 TCA).	264
Appendix D. 2: Amplicon pyrosequencing data in background monitoring points. Results are grouped by phylum showing that the microbial communities are similar throughout the site prior to injection. A high percentage of community is identified from Green genes database.	266
Appendix D. 3: High resolution version of Figure 5d showing ordination of species and ORP contours.....	267
Appendix D. 4: Ethene Data collected following injection. Downgradient and injection wells have the highest Ethene concentrations one year after injection. Ethene was not analyzed prior to 246 days.	268

Chapter 1

1 Introduction

1.1 Background

Groundwater is a vital resource, sustaining life processes and communities worldwide. It provides drinking water for over 30 % of Canadians (Sprague 2007), in particular 80% of rural households use water from an underground source (Nowlan 2007). Unlike surface water where riparian rights exist, groundwater legislation is not as advanced in the prevention or protection of downstream rights to water (Shrubsole 2007). This makes groundwater sources more susceptible to the impacts of contamination and scarcity issues, in comparison to surface water. A lack of testing and proper oversight in public wells (O'Connor 2002) or a lack of knowledge in private wells can lead to dire consequences, such as was the case in Walkerton, Ontario in May of 2000 (CIDNews 2000). This is a recent tragedy affecting the public at large but there have sadly been many groundwater tragedies in the past (Harr 1996). Economic and population growth continue to stress water resources leading to scarcity of water. Compounding the current threats to groundwater the legacy of neglectful industrial practices that have contaminated groundwater aquifers is an ongoing issue. Although decades of research and development have provided alternatives to remediate recalcitrant industrial contaminants, current technologies are incapable of returning the nearly 400,000 contaminated sites in North America to pristine levels.

The most reliable degradation method for these recalcitrant compounds is natural biological attenuation by microorganisms that reside in the subsurface. Organohalide-respiring microorganisms are a group of organisms that are able to respire halogenated groups found on chlorinated compounds, degrading and rendering the compounds harmless (Hug et al. 2013, Edwards 2014). This class of organisms has been described in great detail (Maymó-Gatell et al. 1997) and enriched in cultures to exploit their abilities (Waller et al. 2005). These microbially mediated processes, however, take considerable amounts of time and must be monitored, managed, and supplemented with pretreatment in order to achieve reasonable cleanup times.

One technology that has generated a lot of interest, is Zero Valent Iron (ZVI), a chemical reductant that is capable of degrading many recalcitrant compounds and has been noted as an effective pre-cursor to biodegradation. ZVI was first used in passive plume remediation (Gillham et al. 1994) for the treatment of low concentration chlorinated solvents. Nanoscale particles of Zero Valent Iron (nZVI) was developed, showing improved reactivity (Wang et al. 1997, Zhang et al. 1997). However, early field applications of bare-nZVI resulted in limited mobility in porous media in early field studies (Elliott et al. 2001). This limited mobility has been since described as “a few inches to a few feet” (Sun et al. 2007) due to the ferromagnetic properties that cause rapid aggregation and settling (Phenrat et al. 2007). Further development led to versions of nZVI that were polymer coated to mitigate aggregation and settling (Schrack et al. 2004), and methods were implemented for controlling the particle size (He et al. 2005, He et al. 2007). These nZVI particles demonstrated improved colloidal stability (Phenrat et al. 2008) and improved mobility in porous media (He et al. 2009, Phenrat et al. 2009, Kocur et al. 2013), which has led to the successful field implementation of the technology (Henn 2006, Bennett et al. 2010, He et al. 2010, Johnson et al. 2013, Kocur et al. 2014). An unexpected consequence of nZVI injection was that microbial degradation also increased (Henn 2006, He et al. 2010). Contradictory results have been shown several studies in the laboratory and have noted the enhanced microbial activity following nZVI in laboratory studies, however, there have not been any successful field studies that have demonstrated this property.

1.2 Scope of Work

The chemists and chemical engineers that originally invented and patented nZVI were able to demonstrate its capabilities in the laboratory with the intention of field scale site remediation. Along the way many researchers have worked on improving the state of the art, improving the understanding of nanoparticle stability, mobility, and reaction. Concerns over the eco-toxicity of nanoparticles in general have also promoted numerous environmental risk investigations from nZVI use. Despite being a very active research topic, there have been very few studies that have demonstrated successful implementation of the technology at the field scale. This requires a multidisciplinary approach to field work implementing aspects of site characterization, nanoparticle synthesis chemistry, groundwater hydrogeology, and microbiology throughout the project.

1.3 Research Objectives

The goal of this research is to substantiate speculation in earlier field studies. Through the use of analytical and microbiological techniques and a well-coordinated field sampling campaign this study evaluates the following objectives.

- Demonstrate the feasibility of nZVI/CMC gravity injection as a method of delivery. Track the mobility of nZVI/CMC within the contaminated utility corridor during injection.
- Present definitive evidence of nZVI/CMC presence in the subsurface; delineating the extent of amendment delivery and validating Fe^0 reactive potential upon delivery
- Evaluate nZVI impact on the dechlorinating microorganism *Dehalococcoides spp.* in-situ immediately following injection.
- Substantiate earlier claims that nZVI enhances microbially mediated degradation in the subsurface.
- Appraise the microbial community response to nZVI/CMC injection using a phylum level analysis.

1.4 Thesis Outline

This thesis is written in “Integrated Article Format.” A brief description of each chapter is presented below.

Chapter 1 provides a brief introduction to groundwater, nZVI, biodegradation, and delineates the objectives of this thesis.

Chapter 2 reviews current literature on the relevant aspects of contaminated site regulations, site-specific characterization in remediation using nZVI, nZVI laboratory studies, field scale implementation techniques for amendment injection, and best practices for nZVI use. This chapter was written as the literature review for this thesis and was submitted for publication in the book: *Nanoscale Zerovalent Iron Particles for Environmental Restoration: From Fundamental Science to Field Scale Engineering Applications*. Edited by Greg Lowry and Tanapon Phenrat.

Chapter 3 titled “Characterization of nZVI in a field scale test” is a manuscript that quantifies mobility of nZVI/CMC following injection, delineated the extent of injection through characterization of nanoparticle samples retrieved from wells. This chapter was published on January 30th 2014 in the journal of *Environmental Science and Technology*. [dx.doi.org/10.1021/es4044209](https://doi.org/10.1021/es4044209)

Chapter 4 titled “Contributions of abiotic and biotic dechlorination following carboxymethyl cellulose stabilized nanoscale zero valent iron injection” presents the short term effects of nZVI/CMC injection in the subsurface. cVOCs degradation and dechlorinating microbial species are monitored following injection. Estimated contributions of abiotic and biotic degradation are evaluated from water sample parameters and obligate dechlorinating species growth. This chapter was accepted for publication in the journal *Environmental Science and Technology* on June 19th 2015.

Chapter 5 titled “Long Term Dechlorination Following nZVI/CMC Injection and Impact on Microbial Communities, Including Organohalide-Respiring Microorganisms” is a manuscript that evaluates the long term cVOC degradation in the utility corridor by comparing the wells that were impacted by nZVI/CMC and those that were not. Next-generation pyrosequencing obtained microbial community data that was classified on the phylum level. Implications of the injection amendments on organohalide-respiring microorganisms are discussed along with analysis of the predominant environmental parameters that affect microbial communities during remediation.

Chapter 6 summarizes the major conclusions of the thesis, discusses the practical and environmental implications of the work, and recommends future research need.

Appendix A titled “Nanoscale zero valent iron and bimetallic particles for contaminated site” was a literature review that was collaboratively written and presents the state of the art as of 2011. This chapter was published in 2013 as a special edition of the journal *Advanced in Water Resources* as an invited review. [doi:10.1016/j.advwatres.2012.02.005](https://doi.org/10.1016/j.advwatres.2012.02.005)

1.5 References

- Bennett, P., F. He, D. Zhao, B. Aiken and L. Feldman (2010). "In Situ Testing of Metallic Iron Nanoparticle Mobility and Reactivity in a Shallow Granular Aquifer." Journal of Contaminant Hydrology **116**(1-4): 35-46.
- CIDNews (2000). "E. coli O157:H7 outbreak in Walkerton, Ontario." Clinical Infectious Diseases **31**(2): i-iii.
- Edwards, E. A. (2014). "Breathing the unbreathable." Science **346**(6208): 424-425.
- Elliott, D. W. and W.-x. Zhang (2001). "Field Assessment of Nanoscale Bimetallic Particles for Groundwater Treatment." Environmental Science & Technology **35**(24): 4922-4926.
- Gillham, R. W. and S. F. O'Hannesin (1994). "Enhanced Degradation of Halogenated Aliphatics by Zero-Valent Iron." Ground Water **32**(6): 958-967.
- Harr, J. (1996). A Civil Action, Vintage Books.
- He, F., M. Zhang, T. Qian and D. Zhao (2009). "Transport of carboxymethyl cellulose stabilized iron nanoparticles in porous media: Column experiments and modeling." Journal of Colloid and Interface Science **334**(1): 96-102.
- He, F. and D. Zhao (2005). "Preparation and Characterization of a New Class of Starch-Stabilized Bimetallic Nanoparticles for Degradation of Chlorinated Hydrocarbons in Water." Environmental Science & Technology **39**(9): 3314-3320.
- He, F. and D. Zhao (2007). "Manipulating the Size and Dispersibility of Zerovalent Iron Nanoparticles by Use of Carboxymethyl Cellulose Stabilizers." Environmental Science & Technology **41**(17): 6216-6221.
- He, F., D. Zhao and C. Paul (2010). "Field assessment of carboxymethyl cellulose stabilized iron nanoparticles for in situ destruction of chlorinated solvents in source zones." Water Research **44**(7): 2360-2370.
- Henn, K. W., Waddill, D.W. (2006). "Utilization of nanoscale zero-valent iron for source remediation - A case study." Remediation Journal **16**(2): 57-77.

- Hug, L. A., F. Maphosa, D. Leys, F. E. Löffler, H. Smidt, E. A. Edwards and L. Adrian (2013). "Overview of organohalide-respiring bacteria and a proposal for a classification system for reductive dehalogenases." Philosophical Transactions of the Royal Society B: Biological Sciences **368**(1616).
- Johnson, R. L., J. T. Nurmi, G. S. O'Brien Johnson, D. Fan, R. L. O'Brien Johnson, Z. Shi, A. J. Salter-Blanc, P. G. Tratnyek and G. V. Lowry (2013). "Field-Scale Transport and Transformation of Carboxymethylcellulose-Stabilized Nano Zero-Valent Iron." Environmental Science & Technology **47**(3): 1573-1580.
- Kocur, C. M., A. I. Chowdhury, N. Sakulchaicharoen, H. K. Boparai, K. P. Weber, P. Sharma, M. M. Krol, L. Austrins, C. Peace, B. E. Sleep and D. M. O'Carroll (2014). "Characterization of nZVI Mobility in a Field Scale Test." Environmental Science & Technology **48**(5): 2862-2869.
- Kocur, C. M., D. M. O'Carroll and B. E. Sleep (2013). "Impact of nZVI stability on mobility in porous media." Journal of Contaminant Hydrology **145**(0): 17-25.
- Maymó-Gatell, X., Y.-t. Chien, J. M. Gossett and S. H. Zinder (1997). "Isolation of a Bacterium That Reductively Dechlorinates Tetrachloroethene to Ethene." Science **276**(5318): 1568-1571.
- Nowlan, L. (2007). Out of Sight, Out of Mind? Taking Canada's Groundwater for Granted. Eau Canada: The Future of Canada's Water. K. Bakker, UBC Press: 4.
- O'Connor, H. D. R. (2002). Report of the Walkerton Inquiry.
- Phenrat, T., H.-J. Kim, F. Fagerlund, T. Illangasekare, R. D. Tilton and G. V. Lowry (2009). "Particle Size Distribution, Concentration, and Magnetic Attraction Affect Transport of Polymer-Modified Fe⁰ Nanoparticles in Sand Columns." Environmental Science & Technology **43**(13): 5079-5085.
- Phenrat, T., N. Saleh, K. Sirk, H.-J. Kim, R. Tilton and G. Lowry (2008). "Stabilization of aqueous nanoscale zerovalent iron dispersions by anionic polyelectrolytes: adsorbed anionic

polyelectrolyte layer properties and their effect on aggregation and sedimentation." Journal of Nanoparticle Research **10**(5): 795-814.

Phenrat, T., N. Saleh, K. Sirk, R. D. Tilton and G. V. Lowry (2007). "Aggregation and Sedimentation of Aqueous Nanoscale Zerovalent Iron Dispersions." Environmental Science & Technology **41**(1): 284-290.

Schrick, B., B. W. Hydutsky, J. L. Blough and T. E. Mallouk (2004). "Delivery Vehicles for Zerovalent Metal Nanoparticles in Soil and Groundwater." Chemistry of Materials **16**(11): 2187-2193.

Shrubsole, D., Draper, D. (2007). On Guard for Thee? Water (Ab)uses and Management in Canada Eau Canada: The Future of Canada's Water. K. Bakker, UBC Press: 3.

Sprague, J. B. (2007). Great Wet North? Canada's Myth of Water Abundance. Eau Canada: The Future of Canada's Water. K. Bakker, UBC Press: 2.

Sun, Y.-P., X.-Q. Li, W.-X. Zhang and H. P. Wang (2007). "A method for the preparation of stable dispersion of zero-valent iron nanoparticles." Colloids and Surfaces A: Physicochemical and Engineering Aspects **308**(1-3): 60-66.

Waller, A. S., R. Krajmalnik-Brown, F. E. Löffler and E. A. Edwards (2005). "Multiple Reductive-Dehalogenase-Homologous Genes Are Simultaneously Transcribed during Dechlorination by Dehalococcoides-Containing Cultures." Applied and Environmental Microbiology **71**(12): 8257-8264.

Wang, C.-B. and W.-x. Zhang (1997). "Synthesizing Nanoscale Iron Particles for Rapid and Complete Dechlorination of TCE and PCBs." Environmental Science & Technology **31**(7): 2154-2156.

Zhang, L. and A. Manthiram (1997). "Chains composed of nanosize metal particles and identifying the factors driving their formation." Applied Physics Letters **70**(18): 2469-2471.

Chapter 2

2 Field scale evaluation of nZVI

Adequately assessing remediation performance in the field requires a detailed understanding of the remediation technology that has been implemented in addition to comprehensive understanding of the site that is being remediated. When an amendment injection is involved, such as nanoscale zero valent iron (nZVI), it is also important to ensure that the amendment has been effectively administered. nZVI has important and unique geochemical characteristics that are often used in the interpretation of remedial processes. These geochemical interactions have been extensively studied in controlled laboratory studies, leading to a good understanding of nZVI as a remediation technology. The use of nZVI in the field, however, has many complicating factors. This is compounded by the fact that adequately evaluating remediation performance suffers from poor site characterization (Preslo 2005, Kueper 2014). Examples from previous nZVI field studies will be used to illustrate the many important considerations involved in assessing delivery and performance monitoring following nZVI application. The different metrics used to evaluate nZVI as a remediation technology will be compared. In addition examples of site characterization techniques will be used to stress the importance of developing an adequate conceptual model of field activities. Finally interpretation of field results must include a multi-disciplinary approach incorporating the reaction chemistry along with the environmental biogeochemistry. Strategies will be discussed for best assessing the site prior to amendment injection, during injection, and during long term monitoring.

2.1 Contaminated site management and technology evaluation

The motivation for remediation of a contaminated site can come in several forms but is almost always due to monetary considerations. Liability reduction, avoidance of penalty, and capital gains from the standpoint of asset transfer, are three of the largest motivators for remediation (Preslo 2005). Jurisdiction also dictates, to a large degree, the extent to which remediation is a driver. Governmental bodies incentivize remediation through regulations and

enforcement to different degrees throughout the world. Similarly, insurance companies, to a great extent, drive motivation for remediation through the requirement of dispensation to regional laws and business practices. Industrial standards and environmental stewardship has improved over the last several decades, curbing the release of some contaminants, however, the legacy of recalcitrant contaminants still represents a considerable challenge. Discovery of emerging contaminants also continues to challenge researchers, regulators and society. The equalizing factor in this situation can be technological advances of remediation technologies, both in the development of the technology, but also in the advancement of how it is used.

2.1.1 Contamination and legislation

Prior to the 1970s there was little legislative oversight of the creation, transportation, treatment, and disposal of hazardous materials. In 1976 the United States passed the Resource Conservation and Recovery Act (RCRA), the first comprehensive attempt to regulate hazardous materials. Since then, similar “polluter pays” legislation has been enacted throughout the developed world and in many cases extends to environmental damage in addition to direct threat to human health. In 1980, the Comprehensive Environmental Response, Compensation and Liability Act (CERCLA) was passed in response to the discovery of a large number of hazardous waste sites that were contaminated prior to 1976 in the United States, accompanied by the realization that a number of sites were abandoned. CERCLA sites are commonly called “Superfund” sites and represent the largest, highest priority, and most hazardous sites in the United States. Following CERCLA, there were a number of important programs that were created, including the Superfund Amendments and Reauthorization Act (SARA) of 1986. SARA protected workers during the clean-up of hazardous materials through amendments to the Occupational Safety and Health Act (OSHA) of 1970 and also encouraged the continued adaptation and improvement of public health standards surrounding hazardous contaminants. These working standards and legislated directives for release of hazardous materials and contaminants cover numerous industries and help drive remediation (Makeig 2005).

2.1.2 The cost and endpoints of remediation

Two challenges arise from the restoration and remediation of contaminated sites. First, there is great difficulty in degrading contaminants to satisfactory levels using existing

techniques. The recalcitrant properties of chlorinated solvents is the reason for their widespread use, making degradation challenging. Second, there is difficulty in definitively proving that remediation goals have been attained and the site is sufficiently restored. Alongside advances in remediation are the advances in analytical methods. Improving detection limits allows researchers to better understand the fate of contaminants. Remediation standards can be more confidently established if the contamination on site can be better characterized.. One initial goal of RCLA was that an impacted groundwater resource should be returned to a useful drinking water resource through remediation, however, it has since been shown that the cost of cleaning up such resources to pristine conditions is prohibitively expensive. Figure 2.1 shows a conceptual curve of the capital costs needed to achieve cleanup goals. The cost associated with remediation increases as the endpoint remediation contaminant concentration decreases. This is in part due to the increased volume of cleanup area, but also the technical challenges in achieving low concentrations.

In practice alternative remediation endpoints are often pursued due to the prohibitive cost of cleaning up groundwater to strict standards (MCLs). Such alternative endpoints provide a means of restoring impacted lands to serve a useful purpose, even though the resource is not restored to pristine levels. Tiered systems of regulation have been adopted throughout the developed world. The most stringent regulations would be ascribed to maximum concentration levels (MCLs) targets for drinking water while the lower tiers of remediation goals would be for scenarios with lower risk, such as land use and zoning. Public use lands, private residential, commercial and industrial areas may be assigned different standardized evaluation of contamination and remediation criteria (e.g, Ontario Reg. 153/11). Contaminant exposure in the context of planned site use and potential future exposure to surrounding and downstream ecosystems are often considered when determining regulatory targets for a particular contaminant. Remediation goals may also be set based on a site-by-site evaluation of specific contaminants and associated risks. These site-specific goals can be based on practicality and cost of remediation (e.g. Technical Impracticability waivers) or site-specific risk analysis.

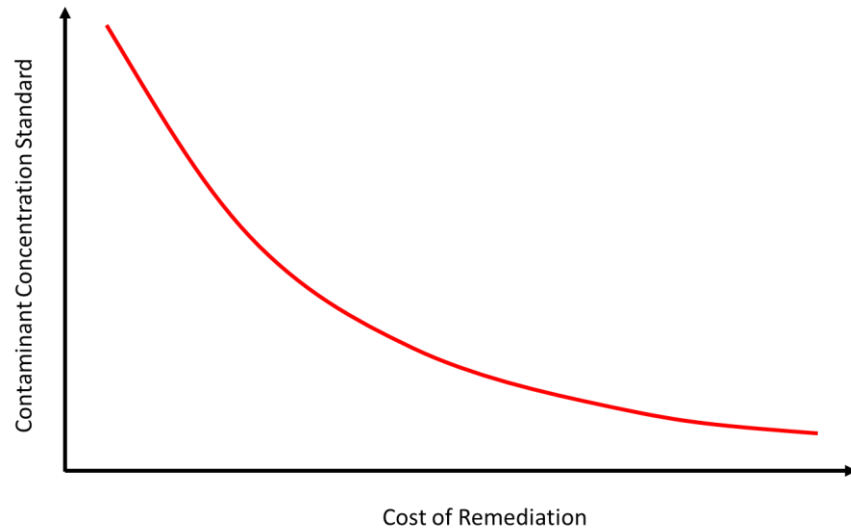


Figure 2.1: Contaminant Removal Level (concentration standard, MCL) vs Remediation Cost. The cost of remediating contaminated sites to strict concentrations can exponentially increase as the extent of remediation grows.

2.1.3 Conceptual site model

Although the goal of reducing contamination at a site is the site remediation goal this is complicated by a variety of factors including back diffusion from low permeability media or uncharacterized secondary sources. Given this, development of a robust conceptual model after rigorous site characterization helps ensure desired remediation outcomes can be achieved.

Identification of the sources of contamination, the potential avenues of migration and transfer between phases is not only important for understanding the pre-remediation conditions on site, but also imperative in selecting a remediation alternative and throughout the remediation monitoring phase. Knowledge of the distribution of contaminants within high and low permeability zones allows for targeted remediation and an understanding of the current state of contaminant fluxes can allow for better prediction of the fate of contaminants on site. The age of the site and the mass of contaminants that were released are also important factors to consider in site characterization.

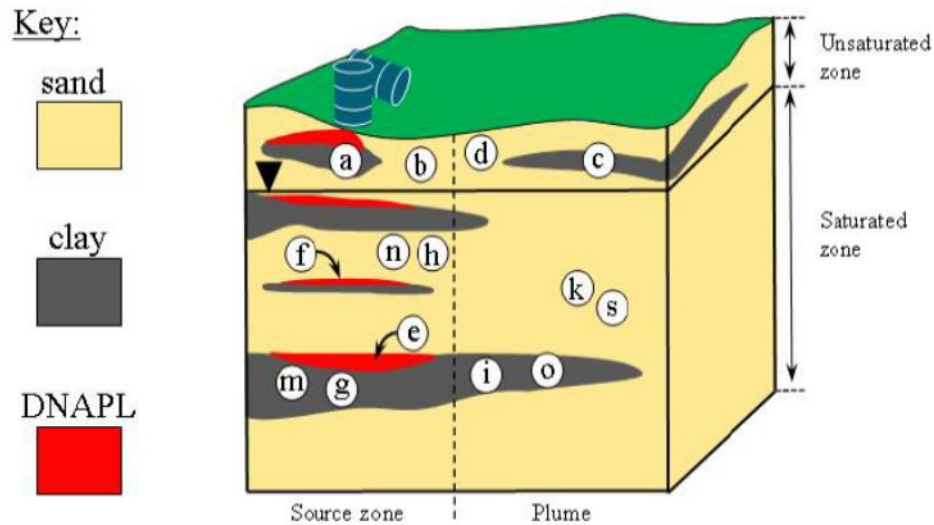


Figure 2.2: Site conceptual model of subsurface contamination showing all possible phases of contamination within the 14 compartment model: DNAPL, sorbed, aqueous, vapor. (from IRTC 2011)

The fourteen compartment model in Figure 2.2 is an example of a contaminated site conceptual model. The example assumes chlorinated solvents are the contaminant as they are among the most prevalent target compounds in site remediation operations (ITRC 2011). The model accounts for the contaminant mass distributed in different phases (Table 2.1) with different subsurface formations simplified as high and low conductivity zones. Initially contaminants enter the system through high conductivity zones, perhaps as a NAPL, and then sorb and diffuse into lower conductivity media. The model can therefore also allow for the understanding of contaminant fluxes that occur as the contamination persists, migrates, and degrades within the model. An accurate conceptual model, including knowledge of how the contamination impacted the site in the source zone, how long the contamination has persisted and how long the aqueous plume extends, as well as an accurate profile of the lithology and media, is the first step in effective remediation. This allows for strategic selection of a remediation approach and allows for the implementation of technologies that will most effectively remove the highest priority contaminants. This will also facilitate an assessment of remediation performance and the identification of remediation stop points, or assist in the transition to another remediation technology in the treatment train.

Table 2.1: Phases of contamination in the site conceptual model laid out in the 14 compartment model. The 14 compartment model is an example of a tool for evaluating chlorinated solvent sites.

Zone	Source Zone		Plume	
	Lower K	Higher K	Lower K	Higher K
Vapour	a	b	c	d
DNAPL	e	f		
Aqueous	g	h	i	k
Sorbed	m	n	o	s

2.1.4 Remediation timeline & performance objectives

The motivation for remediation may be derived from a requirement to limit the migration of contamination, the need to conform to a standard by a prescribed deadline, or otherwise reach a site-specific performance objective under a deadline. Regardless of the motivation for remedial action, a temporal component is typically prescribed. Site cleanup approaches that allow for the highest discounted time or money, shown in Figure 2.1, will be preferred. Understanding the limitations of each remediation technology will allow for effective technology selection for each stage along the cost-time curve. Applying appropriate performance objectives for the technology will enable a transition plan between one remediation technology and another. For example, thermal remediation techniques, solvent extraction, or flushing techniques are cost effective for removing NAPL phase contamination and for high concentration source zone removal, however, for residual NAPL or highly sorbed contamination, injection techniques such as in-situ chemical oxidation and in-situ chemical reduction have become popular (Tratnyek 2014).

Successful remediation will inevitably lead to bioremediation of aqueous contaminants at low level concentrations either through optimized delivery of amendments or through natural attenuation and monitoring. Performance objectives can include targeted remediation within areas of high contaminant flux, preventing off site contaminant migration or to achieve MCL standards in certain areas, avoiding liability or legal repercussions. When the

contamination is contained through engineering controls and low concentrations of contaminants can be achieved on the site, often the contamination can be monitored as it naturally attenuates. At the low concentration end of the curve in Figure 2.1, engineering controls and risk assessment can also be useful. Engineering controls include gas collection and treatment systems, sub-slab collection systems, and positive pressure mitigation systems to reduce the hazards due to vapour intrusion. Building design and planning can also work to strategically place structures and parking lots in such a way as to minimize hazards to occupants.

Most remediation technologies can be divided into two general strategies: active or passive remediation. Active remediation of a contaminated site involves removing the source of contamination. This is often necessary but can lead to very high capital costs. Complete removal of the mass is also rarely achieved using a single remediation technology, necessitating additional investment to treat residual contamination. Passive remediation involves the treatment of the contaminant plume, limiting the spread of downstream contamination. This can mitigate the immediate threat to downstream receptors and can bring a site into compliance with emission and discharge standards. Treating the plume does not, however, address source zone contamination and can lead to indefinite operating costs.

2.1.5 nZVI alternatives for remediation

ZVI based technologies can treat a broad range of contaminated site problems. Table 2.2 shows a comparative summary of the properties, attributes, and limitations of ZVI based technologies. The conditions of use will be site-specific and depend on many factors, however, general criteria for the effective use of each ZVI variant has been briefly outlined in Table 2.2. nZVI is particularly attractive due to its ability to treat higher concentrations of contaminants close to the source zone and also its ability to create ideal conditions for in-situ bioremediation.

Table 2.2: Comparative summary of ZVI remediation alternatives in wide use and in development.

Type of ZVI	Granular ZVI	mZVI	nZVI			
			nZVI (bare)	with stabilizers	with Carbon Substrate	Bimetallic
Size Range	Silt to medium sand	1-1000 μm	5-100 nm	Tunable depending on stabilizer (5-100nm)		
Specific Surface area	Low	Moderate	Variable	High, depending on stabilizer		
Mobility	Not mobile	Very limited	Very limited	Moderate to high depending on stabilizer		
Longevity of Reaction	years of use in PRBs, depending on conditions	months to years, susceptible to passivation	weeks to months, depending on passivation and method of synthesis	days to weeks, depending on contaminant loading	days to weeks, longer if coupled with biodegradable stabilizer	weeks to months due to more efficient use of electrons
Reaction Rate	Slow compared to alternatives	Moderate, depending on surface area	High with many contaminants	High, depending on stabilizer		Rapid reaction with most chlorinated contaminants
Aggregation	N/A	N/A	Rapid, especially at high concentrations	Low, forms stable aggregates depending on stabilizer		
Use cases (targeted zone)	Soil mixing (i,k,o,s), PRBs (i,k), fracture and injection (g)	Soil mixing (i,k), fracture and injection (g), PRBs (i,k), slurry walls (i,k), high viscosity injection (f,h,n)	High viscosity injection (f,h,n), EZVI (f,h,n)	Hot spot injection/source zone (e,f,g,h,m,n), high contaminant flux zones (h,n,k,s)	hot spots injection / biostimulation (e,f,g,h,m,n)	High contaminant concentrations, hotspots, troubled contaminants, tight timeline (g,h,m,n)

2.1.6 Role of nZVI

Advances in delivery techniques and particle mobility have allowed for the successful application of nZVI at dozens of sites in North America, Asia, and Europe. At many of these sites nZVI was not applied for full scale remediation but as pilot trials to develop a knowledge set for future applications. What is becoming apparent from the numerous examples of nZVI application is the necessity for a scalable and reliable deployment in order to treat problem areas of contamination. These “hot spots” may need to be treated due to accidental spills or re-mobilization of NAPL, or there may be areas not remediated using

other technologies, under characterized source zones, or secondary sources of contamination. In all these scenarios, nZVI provides a viable alternative to time-bound remediation. Figure 2.3 presents several examples of contamination scenarios for which there are limited viable remediation options. In addition, nZVI application requires minimal above ground infrastructure and can be effective for remediation around active infrastructure and utilities.

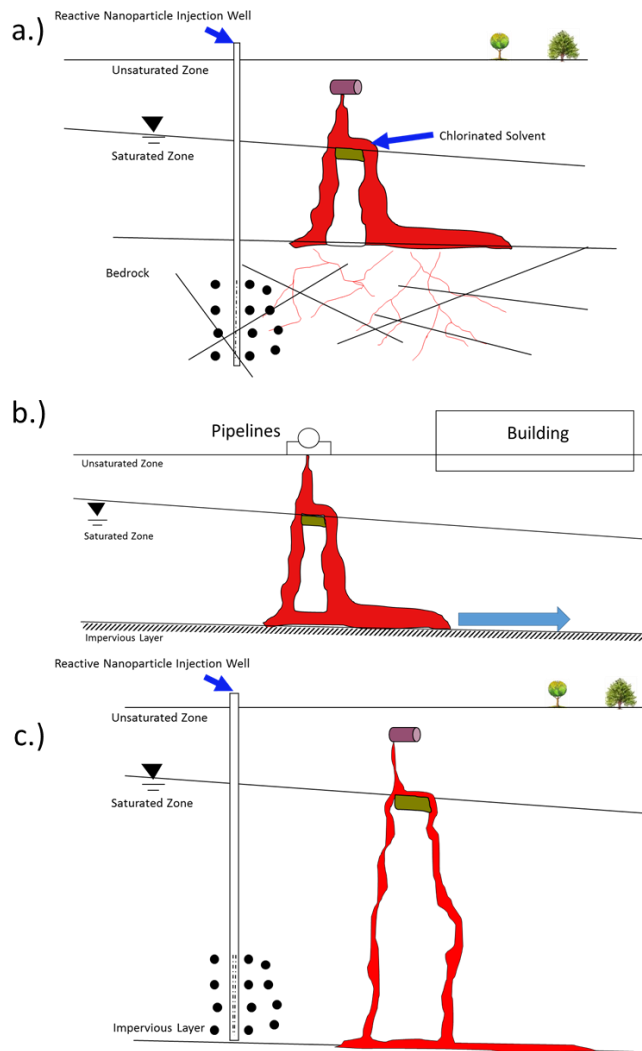


Figure 2.3: Three cases where nZVI may be a suitable remediation alternative. a.) contamination in fractured bedrock b.) existing critical infrastructure is too expensive to dismantle prior to remediation. c.) contamination reaches depths unattainable by other remediation methods.

2.2 Site characterization

Initial on site investigations and use of historical activity records can identify the potential sources of contamination. Site topology and lithology information can be gathered on regional, local, and site levels from borings and can be used to build a conceptual site model. Through further investigation more detailed elements of the conceptual site model can be identified and decisions about remediation made. Site characteristics including the type of subsurface media, hydraulic gradient, property boundaries and infrastructure help inform selection and design of remediation alternatives. The decision on whether an amendment injection remediation approach is appropriate requires information related to whether the permeable media is appropriate for delivery. This section provides a summary of some of the site characterization methods that should be considered prior to the application of nZVI. The lithology, depth of contamination, target contaminants, and possible co-contaminants, as well as site-specific considerations (e.g., below and above ground infrastructure) will strongly influence design.

2.2.1 Conceptual model development for nZVI applications

It is essential to delineate site contamination. Site lithology is often logged in detail during bore-hole investigations. In the past this information has been used to guide engineers and geologists about where to install water wells or petroleum hydrocarbon extraction networks. For environmental remediation knowledge of the geological, lithological and hydrological conditions is not enough to inform decisions. Delineation of contamination is also required at the same level of detail.

Monitoring wells for environmental contamination investigation require a modified approach than that for drinking water extraction wells. Decades of research and development of site investigation on Superfund sites has found that traditional monitoring wells are incapable of adequately characterizing contamination. Figure 2.4 provides an example of typical long screen monitoring wells and some of the shortcomings when applied to environmental remediation (Einarson 2005). Table 2.3 describes the implications of different screen intervals on site characterization. The example contaminant contours can represent any soluble compound sampled in an aqueous matrix. For example for nZVI the solute could be

cVOCs (e.g. TCE). Well screen lengths can be as long as 20 feet on some sites which can lead to large discrepancies between the conceptual site model and actual site conditions.

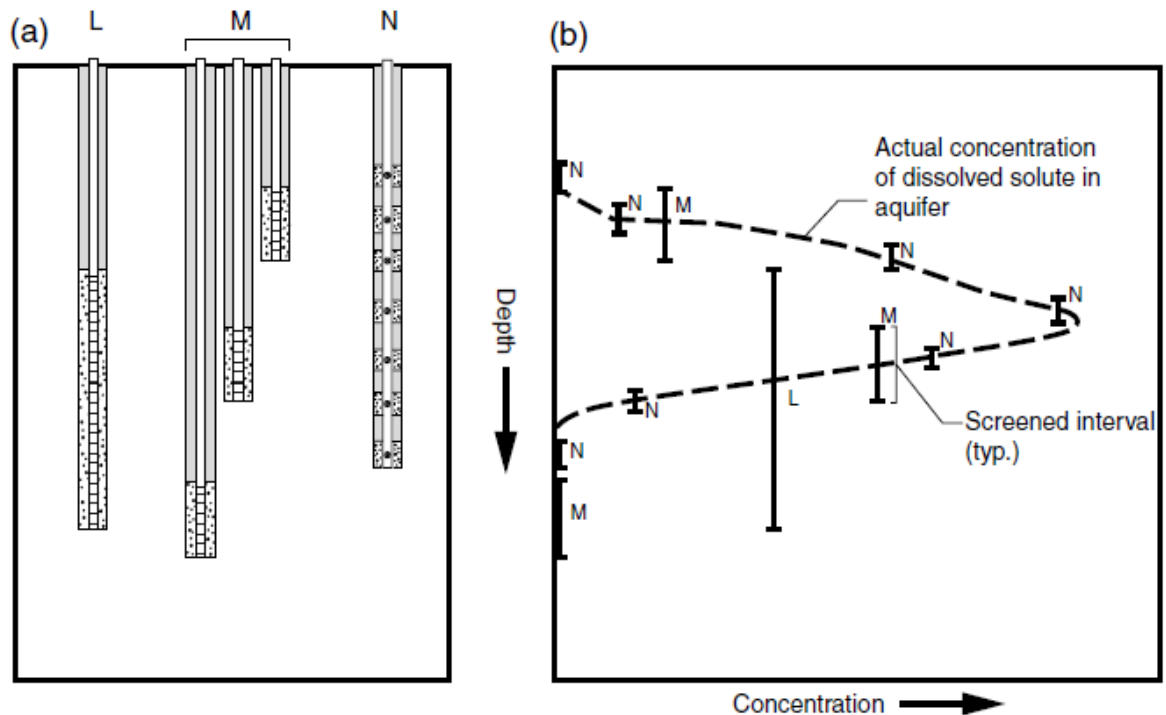


Figure 2.4: a.) Illustration of three different wells screen lengths (Long screened interval (L), Medium (M), and Multilevel (N)) and b.) an example of possible concentrations of solute measured with these different screened intervals. (Einerson 2005)

Table 2.3: Impact of monitoring well design on conceptual model of the cVOC contamination on site (modified from Einerson 2005)

Bias in monitoring well	Implications on site conceptual model	Resulting consequences on nZVI remediation
Long well screen dilutes cVOCs in samples	Maximum concentration is underestimated	nZVI dose may not treat most of the contaminated zone
Well screen only partially captures contaminated interval	Position of maximum cVOC concentration is inaccurate	Targeted nZVI injection depth may miss contamination
Complex layering of media present along well screen	No information about contaminant distribution	Injection may only enter the most conductive media, but miss the contaminated zone
Long well installed and a vertical hydraulic gradient is present	Contamination may migrate upwards or downwards within well screen	nZVI injection (often viscous) may mobilize contamination downwards.

Use of a transect of multilevel wells can provide a detailed conceptual understanding of the extent of contamination. Figure 2.5 is an example transect detailing a cVOC plume travelling through section A-A'. This level of detail helps delineate more precisely plume extent. This type of plume delineation can be combined with known hydraulic gradient and estimates of hydraulic conductivity to estimate contaminant flux across the transect. The transect can also be oriented longitudinally to the direction of groundwater flow to delineate plume length, and potentially providing information related to plume attenuation.

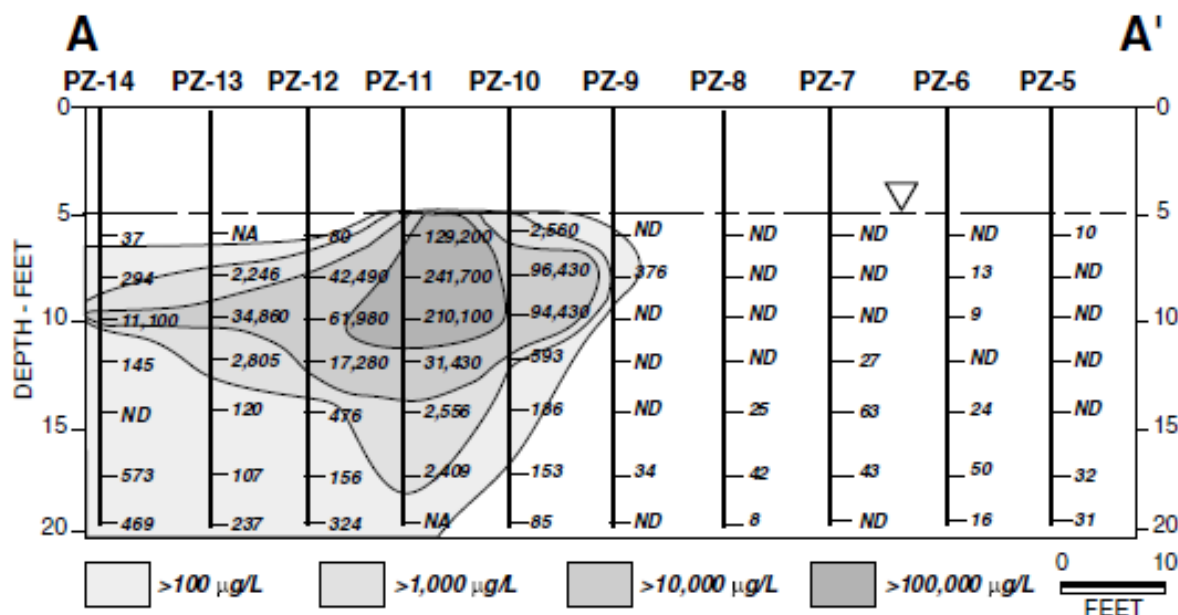


Figure 2.5: Transect of a groundwater plume with total cVOC concentrations shaded at different contour intervals. The transect was installed transverse to the direction of travel of a groundwater plume (Einarson and Cherry 2002).

The same transect approach can be used to delineate contamination within a source zone. nZVI and other amendments can be targeted to zones where elevated concentrations are detected.

An EZVI field application has taken advantage of the multilevel well approach to estimate mass flux using integral pump tests (Krug 2010). Two monitoring wells were installed with a small transect of three multilevel wells in between. Over time the multilevel concentrations were monitored while the groundwater velocity was controlled across the transect using the two surrounding monitoring wells. Over a course of several years the mass flux was periodically measured in this manner, providing a method for NAPL mass loss determination (SERDP report). Generally, more informed decisions regarding remediation success can be made using contamination profiles along transects in comparison to traditional long screen wells.

2.2.2 Subsurface characterizing using well methods

Quantification of subsurface aquifer properties (e.g., storage, hydraulic conductivity and groundwater direction) are vital in conceptual model development. There is a range of established techniques to rigorously evaluate subsurface hydrogeological parameters of interest (Fetter 2001, Pinder 2006). Pumping tests can provide information about hydraulic conductivity or transmissivity, specific yield (for unconfined aquifers) or storage (for confined aquifers) and connectivity of wells or layers. Slug tests can be performed for a screened well, within an open borehole, or through the use of packers along multiple discrete intervals to provide estimates of transmissivity, and ultimately hydraulic conductivity (Butler 1997). Other considerations related to development of a site hydraulic conceptual model include the position and seasonal fluctuation in the water table. The conceptual model may have to be modified on some sites as seasonal changes in the water table can change the groundwater flow direction and magnitude.

Tracer testing can be used to identify horizontal hydraulic conductivity using arrival times between wells. This information can subsequently be used to benchmark solute transport against a conservative tracer (Bennett et al. 2010, He et al. 2010). This helps quantify the extent of adsorption and desorption of a given media. Tracers are used in column tests to compare water flow to nZVI transport, and have been used as the basis for comparison in pilot scale tests for nZVI injection as well (He et al. 2010, Johnson et al. 2013, Kocur et al. 2014).

Constituents in the injection fluid can also be used as conservative tracers. The electrical signal of the amendment injected can be used as a tracer to monitor extent of migration (Wei et al. 2010, Johnson et al. 2013). The extent of polymer amendment transport has also been demonstrated to correlate well with nZVI travel (Kocur et al. 2014). Reactive tracers employing tracers that possess known sorption properties to the oil/water interface can be used in combination with a conservative tracer to quantify the NAPL/water surface area Annable et al. (1998). The effects of any tracer on nZVI reactivity and mobility should be considered prior to field application.

2.2.3 Investigating the subsurface using alternative methods

Alternative methods for site investigation may greatly aid or replace conventional methods, depending on the situation. When permanent well infrastructure is not feasible (e.g.,

creeks or riverbeds, other low lying areas prone to flooding) or permitted by regulators alternative techniques can be the only methods available for site characterization. These alternative methods include a range of probe techniques:

- Waterloo profiler – Geoprobe tip with machined holes and screen allowing for relative hydraulic conductivity testing at discrete intervals as the probe is driven into the subsurface. The peristaltic pump at the surface can reverse direction allowing sample collection.
- Membrane interface probe (MIP) – Membrane sleeve that allows for volatile compounds sampling as the probe is driven into the ground. When the tip encounters high aqueous concentrations or NAPL, the inert gas pumped on the inside of the membrane will carry the volatile compounds to the surface for analysis on a portable gas chromatograph with the detector of choice.
- Hydrosparge – Probe allows water to enter an internal chamber at a discrete depth where gas is bubbled through the sample and passed to the surface where a gas analysis system determines the volatile compounds in the sample.
- In situ solvent injection and extraction – Similar to the hydrosparge technique but a solvent is released into the formation through the drive tip, then gathered by the probe and analyzed at the surface.
- Downhole microscope/Camera – Visual evidence of NAPL in the subsurface at depth based on the color (usually weathered and black).
- Laser induced fluorescence (LIF) – Emission of a specific wavelength that is compound specific and fluorescent detection can be used to identify polychlorinated biphenyls polycyclic aromatic hydrocarbons in the subsurface.

A relatively recent example of the application of a probe at an nZVI field site is the study of Bennett *et al* (2010) who successfully used a MIP for aqueous phase sampling prior to nZVI injection into a layered sand aquifer that was contaminated with PCE and TCE. More detailed descriptions of probes are available (Kram 2005). . Another suite of site characterization techniques are geophysical methods that can be implemented above ground or in boreholes. Information from geophysical methods can be used to provide a continuum of data on the site when properly calibrated to borehole data (Benson 2005). Probe techniques have the added benefit of reducing waste as only samples are brought up to the surface. This can reduce exposure at highly contaminated sites.

2.2.4 Pre-screening porous media with nZVI

Transport through idealized porous media has been tested for a number of nZVI formulations, and a growing understanding of nZVI/media interaction exists. However laboratory testing, using permeable media recovered from the site of interest and under the range of conditions that are planned at the site, is the best way to ensure that nZVI will be mobile in the field. Kocur *et al* (2013) discussed the importance of replicating field conditions in laboratory tests to avoid overestimating nZVI transport in the field.

A number of studies have used unrealistically high pore water velocities in laboratory experiments when attempting to determine the extent of field transport (Zhan 2008). During site investigation core logs, and testing, can be used to estimate the range of hydraulic conductivity expected on site and select appropriate conditions for column experiments. Additionally groundwater and soils constituents, that could impact nZVI mobility, should be identified (e.g., high clay content and mineralogical anomalies). For example, nZVI had limited mobility in soils rich in calcium carbonates (Laumann *et al.* 2013). Previous studies have also noted a decline in mobility in natural soils (Schrack *et al.* 2004, He *et al.* 2009).

The design and upscaling of nZVI remediation systems from batch, to laboratory, to pilot scale has been done for a range of nZVI formulations and site conditions. Bennett *et al* (2010) provides a model for pilot testing using a single well pilot testing method. Coupling nZVI injection and extraction generated important information related to nZVI sorption, interaction, and reaction with porous media. This is particularly important on sites that differ from previous studies.

2.3 Evaluating injection and mobility

The injection of nZVI at an injection well is governed by Darcy's Law:

$$q = \frac{k\rho g}{\mu} \frac{dh}{dr} \quad (1)$$

Where q is the Darcy velocity, k is the permeability, ρ is the fluid density, μ is the fluid viscosity, h is hydraulic head, and r is the radius from the well.

nZVI can be injected using the following techniques:

- Constant head injection with a constant head at the well head.
- Gravity feed injection is a constant head injection that is limited by the height of the injection well, allowing only head from the standpipe.
- Constant flux injection ensures that the Darcy flux is constant throughout the injection.

In column experiments, linear head loss across a column is determined from Darcy's law, resulting in a constant velocity throughout the column. Radial flow from an injection well is often idealized as cylindrical flow emanating from the well. In radial flow as the radius from the well increases the Darcy velocity decreases due to a head drop throughout the system. Thus the radius of travel from a well can be predicted using:

$$r_{max} = \sqrt{\frac{V}{\pi n L} + r_{well}^2} \quad (2)$$

Where r_{max} is the maximum extent of the injection due to injection, V is the volume injected, L is the screen length, n is porosity (Bennett et al. 2010).

Radius of influence

The first nZVI field trials employed gravity injection and reported travel distances of only a few feet due to poor nZVI suspension stability (Elliott et al. 2001). Unfortunately, in these studies the methods of evaluating nZVI transport were not well established and it is likely that the radius of influence was likely closer to a few inches rather than to a few feet (Sun et al. 2007). Advances in particle stability resulted in nZVI suspensions that were easier to handle and inject (He et al. 2009, He et al. 2010). The most successful method to inject a large volume of nZVI at a large rate is to increase the injection head. This can be achieved using constant head or constant flux injection techniques yielding a radius of influence on the order of 5-7 feet, (Quinn 2005, Krug 2010) as compared to the 2-3 feet with gravity injection (He et al.

2010, Krug 2010). Shear thinning polymers are now being used for mZVI injection under pressure (Köber et al. 2014, Velimirovic et al. 2014, Luna et al. 2015). Krug *et al* (2010) tested injection alternatives prior to selecting full scale delivery method for EZVI. Luna *et al* (2015) tested pressurized injection methods and investigated which pressure discharge profile was able to inject the most stabilized mZVI on their pilot site.

Effect of viscosity

Increasing nZVI suspension viscosity is advantageous as it improves nZVI suspension stability. This has been noted in numerous laboratory studies that have used polymers (Tiraferri et al. 2009, Kocur et al. 2013), sheer thinning polymers (Tosco et al. 2010), and an oil in water emulsion (Berge et al. 2009). Although a viscosity increase potentially increases the radius of influence due to improved mobility, it has been noted that even a moderate increase in viscosity can significantly increase injection pressure (Krol et al. 2013). Injection of a viscous fluids also improves the stability of the injection front, however, increases in viscosity could also result in mobilization of NAPL (Pennell et al. 1994, Johnson et al. 2009, Abriola 2011).

Delivery in less permeable media

Low permeability zones, when contaminated directly or through long term diffusive transport from higher permeability zones, can act as long term sources of contamination. Back diffusion has long been established as a cause of long asymptotic concentration decline. This causes particular problems in site closure and a reliance on concentration-based criteria can result in extended monitoring because of the diffusive flux from low permeability zones. Advanced techniques for accessing and remediating impermeable zones are being explored.

Delivering electron donors using shear thinning polymers has been investigated for many remediation technologies, including nZVI (Cantrell et al. 1997, Cantrell et al. 1997, Comba et al. 2009, Vecchia et al. 2009, Truex et al. 2011) and mZVI (Cantrell et al. 1997, Vecchia et al. 2009, Truex et al. 2011). Most recently shear thinning polymers have been investigated for the injection of nZVI in column experiments (Zhong et al. 2008, Comba et al. 2012), in sand box experiments (Oostrom et al. 2007), and in the field (Truex et al. 2011, Truex et al. 2011). The shear rate is related to velocity (v), permeability (k), and porosity (n) (Martel et al. 1998)

$$Shear\ Rate\ (\gamma) = \alpha \frac{4v}{\sqrt{8\frac{k}{n}}} \quad (3)$$

Although more complex shear rate in porous media relationships have been described (Phenrat et al. 2009), Equation 3 demonstrates that shear rate increases with velocity. Thus, a shear thinning agent in the injection will result in a lower viscosity when shear rate is high (i.e., while passing through low permeability media), making it more likely for the fluid to pass through less permeable media. Injection with the aid of shear thinning fluids will cause more uniformly distributed amendment along the injection front in heterogeneous media because higher shear forces will thin the fluid in lower permeability media (Zhong et al. 2008). This generally causes an equalizing sweeping effect on the injection front and increases penetration in to low permeability lenses, areas that would otherwise be bypassed.

Amendments can also be delivered through low permeability media with the aid of electrokinetics. In this case electrodes are used to apply a direct current and transmit charged particles through the subsurface. This has been utilized for heavy metals and waste rock remediation (Acar et al. 1993, Mulligan et al. 2001). Electrokinetic enhanced nZVI transport through low permeability media has been demonstrated in laboratory studies (Chowdhury et al. 2012). This technology has not been demonstrated for field scale transport of nZVI, however, it has been used for the delivery of bioremediation amendments in the field (Mao et al. 2012).

Pneumatic and hydraulic fracturing techniques have been adopted from the oil and gas extraction industry to enhance subsurface ZVI distribution. Fracturing of media increases the permeability by intentionally exceeding the overburden effective stress, fracturing the media (Murdoch et al. 2002). Microscale and granular ZVI can be delivered in this manner. The technique can also introduce sand or other permeable media into the fracture creating a conduit that remains permeable. Such techniques are effective for creating delivery pathways for electron donors in tight media, however, this technique is subject to frequent daylighting of fractures.

2.4 nZVI detection and evaluation methods

The most reliable methods of directly quantifying nZVI mobility have, to date, involved sophisticated analysis of well-preserved samples, or analysis of samples very soon after sampling. The highly reactive nature of nZVI can also indirectly characterize nZVI. In a field setting this approach of indirect observation (i.e., monitoring geochemical changes due to nZVI oxidation and contaminant degradation at monitoring wells) is often the only available means of evaluation. Well methods are particularly useful for providing screening level analysis, but should be complemented with additional analysis to gain a better conceptual understanding of governing nZVI processes on site

2.4.1 Techniques and approaches for evaluating nZVI in wells

Well infrastructure is used for several purposes during site characterization, remediation, and in post-remediation monitoring. The most commonly reported method of evaluating nZVI mobility is quantification of total Fe recovered from aqueous samples from monitoring wells. Total Fe has been used in many column studies to delineate nZVI distribution (Saleh et al. 2008, He et al. 2009, Phenrat et al. 2009, Raychoudhury et al. 2012, Kocur et al. 2013), and thus many field studies extend this technique to delineate nZVI distribution following injection (Henn 2006, He et al. 2010). This method has been criticized as nZVI is rapidly oxidized and quantification of total Fe isn't necessarily an indicator of nZVI particle transport (Shi et al. 2015).

Kocur *et al* (2014) measured total Fe and the Fe⁰ content following injection of nZVI at a contaminated site. After 24 hrs of injection, samples were collected at a monitoring well where nZVI had travelled and it was found that nZVI content decreased from 55% to only 17 % in the particles. Column studies evaluating nZVI transport are commonly conducted for relatively short durations as such it is assumed that nZVI oxidation over the course of an experiment can be neglected. Field studies, however, involving longer duration injections cannot neglect oxidation and sophisticated analysis is therefore required to assess nZVI particle transport.

Geochemical indicators have also been widely used as evidence of nZVI mobility in the field (Henn 2006, He et al. 2010, Wei et al. 2010, Johnson et al. 2013, Kocur et al. 2014).

Fe⁰ oxidation increases pH and decreases ORP as it rapidly consumes dissolved oxygen. . Geochemical indicators of nZVI oxidation do not definitively prove that nZVI is present, only that the vicinity of the well has been impacted by oxidation products. Geochemical data is best suited as complementary data, or for screening purposes to identify the best time to collect additional samples for further analysis. Early field studies, and many applications of PRBs, rely on minimum ORP values in order to ensure that reductive dechlorination is occurring. Thermodynamically, low ORP conditions are necessary for reductive elimination of chlorinated compounds, however, as Bennett et al (2010) discussed low ORP does not necessarily mean that reductive dechlorination is occurring; only that it is possible. Reductive dehalogenation and beta-elimination both require electron and proton donors, thus evidence of their presence should also be explored. Recent work by Shi *et al* (2011, 2015) discussed the importance of additional analysis to support ORP measurements.

Conservative tracers (e.g., conservative ions) are another way that wells can be used to gather supporting information to improve the understanding of nZVI mobility. Many studies have demonstrated a strong correlation between tracer migration and total Fe distribution in aqueous samples during or immediately after injection. Bromide has been used as a tracer during injection of nZVI at a field test (He et al. 2010) and in push-pull tests (Bennett et al. 2010). Specific conductance has been used as a tracer when SO₄²⁻ and Na⁺ were the predominant ions in the system (Johnson et al. 2013). Bennett et al (2010) also showed a strong correlation between Fe and TOC immediately following injection due to the signal produced by the stabilizing polymer, a relationship that was shown to be useful in calibrating viscosity (Krol et al. 2013). Wei et al (2010) suggested total Fe correlated with suspended and total solids as an analog of mobility.

2.4.2 Challenges in interpretation of well data

Use of monitoring wells, which are essentially a point measure in space, inherently assumes that this point is representative of a larger domain and that an analyte is intercepted by the well. As such it can be sometimes be challenging to use monitoring wells to definitive determine transport of nZVI, or any amendment. Non-detection of nZVI can be due to the injection solution bypassing a well that is installed in a less permeable zone. Heterogeneity or flow along preferential pathways may also allow for nZVI to travel further than detected. This

can be a particular problem when budgetary constraints limit spatial sample resolution. Detection of dissolved Fe at a well can be misinterpreted as nZVI travel however it could be the transport of nZVI oxidation products. In order to definitively determine the extent to which nZVI has travelled and deposited in the subsurface, additional analysis should be undertaken. Sampling of zones with both high nZVI content and low concentrations will result in dilution and can complicate sample characterization. Some particle analysis methods require a minimum number of particles (ie. particle counts) and dilution of any analyte only serves to make detection more difficult. Well dilution can be mitigated by identifying the highly transmissive zones, prior to injection, and discrete interval sampling through the use of multi-level wells.

2.4.3 Methods of evaluating and characterizing particles

nZVI particles have been characterized using numerous approaches and analytical techniques in studies ranging from batch to field scale. The addition of polymeric coatings will alter nZVI suspension properties and will therefore have an effect on the interpretation of results. Below is a summary and critical analysis of the most widely used methods for nZVI characterization.

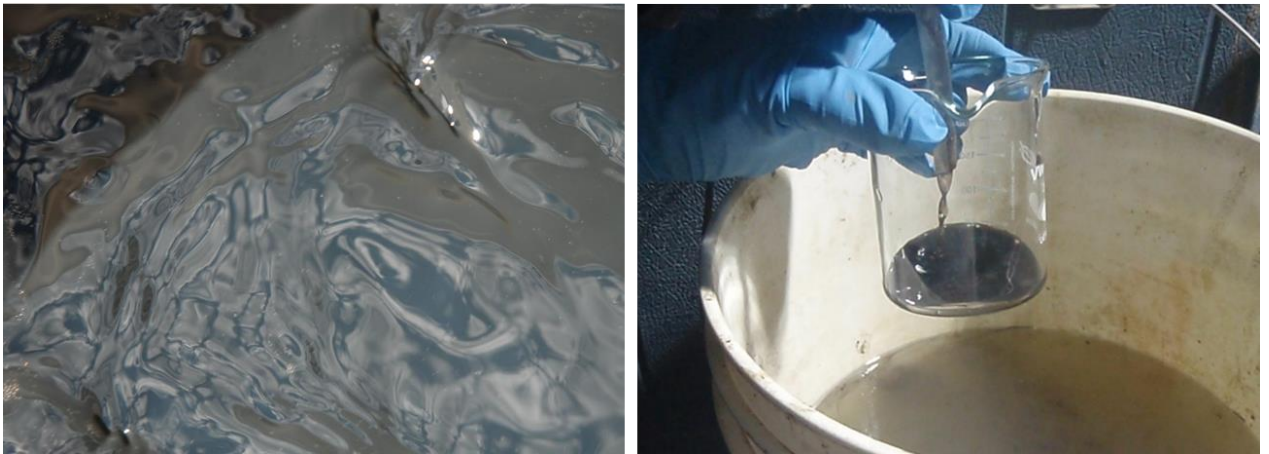


Figure 2.6: nZVI slurry synthesized at 1 g/L in 0.8 % wt CMC prior to injection (Left). nZVI sample collection at a monitoring well downstream of the injection (right)

Optical methods

A jet black color of an aqueous solution is often an indication of nZVI presence (Wang et al. 1997, Zhang et al. 1997, Elliott et al. 2001). nZVI is visible, depending on the Fe^0 content, at concentrations as low as 20mg/L (Shi et al. 2015). Visual indication of nZVI has been used in interpretation of 2-D sand box experiments (Kanel et al. 2008, Phenrat et al. 2010) and provides evidence of nZVI transport in column experiments as shown in Figure 2.7. Visual techniques has also been used as evidence of nZVI transport in field studies (Henn 2006, He et al. 2010, Kocur et al. 2014). Figure 2.6 shows a jet black nZVI slurry prior to injection and a black solution sampled at a downstream monitoring well. Field samples can contain silt and naturally occurring matter that can interfere with visual techniques. Fe sulfides, other metals (e.g., Mn), and other black or dark substances may be interpreted as nZVI, thus caution is advisable in relying on only visual evidence. Geochemical evidence of nZVI transport will typically accompany or precede visual observations of nZVI in the field.

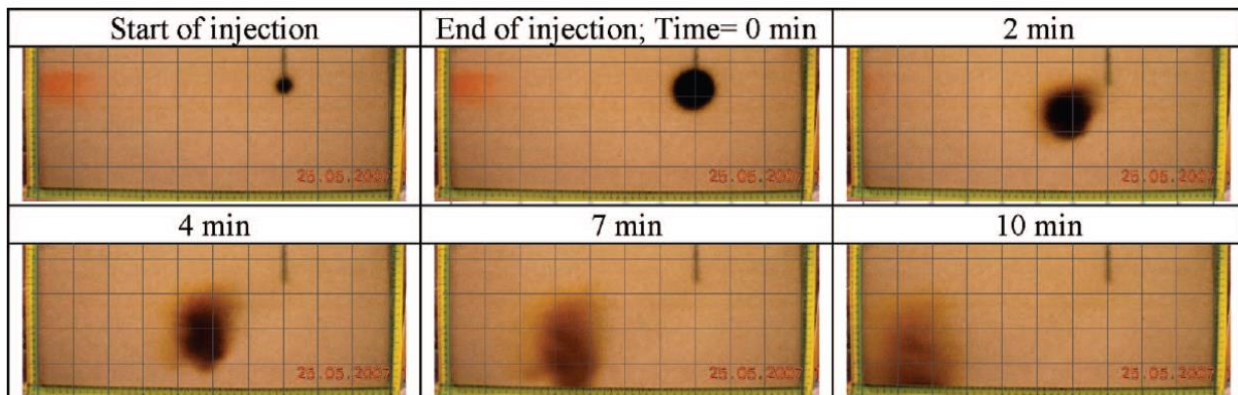


Figure 2.7: Demonstration of 4 g/L nZVI stabilized with PAA moving through a heterogeneous sandbox (Kanel 2008)

More advanced optical methods rely on absorbance quantification. UV/vis techniques specific to nZVI have been used to determine Fe concentrations in stability studies (Saleh et al. 2005, He et al. 2007, Phenrat et al. 2007, Phenrat et al. 2008, Tiraferri et al. 2008, Comba et al. 2009, Johnson et al. 2009, Raychoudhury et al. 2010, Sakulchaicharoen et al. 2010, Kocur et al. 2013) and have been extended to column studies by calibrating absorbance of light at 508nm (Schrack et al. 2004, Saleh et al. 2007, Saleh et al. 2008, He et al. 2009, Johnson et al. 2009, Phenrat et al. 2009, Tiraferri et al. 2009, Raychoudhury et al. 2010, Kocur et al. 2013).

In well controlled studies in the laboratory, the use of total Fe to quantify nZVI transport is considered to be acceptable. This assumption should be used with caution in field studies, or when there is sufficient time and conditions favorable to nZVI oxidation.

When possible a standard method (e.g., Ferrozine method (Stookey 1970, Viollier et al. 2000)) should be used to distinguish Fe phases to determine the extent of oxidation and the remaining nZVI content. Field sampling techniques have prescribed collection and Fe preservation techniques. The first sample will be filtered using a 0.45 μm or 0.2 μm media and the second will be preserved unfiltered. The dissolved species, predominantly ferrous iron will be preserved in the filtered sample, while the unfiltered sample will constitute the total Fe. These methods for quantification of total Fe and dissolved Fe rely on the operational definition of dissolved and solid Fe based on the filter size, however nZVI can pass through such filter sizes, complicating analysis

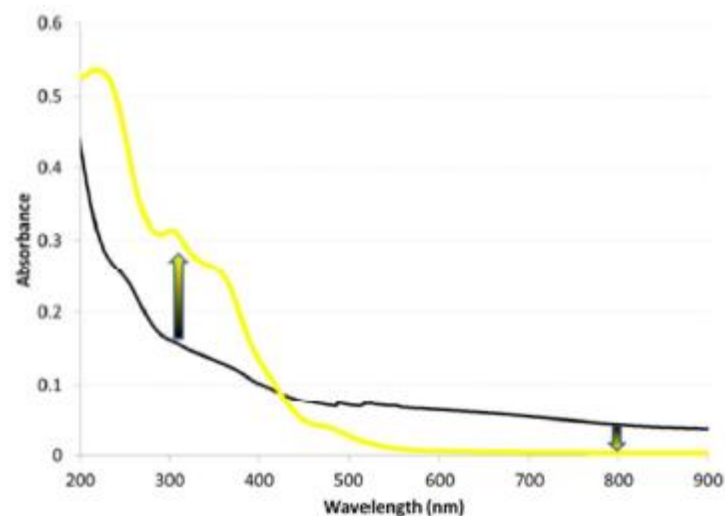


Figure 2.8: UV/Vis spectra of nZVI (black) and oxidized ZVI (yellow), showing the peaks used in two wavelength calibration. (Johnson et al 2013)

Oxidized iron and nZVI can be quantitatively distinguished using UV/vis spectroscopy (Figure 2.8) (Johnson et al. 2013). nZVI is quantified at 800nm and oxidized Fe at 325nm. Use of UV/vis methods can require dilution, complicating analysis.

Scattering methods

Dynamic light scattering (DLS) and measurement of zeta potential are light scattering methods that have been used as bulk particle characterization analyses. Zeta potential is calculated based on the Schmolukowski equation and measurement of the electrophoretic mobility. This technique is a well-established tool in characterizing colloids (Nurmi et al. 2005) and has been extended to nZVI characterization in laboratory experiments (Saleh et al. 2005, Saleh et al. 2007, Phenrat et al. 2008, Tiraferri et al. 2008, Chowdhury et al. 2012, Kocur et al. 2013). DLS has been used to characterize nZVI and other nanoparticles (Nurmi et al. 2005, Saleh et al. 2008, Tiraferri et al. 2008, Tiraferri et al. 2009, Chowdhury et al. 2012, Kocur et al. 2013). These techniques are easy to implement and are transferable to field analysis with little difficulty (Kocur et al. 2014). For polymer coated particles scattering techniques cannot quantify properties of the metallic surface. As such DLS and zeta potential measurements are reported for the apparent surface (Saleh et al. 2008).

Other novel methods for particle charge and size measurement have been employed. Acoustic methods have been used to determine nZVI size distribution and estimation of apparent surface charge (i.e., zeta potential) in a custom made apparatus (Dukhin et al. 2001, Sun et al. 2006). Refractive laser analysis (e.g., nanoparticle tracking analysis, NTA) is a microscopic method capable of calculating zeta potential and particles size for low concentrations of nanoparticles, including nZVI (Raychoudhury et al. 2012, Adeleye et al. 2013, Raychoudhury et al. 2014). NTA tracks single particles using image analysis to calculate the parameters.

Limitations of scattering methods are similar to UV/vis for field methods and dilution is often required. The particle concentrations must be low to allow light transmission, but the suspension must contain sufficient particle counts for measuring particle scattering. DLS analysis yield erroneously small hydrodynamic diameters when concentration is too high due to scattering of light off of multiple particles. The limitations of NTA have not been tested in a field setting. For all optical techniques application to field samples requires a careful sampling procedure to minimize the presence of sediment, silt or clay in samples. A sampling program that facilitates low flow sampling techniques should produce samples suitable for UV/vis and light scattering methods.

Microscopic and energy techniques

Classical light microscopy cannot resolve nanoscale dimensions, thus the techniques in this section focus on electron emission and x-ray microscopy. The characterization tools summarized in this section, provided in Table 2.4, have been used for characterization of nZVI in laboratory experiments. The methods also lend themselves to field studies to a limited degree as care must be taken in sampling and interpretation can become more difficult as the field matrix is more complex than that present in lab samples.

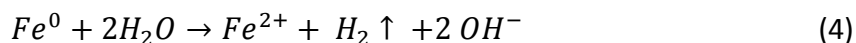
Table 2.4: Analytical electron spectroscopic and x-ray tools for characterizing nZVI

Technique		Analysis	Reference
TEM	Transmission electron microscopy	Size and Morphology detection by phase-contrast focusing	(Schrack et al. 2004, Sakulchaicharoen et al. 2010, Kocur et al. 2014)
SEM	Scanning electron microscopy	Topography of larger sample area	(Wei et al. 2010)
STEM	Scanning transmission electron microscopy	Size, morphology, topology Narrow beam transmission	(Chang et al. 2009, Yan et al. 2010)
EDS	Energy dispersive x-ray spectroscopy	Elemental composition using scanning x-ray	(Sun et al. 2006, Sun et al. 2008, Chang et al. 2009, Yan et al. 2010, Kocur et al. 2014)
XRD	X-ray diffraction	Identification of crystalline structure in nanoparticle	(Nurmi et al. 2005, Sun et al. 2006, Sun et al. 2008)
XPS	X-ray photospectroscopy	Surficial elemental composition	(Nurmi et al. 2005, Li et al. 2007)

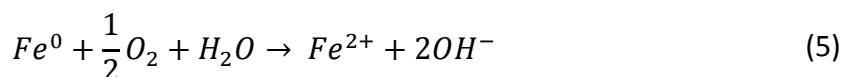
EXAFS/ XANES	Extended x-ray absorption spectroscopy / X-ray absorption near edge structure spectroscopy	Determination of oxidation state of the surface.	(Nurmi et al. 2005, Sun et al. 2006, Li et al. 2007, Reinsch et al. 2010)
-----------------	--	--	---

2.5 Geochemical methods

There are no standard method for reporting results and although successful application has been reported in several cases the metrics of success are unclear. ORP has commonly been reported in field studies investigating nZVI transport (Elliott et al. 2001, Henn 2006). The determination of low ORP may not immediately point to effective transport in the subsurface, rather it provides evidence that nZVI is in the vicinity and has been oxidized by water following equation 4.



A pH change in the system can occur due to equation 4 along with the reaction of nZVI with dissolved oxygen.



pH and ORP have been used as an indicator of nZVI mobility (Henn 2006, He et al. 2010, Wei et al. 2010, Kocur et al. 2014). This should be used with caution as reducing conditions (less than -50 mV) may not necessarily indicate reductive dechlorination (Bennett et al. 2010), especially given that ORP readings are prone to error. Shi et al, in several studies have investigated uses of ORP probes that lead to poor measurements of redox potential. For example nZVI particles can attach to the probe yielding low ORP (Shi et al. 2011, Shi et al. 2015). Given this rotating disk electrodes have been proposed in place of stationary electrodes for measurement of redox couples that are associated with nZVI formulations.

Screening methods for the determination of the natural reductant demand on site are limited. ORP provides a measurement of the geochemical conditions on site during site investigation, however the measurement does not estimate the capacity of reducing species. For example, the use of nZVI has been called into question where high levels of nitrates in the

groundwater persist as the (hydr)oxide surface of nZVI can become passivated (Reinsch et al. 2010), thus nitrates should be pre-screened prior to nZVI use. Geochemical characterization during site investigation has been proposed using assays for chemical reductant demand (Tratnyek 2014). Such a technique is available for in situ chemical oxidant demand (Haselow et al. 2003) and provides a tool for technology selection. Similar reducing demand tools could be built for screening sites for the feasibility of nZVI application. Such standard methodology would systematically evaluate compatibility issues.

2.6 Determining Fe⁰ content

Determining and distinguishing all phases of Fe can be difficult. In an environmentally relevant system Fe⁰ is rapidly oxidized to Fe²⁺, Fe³⁺ and Fe (hydr)oxides. Qualitative measurements, like TEM, can quantify the core/shell structure of nZVI particles as well as size and shell thickness (Matheson et al. 1994, Wang et al. 1997, Zhang et al. 1997, Schrick et al. 2004, Nurmi et al. 2005). However, other analytical tools summarized above are needed to determine elemental compositions and structure of these surface layers. Groundwater composition impacts the formation of different oxide phases in the shell (e.g., magnetite and maghemite) (Reinsch et al. 2010). Reinsch *et al* (2010) also suggest that the entire ZVI core will become oxidized when dissolved oxygen is present except in cases where high nitrates passivate the surface. Laboratory evaluation allows for investigation of surface layer formation under controlled conditions, however, field applications tend to rely on bulk measurements to determine nZVI reaction potential.

ZVI content can be determined through digestion with acid to completely transform Fe⁰ to Fe²⁺ following equation 4. Analysis of the gas composition evolved from the complete oxidation of iron particles along with stoichiometric calculations, based on knowledge of the total Fe, will yield the Fe⁰ content in the sample. Several methods have been proposed for analysis of hydrogen including gas chromatography (Liu et al. 2005, Liu et al. 2006) as well as gas displacement for large sample volumes.

2.7 Fe⁰ in a complex matrix

Not only does naturally occurring subsurface material need to be considered in the context of measurement interference, the effect on nZVI stability and reaction longevity, nZVI

interactions with porous media also need to be considered. Bench scale tests have provided black-box observations of interaction with clay and fine soils, showing that there is more interaction than with homogeneous glass beads or sands (Schrack et al. 2004, He et al. 2009). Other studies have reported increased interaction with silica surfaces at high ionic strengths (Saleh et al. 2008, He et al. 2009, Phenrat et al. 2010, Laumann et al. 2013). Laboratory transport experiments with natural soils and nZVI retention in field studies suggest a significant portion of the nZVI will become associated with the solid phase in the subsurface. Bennett *et al* (2010) and Kocur *et al* (2014) have suggested that nZVI is not mobile over the long term and under natural flow conditions. This stationary nZVI is not accounted for in aqueous sampling methods, or in many analysis techniques, however this nZVI could still be reactive towards the target contaminant. This suggests that soil surface analysis techniques should be considered to assess the reactive potential of injected nZVI.

2.7.1 Alternative and emerging methods of nZVI determination

Alongside the development of particle characterization and identification techniques discussed in section 7.4.3, there is a need to link these results to continuum scale evaluation techniques (Shi et al. 2015). Remote sensing techniques, sensors and probes are being explored for their utility in linking bulk fluid properties to nZVI delivery and in some cases reaction and oxidation.

Geophysical methods can take advantage of the differential attenuation of electrochemical and electromagnetic properties between the solute or constituent in the plume (e.g., nZVI, NaBr) and the surrounding groundwater. Different media and fluids will have different properties including electrical conductivity and dielectric constants. Complications can arise in implementing geophysical methods as fluid or solid properties can limit use. For example ground penetrating radar (GPR) and electrical resistance tomography (ERT) are best suited to shallow subsurface cases. Shi et al (2015) review several types of geophysical techniques specifically for ZVI applications. Large scale use for ZVI has been limited to verification of PRB placement (Slater et al. 2003) although laboratory studies have been extended to track emplacement and geochemical changes in iron column experiments (Slater et al. 2005, Wu et al. 2005, Wu et al. 2006, Wu et al. 2008, Wu et al. 2009). Geophysical methods have been used to identify nanoparticles in laboratory studies with induced

polarization (Joyce et al. 2012). Induced polarization has been previously established as a tool in PRB column experiments (Slater et al. 2005).

The limitations of resistivity methods and subsurface tomography are associated with the proximity of measurements to the targeted ZVI (Shi et al. 2015). Thus, chemical threshold indicators for isolating specific redox couples have been proposed as a complementary method for sensing nZVI distribution and oxidation (Jones et al. 2001, Tratnyek et al. 2001, Jones et al. 2005). The use of specific redox couples as indicators in reactive chemical probes can differentiate target reducing species by color (e.g., Resazurine indicator in batch tests with iron filings) (Tratnyek et al. 2001). These reactive redox couples have potential to determine the specific redox state of the injected amendment. This provides an advantage over some redox electrodes, as static electrodes have can result in erroneously low ORP measurements. The effective use of redox electrodes has been explored in laboratory studies (Shi et al. 2011, Su et al. 2014).

Magnetic susceptibility has also recently been studied as a means of remote geophysical detection of ZVI (Vecchia et al. 2009, Buchau et al. 2010, Köber et al. 2014). Viacchia et al 2009, quantified ZVI mass using magnetic resonance in column experiments. A field study by Kober et al (2014) characterized soil cores following the injection of nanoscale/microscale iron filings with a magnetic susceptibility coil developed to delineate total Fe⁰ deposited in the subsurface. The study was able to determine the distribution of iron filings at a resolution of <10cm along soil cores. Similar technique has also been demonstrated for ZVI fracture injection profiling (Arnason et al. 2014). Bachau et al (2010) developed inductive coils as remote sensors for the in situ detection of ZVI. The planned emplacement of the coils prior to subsurface injection provided quantitative evaluation of ZVI migration. Single particle inductively coupled plasma mass spectroscopy techniques have also been developed with the potential of evaluating nanoparticles (e.g., nZVI in environmental samples) (Lee et al. 2014). A combination of techniques may provide a clearer conceptual model of nZVI transport, deposition, and reaction in the subsurface.

2.7.2 Modelling field scale nZVI transport

Accurate prediction of nZVI transport in porous media relies on many important parameters and a process level understanding of complex interconnected physical and chemical

mechanisms governing transport. To date, there has not been a comprehensive nZVI model that incorporates every aspect of delivery, contaminant interaction, and degradation, however, models are currently available that capture many of the important physical and chemical processes that occur.

Laboratory studies have investigated the transport of nZVI in column studies, and in 2-D sand boxes. Many of these studies used colloid filtration theory to predict retention of particles in porous media. Colloid filtration theory (CFT) was originally developed to predict colloid retention in water systems (Yao et al. 1971), but has been extended to include a broad range of colloid-collector conditions (Bai et al. 1996, Bai et al. 1999, Tufenkji et al. 2004) including nZVI transport experiments (Saleh et al. 2008, He et al. 2009, Johnson et al. 2009, Phenrat et al. 2009, Tiraferri et al. 2009). Care must be taken applying these models to field conditions as the conditions used for model verification can be different than those in the field.

For example CFT assumes particle stability however nZVI particles are prone to aggregation. Some have included aggregation and aggregate settling through an empirical correlation (Phenrat et al. 2010) or through the manipulation of the already widely adopted predictive physiochemical estimation of colloid interaction forces to include inter-particle interaction (Petosa et al. 2010). Stabilizers that inhibit particle-particle interaction, however, allow for extension of CFT to polymer/nZVI systems because stable aggregates are formed (Baalousha 2009, Kocur et al. 2013). Kocur *et al* (2013) showed that inclusion of aggregation and sedimentation along with CFT yields good prediction of nZVI transport behavior. Other mathematical formulations have been suggested including general nanoparticle aggregation (Chatterjee et al. 2009), and other retention mechanisms (e.g., straining and blocking) (Tosco et al. 2010, Köber et al. 2014). These colloid retention mechanisms have been proposed to be operable in nZVI systems (Raychoudhury et al. 2014).

Other modelling approaches include simulation of the bulk movement of the fluid containing the nanoparticles. This is particularly useful in the design of nZVI delivery systems. For example consideration of the density of an nZVI suspension in SEAWAT yielded good predictions of the plunging behavior observed in 2-D sandbox experiments in homogeneous porous media (Kanel et al. 2008). Analogs of heterogeneous porous media have been investigated in small-scale 2-D experiments (Phenrat et al. 2010, Phenrat et al. 2011) and at

the pilot scale in a packed aquifer model (Johnson et al. 2013). Phenrat et al (2010) showed that a predictive model could capture nZVI transport in a 2-D sand box. Modelling the interaction and reaction of nZVI with contaminants has been limited as few studies consider mass transfer or reaction. Phenrat et al (2011) modelled the interaction of nZVI and PCE in laboratory experiments (Fagerlund et al. 2012) showing the improved interaction of TCE and nZVI that functionalized polymer coatings. nZVI transport experiments through 1-D columns at residual PCE saturation were used to validate a 1-D reactive transport model (Taghavy et al. 2010). Using a sensitivity analysis Taghavy et al (2010) investigated the contact time required to achieve PCE degradation to ethene. These types of simulations aid in the design and testing of remediation strategies prior to implementation.

2.8 Evaluating degradation

Numerous contaminants can be degraded through chemical reduction with nZVI. The degradation of these contaminants has been well documented and many good reviews have been published (Li et al. 2006, Karn 2009, Mueller et al. 2012, O'Carroll et al. 2013, Tratnyek 2014). The most prevalent contaminants in field studies have historically been chlorinated ethenes, ethanes, and methanes as these make up the widest group of persistent contaminants worldwide. Chlorinated ethenes have been the focus of many of the early field studies that used unstabilized nZVI (Elliott et al. 2001, Glazier et al. 2003, Gavaskar 2005, Mace 2006). As polymers emerged as a superior delivery vehicle the first field tests primarily involved chlorinated ethenes (Gavaskar 2005, Henn 2006, Bennett et al. 2010, He et al. 2010). Chlorinated ethane and sites with lesser chlorinated ethene have been investigated more recently in the field (Wei et al. 2010) and mZVI (Truex et al. 2011, Köber et al. 2014, Velimirovic et al. 2014, Luna et al. 2015).

2.8.1 Reactivity in closed systems

Closed batch systems are ideal for feasibility studies investigating chlorinated solvent degradation using nZVI. Batch experiment studies have been able to provide first order kinetic constants for numerous contaminants (Arnold et al. 2000, Song et al. 2005). These experiments are useful in that they provide estimates of the theoretical maximum reaction rate

of nZVI with target contaminants. The rate constant k_{obs} can be quantified by fitting the first order decay of contaminants as demonstrated in figure 2.9:

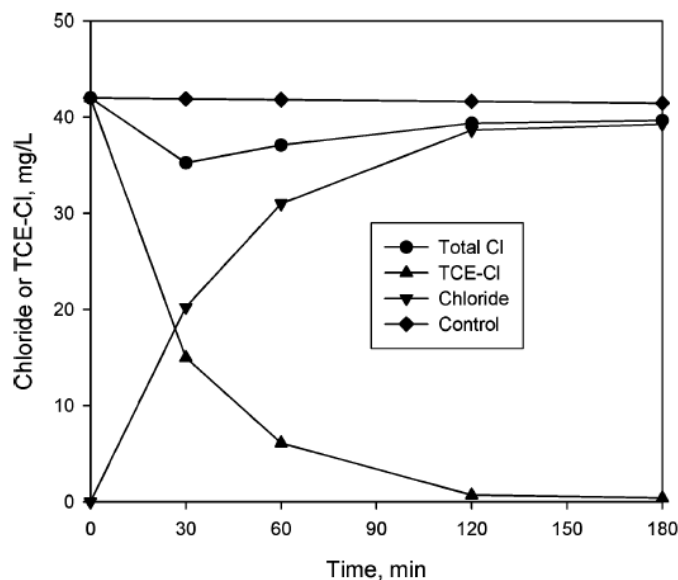


Figure 2.9: First order decay of TCE with nZVI (modified from He ES&T 2005).

$$C = C_0 e^{-k_{obs}t} \quad (6)$$

Where C_0 and C are the concentrations of cVOCs initially and after time t .

These results are often reported as a normalized rate constant k_{SA} ,

$$k_{obs} = k_{SA} a_s \rho_m \quad (7)$$

Where ρ_m is the mass concentration of nZVI, and a_s is the specific surface area of the particles.

Such batch experiments have some limitations including ideal mixing of reactants. The availability of electrons in nZVI is inherent in equation 7, however, it has been shown that reaction with nZVI is second order because of the reduction of Fe^0 mass with time (Taghavy et al. 2010). This is an important consideration that is often overlooked, and may change the mechanisms of reaction (Liu et al. 2005)

2.8.2 Pathways of degradation

The study of closed systems and mass balance analysis allows for the determination of degradation pathways. Figure 2.10 shows the pathways of degradation for nZVI for chlorinated methanes, ethanes, and ethenes (Arnold et al. 2000, Liu et al. 2005, Song et al. 2005, Song et al. 2008). The progressive degradation along the pathways in Figure 2.10 provides evidence of contaminant degradation on site.

- **Hydrogenolysis** is a relatively slow reaction involving the replacement of one chloride atom on the compound with one hydrogen (Eykholt et al. 1998, Arnold et al. 2000). This requires donation of electrons and hydrogen. (e.g., TCE degradation to cis-1,2 DCE) .
- **Beta-Elimination** is the dominant reaction pathway releasing chloride atoms while saturating a carbon-carbon bond (Arnold et al. 2000). This requires a surface and electrons (e.g., TCE degradation to chloro-acetylene)
- **Alpha elimination** is a dechlorination reaction removing two chloride atoms from a single carbon in the compound (e.g., degradation from 1,1 DCA to ethane).
- **Hydrogenation and hydrolysis** are rapid pathways that involve water. These mechanisms occur mainly with unstable daughter compounds formed via other reactions. (e.g., the breakdown of acetylene to ethene)

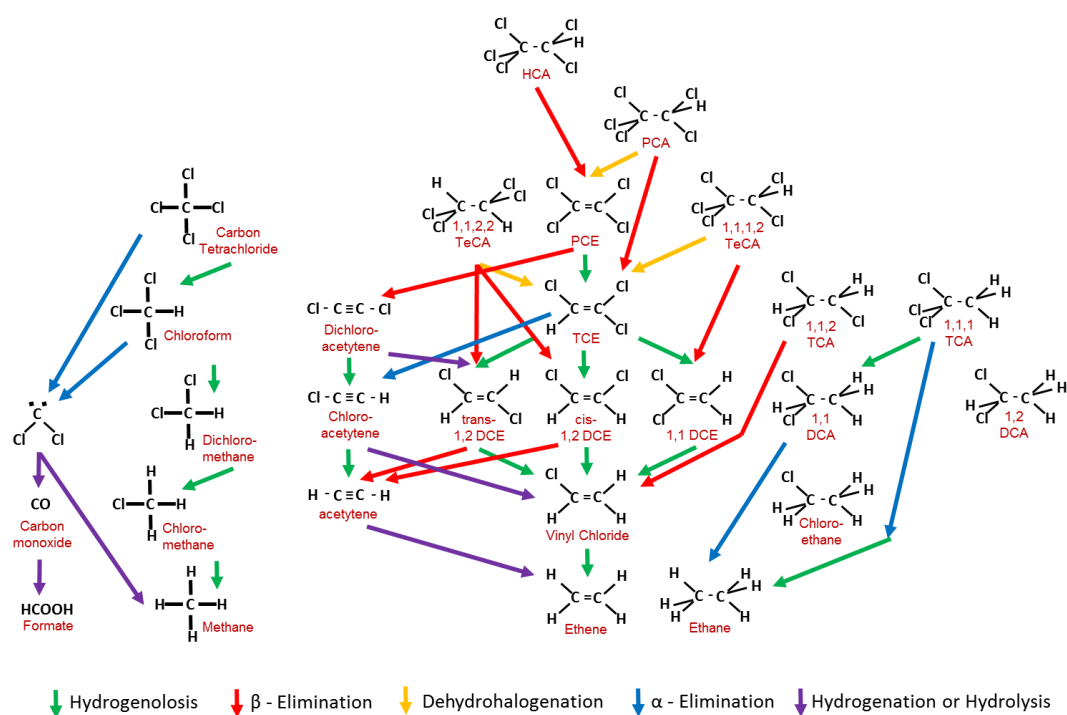


Figure 2.10: Reductive dechlorination pathways of chlorinated methanes, ethanes, and ethenes. (Modified from Song and Carraway 2005, Arnold and Roberts 2000, Tratnyek et al 2014)

The most common degradation pathway in nZVI studies is β -elimination, however, it has been reported that for granular ZVI, up to 10% by mole undergoes a less efficient hydrogenolysis reaction (Gillham et al. 1994). This can create buildup of degradation byproduct (Gillham 2010). ZVI has typically been reported to preferably degrade compounds with higher degrees of chlorination (e.g. k_{obs} for PCE>TCE>cDCE>VC) (Gillham et al. 1994, Johnson et al. 1996, Liang et al. 1997). For nZVI, the opposite reaction order has been observed (e.g. k_{obs} for VC > cDCE > TCE > PCE) (Arnold et al. 2000, Song et al. 2005). nZVI has a large surface area to mass ratio which allows rapid transfer of electrons across a relatively thin oxide shell increasing reaction rate. Studies have shown that adding a catalyst facilitates rapid electron transfer to the surface with k_{obs} for VC>cDCE>TCE>PCE due to involvement of hydrogen as the reductant (Song et al. 2008).

A potential concern is that polymer coated nZVI exhibits decreased reactivity as reactive sites are blocked because of surface coverage (He et al. 2008). The polymer creates a

barrier to the diffusive flux of contaminants to the surface along with reaction products from the surface, which contributes to the lower reactivity (Phenrat et al. 2009, Wang et al. 2010).

2.8.3 Considerations for field applications

Interpretation of field data requires a validated conceptual model. This includes knowledge of the contribution of natural reductant demand and additional metals or contaminants that may interfere with target contaminant degradation. Byproducts may build up due to competition for reactive sites when high cVOC concentrations are present on site or in multi-component systems (Arnold et al. 2000). Byproducts may also already be present on site due to microbially mediated degradation.

Dose

The appropriate nZVI dose for a given level of contamination on a per soil volume unit basis has not been systematically studied. Vendors and practitioners may have rules of thumb for specific cases, however, an appropriate dose is likely site specific, as no two scenarios are identical. Fe/soil ratio of 0.004 or 4 g/ kg of soil has been used as a qualitative threshold to achieve low ORP (e.g. -400 mV) throughout a treatment area (Gavaskar 2005). This estimated loading of Fe⁰ has not significantly changed since initial PRB installations (Cantrell et al. 1995) although some granular PRB loadings can be as high as 10-22% wt of soil (Gillham 2010). PRB operation at a loading of 0.4 % Fe⁰ has been estimated to be sufficient to last for several decades if this loading has been delivered in columns (Kaplan et al. 1996, Cantrell et al. 1997). In-situ soil mixing applications target Fe loadings between 0.5-2% (Tratnyek 2014).

Delivery

There is concern that nZVI and mZVI cannot be delivered at the required dose to treat in-situ source zones. Gavaskar *et al* (2005) commented that Fe/soil ratios associated with soil mixing and PRB applications in the literature were not attainable via injection methods. This is based on the limited success in early field studies prior to the development of polymer coatings. Considering that many pilot injections involve nZVI at a dose of 0.3-1 g/L there may be a need for multiple injections. There have been significant advances in the delivery of mZVI and nZVI (Quinn et al. 2005, O'Hara et al. 2006, Truex et al. 2011, Truex et al. 2011, Su et al. 2012, Köber et al. 2014, Luna et al. 2015). The addition of a stabilizer has the added advantage

of allowing more time for delivery than with an unstable slurry (Kocur et al. 2013) and the ability to stabilize high concentrations of nZVI (Comba et al. 2009). Improved stability leads to better mobility as discussed previously (Saleh et al. 2008, He et al. 2009, Phenrat et al. 2009, Kocur et al. 2013). This provides the opportunity to inject more nZVI mass initially, either through multiple injections, or with a more concentrated slurry. Methods of injecting amendments into the ground have been developed, however, methods of evaluating and accurately analyzing the delivery and performance are not as developed.

Analytical difficulties with polymers

The interaction of polymers with subsurface materials can interfere with some analysis. The solubility of solvents is affected when a polymer is present (Phenrat et al. 2009), which makes closure of mass balance difficult, even in a closed system. No studies have rigorously investigated cVOC reaction pathways in polymer systems. Additional uncertainties are introduced when polymer breakdown products that interact with cVOCs create more complex mixtures with unknown sorption properties. The separation of nZVI, cVOC, and organic content in samples also becomes more difficult with stable nanoparticles. There is work to be done to establish a mechanistic understanding of nZVI and polymer interaction with cVOCs.

Longevity

Depending on the mass of Fe^0 that is injected loss of electron donors prior to contaminant mass destruction will lead to a rebound in contaminant concentrations. This is commonly reported in early field studies with nZVI where between 80-99% reduction in VOC concentrations within the vicinity of injection wells was observed but was followed by rebound several months later (Mace 2006). This is caused by the return of contaminated pore water that is pushed out of the test area by the injection process (Bennett et al. 2010). In these cases it is likely that dilution of the injection mixture will cause the oxidation of nZVI with dissolved oxygen and water following equations 4 and 5, causing Fe^0 mass consumption. It has been suggested that nZVI injection is best utilized for stationary phase contamination (Bennett 2010). Estimates of reaction longevity vary and depend on subsurface conditions. Batch studies have determined that nZVI is reactive for months, but only reactive in sediment aqueous mixtures for about one month (Adeleye et al. 2013). In situ reaction longevity, however, has

yet to be fully explored. Contaminant interaction and degradation with deposited nZVI is not well studied and remains an open question.

Site screening using laboratory tests

Prior to the implementation of nZVI at a field site subsurface conditions can be evaluated for nZVI compatibility. Batch tests can be designed to evaluate the feasibility of nZVI with site specific contaminants. Geochemical parameters are a good starting point as nZVI will work best in a reducing environment, with a neutral or slightly basic pH. Quantifying the natural reductant demand and simple estimates of contaminant mass distribution in the subsurface can be used for technology selection. Batch tests can evaluate the need for pretreatment or the addition of a catalyst. These batch tests can also guide monitoring protocol and methods as well as nZVI dose. The nZVI formulation can be tested in laboratory column tests in model media or site media to determine mobility. The slurry can be injected using several different methods to determine the best method of delivery or to screen contractors with different equipment. Considering the inevitable need for some polishing treatment prior to site closure, the site groundwater can be screened to determine the impact to microbial species.

2.8.4 Monitoring VOCs in the Field

Aqueous sampling methods are commonly adopted for monitoring nZVI remediation. This is especially true when regulatory site closure is based on aqueous criteria. Highly contaminated sites may require analysis of soils to evaluate sorbed or free phase contaminant mass.

Concentration-based sampling methods have been problematic in nZVI field studies in the past. Injection of an amendment inherently pushes contaminants in the aqueous phase out of the treatment area. Thus, VOC concentrations decline, especially in injection wells, and may be the result of replacing pore fluid with injected fluid (Gavaskar 2005). A rebound in cVOC concentrations can be due to groundwater flow that carries aqueous contaminants back into the treated area. Early studies and some ongoing studies inaccurately associate dilute cVOC samples in injection wells to nZVI treatment without accounting for the dilution in the well and the fact that the injected fluid is being sampled (Němeček et al. 2014).

Quantification of target contaminant degradation can be used as evidence of nZVI performance. Field application of polymer stabilized nZVI was demonstrated to be effective by monitoring a suite of cVOCs showing that the aqueous cVOC degraded over time (Henn 2006). Quinn *et al* (2005) showed high TCE removal efficiencies following EZVI treatment by monitoring soil VOCs. He *et al* (2010) monitored VOCs over a two year period, reporting degradation for longer than expected due to the onset of microbially mediated degradation. Long term NAPL mass reduction due to treatment with nZVI in an emulsion of vegetable oil was reported and accredited to microbial processes (Su et al. 2012).

2.9 Lessons learned from nZVI field applications

2.9.1 Occupational health and safety considerations

Handling nZVI in the field

There are precautions that should be taken when handling nZVI, or other reactive particles. These precautions and the risk associated with the work stems from the novelty of the technology and the unknown repercussions of exposure to these substances. Toxicologists have not yet had sufficient time to fully characterize the effects of nZVI on human and ecosystem health, although there is some indication that nZVI can have toxic effects (Keenan et al. 2009). Dermal and respiratory protection should be employed on site when there is potential exposure to nZVI.

nZVI may come to the field site in one of several forms: raw materials may be delivered for on-site synthesis; slurry may arrive in containers ready for injection; or dry powders may be supplied for mixing of the slurry on site. Regardless of the form in which nZVI is supplied, appropriate protection should be taken.

Rapid oxidation of dry ZVI

ZVI can oxidize rapidly in the presence of oxygen. The increased surface area associated with small particles sizes allows this process to occur spontaneously, creating

flames and sparks. This can be of particular concern for bare nZVI that has been shipped in an inert atmosphere. Large quantities of slurry that have dried may also be subject to rapid oxidation (Figure 2.11). Slurry that is preserved in ethanol or another solvent should be handled according to the Material Safety Data Sheets. In all cases, the supplier or vendor should provide information on handling in order to maintain quality and also instruction on safe handling of the material.

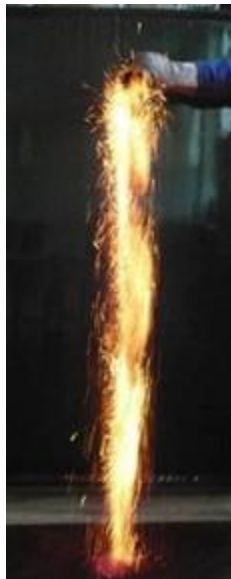
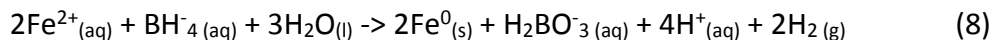


Figure 2.11: Photo of nZVI rapidly oxidizing as it is poured out of a beaker
(www.nanoiron.cz)

Mitigating hydrogen emission during nZVI synthesis

The synthesis of nZVI using chemical precipitation requires a strong reductant. The reaction below involves the reduction of dissolved ferrous iron with a reducing agent, sodium borohydride (NaBH_4), forming solid ZVI particles in aqueous solution:



The hydrogen that is off-gassed from this reaction should be managed and monitored during the synthesis process. A gas meter can be used to monitor the hydrogen and oxygen in the working zones. Hydrogen will be generated during the preparation of NaBH_4 in the chemical handling area and during the reduction of Fe^{2+} to Fe^0 in the reaction vessel. Air monitoring in these areas, as well as at the perimeter of an out-gas emission area, during

chemical handling and reaction will ensure that hydrogen levels satisfy safe working conditions and is well under the Lower Explosive Limit (LEL) (4% of total gas for Hydrogen). All sources of ignition (e.g. lighters, cell phones, smoking, electrical equipment that sparks, heat, generators, vehicle engines, etc.) and flammable materials (e.g. flammable solvents, flammable clothes, paper) should be removed from the working zones and kept at a safe distance.

2.9.2 nZVI performance evaluation

A growing number of field tests have been performed and summaries of many of these injections are available. In Europe alone, more than 15 pilot and full scale injections have taken place (Mueller et al. 2012). As discussed in this chapter, a number of effective methods have been developed for delivering different formulations and types of nZVI. Unfortunately the rigorous methods that are essential for the evaluation of nZVI technology has not evolved at the same pace. Often field injections assume that successful injection and delivery to the subsurface is enough to remediate the site, however, several decades ago, performance of in-situ chemical oxidants was evaluated in a similar manner. At many sites where oxidants were used concentrations rebounded to pre-treatment concentrations in relatively short periods of time. Methods of site characterization have improved since this time. Performance evaluation of the mobility and in-situ degradation of nZVI is just as important as optimizing the injection and delivery of nZVI, necessitating the development of more rigorous monitoring methods.

2.9.3 Coupling technologies with nZVI

According to the environmental security technology certification program (ESTCP) the most widely used remediation technologies are thermal, enhanced bioremediation, monitored natural attenuation, and in-situ chemical oxidation. These technologies can be reliably employed for the cleanup of contaminated sites along with many other technological alternatives that have been around for longer than chemical reduction using nZVI. However, nZVI has many important benefits and can be used in the treatment train coupled with many of these technologies.

Source removal approaches that treat highly NAPL-saturated media (e.g., Thermal treatment or flushing technologies) would precede nZVI injection in a treatment train. NAPL source removal by flushing, solvent extraction, and hot water flushing may represent

opportunities for coupled use with nZVI injection. Flushing techniques work well for NAPL pools and higher-residual NAPL, but less well with lower-residual and sorbed contaminants. The infrastructure that would be used for solvent flushing would be similar to nZVI injection wells leading to cost savings as installed wells can be used for both purposes. Another example of sequential treatment was investigated by coupling nZVI and electrical resistive heating (ERH). In order to increase contaminant interaction with nZVI by increasing the mass flux from NAPL residual, in situ ERH has been pilot tested as a coupled technology with nZVI (Truex et al. 2011). nZVI application would degrade contaminants that were not removed during flooding or heating.

Sequential treatment using monitored natural attenuation may also couple with nZVI application in a treatment train. nZVI that is deposited in the subsurface will oxidize to Fe^{2+} and furthermore to Fe^{3+} species serving as an electron donor. This approach has been demonstrated to degrade low levels of aqueous contaminants as they flow through the reduced media (i.e., insitu redox manipulation) (Szecsody et al. 2004). Such a technique can also immobilize contaminant metals (Cantrell et al. 1995, Li et al. 2007, O'Carroll et al. 2013).

Enhanced bioremediation by organohalide-respiring microorganisms has the most potential when coupled with nZVI application. The reducing conditions created as a result of the oxidation of nZVI and the hydrogen that is produced eliminates any significant acclimatization period required for bioremediation. Unintended microbially mediated degradation has been observed following nZVI/CMC injection (He et al. 2010). ZVI emulsified in vegetable oil has also shown to abiotically degrade PCE and TCE, while biodegradation products (e.g., Methane and volatile fatty acids) increased over a 2 year period, suggesting microbially mediated degradation was stimulated (Su et al. 2012).

Laboratory studies have shown that naturally occurring microorganisms will utilize the cathodically produced hydrogen in anaerobic systems. Increased microbial degradation has been attributed to abiotic redox and electron donor processes derived from nZVI oxidation in water (Lampron et al. 1998, Lampron et al. 2001, Fernandez-Sanchez et al. 2004, Jeon et al. 2013). This has led to number of studies investigating the effects of nZVI on microorganisms. Stimulation of bioactivity by ZVI was noted in microcosms evaluating PRB performance (Lampron et al. 1998, Lampron et al. 2001, Fernandez-Sanchez et al. 2004) and in enriched

cultures isolating *dehalobacter* in the degradation of carbon tetrachloride (Lee et al. 2015), *Dehalococcoides* in the degradation of chlorinated ethenes (Rosenthal et al. 2004) and the degradation of chlorobenzenes (Rosenthal et al. 2004, Zhu et al. 2012, Zhu et al. 2013). General dehydrogenase activity was enhanced in soil activity tests with nZVI (Cullen et al. 2011) in addition to upregulation of reductive dehydrogenases genes, *tceA* and *vcrA* (Xiu et al. 2010) in microcosms.

Many of these studies are limited as they evaluate single organisms or evaluate single organism functions. However, they are important in the development of remediation biomarkers. Specific studies have noted that enhanced microbial activity is aided by the polymer coating that stabilizes the nanoparticles (Zhou et al. 2014) while others have suggested that the polymer screens the organism from harmful oxidative stress (Li et al. 2010, Xiu et al. 2010). It has also been reported that this biostimulation occurs only after a lag period (Xiu et al. 2010). These remediation focused papers are accompanied by numerous toxicity studies focused on evaluating the oxidative stress and negative impacts of nZVI on bacteria (Jiang et al. 2013), aquatic organisms (Li et al. 2009), soils organisms (Pawlett et al. 2013, Saccà et al. 2014), and mammalian cells (Phenrat et al. 2009), and human cells (Sun et al. 2011).

Fewer studies have taken a focus on the effects of nZVI on microbial community. Kirschling *et al* (2010) observed changes in Eubacteria diversity in aquifer media microcosms but no change in abundance was observed due to exposure to nZVI. Barnes *et al* (2010) studied aquifer derived microbial microcosms, finding that nZVI inhibited chlorinated ethene degradation. Zaa et al (2010) comprehensively characterized the organohalide respiring microorganisms in a chlorinated ethene plume undergoing natural attenuation. The most rigorous community focused analysis was reported in soil mixing mesocosms experiments evaluating pesticide degradation resulting in shifting microbial communities in real soil (Tilston et al. 2013). These studies provide a step forward, evaluating field relevant soils and groundwater in their laboratory studies. However, it is difficult to replicate field relevant exposure conditions on microbial communities in microcosms.

2.10 References

- Abriola, L. R., A., Pennell, K. (2011). Final Report: Development and Optimization of Targeted Nanoscale Iron Delivery Methods for Treatment of NAPL Source Zones. Strategic Environmental Research and Development Program, Tufts University.
- Acar, Y. B. and A. N. Alshawabkeh (1993). "Principles of electrokinetic remediation." Environmental Science & Technology **27**(13): 2638-2647.
- Adeleye, A., A. Keller, R. Miller and H. Lenihan (2013). "Persistence of commercial nanoscaled zero-valent iron (nZVI) and by-products." Journal of Nanoparticle Research **15**(1): 1-18.
- Annable, M. D., J. W. Jawitz, P. S. C. Rao, D. P. Dai, H. Kim and A. L. Wood (1998). "Field evaluation of interfacial and partitioning tracers for characterization of effective NAPL-water contact areas." Ground Water **36**(3): 495-502.
- Arnason, J. G., M. Harkness and B. Butler-Veytia (2014). "Evaluating the Subsurface Distribution of Zero-Valent Iron Using Magnetic Susceptibility." Groundwater Monitoring & Remediation **34**(2): 96-106.
- Arnold, W. A. and A. L. Roberts (2000). "Pathways and Kinetics of Chlorinated Ethylene and Chlorinated Acetylene Reaction with Fe(0) Particles." Environmental Science & Technology **34**(9): 1794-1805.
- Baalousha, M. (2009). "Aggregation and disaggregation of iron oxide nanoparticles: Influence of particle concentration, pH and natural organic matter." Science of the Total Environment **407**(6): 2093-2101.
- Bai, R. and C. Tien (1996). "A New Correlation for the Initial Filter Coefficient under Unfavorable Surface Interactions." Journal of Colloid and Interface Science **179**(2): 631-634.
- Bai, R. and C. Tien (1999). "Particle Deposition under Unfavorable Surface Interactions." Journal of Colloid and Interface Science **218**(2): 488-499.

Bennett, P., F. He, D. Zhao, B. Aiken and L. Feldman (2010). "In Situ Testing of Metallic Iron Nanoparticle Mobility and Reactivity in a Shallow Granular Aquifer." Journal of Contaminant Hydrology **116**(1-4): 35-46.

Benson, R. C. (2005). Remote Sensing and Geophysical Methods for Evaluation of Subsurface Conditions. Practical Handbook of Environmental Site Characterization and Ground-Water Monitoring, Second Edition, CRC Press: 249-295.

Berge, N. D. and C. A. Ramsburg (2009). "Oil-in-Water Emulsions for Encapsulated Delivery of Reactive Iron Particles." Environmental Science & Technology **43**(13): 5060-5066.

Buchau, A., W. M. Rucker, C. V. De Boer and N. Klaas (2010). "Inductive detection and concentration measurement of nano sized zero valent iron in the subsurface." IET Science, Measurement and Technology **4**(6): 289-297.

Butler, J. J. (1997). The Design, Performance, and Analysis of Slug Tests, Taylor & Francis.

Cantrell, K. J., D. I. Kaplan and T. J. Gilmore (1997). "Injection of colloidal Fe-0 particles in sand with shear-thinning fluids." Journal of Environmental Engineering-Asce **123**(8): 786-791.

Cantrell, K. J., D. I. Kaplan and T. J. Gilmore (1997). "Injection of colloidal size particles of Fe0 in porous media with shear thinning fluids as a method to emplace a permeable reactive zone." Land Contamination and Reclamation **5**(3): 253-257.

Cantrell, K. J., D. I. Kaplan and T. W. Wietsma (1995). "Zero-valent iron for the in situ remediation of selected metals in groundwater." Journal of Hazardous Materials **42**(2): 201-212.

Chang, M. C. and H. Y. Kang (2009). "Remediation of pyrene-contaminated soil by synthesized nanoscale zero-valent iron particles." Journal of Environmental Science and Health, Part A **44**(6): 576-582.

Chatterjee, J. and S. K. Gupta (2009). "An Agglomeration-Based Model for Colloid Filtration." Environmental Science & Technology **43**(10): 3694.

- Chowdhury, A. I. A., D. M. O'Carroll, Y. Xu and B. E. Sleep (2012). "Electrophoresis enhanced transport of nano-scale zero valent iron." Advances in Water Resources **40**(0): 71-82.
- Comba, S., D. Dalmazzo, E. Santagata and R. Sethi (2012). "Rheological characterization of xanthan suspensions of nanoscale iron for injection in porous media." Journal of Hazardous Materials **185**(2-3): 598-605.
- Comba, S. and R. Sethi (2009). "Stabilization of highly concentrated suspensions of iron nanoparticles using shear-thinning gels of xanthan gum." Water Research **43**(15): 3717-3726.
- Cullen, L. G., E. L. Tilston, G. R. Mitchell, C. D. Collins and L. J. Shaw (2011). "Assessing the impact of nano- and micro-scale zerovalent iron particles on soil microbial activities: Particle reactivity interferes with assay conditions and interpretation of genuine microbial effects." Chemosphere **82**(11): 1675-1682.
- Dukhin, A. S., P. J. Goetz and S. Truesdail (2001). "Titration of concentrated dispersions using electroacoustic ζ -potential probe." Langmuir **17**(4): 964-968.
- Einarson, M. (2005). Multilevel Ground-Water Monitoring. Practical Handbook of Environmental Site Characterization and Ground-Water Monitoring, Second Edition, CRC Press: 807-848.
- Elliott, D. W. and W.-x. Zhang (2001). "Field Assessment of Nanoscale Bimetallic Particles for Groundwater Treatment." Environmental Science & Technology **35**(24): 4922-4926.
- Eykholt, G. R. and D. T. Davenport (1998). "Dechlorination of the Chloroacetanilide Herbicides Alachlor and Metolachlor by Iron Metal." Environmental Science & Technology **32**(10): 1482-1487.
- Fagerlund, F., T. H. Illangasekare, T. Phenrat, H. J. Kim and G. V. Lowry (2012). "PCE dissolution and simultaneous dechlorination by nanoscale zero-valent iron particles in a DNAPL source zone." Journal of Contaminant Hydrology **131**(1-4): 9-28.

Fernandez-Sanchez, J. M., E. J. Sawvel and P. J. J. Alvarez (2004). "Effect of Fe₀ quantity on the efficiency of integrated microbial-Fe₀ treatment processes." Chemosphere **54**(7): 823-829.

Fetter, C. W. (2001). Applied Hydrogeology. Upper Saddle River, NJ, Prentice-Hall, Inc.

Gavaskar, A., Tatar L., Condit W., (2005). Contract Report: Cost and Performance Report: nanoscale zerovalent iron technologies for source remediation. Port Huenema, CA, NAVFAC: Naval Facilities Engineering Command. **CR-05-007-ENV**.

Gillham, R., Vogan, J., Gui, L., Duchene, M., Son, J., (2010). Iron Barrier Walls for Chlorinated Solvent Remediation. In Situ Remediation of Chlorinated Solvent Plumes. H. F. Stroo, Ward, C.H.,. New York, Springer Science Media: 537-571.

Gillham, R. W. and S. F. O'Hannesin (1994). "Enhanced Degradation of Halogenated Aliphatics by Zero-Valent Iron." Ground Water **32**(6): 958-967.

Glazier, R., R. Venkatakrishnan, F. Gheorghiu, L. Walata, R. Nash and Z. Wei-xian (2003). "Nanotechnology Takes Root." Civil Engineering (08857024) **73**(5): 64.

Haselow, J. S., R. L. Siegrist, M. Crimi and T. Jarosch (2003). "Estimating the total oxidant demand for in situ chemical oxidation design." Remediation Journal **13**(4): 5-16.

He, F., M. Zhang, T. Qian and D. Zhao (2009). "Transport of carboxymethyl cellulose stabilized iron nanoparticles in porous media: Column experiments and modeling." Journal of Colloid and Interface Science **334**(1): 96-102.

He, F., D. Zhao, J. Liu and C. B. Roberts (2007). "Stabilization of Fe-Pd Nanoparticles with Sodium Carboxymethyl Cellulose for Enhanced Transport and Dechlorination of Trichloroethylene in Soil and Groundwater." Industrial & Engineering Chemical Research **46**(1): 29-34.

He, F., D. Zhao and C. Paul (2010). "Field assessment of carboxymethyl cellulose stabilized iron nanoparticles for in situ destruction of chlorinated solvents in source zones." Water Research **44**(7): 2360-2370.

- He, F. and D. Y. Zhao (2008). "Hydrodechlorination of trichloroethene using stabilized Fe-Pd nanoparticles: Reaction mechanism and effects of stabilizers, catalysts and reaction conditions." Applied Catalysis B-Environmental **84**(3-4): 533-540.
- Henn, K. W., Waddill, D.W. (2006). "Utilization of nanoscale zero-valent iron for source remediation - A case study." Remediation Journal **16**(2): 57-77.
- ITRC, I. T. R. C. (2011). Integrated DNAPL Site Strategy. Washington, D.C, Interstate Technology & Regulatory Council, Integrated DNAPL Site Strategy Team.
- Jeon, J.-R., K. Murugesan, I.-H. Nam and Y.-S. Chang (2013). "Coupling microbial catabolic actions with abiotic redox processes: A new recipe for persistent organic pollutant (POP) removal." Biotechnology Advances **31**(2): 246-256.
- Jiang, C., Y. Liu, Z. Chen, M. Megharaj and R. Naidu (2013). "Impact of iron-based nanoparticles on microbial denitrification by *Paracoccus* sp. strain YF1." Aquatic Toxicology **142–143**(0): 329-335.
- Johnson, R. L., G. O. B. Johnson, J. T. Nurmi and P. G. Tratnyek (2009). "Natural Organic Matter Enhanced Mobility of Nano Zerovalent Iron." Environmental Science & Technology **43**(14): 5455-5460.
- Johnson, R. L., J. T. Nurmi, G. S. O'Brien Johnson, D. Fan, R. L. O'Brien Johnson, Z. Shi, A. J. Salter-Blanc, P. G. Tratnyek and G. V. Lowry (2013). "Field-Scale Transport and Transformation of Carboxymethylcellulose-Stabilized Nano Zero-Valent Iron." Environmental Science & Technology **47**(3): 1573-1580.
- Johnson, T. L., M. M. Scherer and P. G. Tratnyek (1996). "Kinetics of Halogenated Organic Compound Degradation by Iron Metal." Environmental Science & Technology **30**(8): 2634-2640.
- Jones, B. D. and J. D. Ingle Jr (2001). "Evaluation of immobilized redox indicators as reversible, in situ redox sensors for determining Fe(III)-reducing conditions in environmental samples." Talanta **55**(4): 699-714.

Jones, B. D. and J. D. Ingle Jr (2005). "Evaluation of redox indicators for determining sulfate-reducing and dechlorinating conditions." Water Research **39**(18): 4343-4354.

Joyce, R. A., D. R. Glaser, D. D. Werkema and E. A. Atekwana (2012). "Spectral induced polarization response to nanoparticles in a saturated sand matrix." Journal of Applied Geophysics **77**: 63-71.

Kanel, S. R., R. R. Goswami, T. P. Clement, M. O. Barnett and D. Zhao (2008). "Two Dimensional Transport Characteristics of Surface Stabilized Zero-valent Iron Nanoparticles in Porous Media." Environmental Science & Technology **42**(3): 896-900.

Kaplan, D. I., K. J. Cantrell, T. W. Wietsma and M. A. Potter (1996). "Retention of Zero-Valent Iron Colloids by Sand Columns: Application to Chemical Barrier Formation." Journal of Environmental Quality **25**(5): 1086-1094.

Karn, B., Kuiken, T., Otto, M. (2009). "Nanotechnology and in Situ Remediation: A Review of the Benefits and Potential Risks." Environ Health Perspect **117**(12): 1823-1831.

Keenan, C. R., R. Goth-Goldstein, D. Lucas and D. L. Sedlak (2009). "Oxidative Stress Induced by Zero-Valent Iron Nanoparticles and Fe(II) in Human Bronchial Epithelial Cells." Environmental Science & Technology **43**(12): 4555-4560.

Köber, R., H. Hollert, G. Hornbruch, M. Jekel, A. Kamptner, N. Klaas, H. Maes, K. M. Mangold, E. Martac, A. Matheis, H. Paar, A. Schäffer, H. Schell, A. Schiwy, K. R. Schmidt, T. J. Strutz, S. Thümmeler, A. Tiehm and J. Braun (2014). "Nanoscale zero-valent iron flakes for groundwater treatment." Environmental Earth Sciences **72**(9): 3339-3352.

Kocur, C. M., A. I. Chowdhury, N. Sakulchaicharoen, H. K. Boparai, K. P. Weber, P. Sharma, M. M. Krol, L. Austrins, C. Peace, B. E. Sleep and D. M. O'Carroll (2014). "Characterization of nZVI Mobility in a Field Scale Test." Environmental Science & Technology **48**(5): 2862-2869.

Kocur, C. M., D. M. O'Carroll and B. E. Sleep (2013). "Impact of nZVI stability on mobility in porous media." Journal of Contaminant Hydrology **145**(0): 17-25.

Kram, M. L. (2005). Dnapi Characterization Methods and Approaches. Practical Handbook of Environmental Site Characterization and Ground-Water Monitoring, Second Edition, CRC Press: 473-515.

Krol, M. M., A. J. Oleniuk, C. M. Kocur, B. E. Sleep, P. Bennett, X. Zhong and D. M. O'Carroll (2013). "A Field-Validated Model for In Situ Transport of Polymer-Stabilized nZVI and Implications for Subsurface Injection." Environmental Science & Technology **47**(13): 7332-7340.

Krug, T., O'Hara, S., Watling, M., Quinn, J., (2010). Final Report: Emulsified Zero-Valent Nano-Scale Iron Treatment of Chlorinated

Solvent DNAPL Source Areas ESTCP Project ER-0431, Environmental Security Technology Certification Program.

Kueper, B. H. (2014). Chlorinated Solvent Source Zone Remediation, Springer.

Lampron, K. J., P. C. Chiu and D. K. Cha (1998). "Biological reduction of trichloroethene supported by Fe(0)." Bioremediation Journal **2**(3-4): 175-181.

Lampron, K. J., P. C. Chiu and D. K. Cha (2001). "Reductive Dehalogenation of Chlorinated Ethenes with Elemental Iron: The Role of Microorganisms." Water Research **35**(13): 3077-3084.

Laumann, S., V. Micić, G. V. Lowry and T. Hofmann (2013). "Carbonate minerals in porous media decrease mobility of polyacrylic acid modified zero-valent iron nanoparticles used for groundwater remediation." Environmental Pollution **179**(0): 53-60.

Lee, M., E. Wells, Y. K. Wong, J. Koenig, L. Adrian, H. H. Richnow and M. Manefield (2015). "Relative Contributions of Dehalobacter and Zerovalent Iron in the Degradation of Chlorinated Methanes." Environmental Science & Technology **49**(7): 4481-4489.

Lee, S., X. Bi, R. B. Reed, J. F. Ranville, P. Herckes and P. Westerhoff (2014). "Nanoparticle Size Detection Limits by Single Particle ICP-MS for 40 Elements." Environmental Science & Technology **48**(17): 10291-10300.

- Li, H., Q. Zhou, Y. Wu, J. Fu, T. Wang and G. Jiang (2009). "Effects of waterborne nano-iron on medaka (*Oryzias latipes*): Antioxidant enzymatic activity, lipid peroxidation and histopathology." Ecotoxicology and Environmental Safety **72**(3): 684-692.
- Li, L., M. Fan, R. C. Brown, J. Van Leeuwen, J. Wang, W. Wang, Y. Song and P. Zhang (2006). "Synthesis, Properties, and Environmental Applications of Nanoscale Iron-Based Materials: A Review." Critical Reviews in Environmental Science and Technology **36**(5): 405 - 431.
- Li, X.-q. and W.-x. Zhang (2007). "Sequestration of metal cations with zerovalent iron nanoparticles - A study with high resolution X-ray photoelectron spectroscopy (HR-XPS)." Journal of Physical Chemistry C **111**(19): 6939-6946.
- Li, Z. Q., K. Greden, P. J. J. Alvarez, K. B. Gregory and G. V. Lowry (2010). "Adsorbed Polymer and NOM Limits Adhesion and Toxicity of Nano Scale Zerovalent Iron to *E. coli*." Environmental Science & Technology **44**(9): 3462-3467.
- Liang, L., N. Korte, J. D. Goodlaxson, J. Clausen, Q. Fernando and R. Muftikian (1997). "Byproduct Formation During the Reduction of TCE by Zero-Valence Iron and Palladized Iron." Ground Water Monitoring & Remediation **17**(1): 122-127.
- Liu, Y. and G. V. Lowry (2006). "Effect of Particle Age (Fe⁰ Content) and Solution pH On NZVI Reactivity: H₂ Evolution and TCE Dechlorination." Environmental Science & Technology **40**(19): 6085-6090.
- Liu, Y., S. A. Majetich, R. D. Tilton, D. S. Sholl and G. V. Lowry (2005). "TCE Dechlorination Rates, Pathways, and Efficiency of Nanoscale Iron Particles with Different Properties." Environmental Science & Technology **39**(5): 1338-1345.
- Luna, M., F. Gastone, T. Tosco, R. Sethi, M. Velimirovic, J. Gemoets, R. Muyschondt, H. Sapon, N. Klaas and L. Bastiaens (2015). "Pressure-controlled injection of guar gum stabilized microscale zerovalent iron for groundwater remediation." Journal of Contaminant Hydrology.

- Mace, C. (2006). "Controlling Groundwater VOCs: do nanoscale ZVI particles have any advantages over microscale ZVI of BNP." Pollution Engineering **38**(4): 24-28.
- Makeig, K. S., Nielsen, D.M., (2005). Regulatory Mandates for Ground-Water Monitoring. Practical Handbook of Environmental Site Characterization and Ground-Water Monitoring, Second Edition, CRC Press: 1-34.
- Mao, X., J. Wang, A. Ciblak, E. E. Cox, C. Riis, M. Terkelsen, D. B. Gent and A. N. Alshawabkeh (2012). "Electrokinetic-enhanced bioaugmentation for remediation of chlorinated solvents contaminated clay." Journal of Hazardous Materials **213–214**(0): 311-317.
- Martel, K. E., R. Martel, R. Lefebvre and P. J. Gélinas (1998). "Laboratory Study of Polymer Solutions Used for Mobility Control During In Situ NAPL Recovery." Ground Water Monitoring & Remediation **18**(3): 103-113.
- Matheson, L. J. and P. G. Tratnyek (1994). "Reductive Dehalogenation of Chlorinated Methanes by Iron Metal." Environmental Science & Technology **28**(12): 2045-2053.
- Mueller, N. C., J. Braun, J. Bruns, M. Cernik, P. Rissing, D. Rickerby and B. Nowack (2012). "Application of nanoscale zero valent iron (NZVI) for groundwater remediation in Europe." Environmental Science and Pollution Research **19**(2): 550-558.
- Mulligan, C. N., R. N. Yong and B. F. Gibbs (2001). "Remediation technologies for metal-contaminated soils and groundwater: an evaluation." Engineering Geology **60**(1–4): 193-207.
- Murdoch, L. and W. Slack (2002). "Forms of Hydraulic Fractures in Shallow Fine-Grained Formations." Journal of Geotechnical and Geoenvironmental Engineering **128**(6): 479-487.
- Němeček, J., O. Lhotský and T. Cajthaml (2014). "Nanoscale zero-valent iron application for in situ reduction of hexavalent chromium and its effects on indigenous microorganism populations." Science of The Total Environment **485–486**(0): 739-747.
- Nurmi, J. T., P. G. Tratnyek, V. Sarathy, D. R. Baer, J. E. Amonette, K. Pecher, C. Wang, J. C. Linehan, D. W. Matson, R. L. Penn and M. D. Driessen (2005). "Characterization and

Properties of Metallic Iron Nanoparticles: Spectroscopy, Electrochemistry, and Kinetics." Environmental Science & Technology **39**(5): 1221-1230.

O'Carroll, D., B. Sleep, M. Krol, H. Boparai and C. Kocur (2013). "Nanoscale zero valent iron and bimetallic particles for contaminated site remediation." Advances in Water Resources **51**: 104-122.

O'Hara, S., T. Krug, J. Quinn, C. Clausen and C. Geiger (2006). "Field and laboratory evaluation of the treatment of DNAPL source zones using emulsified zero-valent iron." Remediation Journal **16**(2): 35-56.

Oostrom, M., T. W. Wietsma, M. A. Covert and V. R. Vermeul (2007). "Zero-valent iron emplacement in permeable porous media using polymer additions." Ground Water Monitoring and Remediation **27**(1): 122-130.

Pawlett, M., K. Ritz, R. A. Dorey, S. Rocks, J. Ramsden and J. A. Harris (2013). "The impact of zero-valent iron nanoparticles upon soil microbial communities is context dependent." Environmental Science and Pollution Research International **20**(2): 1041-1049.

Pennell, K. D., M. Jin, L. M. Abriola and G. A. Pope (1994). "Surfactant enhanced remediation of soil columns contaminated by residual tetrachloroethylene." Journal of Contaminant Hydrology **16**(1): 35-53.

Petosa, A. R., D. P. Jaisi, I. R. Quevedo, M. Elimelech and N. Tufenkji (2010). "Aggregation and Deposition of Engineered Nanomaterials in Aquatic Environments: Role of Physicochemical Interactions." Environmental Science & Technology **44**(17): 6532-6549.

Phenrat, T., A. Cihan, H.-J. Kim, M. Mital, T. Illangasekare and G. V. Lowry (2010). "Transport and Deposition of Polymer-Modified Fe⁰ Nanoparticles in 2-D Heterogeneous Porous Media: Effects of Particle Concentration, Fe⁰ Content, and Coatings." Environmental Science & Technology **44**(23): 9086-9093.

Phenrat, T., F. Fagerlund, T. Illangasekare, G. V. Lowry and R. D. Tilton (2011). "Polymer-Modified Fe⁰ Nanoparticles Target Entrapped NAPL in Two Dimensional Porous Media:

Effect of Particle Concentration, NAPL Saturation, and Injection Strategy." Environmental Science & Technology **45**(14): 6102-6109.

Phenrat, T., H.-J. Kim, F. Fagerlund, T. Illangasekare, R. D. Tilton and G. V. Lowry (2009). "Particle Size Distribution, Concentration, and Magnetic Attraction Affect Transport of Polymer-Modified Fe⁰ Nanoparticles in Sand Columns." Environmental Science & Technology **43**(13): 5079-5085.

Phenrat, T., H. J. Kim, F. Fagerlund, T. Illangasekare and G. V. Lowry (2010). "Empirical correlations to estimate agglomerate size and deposition during injection of a polyelectrolyte-modified Fe⁰ nanoparticle at high particle concentration in saturated sand." Journal of Contaminant Hydrology **118**(3-4): 152-164.

Phenrat, T., Y. Liu, R. D. Tilton and G. V. Lowry (2009). "Adsorbed Polyelectrolyte Coatings Decrease Fe⁰ Nanoparticle Reactivity with TCE in Water: Conceptual Model and Mechanisms." Environmental Science & Technology **43**(5): 1507-1514.

Phenrat, T., T. C. Long, G. V. Lowry and B. Veronesi (2009). "Partial Oxidation ("Aging") and Surface Modification Decrease the Toxicity of Nanosized Zerovalent Iron." Environmental Science & Technology **43**(1): 195-200.

Phenrat, T., N. Saleh, K. Sirk, H.-J. Kim, R. Tilton and G. Lowry (2008). "Stabilization of aqueous nanoscale zerovalent iron dispersions by anionic polyelectrolytes: adsorbed anionic polyelectrolyte layer properties and their effect on aggregation and sedimentation." Journal of Nanoparticle Research **10**(5): 795-814.

Phenrat, T., N. Saleh, K. Sirk, R. D. Tilton and G. V. Lowry (2007). "Aggregation and Sedimentation of Aqueous Nanoscale Zerovalent Iron Dispersions." Environmental Science & Technology **41**(1): 284-290.

Pinder, G. F., Celia, M.A. (2006). Subsurface Hydrology. Hoboken, NJ, John Wiley & Sons, Inc.

- Preslo, L. M., Nielsen, G.L., Nielsen, D.M., (2005). Environmental Site Characterization. Practical Handbook of Environmental Site Characterization and Ground-Water Monitoring, Second Edition, CRC Press: 35-205.
- Quinn, J., C. Geiger, C. Clausen, K. Brooks, C. Coon, S. O'Hara, T. Krug, D. Major, W.-S. Yoon, A. Gavaskar and T. Holdsworth (2005). "Field Demonstration of DNAPL Dehalogenation Using Emulsified Zero-Valent Iron." Environmental Science & Technology **39**(5): 1309-1318.
- Raychoudhury, T., G. Naja and S. Ghoshal (2010). "Assessment of transport of two polyelectrolyte-stabilized zero-valent iron nanoparticles in porous media." Journal of Contaminant Hydrology **118**(3-4): 143-151.
- Raychoudhury, T., N. Tufenkji and S. Ghoshal (2012). "Aggregation and deposition kinetics of carboxymethyl cellulose-modified zero-valent iron nanoparticles in porous media." Water Research **46**(6): 1735-1744.
- Raychoudhury, T., N. Tufenkji and S. Ghoshal (2014). "Straining of polyelectrolyte-stabilized nanoscale zero valent iron particles during transport through granular porous media." Water Research **50**(0): 80-89.
- Reinsch, B. C., B. Forsberg, R. L. Penn, C. S. Kim and G. V. Lowry (2010). "Chemical Transformations during Aging of Zerovalent Iron Nanoparticles in the Presence of Common Groundwater Dissolved Constituents." Environmental Science & Technology **44**(9): 3455-3461.
- Rosenthal, H., L. Adrian and M. Steiof (2004). "Dechlorination of PCE in the presence of Fe⁰ enhanced by a mixed culture containing two Dehalococcoides strains." Chemosphere **55**(5): 661-669.
- Saccà, M. L., C. Fajardo, G. Costa, C. Lobo, M. Nande and M. Martin (2014). "Integrating classical and molecular approaches to evaluate the impact of nanosized zero-valent iron (nZVI) on soil organisms." Chemosphere **104**(0): 184-189.

Sakulchaicharoen, N., D. M. O'Carroll and J. E. Herrera (2010). "Enhanced stability and dechlorination activity of pre-synthesis stabilized nanoscale FePd particles." Journal of Contaminant Hydrology **118**(3-4): 117-127.

Saleh, N., H.-J. Kim, T. Phenrat, K. Matyjaszewski, R. D. Tilton and G. V. Lowry (2008). "Ionic Strength and Composition Affect the Mobility of Surface-Modified Fe⁰ Nanoparticles in Water-Saturated Sand Columns." Environmental Science & Technology **42**(9): 3349-3355.

Saleh, N., T. Phenrat, K. Sirk, B. Dufour, J. Ok, T. Sarbu, K. Matyjaszewski, R. D. Tilton and G. V. Lowry (2005). "Adsorbed Triblock Copolymers Deliver Reactive Iron Nanoparticles to the Oil/Water Interface." Nano Letters **5**(12): 2489-2494.

Saleh, N., K. Sirk, Y. Liu, T. Phenrat, B. Dufour, K. Matyjaszewski, R. D. Tilton and G. V. Lowry (2007). "Surface Modifications Enhance Nanoiron Transport and NAPL Targeting in Saturated Porous Media." Environmental Engineering Science **24**(1): 45-57.

Schrick, B., B. W. Hydutsky, J. L. Blough and T. E. Mallouk (2004). "Delivery Vehicles for Zerovalent Metal Nanoparticles in Soil and Groundwater." Chemistry of Materials **16**(11): 2187-2193.

Shi, Z., D. Fan, R. L. Johnson, P. G. Tratnyek, J. T. Nurmi, Y. Wu and K. H. Williams (2015). "Methods for Characterizing the Fate and Effects of Nano Zerovalent Iron during Groundwater Remediation." Journal of Contaminant Hydrology(0).

Shi, Z., J. T. Nurmi and P. G. Tratnyek (2011). "Effects of Nano Zero-Valent Iron on Oxidation Reduction Potential." Environmental Science & Technology **45**(4): 1586-1592.

Slater, L. and A. Binley (2003). "Evaluation of permeable reactive barrier (PRB) integrity using electrical imaging methods." GEOPHYSICS **68**(3): 911-921.

Slater, L. D., J. Choi and Y. Wu (2005). "Electrical properties of iron-sand columns: Implications for induced polarization investigation and performance monitoring of iron-wall barriers." Geophysics **70**(4): G87-G94.

- Song, H. and E. R. Carraway (2005). "Reduction of Chlorinated Ethanes by Nanosized Zero-Valent Iron: Kinetics, Pathways, and Effects of Reaction Conditions." Environmental Science & Technology **39**(16): 6237-6245.
- Song, H. and E. R. Carraway (2008). "Catalytic hydrodechlorination of chlorinated ethenes by nanoscale zero-valent iron." Applied Catalysis B: Environmental **78**(1–2): 53-60.
- Stookey, L. L. (1970). "Ferrozine - A New Spectrophotometric Reagent for Iron." Analytical Chemistry **42**(7).
- Su, C., R. W. Puls, T. A. Krug, M. T. Watling, S. K. O'Hara, J. W. Quinn and N. E. Ruiz (2012). "A two and half-year-performance evaluation of a field test on treatment of source zone tetrachloroethene and its chlorinated daughter products using emulsified zero valent iron nanoparticles." Water Research **46**(16): 5071-5084.
- Su, Y., A. S. Adeleye, X. Zhou, C. Dai, W. Zhang, A. A. Keller and Y. Zhang (2014). "Effects of nitrate on the treatment of lead contaminated groundwater by nanoscale zerovalent iron." Journal of Hazardous Materials **280**: 504-513.
- Sun, J., S. Wang, D. Zhao, F. H. Hun, L. Weng and H. Liu (2011). "Cytotoxicity, permeability, and inflammation of metal oxide nanoparticles in human cardiac microvascular endothelial cells: Cytotoxicity, permeability, and inflammation of metal oxide nanoparticles." Cell Biology and Toxicology **27**(5): 333-342.
- Sun, Q., A. J. Feitz, J. Guan and T. D. Waite (2008). "Comparison of the reactivity of nanosized zero-valent iron (nZVI) particles produced by borohydride and dithionite reduction of iron salts." Nano **3**(5): 341-349.
- Sun, Y.-P., X.-q. Li, J. Cao, W.-x. Zhang and H. P. Wang (2006). "Characterization of zero-valent iron nanoparticles." Advances in Colloid and Interface Science **120**(1-3): 47-56.
- Sun, Y.-P., X.-Q. Li, W.-X. Zhang and H. P. Wang (2007). "A method for the preparation of stable dispersion of zero-valent iron nanoparticles." Colloids and Surfaces A: Physicochemical and Engineering Aspects **308**(1-3): 60-66.

- Szeconsdy, J. E., J. S. Fruchter, M. D. Williams, V. R. Vermeul and D. Sklarew (2004). "In situ chemical reduction of aquifer sediments: Enhancement of reactive iron phases and TCE dechlorination." Environmental Science and Technology **38**(17): 4656-4663.
- Taghavy, A., J. Costanza, K. D. Pennell and L. M. Abriola (2010). "Effectiveness of nanoscale zero-valent iron for treatment of a PCE-DNAPL source zone." Journal of Contaminant Hydrology **118**(3-4): 128-142.
- Tilston, E. L., C. D. Collins, G. R. Mitchell, J. Princiville and L. J. Shaw (2013). "Nanoscale zerovalent iron alters soil bacterial community structure and inhibits chloroaromatic biodegradation potential in Aroclor 1242-contaminated soil." Environmental Pollution **173**(0): 38-46.
- Tiraferrri, A., K. L. Chen, R. Sethi and M. Elimelech (2008). "Reduced aggregation and sedimentation of zero-valent iron nanoparticles in the presence of guar gum." Journal of Colloid and Interface Science **324**(1-2): 71-79.
- Tiraferrri, A. and R. Sethi (2009). "Enhanced transport of zerovalent iron nanoparticles in saturated porous media by guar gum." Journal of Nanoparticle Research **11**(3): 635-645.
- Tosco, T. and R. Sethi (2010). "Transport of Non-Newtonian Suspensions of Highly Concentrated Micro- And Nanoscale Iron Particles in Porous Media: A Modeling Approach." Environmental Science & Technology **44**(23): 9062-9068.
- Tratnyek, P. G., Johnson R.L., Lowry, G.V., Brown, R.A. (2014). In Situ Chemical Reduction for Source Remediation, Springer.
- Tratnyek, P. G., T. Reilkoff, A. Lemon, M. Scherer, B. Balko, L. Feik and B. Henegar (2001). "Visualizing Redox Chemistry: Probing Environmental Oxidation–Reduction Reactions with Indicator Dyes." The Chemical Educator **6**(3): 172-179.
- Truex, M. J., T. W. Macbeth, V. R. Vermeul, B. G. Fritz, D. P. Mendoza, R. D. Mackley, T. W. Wietsma, G. Sandberg, T. Powell, J. Powers, E. Pitre, M. Michalsen, S. J. Ballock-Dixon, L. Zhong and M. Oostrom (2011). "Demonstration of Combined Zero-Valent Iron and

Electrical Resistance Heating for In Situ Trichloroethene Remediation." Environmental Science & Technology **45**(12): 5346-5351.

Truex, M. J., V. R. Vermeul, D. P. Mendoza, B. G. Fritz, R. D. Mackley, M. Oostrom, T. W. Wietsma and T. W. Macbeth (2011). "Injection of Zero-Valent Iron into an Unconfined Aquifer Using Shear-Thinning Fluids." Ground Water Monitoring and Remediation **31**(1): 50-58.

Tufenkji, N. and M. Elimelech (2004). "Correlation Equation for Predicting Single-Collector Efficiency in Physicochemical Filtration in Saturated Porous Media." Environmental Science & Technology **38**(2): 529-536.

Vecchia, E. D., M. Luna and R. Sethi (2009). "Transport in Porous Media of Highly Concentrated Iron Micro- and Nanoparticles in the Presence of Xanthan Gum." Environmental Science & Technology.

Velimirovic, M., T. Tosco, M. Uyttebroek, M. Luna, F. Gastone, C. De Boer, N. Klaas, H. Sapion, H. Eisenmann, P.-O. Larsson, J. Braun, R. Sethi and L. Bastiaens (2014). "Field assessment of guar gum stabilized microscale zerovalent iron particles for in-situ remediation of 1,1,1-trichloroethane." Journal of Contaminant Hydrology **164**(0): 88-99.

Viollier, E., P. W. Inglett, K. Hunter, A. N. Roychoudhury and P. Van Cappellen (2000). "The ferrozine method revisited: Fe(II)/Fe(III) determination in natural waters." Applied Geochemistry **15**(6): 785-790.

Wang, C.-B. and W.-x. Zhang (1997). "Synthesizing Nanoscale Iron Particles for Rapid and Complete Dechlorination of TCE and PCBs." Environmental Science & Technology **31**(7): 2154-2156.

Wang, W., M. Zhou, Z. Jin and T. Li (2010). "Reactivity characteristics of poly(methyl methacrylate) coated nanoscale iron particles for trichloroethylene remediation." Journal of Hazardous Materials **173**(1-3): 724-730.

- Wei, Y. T., S. C. Wu, C. M. Chou, C. H. Che, S. M. Tsai and H. L. Lien (2010). "Influence of nanoscale zero-valent iron on geochemical properties of groundwater and vinyl chloride degradation: A field case study." Water Research **44**(1): 131-140.
- Wu, Y., L. Slater, R. Versteeg and D. LaBrecque (2008). "A comparison of the low frequency electrical signatures of iron oxide versus calcite precipitation in granular zero valent iron columns." Journal of Contaminant Hydrology **95**(3-4): 154-167.
- Wu, Y., L. D. Slater and N. Korte (2005). "Effect of precipitation on low frequency electrical properties of zerovalent iron columns." Environmental Science and Technology **39**(23): 9197-9204.
- Wu, Y., L. D. Slaters and N. Korte (2006). "Low frequency electrical properties of corroded iron barrier cores." Environmental Science and Technology **40**(7): 2254-2261.
- Wu, Y., R. Versteeg, L. Slater and D. LaBrecque (2009). "Calcite precipitation dominates the electrical signatures of zero valent iron columns under simulated field conditions." Journal of Contaminant Hydrology **106**(3-4): 131-143.
- Xiu, Z.-m., K. B. Gregory, G. V. Lowry and P. J. J. Alvarez (2010). "Effect of Bare and Coated Nanoscale Zerovalent Iron on tceA and vcrA Gene Expression in Dehalococcoides spp." Environmental Science & Technology **44**(19): 7647-7651.
- Xiu, Z.-m., Z.-h. Jin, T.-l. Li, S. Mahendra, G. V. Lowry and P. J. J. Alvarez (2010). "Effects of nano-scale zero-valent iron particles on a mixed culture dechlorinating trichloroethylene." Bioresource Technology **101**(4): 1141-1146.
- Yan, W., A. A. Herzing, C. J. Kiely and W.-x. Zhang (2010). "Nanoscale zero-valent iron (nZVI): Aspects of the core-shell structure and reactions with inorganic species in water." Journal of Contaminant Hydrology **118**(3-4): 96-104.
- Yao, K.-M., M. T. Habibian and C. R. O'Melia (1971). "Water and waste water filtration. Concepts and applications." Environmental Science & Technology **5**(11): 1105-1112.
- Zhang, L. and A. Manthiram (1997). "Chains composed of nanosize metal particles and identifying the factors driving their formation." Applied Physics Letters **70**(18): 2469-2471.

Zhong, L., M. Oostrom, T. W. Wietsma and M. A. Covert (2008). "Enhanced remedial amendment delivery through fluid viscosity modifications: Experiments and numerical simulations." Journal of Contaminant Hydrology **101**(1-4): 29-41.

Zhou, L., T. L. Thanh, J. Gong, J.-H. Kim, E.-J. Kim and Y.-S. Chang (2014). "Carboxymethyl cellulose coating decreases toxicity and oxidizing capacity of nanoscale zerovalent iron." Chemosphere **104**(0): 155-161.

Zhu, L., H.-z. Lin, J.-q. Qi, X.-y. Xu and H.-y. Qi (2012). "Effect of H₂ on reductive transformation of p-ClNB in a combined ZVI-anaerobic sludge system." Water Research **46**(19): 6291-6299.

Zhu, L., H. Lin, J. Qi and X. Xu (2013). "Enhanced transformation and dechlorination of p-chloronitrobenzene in the combined ZVI-anaerobic sludge system." Environmental Science and Pollution Research **20**(9): 6119-6127.

Chapter 3

3 Characterization of nZVI Mobility in a Field Scale Test.

Chris M. Kocur ^{a,c}, Ahmed I. Chowdhury ^a, Nataphan Sakulchaicharoen ^a, Hardiljeet K. Boparai ^a, Kela P. Weber, ^{a,d}, Prabhakar Sharma ^a, Magdalena M. Krol ^{a,b}, Leanne Austrins ^c, Christopher Peace ^c, Brent E. Sleep ^b, Denis M. O'Carroll ^{a*}

^a Civil & Environmental Engineering, University of Western Ontario, 1151 Richmond Rd. London, ON, N6A 5B8

^b Civil Engineering, University of Toronto, 35 St. George St. Toronto, ON, M5S 1A4

^c CH2M Hill Canada Ltd. Suite 300, 72 Victoria Street South, Kitchener, ON, N2G 4Y9

^d Department of Chemistry and Chemical Engineering, Royal Military College of Canada, PO Box 17000 Station Forces, Kingston, ON, K7K 7B4

Keywords: nZVI, nanometals, nanoparticle transport, field injection, nanoparticle characterization

3.1 Abstract

Nanoscale zero valent iron (nZVI) particles were injected into a contaminated sandy subsurface area in Sarnia, Ontario. The nZVI was synthesized on site, creating a slurry of 1 g/L nanoparticles using the chemical precipitation method with sodium borohydride (NaBH_4) as the reductant in the presence of 0.8% wt. sodium carboxymethylcellulose (CMC) polymer to form a stable suspension. Individual nZVI particles formed during synthesis had a transmission electron microscopy (TEM) quantified particle size of 86.0 nm and dynamic light scattering (DLS) quantified hydrodynamic diameter for the CMC and nZVI of 624.8 nm. The nZVI was delivered to the subsurface via gravity injection. Peak normalized total Fe breakthrough of 71% was observed 1m from the injection well and remained above 50% for the 24 h injection period. Samples collected from a monitoring well 1 m from the injection contained nanoparticles with TEM-measured particle diameter of 80.2 nm and hydrodynamic diameter of 562.9 nm. No morphological changes were discernible between the injected nanoparticles and nanoparticles recovered from the monitoring well. Energy dispersive X-ray spectroscopy (EDS) was used to confirm the elemental composition of the iron nanoparticles sampled from the downstream monitoring well, verifying the successful transport of nZVI particles. This study suggests that CMC stabilized nZVI can be transported at least 1 m to the contaminated source zone at significant Fe^0 concentrations for reaction with target contaminants.

3.2 Introduction

Nanoscale zero valent iron (nZVI) has shown great potential for remediation of chlorinated solvents, especially at the bench scale (Wang et al. 1997, Zhang 2003, Liu et al. 2005, Liu et al. 2005). However, attempts to scale up from bench scale studies suggest that achieving adequate nZVI mobility in the subsurface could be problematic (Kanel et al. 2008, Phenrat et al. 2010). In the nZVI field tests of Elliot and Zhang (Elliott et al. 2001), nZVI rapidly deposited on the well screen with the remaining nZVI travelling only a “few inches to a few feet” before becoming immobilized (Elliott et al. 2001, Zhang 2003). Limited nZVI mobility is due to the tendency of nZVI to quickly aggregate and settle, primarily due to magnetic attractive forces (Phenrat et al. 2007). A variety of methods have been developed to stabilize nZVI (He et al. 2005, Hoch et al. 2008, Berge et al. 2009). Most methods use polymers to provide electrosteric repulsion to minimize particle aggregation (Saleh et al. 2005, He et al. 2007, Sun et al. 2007, Tiraferri et al. 2008, Comba et al. 2009, Sakulchaicharoen et al. 2010). Electrosteric stabilization has been shown to increase nZVI mobility in porous media column studies (He et al. 2009, Johnson et al. 2009, Phenrat et al. 2009, Tiraferri et al. 2009), although deposition of nZVI is reported to be greater when natural soil was used (He et al. 2009). Despite the recent advances in enhancing nZVI stability and improved understanding of nZVI mobility in porous media, it is still uncertain if nZVI will retain nanoscale dimension (1-100nm) during transport and reaction in the field when used for remediation purposes (Wang et al. 1997, Zhang 2003, Liu et al. 2005, Liu et al. 2005). As reaction with nZVI is surface mediated, it is important to retain nano-scale dimensions during transport through the subsurface to benefit from a high surface area upon arrival in the targeted treatment zone. Most nZVI transport studies have used relatively high groundwater velocities with short residence times in porous media column experiments. Pore velocities in column experiments typically ranged between 15 m/day and 100 m/day in studies reporting nZVI mobility (Kanel et al. 2007, He et al. 2009, Phenrat et al. 2009). In a field setting much lower delivery velocities would be typical, especially considering that injection velocities in groundwater rapidly dissipate as nZVI moves radially from the injection well (Krol et al. 2013). In addition, current bench scale experiments do not adequately represent the required time for delivery of nZVI in the field. For example, laboratory residence times range from 2 – 30min (Saleh et al. 2007, Zhan et al. 2008), whereas field scenarios can take several hours (Elliott et al. 2001, Bennett et al. 2010, He et al. 2010) to days for injection and subsequent nZVI transport to the target treatment zone

(Henn 2006, Wei et al. 2010). Recent column studies have evaluated nZVI mobility at field relevant pore velocities (Berge et al. 2009, Johnson et al. 2009, Tiraferri et al. 2009) and over longer injection periods (Berge et al. 2009, Kocur et al. 2013) and demonstrated that stabilized nZVI is mobile in porous media in the laboratory.

Nano-materials, predominantly nZVI, have been injected into the subsurface for remediation purposes at many locations worldwide (Karn 2009, Mueller et al. 2012). An EPA factsheet in 2008 reported 26 sites in North America where some form of nZVI technology was used for subsurface remediation (EPA 2008). Sites where nZVI has been utilized range from fractured bedrock (Glazier et al. 2003, Zhang 2003) to sandy aquifers (Gavaskar A. 2005, Quinn et al. 2005, Henn 2006, He et al. 2010, Wei et al. 2010) to confined water bearing zones of stratified sediment (Varadhi 2005, Bennett et al. 2010) to large scale sandbox injections (Johnson et al. 2013). Geochemical parameters such as pH, oxidation reduction potential (ORP), and dissolved oxygen have been used to indicate the presence of nZVI within a treatment zone, however, these parameters alone do not confirm the presence of nZVI (Shi et al. 2011), nor does the measurement of elevated total or dissolved Fe down gradient (i.e., constituents that dissolved upstream could have migrated downstream). There is an inadequate understanding of the utility of these parameters with regards to the understanding of nZVI transport in field systems.

This study evaluates the mobility of field-synthesized nZVI within a utility corridor in Sarnia, ON that contained free phase chlorinated solvents. A scalable method of on-site synthesis (He et al. 2010) was used to produce nZVI for subsequent gravity feed injection for hotspot remediation. Objectives of the study were to: 1) evaluate the ability of direct-push wells to deliver nZVI to the contaminated unit via gravity feed injection; 2) monitor the mobility of nZVI within the utility corridor containing sandy soil and; 3) determine the characteristics and quality of nZVI particles synthesized in the field as well as after transport in the subsurface within the treatment area. Field studies have inferred mobility of polymer stabilized nZVI using different approaches, noting black color in downstream water samples (Henn 2006), or geochemical evidence of nZVI transport (Bennett et al. 2010, He et al. 2010). However few studies have collected and characterized nZVI particles recovered downstream from injection wells (Johnson et al. 2013). Although the techniques used in this study have

been used in the laboratory setting (Nurmi et al. 2005, Liu et al. 2006, Sun et al. 2006), this is the first time nZVI mobility has been characterized in such detail at a contaminated site.

3.3 Site Background

3.3.1 Site Description

The study site is located near Sarnia, Ontario on a plain of glacially deposited clay. The first unit is a 3.6-6.7 m thick layer of brown weathered clay, underlain by 20+ m layer of grey (un-weathered and nearly impervious) clay, previously characterized with hydraulic conductivities of 2.1×10^{-9} m/s and 1.6×10^{-10} m/s respectively (Husain et al. 1998). The water table is approximately 1.5 m below ground surface (bgs), but varies spatially and seasonally. The study area is within a continuous (approximately 3 m wide) channel of non-native, porous, sandy material running east to west several hundred meters through the native clay (See Appendix B.1). This North Utility Corridor (NUC) is adjacent to retired and demolished trichloroethylene (TCE) and perchloroethylene (PCE) production facilities. The NUC is approximately 2.5-5 m bgs and hydraulically conductive but capped from direct infiltration by an engineered clay layer. The base of the NUC contains abandoned sewers and utilities, some of which may have been the source of spills and release of chlorinated solvents. The NUC has three sumps which provide a means of controlling the hydraulic gradient in the study area during the injection and monitoring period. Contaminants migrate on site primarily through clay fractures and other permeable pathways such as those surrounding infrastructure and within backfilled zones.

3.3.2 Site Characterization

To confirm the conceptual model of the subsurface, several techniques were used to characterize the study site prior to testing. Examination of soil cores revealed that the site is consistently clay to a depth of 1.5 m, after which, in the NUC, a highly complex emplaced fill mixture of sand and clay units exists. The NUC has heterogeneous zones that vary in composition from clay to medium sand with no obvious connection or layering of units between boreholes. During well installation drill cuttings were closely examined to determine the most conductive intervals for screen placement. A 5.08 cm diameter primary injection well was installed using a 10.16 cm diameter hollow stem auger and was screened 2.5-3 m bgs to intercept the top of the permeable utility corridor 6 m from the hydraulic control sump (Sump

1). Monitoring wells were screened over a length of 1.5 m to intersect sandy units suspected to be connected to the injection well at a minimum depth of 1.5 m.

Prior to flow tests (tracer or nZVI injection) the hydraulic gradient in the study area was measured to be 0.002 with westward flow from the injection well through the monitoring well field to Sump 1 (see Figure 3.1). Slug tests were performed on each well, before and after nZVI injection. In addition, a pump test was conducted prior to the tracer test by pumping Sump 1 at 150 L/min for 1 hour. This induced a hydraulic gradient of 0.055 within the study area. All wells were responsive during the pumping test suggesting hydraulic connection with Sump 1. Following the hydraulic testing, a tracer test was performed by injecting 155L of 6 g/L NaBr solution for 2.75 hours through gravity feed injection at the injection well. During tracer and nZVI injection the hydraulic gradient was controlled in the study area by reproducing pump test conditions (i.e., hydraulic gradient = 0.055).

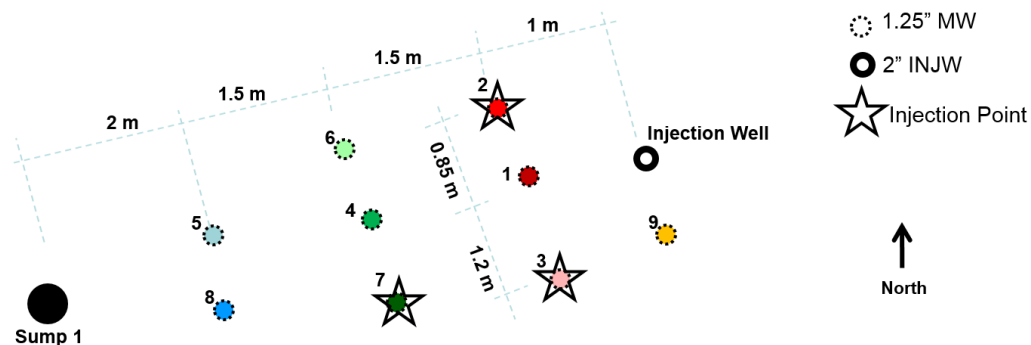


Figure 3.1: Site layout showing the injection and monitoring wells in the study area.

3.4 Field Methods and Materials

3.4.1 nZVI Synthesis on Site

nZVI was synthesized on site over an 8 hr period using 5 batch reactors to produce a total of 760 L of nZVI solution. Preliminary work was done to optimize the nZVI recipe for the production of 1 g/L nZVI in a polymer solution containing 0.8 % carboxymethyl cellulose (CMC). The synthesis reaction was carried out in 208 L HDPE drums (Uline, Brampton, ON) containing 152 L of ZVI slurry and 56 L headspace. Synthesis conditions closely resembled

laboratory conditions in the anaerobic chamber through the use of a nitrogen diffuser installed at the bottom of the HDPE drums. A pneumatic mixer was operated in the drum to keep the reactor mixed at all times and all metal parts were latex coated to maintain chemical compatibility. A second nitrogen diffuser maintained an inert atmosphere in the drum headspace and also diluted any hydrogen gas produced during synthesis, reducing hydrogen gas explosion hazards.

Food grade CMC (Cellogen HP-8A, Dai-Ichi Kogyo Seiyaki Co. Japan) with an estimated molecular weight of 90 kg/mol was used to stabilize nZVI, yielding a solution viscosity of 7 cP. Viscosity was measured using an axial rheometer (Brookfield LVDV-III U, Middleboro MA). Reagents were pre-dissolved in de-oxygenated, de-ionized water before being pumped to the reaction drum (e.g., 0.018 M FeSO₄ (A&K Petrochem Ind. Ltd., Vaughn, ON)). 0.036 M NaBH₄ (GFS Chemicals Inc., Columbus, OH) solution was then titrated to provide optimal nZVI nucleation (He et al. 2007) and achieve a final ZVI concentration of 1 g/L. The ambient temperature of the air and fluids was around 7°C on the day of synthesis. After titration, the reaction drum was mixed for 30 minutes to complete the reaction and samples of nZVI were collected and shipped to the laboratory for particle characterization.

3.4.2 Injection Schedule and Sampling

Table 3.1 outlines the injection schedule for delivery of nZVI into the study area. 380 L of 1 g/L nZVI was introduced into INJW, the primary injection well, (shown in Figure 3.1) at an initial rate of 1 L/min using a constant head gravity feed. It is estimated that 0.375 kg of nZVI was introduced at INJW over the primary injection period. nZVI was subsequently injected into MW2, MW3, and MW7 in order to gather more injection information and distribute nZVI throughout the study area. All nZVI was injected within 24 hours of synthesis using gravity feed injection with the aid of a local gradient that was created by circulating water from Sump 1, 6m upgradient of the study area. Following the 24 hr injection period the injection and recirculation pumps were turned off. The re-circulation resumed for 6 hours each day for 3 days to induce further movement of the injected amendments, after which recirculation was discontinued.

Table 3.1: Summary of the nZVI injection schedule

Injection Location	Initial Rate of Injection (L/min)	Total Mass of Fe Injected (kg)	Start of Injection (hr)	Injection Period (hr)
INJW	1.0	0.375	0	24
MW2	1.8	0.225	12	12
MW3	1.0	0.075	16	5
MW7	0.4	0.075	21	3

Water samples were collected from the synthesis drums and from MW1 at 2-3 hour intervals using 40mL clear glass EPA vials (Systems Plus Ltd., Baden, ON) for analysis of particle size via dynamic light scattering (DLS), preparation of transmission electron microscopy (TEM) and energy-dispersive x-ray spectroscopy (EDS) grids, and analysis of Fe⁰ content. Samples for total Fe analysis were collected and preserved in H₂SO₄, and samples for anions were collected unpreserved and transported to the lab for analysis. Following the 24hr injection period, sampling occurred at 2, 3, 10, and 21 days to monitor changes in the study area due to the nZVI injection. Geochemical parameters including pH, ORP, EC, and DO were measured during the entire injection and monitoring period using a multi-parameter field probe (YSI 556 MPS, Yellow Springs, OH) equipped with a flow through cell. A low flow sampling technique was used (Puls et al. 1996), sampling < 150 mL/min from monitoring wells to have minimal impact on the hydraulic gradient throughout both the short term and longer term sampling periods.

3.5 Analytical Methods

Analysis of anions (bromide and sulfate) during both the tracer test and nZVI injection period was performed using a high performance liquid chromatograph (HPLC) equipped with a conductivity detector (Model 432, Waters, Milford, MA), a 4.6x50 cm IC-Pak Anion column (#Wat007355) and 12% acetonitrile eluent. Bromide (Br) was selected for the conservative tracer test, whereas sulfate was selected as the tracer for the nZVI injection as FeSO₄ was included in the injection fluid as a reaction precursor for nZVI synthesis. Additional chemicals

typically used as tracers (eg. NaBr) were not used for the primary injection to avoid additional increases in ionic strength and reduced nanoparticle stability.

Total Fe samples were digested using H₂SO₄ and diluted for analysis using inductively coupled plasma - optical emission spectroscopy (ICP-OES) (Varian Vista-Pro Axial, Agilent, Santa Clara, CA) according to EPA-200.7 (Martin 1994). The Fe⁰ content of the nZVI samples was determined using acid digestion (Liu et al. 2005). 5 mL of HCl (1M) and 5 mL of sample was added to a 20 mL headspace vial (5188-2753, Agilent Technologies) immediately following sample collection in the field. H₂ evolved from nanoparticle digestion was measured using a 7890A GC (Agilent, Santa Clara, CA) equipped with a thermal conductivity detector (TCD) and a CarboxenTM-1006 PLOT (30 m x 0.53 mm) capillary column. Nitrogen was used as carrier gas and the oven was isothermal at 60°C. The Fe⁰ content of particles was then stoichiometrically calculated from the amounts of H₂ and Fe in each sample.

Time sensitive samples (e.g., nanoparticle size and stability characteristics) were analyzed or permanently sealed within 16 hours of sampling. The particles were preserved during transport by limiting oxygen through zero headspace sampling and maintaining insitu temperatures as much as possible until analysis. The colloidal stability of nZVI samples was determined by first diluting (10x) the opaque black nZVI sample using de-ionized, de-oxygenated water in an anaerobic chamber. The sample was then transferred into an air tight quartz cuvette and scanned at 508nm using a UV-Vis spectrophotometer (Helios Alpha, Thermo-fischer, Waltham, MA) for 48 hrs at 15 min intervals (Kocur et al. 2013). Identically prepared samples were used to measure the effective hydrodynamic diameter of nZVI samples by DLS using a Zeta Plus particle analyzer (BIC, Brookhaven, Holtsville, NY) and Zeta Plus software. The zeta potentials of nZVI particles were also determined for nZVI field samples using Zeta Plus software.

Parallel samples were permanently preserved for transmission electron microscopy (TEM) and energy dispersive x-ray spectroscopy (EDS). Sample was diluted using deoxygenated water, then 1 drop was dried on a # 300 mesh lacey Formvar/carbon copper grid (Tedpella Inc., Redding, CA) in an anaerobic chamber before being vacuum sealed until analysis. TEM analysis was performed using a FEI Titan 80-300 Cryo-in situ TEM equipped with an Oxford detector for EDS and INCA software (Oxford Instruments, Abingdon, UK). A

representative set of micrographs was obtained for each sample, and diameter distributions were obtained from individual micrographs using Photoshop 7.0 (Adobe, San Jose, CA). The presence of Na, S, Cl, Fe and Br was quantified using EDS analysis at two measurement scales. The larger measurement areas (1.5 μm and 3 μm) provided information regarding the presence of the selected elements in the entire sample whereas the smaller scale (90nm x 90nm) provided information related to elemental composition of single particles.

3.6 Results

3.6.1 Pumping, Slug, and Tracer Testing

Results of the pumping test showed good hydraulic connection between Sump 1 and the monitoring wells, including the injection well, with a hydraulic gradient of 0.012- 0.055 under injection conditions. Hydraulic conductivity (K) in the test area, estimated via slug testing, ranged between 1.2×10^{-6} and 4.6×10^{-6} m/s prior to tracer and nZVI injections (Appendix B.7). These hydraulic conductivities are less than the range of 4.2×10^{-5} to 1.7×10^{-4} m/s measured in laboratory constant head permeability tests of recovered NUC samples (Appendix B.8). K measured in the laboratory was higher because the laboratory tests specifically targeted more permeable zones in the recovered cores and could also be the result of a disturbed sample. Based on the measured hydraulic gradient and the K values determined from slug tests and lab tests, the groundwater pore velocity between the INJW and MW1 during active pumping was estimated to be between 2.1×10^{-7} and 1.0×10^{-5} m/s, assuming a porosity for the sand of 0.32. However, tracer detection at MW1 occurred 15 minutes after injection initiation and reached $C/C_0 = 0.5$ after 5.2 hrs, suggesting a mean tracer velocity between the injection well and MW1 of 5.3×10^{-5} m/s. Given that the tracer arrival time at MW1 is more consistent with laboratory K values, it is anticipated that transport occurred through preferential flow paths of higher K zones. Tracer was detected in MW2 after 2.4 hrs, suggesting good hydraulic connection with the INJW. Tracer concentrations at MW4 only increased to 2.5% of the injection concentration during the 12.9 hrs injection and monitoring period suggesting that the primary flow did not go from INJW to MW4, and also suggesting that the flow field was strongly influenced by subsurface heterogeneity.

3.6.2 nZVI Synthesis, Injection, and Stability

The nZVI suspension showed no visual signs of settling during the injection period and there was no nZVI deposited on the bottom of the drum following injection. Stability tests performed on field synthesized samples commenced in the laboratory 16 hours after field synthesis. In these tests 50% of the nZVI particles remained in suspension for 8-16 hours (i.e., 24-32 hours after the particles were synthesized) (Appendix B.8). Kocur et al (Kocur et al. 2013), reported colloidal stability curves wherein greater than 50% of particles remained in suspension for 8 hrs under closely controlled laboratory conditions, and Sakulchaicharoen et al (Sakulchaicharoen et al. 2010) reported as great as 36 hrs of stability for CMC polymer. Direct comparison between studies is difficult as nZVI and polymer concentrations differed from this study, however the range in literature is consistent with the values observed in this study (Appendix B2). The zeta potential of the synthesized nZVI suspension was -49.2 ± 1.5 mV for nZVI samples prior to injection, which is within the range of values reported in other mobility studies that stabilized nZVI using CMC 90k and used the same synthesis process (i.e., -45 mV to -56 mV) (He et al. 2009, Raychoudhury et al. 2010, Chowdhury et al. 2012).

The rate of nZVI injection was monitored at each injection location (INJW, MW2, MW3, and MW7) to quantify nZVI delivered to the subsurface and to evaluate the performance of the injection wells. The gravity feed at INJW initially delivered 1 L/min of nZVI into the formation over a 0.6 m well screen. The injection well flow rate decreased throughout the injection, ultimately decreasing to 0.08 L/min (Appendix B.3). Similar decreased flow rates occurred in MW2 and MW3, both with 1.5 m screened intervals. Previous field studies using unstabilized nZVI may have had issues delivering the desired amount of nZVI due to well screen clogging or clogging of the pore space immediately outside the well. Similar clogging has been observed for bare nZVI in column experiment studies (Saleh et al. 2008, Johnson et al. 2009, Vecchia et al. 2009). However, in this study there is no other evidence to suggest well clogging. For example, there was no significant aggregation observed in the synthesis drums and the particle hydrodynamic diameter did not appreciably increase, as will be discussed later. A recent modeling study suggests that decreases in injection flow rate with a gravity injection system is unavoidable, but can vary significantly, depending on system conditions (e.g., viscosity, polymer concentration) (Krol et al. 2013). This study showed that under constant head injection, as the viscous injection fluid moves radially outwards from the

injection well the average viscosity of the formation fluid increases, resulting in a corresponding decrease in injection flowrate. Krol et al (Krol et al. 2013) modeled a higher viscosity fluid (13 cP) compared to the 7 cP fluid used in this study, however the behavior observed in this study is similar to that produced using a non-uniform viscosity model. Post injection slug tests revealed that the hydraulic conductivity changes in the vicinity of the well were not permanent as the hydraulic conductivity of the wells remained the same or increased 10 days after injection (Appendix B.7). This temporary decreased well productivity may have been due to the formation of H_2 gas in-situ temporarily clogging the pore space. Shortly after synthesis, the fresh nZVI surface is available for reaction with water, producing H_2 gas (Li 2006). It is also possible that a small amount of residual $NaBH_4$ was present in the delivered injection fluid. $NaBH_4$, once diluted in the vicinity of the well, would undergo self-hydrolysis forming H_2 gas (Schlesinger et al. 1953, Davis et al. 1962).

3.6.3 nZVI Mobility

The breakthrough of total Fe at MW1 was normalized to sulfate breakthrough to account for the fact that not all of the injection fluid is intercepted by MW1 (Figure 3.2.a). Given the relatively short injection period, nZVI breakthrough was only detected in MW1. nZVI reached MW1, 1 m away from the injection well, at the first sampling time (25 min), with normalized concentrations achieving 75% before decreasing to approximately 50% for the majority of the injection. A previous field study observed 37% breakthrough of total Fe normalized to the tracer at a well 1 m away from the gravity feed injection well (He et al. 2010), however the injected nZVI concentration was more dilute (0.2 g/L nZVI). More recently, a 0.9 g/L nZVI injection into a pilot scale model aquifer resulted in similar breakthrough in a monitoring well 0.5m and 1m from the injection (Johnson et al. 2013).

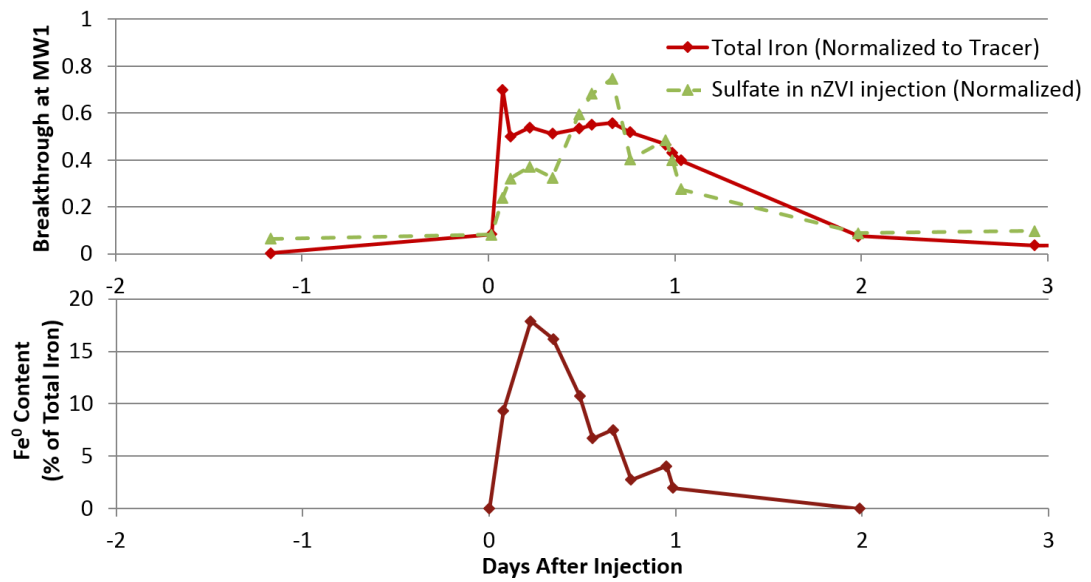


Figure 3.2: Breakthrough data collected at MW1 including a) total Fe and Sulfate (tracer) and b) Fe⁰ content in nZVI particles. $t = 0$ for both plots is denoted by the start of injection at INJW.

Following the 24 hr injection period, injection was stopped and the recirculation pumps were shut off for a period of 16 hrs, after which the hydraulic gradient was re-established and monitoring continued. When the re-circulation pumps were turned on total Fe was 7.8% in MW1. It is possible that the concentration decrease was due to the nZVI suspension being flushed past MW1 during the period of 16 hours when the pumps were turned off. However, given that nZVI was not observed at MW6 after 24 hrs of injection it is more likely that nZVI deposited on the porous media during the 16 hour lag phase. Bennett et al. (Bennett et al. 2010) observed a similar decline in nZVI mobility during injection into a sandy aquifer, and modeling of this field test predicted that an extended lag phase at low pore water velocity ($< 1.2 \times 10^{-5}$ m/s) could immobilize nZVI colloids (Krol et al. 2013). Although previous laboratory studies have demonstrated that nZVI was mobile in column experiments at pore velocities ranging from 1.7×10^{-4} m/s down to 2.9×10^{-6} m/s (He et al. 2009, Raychoudhury et al. 2010, Kocur et al. 2013), mobility at the porewater velocities of $\sim 5.8 \times 10^{-8}$ m/s during the 16 hour reduced gradient period, has not been previously evaluated in laboratory studies.

Monitoring of total Fe from MW1 continued for 3 weeks after the injection. 10 days after injection the total Fe concentration in MW1 was 0.01 g/L, or 1% of the initial injection concentration, suggesting that most of the particles deposited on subsurface porous medium. The pore velocity at the injection front following 24 hours of injection is estimated to be less than 0.1 m/day. Mobility at these pore water velocities has not been reported previously so it is unlikely that nZVI particles migrated further under the background gradient. This is further corroborated by the significant decrease in nZVI particle stability at long times (i.e., $C/C_0 < 0.1$ remained in suspension after 48 hours) (Appendix B.2). Therefore, it is suspected that Fe species sampled at MW1 after 48 hrs would not be mobile Fe nanoparticles, but rather dissolved Fe in low concentrations that have dissolved back into aqueous solution. Previous studies have interpreted measured total Fe downgradient of an injection to be mobile nanoparticles, even after significant transport time (Wei et al. 2010). For example, one field study reported Fe migration at 4.3% of the injection concentration 40 days after nZVI injection 3 m from the injection well and attributed this to nanoparticle mobility. nZVI mobility for extended periods of time and distance would not be expected in the absence of very high groundwater velocities and extremely stable nZVI suspensions.

nZVI induces an immediate drop in ORP when placed in aqueous suspension, creating conditions where the reduction of chlorinated compounds can occur. Reducing conditions were measured in the treatment area before nZVI injection (Appendix B.4.a). Following nZVI injection the largest observed decline in oxidation-reduction potential (ORP) was in the injection well, reaching strongly reducing conditions with an ORP below -400 mV. This magnitude of ORP decline has been measured at injection wells in several field demonstrations (Henn 2006). Strongly reducing conditions were also observed in several other wells directly down gradient of the injection well (MW1, MW6). MW6 exhibited a decline in ORP following nZVI injection (i.e., from -97.7 mV in the background to -192.8 mV at 14 hours) yet total Fe did not significantly increase (i.e., < 4 mg/L, or 0.4% of injected concentration after 10 days) and recovered samples had no black color. A number of field studies have reported decreased ORP as evidence of nZVI transport. However, as demonstrated in this study and as pointed out in a recent study, ORP alone is not an indicator of nZVI (Shi et al. 2011). The presence of hydrogen, ferrous iron, and sulfides, make it difficult to attribute ORP reductions to the presence of nZVI particles alone. pH was monitored following injection (Appendix B.4.b) and exhibits similar behavior as the ORP. This has been previously reported (Elliott et al. 2001, Glazier et al. 2003, Zhang 2003, Varadhi 2005, Wei et al. 2010) and is expected as both ORP and pH change due to the oxidation of Fe^0 in water.

3.6.4 Characterization of nZVI before and after transport

Samples recovered from MW1 were subjected to detailed characterization. TEM micrographs show the presence of individual particles in the nZVI/CMC suspension in the synthesis vessel, as well as in the samples recovered from MW1 at one hour, 12 hours and 24 hours after injection (Appendix B.5). Magnified TEM micrographs (Figure 3.3) indicate that the particles were dark spheres of high molecular weight with no significant morphological changes between injected particles and those recovered from MW1 (Appendix B.5). The diameter of nZVI nanoparticles in the synthesis drum sample (86.0 ± 12 nm ($n = 182$)) and the sample from MW1 after 1 hr (80.2 ± 15 nm ($n = 132$)) were similar. The MW1 samples collected after 12 and 24 hrs had nanoparticle diameters of 65.5 ± 10 nm ($n = 169$), and 79.3 ± 23 nm ($n = 195$) respectively. The quantitative parameters that were characterized are summarized in the supporting information (Appendix B.9). EDS analysis was also performed

on the 4 TEM samples to confirm the chemical composition of the nanoparticles. Wide area scans ($1.5\ \mu\text{m} \times 1.5\ \mu\text{m}$) showed the presence of Na, S, and Fe in all samples as these elements were used as precursors in nZVI synthesis (Appendix B.6). Although quantitative data cannot be extracted from the wide area EDS scans, it is noted that the percentage of Fe in these samples was relatively high. For the recovered nZVI samples from MW1 at 1, 12, and 24 hours after injection the percentage of Fe were 20.3, 42.9, and 69.9% respectively. Elemental analysis of a single particle from MW1 (dotted box in Fig 3.4, $90\text{nm} \times 90\text{nm}$) indicated that this nanoparticle was composed of mainly Fe (61% atomic percentage), Na (20%), Br (11%), S (<5%) and Cl (<3%) were also observed. The presence of Br was likely from the tracer test conducted prior to nZVI injection. Na composition is also expected to be high due to its use as a precursor during injection as well as in the tracer test. Soluble species (eg. Na, and Br) are present on the surface of the particles due to drying during sample preparation. Carbon, silicon and copper were also detected in significant amounts due to their presence in the TEM support media. This is the first time that nZVI particles recovered from sampling wells at an nZVI field trial have been quantified through TEM and EDS analysis.

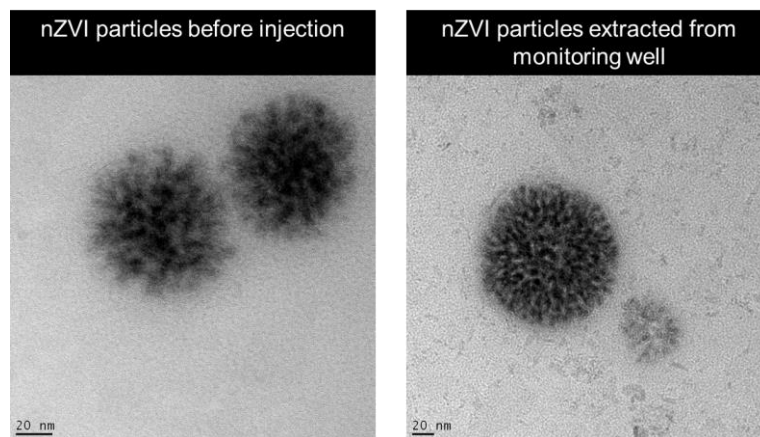


Figure 3.3: TEM Images of nZVI nanoparticles a) freshly synthesized prior to injection and b) recovered from MW1 following transport through the subsurface (12 hrs after injection began).

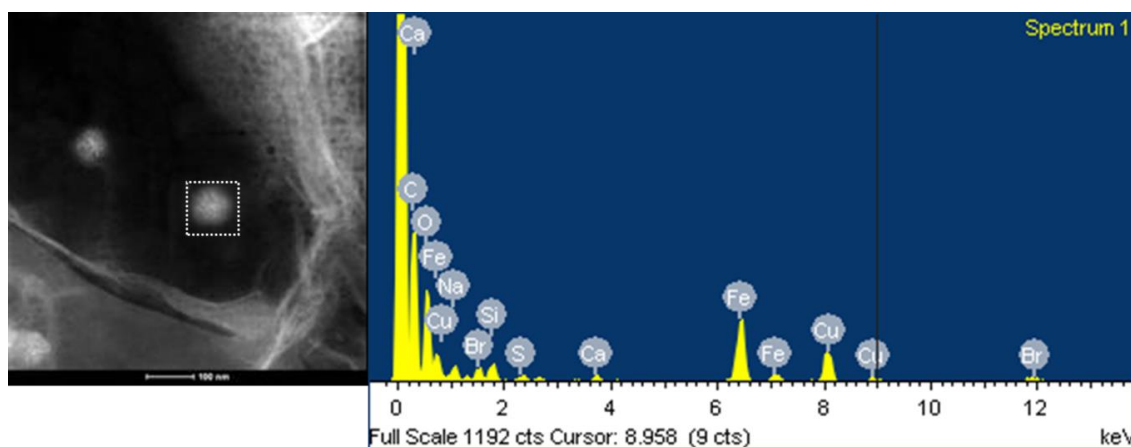


Figure 3.4: Energy dispersive spectroscopy (EDS) spectrum (right) for the nanoparticle (highlighted in left) collected from MW1 - 1hr following injection.

The polymer that stabilizes nZVI particles is indistinguishable from the TEM grid due to the low contrast of the low atomic weight of its constituents, mainly carbon. As such, TEM results provide quantitative information related to the size of the Fe nanoparticle. However, TEM analysis doesn't provide information related to the size of stabilized nanoparticles (i.e., nanoparticle + polymer stabilizer) that governs transport. DLS was therefore used to quantify the hydrodynamic diameter. The hydrodynamic diameter of the nZVI from the 5 synthesis batches was 624.8 ± 47.6 nm. The hydrodynamic diameter of the nZVI particles recovered from MW1 was measured to be 562.9 ± 212.7 nm over the period of injection. Given that the suspension was shown to be stable in batch tests, as discussed in section 5.2, and conditions for subsurface transport are very different than the conditions in the batch stability tests, observed DLS particle sizes are likely due to variability associated with field sampling and are not considered to be significantly different than injected. In addition, the zeta potential of nanoparticles recovered from MW1 was measured to be -48.3 ± 2.3 mV compared to -49.2 ± 1.5 mV in the synthesis vessel. Bare nZVI would be expected to have a lower magnitude of surface charge, zeta-potential for bare-nZVI has been reported to be -31.7 mV (Phenrat et al. 2007). This suggests that, for the recovered nanoparticles, the CMC coating remained intact during transport.

In the injected nZVI suspension, the Fe^0 content was 55% of the total Fe present. The Fe^0 breakthrough at MW1 achieved a maximum of 17.8 % of the total Fe measured at MW1 5 hours after the start of injection (Figure 3.2.b). The Fe^0 content in the particles recovered from MW1 decreased during the test reaching 4% of total Fe at the end of the injection period. This is consistent with the Fe^0 content trend in a recent study demonstrating nZVI transport (Johnson et al. 2013). However, Johnson *et al* (Johnson et al. 2013) observed significant yellow coloring in samples recovered from monitoring wells suggesting that nZVI oxidation occurred. In the present study, no yellow coloring was observed in samples recovered from monitoring wells as there was very limited oxygen present (dissolved oxygen at MW1 was 0.6 mg/L prior to injection and decreased to <0.2mg/L during injection, Appendix B.4.c) in the subsurface. Therefore, the decline in Fe^0 observed in the current study may be due to the decreasing injection rate resulting in residence time increase between INJW and MW1 over the period of injection. With increased residence time, the Fe^0 react with more dissolved oxygen, water, and other oxidizing species in the treatment area. Consequently, even though the dechlorination of PCE and TCE are the targeted reactions within the utility corridor, other constituents in the groundwater will contribute to the rapid decrease of Fe^0 content in the particles.

3.7 Environmental Implications

Results of this study suggest that nZVI synthesized in the presence of CMC polymer is mobile at the field scale, traveling at least 1 meter, to the first monitoring well. It also demonstrates, through very detailed characterization, that Fe^0 nanoparticles are of similar size and morphology after subsurface transport. However it is noted that the zero valent iron content quickly decreases, potentially due to reaction with the target contaminants, with water, or with natural reductant demand. Further work is needed to assess the extent of reaction with target contaminants, water, or natural reductant demand with the ultimate goal of designing nanometal formulations that optimize reactions with the target contaminants while maintaining good mobility. This study also suggests that injection of this type of nZVI/CMC suspension would not result in pore clogging that would limit subsequent remediation efforts. This is, in part, due to the very good nZVI suspension stability and this comes as a step forward in the application of nZVI. With all insitu remediation technologies, consideration must be made for the toxicity and safety of the injected amendments, not only as occupational hazards, but as stressors on ecosystem health. Additional work, is needed to develop a greater understanding

of nZVI transport and the processes governing contaminant degradation at a range of field sites.

3.8 Acknowledgments

The authors would like to acknowledge funding sources for this project for their support including the Natural Science and Engineering Research Council of Canada (NSERC), Dow Chemical Canada LLC. as well as CH2M Hill Canada Ltd. Thank you to Nikolai Mattison for his effort and expertise in laboratory procedures allowing for the expedited characterization of nanoparticle samples; Ambareen Atisha, Bahngmi Jung, Erica Pensini, Matt Horlings, Chris Kuron, Jeremy Meyer, Doug Smith, John Gowings, and Catherine Creber for their assistance in field work and organization; Also, thank you to Lisa Moffatt from CH2M Hill Canada Ltd. for her wisdom and consultation on Health and Safety controls.

3.9 References

- Bennett, P., F. He, D. Zhao, B. Aiken and L. Feldman (2010). "In Situ Testing of Metallic Iron Nanoparticle Mobility and Reactivity in a Shallow Granular Aquifer." Journal of Contaminant Hydrology **116**(1-4): 35-46.
- Berge, N. D. and C. A. Ramsburg (2009). "Oil-in-Water Emulsions for Encapsulated Delivery of Reactive Iron Particles." Environmental Science & Technology **43**(13): 5060-5066.
- Chowdhury, A. I. A., D. M. O'Carroll, Y. Xu and B. E. Sleep (2012). "Electrophoresis enhanced transport of nano-scale zero valent iron." Advances in Water Resources **40**(0): 71-82.
- Comba, S. and R. Sethi (2009). "Stabilization of highly concentrated suspensions of iron nanoparticles using shear-thinning gels of xanthan gum." Water Research **43**(15): 3717-3726.
- Davis, R. E., E. Bromels and C. L. Kibby (1962). "Boron Hydrides. III. Hydrolysis of Sodium Borohydride in Aqueous Solution." Journal of the American Chemical Society **84**(6): 885-892.

Elliott, D. W. and W.-x. Zhang (2001). "Field Assessment of Nanoscale Bimetallic Particles for Groundwater Treatment." Environmental Science & Technology **35**(24): 4922-4926.

EPA, U. S. (2008). EPA Fact Sheet: Nanotechnology for site remediation. S. W. a. E. Response. Washington DC, US.EPA. **EPA 542-F-08-009**.

Gavaskar A., T. L., Condit W., (2005). Contract Report: Cost and Performance Report: nanoscale zerovalent iron technologies for source remediation. Port Huenema, CA, NAVFAC: Naval Facilities Engineering Command. **CR-05-007-ENV**.

Glazier, R., R. Venkatakrishnan, F. Gheorghiu, L. Walata, R. Nash and Z. Wei-xian (2003). "Nanotechnology Takes Root." Civil Engineering (08857024) **73**(5): 64.

He, F., M. Zhang, T. Qian and D. Zhao (2009). "Transport of carboxymethyl cellulose stabilized iron nanoparticles in porous media: Column experiments and modeling." Journal of Colloid and Interface Science **334**(1): 96-102.

He, F. and D. Zhao (2005). "Preparation and Characterization of a New Class of Starch-Stabilized Bimetallic Nanoparticles for Degradation of Chlorinated Hydrocarbons in Water." Environmental Science & Technology **39**(9): 3314-3320.

He, F. and D. Zhao (2007). "Manipulating the Size and Dispersibility of Zerovalent Iron Nanoparticles by Use of Carboxymethyl Cellulose Stabilizers." Environmental Science & Technology **41**(17): 6216-6221.

He, F., D. Zhao, J. Liu and C. B. Roberts (2007). "Stabilization of Fe-Pd Nanoparticles with Sodium Carboxymethyl Cellulose for Enhanced Transport and Dechlorination of Trichloroethylene in Soil and Groundwater." Industrial & Engineering Chemical Research **46**(1): 29-34.

He, F., D. Zhao and C. Paul (2010). "Field assessment of carboxymethyl cellulose stabilized iron nanoparticles for in situ destruction of chlorinated solvents in source zones." Water Research **44**(7): 2360-2370.

Henn, K. W., Waddill, D.W. (2006). "Utilization of nanoscale zero-valent iron for source remediation - A case study." Remediation Journal **16**(2): 57-77.

- Hoch, L. B., E. J. Mack, B. W. Hydutsky, J. M. Hershman, J. M. Skluzacek and T. E. Mallouk (2008). "Carbothermal Synthesis of Carbon-supported Nanoscale Zero-valent Iron Particles for the Remediation of Hexavalent Chromium." Environmental Science & Technology **42**(7): 2600-2605.
- Husain, M. M., J. A. Cherry, S. Fidler and S. K. Frape (1998). "On the long-term hydraulic gradient in the thick clayey aquitard in the Sarnia region, Ontario." Canadian Geotechnical Journal **35**(6): 986-1003.
- Johnson, R. L., G. O. B. Johnson, J. T. Nurmi and P. G. Tratnyek (2009). "Natural Organic Matter Enhanced Mobility of Nano Zerovalent Iron." Environmental Science & Technology **43**(14): 5455-5460.
- Johnson, R. L., J. T. Nurmi, G. S. O'Brien Johnson, D. Fan, R. L. O'Brien Johnson, Z. Shi, A. J. Salter-Blanc, P. G. Tratnyek and G. V. Lowry (2013). "Field-Scale Transport and Transformation of Carboxymethylcellulose-Stabilized Nano Zero-Valent Iron." Environmental Science & Technology **47**(3): 1573-1580.
- Kanel, S., D. Nepal, B. Manning and H. Choi (2007). "Transport of surface-modified iron nanoparticles in porous media and application to arsenic(III) remediation." Journal of Nanoparticle Research **9**(5): 725-735.
- Kanel, S. R., R. R. Goswami, T. P. Clement, M. O. Barnett and D. Zhao (2008). "Two Dimensional Transport Characteristics of Surface Stabilized Zero-valent Iron Nanoparticles in Porous Media." Environmental Science & Technology **42**(3): 896-900.
- Karn, B., Kuiken, T., Otto, M. (2009). "Nanotechnology and in Situ Remediation: A Review of the Benefits and Potential Risks." Environ Health Perspect **117**(12): 1823-1831.
- Kocur, C. M., D. M. O'Carroll and B. E. Sleep (2013). "Impact of nZVI stability on mobility in porous media." Journal of Contaminant Hydrology **145**(0): 17-25.
- Krol, M. M., A. J. Oleniuk, C. M. Kocur, B. E. Sleep, P. Bennett, X. Zhong and D. M. O'Carroll (2013). "A Field-Validated Model for In Situ Transport of Polymer-Stabilized

nZVI and Implications for Subsurface Injection." Environmental Science & Technology **47**(13): 7332-7340.

Li, X. q., Elliot, D.W., Zhang, W.x. (2006). "Zero-Valent Iron Nanoparticles for Abatement of Environmental Pollutants: Materials and Engineering Aspects." Critical Reviews in Environmental Science and Technology **31**: 111-122.

Liu, Y., H. Choi, D. Dionysiou and G. V. Lowry (2005). "Trichloroethene Hydrodechlorination in Water by Highly Disordered Monometallic Nanoiron." Chemistry of Materials **17**(21): 5315-5322.

Liu, Y. and G. V. Lowry (2006). "Effect of Particle Age (Fe⁰ Content) and Solution pH On NZVI Reactivity: H₂ Evolution and TCE Dechlorination." Environmental Science & Technology **40**(19): 6085-6090.

Liu, Y., S. A. Majetich, R. D. Tilton, D. S. Sholl and G. V. Lowry (2005). "TCE Dechlorination Rates, Pathways, and Efficiency of Nanoscale Iron Particles with Different Properties." Environmental Science & Technology **39**(5): 1338-1345.

Martin, T. D., Brockhoff, C.A., Creed, J.T. (1994). Determination of metals and trace elements in water and wastes by inductively coupled plasma - atomic emission spectrometry Cincinnati, OH, U.S EPA National Exposure Research Laboartory: 58.

Mueller, N. C., J. Braun, J. Bruns, M. Cernik, P. Rissing, D. Rickerby and B. Nowack (2012). "Application of nanoscale zero valent iron (NZVI) for groundwater remediation in Europe." Environmental Science and Pollution Research **19**(2): 550-558.

Nurmi, J. T., P. G. Tratnyek, V. Sarathy, D. R. Baer, J. E. Amonette, K. Pecher, C. Wang, J. C. Linehan, D. W. Matson, R. L. Penn and M. D. Driessen (2005). "Characterization and Properties of Metallic Iron Nanoparticles: Spectroscopy, Electrochemistry, and Kinetics." Environmental Science & Technology **39**(5): 1221-1230.

Phenrat, T., A. Cihan, H.-J. Kim, M. Mital, T. Illangasekare and G. V. Lowry (2010). "Transport and Deposition of Polymer-Modified Fe⁰ Nanoparticles in 2-D Heterogeneous

Porous Media: Effects of Particle Concentration, Fe⁰ Content, and Coatings." Environmental Science & Technology **44**(23): 9086-9093.

Phenrat, T., H.-J. Kim, F. Fagerlund, T. Illangasekare, R. D. Tilton and G. V. Lowry (2009). "Particle Size Distribution, Concentration, and Magnetic Attraction Affect Transport of Polymer-Modified Fe⁰ Nanoparticles in Sand Columns." Environmental Science & Technology **43**(13): 5079-5085.

Phenrat, T., N. Saleh, K. Sirk, R. D. Tilton and G. V. Lowry (2007). "Aggregation and Sedimentation of Aqueous Nanoscale Zerovalent Iron Dispersions." Environmental Science & Technology **41**(1): 284-290.

Puls, R. W. and M. J. Barcelona (1996). Ground water issue: Low-flow (minimal drawdown) ground-water sampling procedures. Other Information: DN: See also PB--95-269643; PBD: Apr 1996; Medium: P; Size: 14 p.

Quinn, J., C. Geiger, C. Clausen, K. Brooks, C. Coon, S. O'Hara, T. Krug, D. Major, W.-S. Yoon, A. Gavaskar and T. Holdsworth (2005). "Field Demonstration of DNAPL Dehalogenation Using Emulsified Zero-Valent Iron." Environmental Science & Technology **39**(5): 1309-1318.

Raychoudhury, T., G. Naja and S. Ghoshal (2010). "Assessment of transport of two polyelectrolyte-stabilized zero-valent iron nanoparticles in porous media." Journal of Contaminant Hydrology **118**(3-4): 143-151.

Sakulchaicharoen, N., D. M. O'Carroll and J. E. Herrera (2010). "Enhanced stability and dechlorination activity of pre-synthesis stabilized nanoscale FePd particles." Journal of Contaminant Hydrology **118**(3-4): 117-127.

Saleh, N., H.-J. Kim, T. Phenrat, K. Matyjaszewski, R. D. Tilton and G. V. Lowry (2008). "Ionic Strength and Composition Affect the Mobility of Surface-Modified Fe⁰ Nanoparticles in Water-Saturated Sand Columns." Environmental Science & Technology **42**(9): 3349-3355.

- Saleh, N., T. Phenrat, K. Sirk, B. Dufour, J. Ok, T. Sarbu, K. Matyjaszewski, R. D. Tilton and G. V. Lowry (2005). "Adsorbed Triblock Copolymers Deliver Reactive Iron Nanoparticles to the Oil/Water Interface." Nano Letters **5**(12): 2489-2494.
- Saleh, N., K. Sirk, Y. Liu, T. Phenrat, B. Dufour, K. Matyjaszewski, R. D. Tilton and G. V. Lowry (2007). "Surface Modifications Enhance Nanoiron Transport and NAPL Targeting in Saturated Porous Media." Environmental Engineering Science **24**(1): 45-57.
- Schlesinger, H. I., H. C. Brown, A. E. Finholt, J. R. Gilbreath, H. R. Hoekstra and E. K. Hyde (1953). "Sodium Borohydride, Its Hydrolysis and its Use as a Reducing Agent and in the Generation of Hydrogen1." Journal of the American Chemical Society **75**(1): 215-219.
- Shi, Z., J. T. Nurmi and P. G. Tratnyek (2011). "Effects of Nano Zero-Valent Iron on Oxidation Reduction Potential." Environmental Science & Technology **45**(4): 1586-1592.
- Sun, Y.-P., X.-q. Li, J. Cao, W.-x. Zhang and H. P. Wang (2006). "Characterization of zero-valent iron nanoparticles." Advances in Colloid and Interface Science **120**(1-3): 47-56.
- Sun, Y.-P., X.-Q. Li, W.-X. Zhang and H. P. Wang (2007). "A method for the preparation of stable dispersion of zero-valent iron nanoparticles." Colloids and Surfaces A: Physicochemical and Engineering Aspects **308**(1-3): 60-66.
- Tiraferri, A., K. L. Chen, R. Sethi and M. Elimelech (2008). "Reduced aggregation and sedimentation of zero-valent iron nanoparticles in the presence of guar gum." Journal of Colloid and Interface Science **324**(1-2): 71-79.
- Tiraferri, A. and R. Sethi (2009). "Enhanced transport of zerovalent iron nanoparticles in saturated porous media by guar gum." Journal of Nanoparticle Research **11**(3): 635-645.
- Varadhi, S. N., Gill, H., Apoldo, L.J., Blackman, R.A., Wittman, W.K., (2005). Full-scale Nanoiron Injection for Treatment of Groundwater Contaminated with Chlorinated Hydrocarbons. Natural Gas Technologies Conf. Orlando. FLA.
- Vecchia, E. D., M. Luna and R. Sethi (2009). "Transport in Porous Media of Highly Concentrated Iron Micro- and Nanoparticles in the Presence of Xanthan Gum." Environmental Science & Technology.

Wang, C.-B. and W.-x. Zhang (1997). "Synthesizing Nanoscale Iron Particles for Rapid and Complete Dechlorination of TCE and PCBs." Environmental Science & Technology **31**(7): 2154-2156.

Wei, Y. T., S. C. Wu, C. M. Chou, C. H. Che, S. M. Tsai and H. L. Lien (2010). "Influence of nanoscale zero-valent iron on geochemical properties of groundwater and vinyl chloride degradation: A field case study." Water Research **44**(1): 131-140.

Zhan, J., T. Zheng, G. Piringer, C. Day, G. L. McPherson, Y. Lu, K. Papadopoulos and V. T. John (2008). "Transport Characteristics of Nanoscale Functional Zerovalent Iron/Silica Composites for in Situ Remediation of Trichloroethylene." Environmental Science & Technology **42**(23): 8871-8876.

Zhang, W.-x. (2003). "Nanoscale Iron Particles for Environmental Remediation: An Overview." Journal of Nanoparticle Research **5**(3): 323-332.

Chapter 4

4 Contributions of Abiotic and Biotic Dechlorination Following Carboxymethyl Cellulose Stabilized Nanoscale Zero Valent Iron Injection

Chris M.D. Kocur^{a,d}, Line Lomheim^b, Hardiljeet K. Boparai^a, Ahmed I.A. Chowdhury^a, , Kela P. Weber^c, Leanne M. Austrins^d, Elizabeth A. Edwards^b, Brent E. Sleep^e, Denis M. O'Carroll^{a*},

^a Civil & Environmental Engineering, Western University, 1151 Richmond St. London, Ontario, Canada, N6A 5B8

^b Chemical Engineering & Applied Chemistry, University of Toronto, 200 College Street Toronto, Ontario, M5S 3E5

^c Environmental Sciences Group, Chemistry and Chemical Engineering, Royal Military College of Canada, PO Box 17000, Station Forces, Kingston, Ontario, K7K 7B4

^d CH2M HILL Canada Limited, 72 Victoria St. Kitchener, Ontario, N2G 4Y9

^e Civil Engineering, University of Toronto, 35 St. George Street, Toronto, ON M5S 1A4

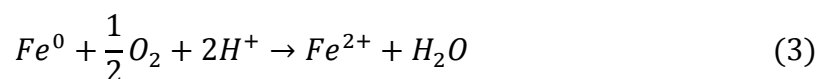
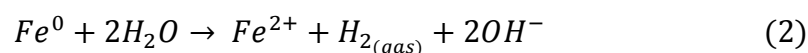
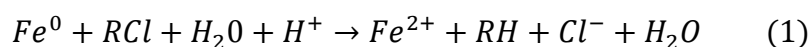
Keywords: nZVI, nanometals, field injection, *Dehalococcoides spp.*, qPCR, cVOC degradation

4.1 Abstract

A pilot scale injection of nanoscale zerovalent iron (nZVI) stabilized with carboxymethyl cellulose (CMC) was performed at an active field site contaminated with a range of chlorinated volatile organic compounds (cVOC). The cVOC concentrations and microbial populations were monitored at the site before and after nZVI injection. The remedial injection successfully reduced parent compound concentrations on site. A period of abiotic degradation was followed by a period of enhanced biotic degradation. Results suggest that the nZVI/CMC injection created conditions that stimulated the native populations of organohalide-respiring microorganisms. The abundance of *Dehalococcoides spp.* immediately following the nZVI/CMC injection increased by an order of magnitude throughout the nZVI/CMC affected area relative to pre-injection abundance. Distinctly higher cVOC degradation occurred as a result of the nZVI/CMC injection over a three week evaluation period when compared to control wells. This suggests that both abiotic and biotic degradation occurred following injection.

4.2 Introduction

Microscale zero valent iron (ZVI) (Matheson et al. 1994, Orth et al. 1995) and nanoscale ZVI (nZVI) (Wang et al. 1997, Zhang et al. 1997, Lien et al. 1999, Lien et al. 2001, Ponder et al. 2001) have been effective electron donors for the reductive dechlorination of a range of chlorinated ethenes and other chlorinated volatile organic compounds (cVOCs) in controlled laboratory studies. nZVI reacts with aqueous species, including cVOCs as follows:



Interpretation of the extent of abiotic degradation following nZVI application at the field scale is much more challenging than for batch experiments. nZVI will react with naturally occurring subsurface constituents limiting the quantity of Fe^0 available to react with target contaminants (Liu et al. 2007). Microorganisms present in the treatment zone may also degrade contaminants, potentially leading to overestimates of the extent of degradation attributable to nZVI. Given this complexity, determining the extent of contaminant degradation caused by reaction with nZVI in field scale tests has proven to be challenging (Henn 2006, Bennett et al. 2010, He et al. 2010, Johnson et al. 2013). Since nZVI addition does not result in complete removal of target contaminants in field application (Mace 2006) it would be desirable to maintain or stimulate long-term biodegradation during and following the period of abiotic nZVI reactivity. Thus, an improved understanding of the effect of nZVI on microbial activity is particularly important for assessments of long term impact of nZVI on contaminant degradation at field sites where biodegradation is known to be occurring.

Potential damage to ecosystem health due to the introduction of nanomaterials into the environment is of concern to regulators and to the public (Dunphy Guzman et al. 2006, Wiesner et al. 2006, Karn 2009, Simonet et al. 2009, Bernhardt et al. 2010, Lowry et al. 2010) due to the high surface activity and bioavailability of nanoparticles in natural systems. nZVI particles

may be toxic or induce stress in organisms in aquatic environments as has been shown for *E. coli* (Auffan et al. 2008, Lee et al. 2008, Li et al. 2010), *Bacillus subtilis* and *Pseudomonas fluorescens* (Diao et al. 2009), *Bacillus cereus* (Fajardo et al. 2013), fish species (Li et al. 2009, Chen et al. 2013), and other freshwater and marine organisms (Keller et al. 2012). Toxicity to rodent cells has also been linked to nZVI (Phenrat et al. 2009).

Reductive dechlorination has also been inhibited for specific consortia of organohalide-respiring organisms at elevated ZVI nanoparticle concentrations (Barnes et al. 2010, Xiu et al. 2010). Xiu *et al.* (2010) found that addition of bare nZVI to microcosms increased methanogenesis but inhibited TCE biodegradation (Xiu et al. 2010). Barnes *et al.* (2010) showed a decline in viable bacterial counts in microcosms containing a mixed culture from a contaminated site (Barnes et al. 2010). These results suggested that nZVI could be detrimental to microbial reductive dechlorination under direct and prolonged contact.

Field scale application of nZVI usually requires the addition of a cellulose polymer (or other anionic polymer or surfactant) to provide colloidal stability and mobility during nZVI injection and delivery (He et al. 2005, He et al. 2007, Phenrat et al. 2008, Sakulchaicharoen et al. 2010, Phenrat et al. 2011) and/or promote NAPL interaction (Saleh et al. 2005, Phenrat et al. 2009, Phenrat et al. 2011). For example, approximately half of previous nZVI field applications have included an amendment with polymers to increase nZVI colloidal stability (Comba et al. 2011). Several lab studies indicate that the polymer coating on nZVI may act as a buffer between microbial cell walls and the highly reductive ZVI surface, mitigating oxidative stress (Phenrat et al. 2009, Li et al. 2010, Xiu et al. 2010). Phenrat et al. (2009) found that a polyaspartate coating reduced toxicity of nZVI to mammalian cells, which they attributed to reduced nZVI sedimentation and reduced contact of nZVI with the cells. In the study of Li et al. (2010) toxicity of nZVI to *E. coli* was reduced by a polyaspartate coating, an effect attributed to reduced adhesion of nZVI to cells due to steric repulsion effects, similar reduced toxicity to *Agrobacterium sp.* has also been attributed to CMC coated nZVI (Zhou et al. 2014). Xiu et al. (2010) found that in a TCE degrading *Dehalococcoides (dhc)* containing culture, the reductive dehalogenases *tceA* and *vcrA* were downregulated when exposed to bare nZVI, but upregulated when exposed to olefin maleic acid copolymer coated nZVI.

Injection of nZVI can generate hydrogen and create strongly reducing conditions (Elliott et al. 2001, He et al. 2010) that are favorable for biotic reductive dechlorination. Strongly reducing conditions have been observed following injection of nZVI in many field studies (Glazier et al. 2003, Gavaskar A. 2005, Henn 2006, Mace 2006, Elliott 2010, He et al. 2010, Wei et al. 2010, Johnson et al. 2013). nZVI has also acted as a source of reducing equivalents for biotic processes in the treatment of nitrates (Shin et al. 2008). Polymers present in the nZVI suspension may also act as a fermentable substrate resulting in production of hydrogen that can be used by organohalide-respiring microorganisms (Kirschling et al. 2011). Kirschling *et al.* (2010) found that addition of polyaspartate coated nZVI did not decrease the count of total bacteria, and sulphate reducing and methanogenic microbial populations increased due to more reduced conditions and H₂ made available from the polymer coated nZVI. One study also found that the polymer coating can be bioavailable when bonded to a nanoparticle (Kirschling et al. 2011). A field study, evaluating the delivery of polymer stabilized nZVI, showed that cVOC degradation products continued to increase much longer than a laboratory based expected reactive lifetime of nZVI of 7 days (He et al. 2008, He et al. 2010). Although these studies showed that injection of polymer stabilized nZVI could lead to degradation of contaminants (Henn 2006, He et al. 2010, Wei et al. 2010), no quantitative field studies have investigated the changes in microbial communities immediately following nZVI/CMC injection.

The objective of this study was to determine the effect of nZVI/CMC injection on cVOC concentrations and microbial activity at a contaminated field site. nZVI/CMC mobility at this site was described in a previous study (Kocur et al. 2014). In the current study changes in cVOC concentrations and abundance of *dhc*, and the associated vinyl chloride reductase gene, were monitored along two flowpaths, only one of which was impacted by the injected nZVI. Balances of reducing equivalents were determined to provide insights into the impact of nZVI/CMC on reductive dechlorination at the site.

4.3 Methods

4.3.1 Site Description

The test site was located in Sarnia, Ontario in an area adjacent to a former cVOC production facility that ceased production 20 years ago. The area is underlain by a glacial deposit of clay that reaches depths between 10 and 50 m. The clay was previously characterized to have hydraulic conductivities on the order of 1.6×10^{-10} m/s with values for the near-surface weathered clay closer to 2.1×10^{-9} m/s (Husain et al. 1998). Due to the low permeability of the glacial deposit, the cVOC contaminants migrated primarily through man-made pathways and installations. One such pathway is a 100m long utility corridor that was excavated and backfilled with clayey sand and fine native clay material, creating a heterogeneous subsurface environment with permeable pathways through sandy areas. The nZVI injection test site was within this 3 m wide, 3-4 m deep corridor that had been capped with clay to prevent surface infiltration. Within the corridor, 0.45m diameter sumps installed at 50 m intervals prior to this study were used to control and monitor water levels.

4.3.2 Sampling and Analytical Methods

Site characterization details, hydraulic testing, sampling methods, and analytical methods for ions (e.g., chloride) were previously described (Kocur et al. 2014). nZVI samples were collected at the well head unpreserved in 40mL glass vials with zero headspace. Subsamples were preserved and analyzed in an anaerobic chamber within 16 hours of the completion of synthesis or emergence from a monitoring well. The primary contaminants that existed within the utility corridor were tetrachloroethene (PCE), trichloroethene (TCE), and chloroform, with other chlorinated ethenes, ethanes, and methanes in various amounts, either present as source contaminants stemming from the cVOC production or as biodegradation products. The groundwater samples for cVOC analysis were collected in 40-mL glass vials with zero headspace. Chlorinated ethenes and ethanes were determined by transferring 250 μ L aliquots to 2-mL GC vials containing 1 mL hexane for cVOC extraction. The extracted samples were then analyzed using an Agilent 7890 GC equipped with an Electron Capture Detector and a DB-624 capillary column (75m x 0.45mm, 2.55 μ m) following a modified EPA 8021 method. Lesser chlorinated ethenes, ethanes and methanes were determined by headspace mode of injection. Aliquots of 1 mL volume were transferred to 2 mL GC vials and equilibrated at 60°C

for 10 min prior to the injection of 0.25 mL of headspace via the autosampler (Agilent G4513A). Compounds were separated using a GS-Gaspro column (30m x 0.32 mm) on an Agilent 7890A GC equipped with a Flame Ionization Detector. External standards were used for calibration and the minimum detection limits range from 0.01 to 0.05 mg/L. Previous remedial work on the site revealed evidence that dechlorinating bacteria, including *dhc* capable of degrading cis-1,2 dichloroethene (cis-DCE) and vinyl chloride (VC), were abundant at the site. Microbiological samples were collected in 1L amber glass bottles with zero headspace and filtered within 48 hours of sampling through sterile 0.22 µm Sterivex filters (Millipore, Billerica, MA), using an Air Cadet Vacuum/Pressure Pump 400-1902 (Barnant Company, Barrington, IL). The filtered volume varied from 0.025 to 1L. The Sterivex filters were frozen at -80°C immediately after filtration.

4.3.3 DNA extraction and quantitative PCR (qPCR) analyses

DNA extractions were done using the UltraClean® Soil DNA isolation kit (Mo Bio Laboratories Inc., Carlsbad, CA). Filters were removed from the filter casing, sliced into small pieces with a sterile surgical blade, and the filter pieces were transferred to the bead-beating tube. The DNA was extracted by following the manufacturer's protocol for maximum yields, except that DNA was eluted in 50µL sterile UltraPure distilled water (Invitrogen, Carlsbad, CA) rather than the eluent provided with the kit. The DNA concentration and quality were assessed using a spectrophotometer (NanoDrop ND-1000; NanoDrop Technologies, Wilmington, DE). DNA samples were diluted 10 and 100 times with sterile UltraPure distilled water, and all subsequent sample manipulations were conducted in a PCR cabinet (ESCO Technologies, Gatboro, PA). Each qPCR reaction was run in duplicate. Two *dhc* genes were targeted by qPCR: 1) the phylogenetic 16S rRNA gene and 2) the functional vinyl chloride reductase gene, *vcrA*. Each qPCR run was calibrated by constructing a standard curve using known concentrations of plasmid DNA containing the gene insert of interest. The standard curve was run with 8 concentrations, ranging from 10 to 10⁸ gene copies/µL. All qPCR analyses were conducted using a CFX96 real-time PCR detection system, with a C1000 Thermo Cycler using SsoFast™ EvaGreen® supermix (Bio-Rad Laboratories, Hercules, CA). Each 20 µL qPCR reaction was prepared in sterile UltraPure distilled water containing 10 µL of EvaGreen® Supermix, 0.5 µL of each primer (forward and reverse, each from 10 µM stock solutions), and 2 µL of diluted template (DNA extract or standard plasmids). The

thermocycling program was as follows: initial denaturation at 95°C for 2 min, followed by 40 cycles of denaturation at 98°C for 5s, annealing at 60°C and 61°C (for 16S rRNA and *vcrA* genes, respectively) for 10s. A final melting curve analysis was conducted at the end of the program. The following primer sets were used: *Dehalococcoides* 16S rRNA Dhc1f (GATGAACGCTAGCGGCG) and Dhc264r (CCTCTCAGACCAGCTACCGATCGAA) (Grostern et al. 2009); and the vinyl chloride reductase gene *vcrA*_642f (GAAAGCTCAGCCGATGACTC) and *vcrA*_846r (TGGTTGAGGTAGGGTGAAGG) (Waller et al. 2005).

4.3.4 nZVI/CMC injection

The nZVI used in this study was synthesized in the field using borohydride precipitation in the presence of a carboxymethyl cellulose polymer (He et al. 2005, He et al. 2007). Detailed description and characterization of this nZVI/CMC slurry can be found in a previous study (Kocur et al. 2014). Briefly, 700 L of 1 g/L nZVI with 0.8% wt CMC polymer was injected at the test site via gravity. The injected nZVI particles averaged 86 ± 12 nm in diameter with a hydrodynamic diameter of 624.8 ± 47.6 nm (including the CMC polymer). Upon injection, the nZVI contained 55.4% Fe⁰ content, as determined by stoichiometric calculation from evolved hydrogen and total iron. The nZVI suspension travelled a distance of over one meter from 4 injection points, distributing nZVI within an areal extent of approximately 3 m² within the sandy test area. This estimate is based on heads measured during the field test, hydraulic conductivity measurements, and porosity (Kocur et al. 2014). Kocur *et al* (2014) also determined that 17% of the zero valent iron content was available for reaction in the aqueous sample recovered in MW1. The injection was vertically distributed over a 0.6-1.6 m screened interval, creating a reactive flowpath where the nZVI travelled. The nZVI distribution, along with tracer distribution and hydraulic test results, was used in the development of the conceptual model of the treatment area (Figure 4.1 and shown in more detail in Appendix A.1). This conceptual model illustrates the nZVI flowpath and an adjacent low-flow pathway that was not significantly affected by nZVI/CMC injection. Appendix C.2.a-c present geochemical data supporting the conceptual model of nZVI distribution.

4.3.5 Estimating abiotic and biotic dechlorination

To assess the biotic and abiotic contributions to the reductive dechlorination of cVOCs, reducing equivalent calculations were performed. This was done by quantifying reducing equivalents introduced to the system and reducing equivalents utilized within the system through reductive dechlorination of cVOCs (abiotic and biotic). The total injected Fe^0 mass was used to calculate the reducing equivalents that were added to the system during the field trial. Reducing equivalents utilized within the system were calculated in three ways. Reducing equivalents that were required for observed cVOC transformation were calculated, as well as reducing equivalents required for the observed chloride production following injection. The change in abundance of *dhc*, an obligate organohalide-respiring microorganism, was also used to estimate reducing equivalents attributable to the biotic degradation of cVOCs. *dhc* was the only strain enumerated using qPCR. Appendices C.3 through C.5 and the surrounding discussion show the methodology for estimating reducing equivalents. Reducing equivalents are presented as a change in molar concentration compared to the background sample. Example calculations are provided along with a summary Appendices C.3-C.5.

4.4 Results and Discussion

4.4.1 Composition of cVOCs along nZVI flowpath

The degradation of cVOCs in the treatment area was monitored immediately following nZVI injection to quantify cVOC degradation downstream of the injection area. Figure 4.1 shows the monitoring wells as well as a conceptual model of the different flowpaths. The data is presented for each well along a given flowpath (e.g., MW1 to MW6 to MW5) at different sampling times. The data represents cVOC composition (pie chart) and total cVOC concentration (i.e., radius is proportional to total concentration) at a given sampling time.

Noticeable shifts in cVOC composition occurred along flowpath #1, where nZVI/CMC migration was reported previously (Kocur et al. 2014). In the three weeks following nZVI injection the composition of cVOCs along flowpath #1 shifted towards lesser chlorinated compounds, creating a distinct pattern of dechlorination that moved downstream from the injection well, through MW1, and towards MW6. This composition change can be attributed to nZVI/CMC injection. For example, at monitoring wells where nZVI migrated (MW1) and further downstream (MW6), cVOC composition prior to nZVI injection was made up of a large

portion of parent compounds. In MW1 and MW6, the PCE and TCE together made up 40% and 25% of the total cVOCs composition, respectively. In the 10 days following nZVI injection, the total cVOCs decreased by 20% in MW1 and the parent compounds decreased to less than 10% of the total cVOCs. At MW6, that is 2.5 m downgradient of the injection well, the total aqueous phase cVOC concentration 10 days after injection approximately doubled, presumably as nZVI reacted with both aqueous phase and sorbed phase parent constituents, creating daughter products, cis-DCE and VC, that are more soluble than the parent compounds. This suggests that in a field scenario intermediate by-products may temporarily exist prior to complete abiotic degradation. However, in a multi-component cVOC system the parent compound in degradation cannot be identified.

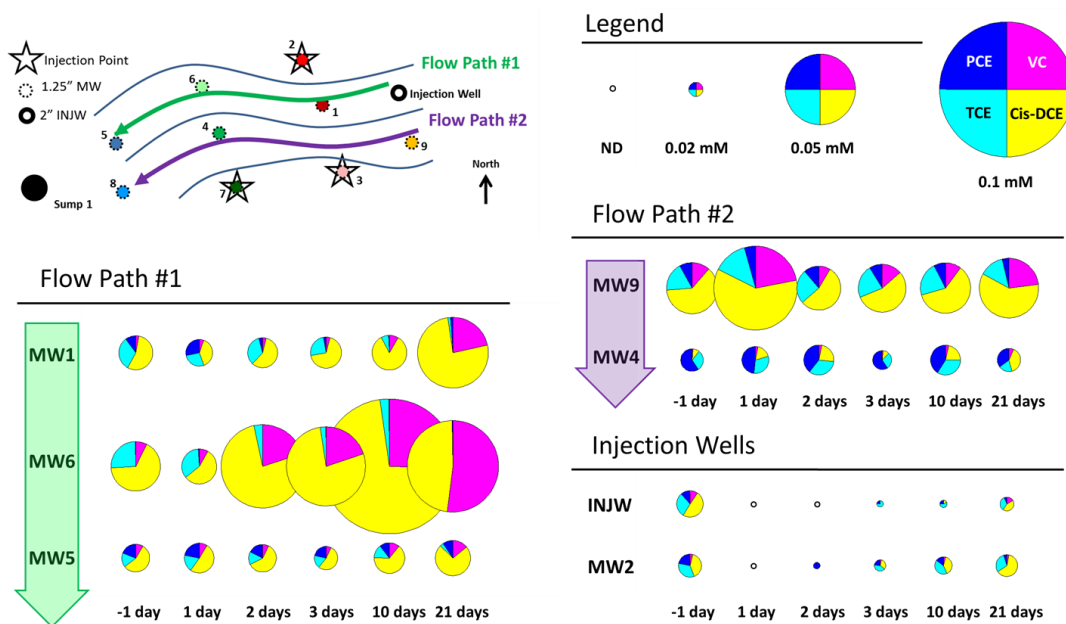


Figure 4.1: Composition of cVOCs shown as a pie chart with the total cVOC concentration represented as the radius for the monitoring wells. Flow path #1, shown in green, shows the path of nZVI travel from the primary injection well. The adjacent flow path #2, shown in purple, was not affected by the nZVI/CMC injection.

In MW6, increasing total cVOC concentrations, particularly of daughter compounds, coincided with the estimated arrival of the injection front that carried the bulk of the degradation products from the nZVI injection 10 days earlier. The cVOC changes in MW6

were the only indication of nZVI/CMC presence as no change in ORP was quantified during injection (Kocur et al. 2014). The changes in cVOCs at MW1 coincided with a significant decrease in oxidation reduction potential (ORP) which is commonly attributed to nZVI travel. In MW1, nZVI/CMC presence was definitively shown through the characterization of nanoparticles in the well (Kocur et al. 2014). Based on the hydraulic gradient and range of hydraulic conductivities along the flowpath, the expected arrival of the injection front was predicted to reach MW6 between 4 and 25 days. Three weeks after injection the cVOC composition shifted to predominantly daughter products, with cis-DCE and VC comprising 90% of the total measured cVOCs at MW1 and MW6. Further downgradient along this flowpath, at MW5 located 3.5 m downgradient of the injection, no buildup of daughter products was observed. cVOC concentrations did not increase, and only a small compositional shift was measured. This suggests that the daughter products within the injection front degraded within the travel time and distance between MW6 and MW5. This is consistent with column studies evaluating nZVI reactivity with PCE, showing that contact time determines the degradation products in reactive transport of nZVI (Taghavy et al. 2010).

The composition shifts within the injection wells (INJW and MW2) were somewhat different than in the nZVI monitoring wells. Parent compound concentrations at INJW and MW2 dropped to below detection limits immediately after injection but rebounded to near pre-injection concentrations after three weeks. These changes are related to dilution from the injection fluid. During the period of rebound, 2 to 10 days after injection at these two injection wells, the cVOCs detected were primarily the same parent compounds as the background. Twenty-one days after injection there was a shift in the cVOC composition in MW2 as more daughter products appeared. It is anticipated that this shift in cVOCs coincided with the onset of stimulated biotic activity on site. This may also have been caused by rebounding aqueous cVOCs from upstream sources. The degradation that was observed in the injection well at this time was likely not the result of abiotic reaction, as the reactivity of nZVI in aqueous suspension is reported to lose reactivity after 7 days (He et al. 2008). nZVI deposited in aquifer material is more likely to persist in the subsurface for longer periods of time. For example nZVI has recently been reported to remain reactive for up to one month under anaerobic conditions (Adeleye et al. 2013). It has been previously reported that the most mobile fraction of nZVI contains the lowest Fe^0 content compared to the less mobile fraction (Phenrat et al.

2009). The effects of dilution due to the volume of nZVI/CMC injected has not been fully investigated to date, but is expected to play a major role following injection. Another issue that complicates analysis following the injection of nZVI/CMC is the change in cVOC solubility (Phenrat et al. 2009) due to the addition of polymer with the injection fluid.

During the field trial, nZVI/CMC was not detected in monitoring wells along the low-flow pathway # 2 (i.e., MW4 and MW9) (Figure 4.1). Therefore, this flow path was used as a control with respect to the effects of nZVI/CMC injection. Minor changes in the cVOC composition and total cVOC concentrations were observed in MW4 over the monitoring period; the total cVOC concentration varied within 30% during the sampling period while the composition of PCE and TCE decreased from about 75% of the total molar concentration to about 40% after 21 days. At MW9, which is located 1 m from the injection well, perpendicular to the flow direction, in flow path #2, individual and total cVOC concentrations fluctuated during the monitoring period. The MW9 catchment may have been partially affected by the nearby injection during early sampling events as a small decrease in ORP was noticed. This may explain some of the cVOC concentration changes at MW9, however, over the monitoring period the cVOCs in MW9 were more similar to MW4 than to any other well on site; with the composition of cis-1,2 DCE steady between 50 to 56% of the total cVOC composition and no increase in the total cVOC concentration.

4.4.2 Short term microbiological response to nZVI

Figure 4.2 shows the gene copies of *dhc* per liter of groundwater from qPCR analysis, a measure of the abundance of the typical organohalide-respiring organisms at chlorinated-ethene contaminated sites. Abundant *dhc* populations present in background samples at all monitoring wells are evidence of biotic reductive dechlorination of cVOCs on site prior to nZVI/CMC injection. There is a distinct increase in *dhc* abundance in wells along the nZVI flowpath following nZVI/CMC injection. For example, *dhc* populations increased in monitoring wells where nZVI/CMC was transported (MW1) and an abundant *dhc* population was also present 2.5 m downgradient of the primary injection well (MW6) 2 days after nZVI/CMC injection. The results suggest that where the nZVI/CMC was transported, significant biotic activity also occurred. In these wells there were also very high measurements

of total organic carbon (TOC) due to the CMC in the injection. In the primary injection well, *dhc* decreased following injection, however, this was presumably due to the large injection volume displacing resident pore fluid. In MW2, where less nZVI/CMC suspension was injected *dhc* populations increased 2 days after injection.

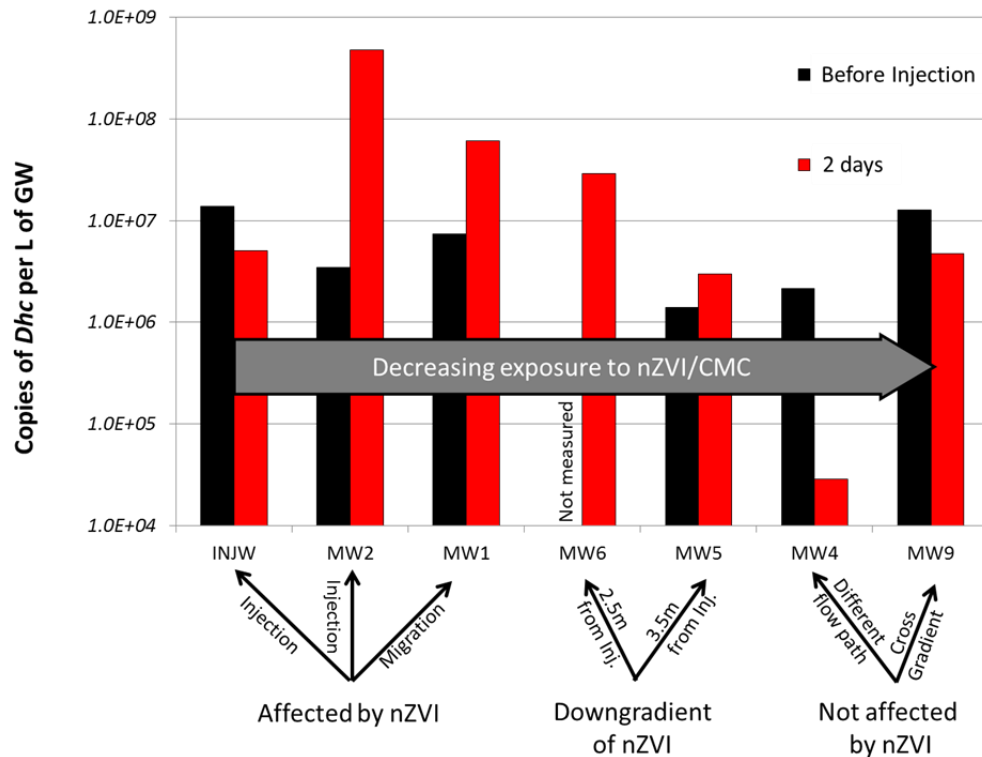


Figure 4.2: qPCR was performed on aqueous samples prior to and two days following nZVI/CMC injection to determine the abundance of *Dehalococcoides* (*dhc*). The wells are ordered by decreasing exposure to nZVI/CMC from left to right. Injection wells (INJW and MW2) and the well where nZVI/CMC travelled (MW1) were most affected, followed by downgradient wells (MW6 and MW5). The wells along the adjacent flow path (MW4 and MW9) were least affected by the nZVI/CMC injection.

Along flowpath #2 (MW4 and MW9), where nZVI did not migrate, *dhc* abundance decreased (Figure 4.2) over the study period. Abundant populations of *dhc* were present prior to nZVI/CMC injection and the presence of some daughter products confirms that biotic degradation of cVOCs was occurring in these areas not impacted by nZVI/CMC injection.

There was no elevated TOC measured in these wells. Decreases in the *dhc* population in MW4 2 days after the injection are believed to be due to the effects of sampling the well. The aqueous sample volume required to retrieve enough biomass for analysis was large and may have contributed to a washout of bacteria in these control wells over this short period of sampling. In the control well (MW9) adjacent to the nZVI flowpath, the *dhc* populations remained constant.

The measurement of *dhc* abundance in this study was complemented by the quantification of *vcrA* gene abundance within the *dhc* population. The abundance of *vcrA* is in good agreement with *dhc* abundance (Appendix C.6) showing that the majority of the *dhc* populations on the site harbor the vinyl chloride reductase gene. This is important because not all species of *dhc* are capable of reducing *cis*-DCE and VC to ethene; only organisms containing vinyl chloride reductase genes such as *vcrA* are capable of transforming chlorinated ethenes completely to ethene (Ritalahti et al. 2006).

4.4.3 Estimating nZVI vs. Biotic Degradation

A summary of calculations for reducing equivalents are shown in Table 4.1, with detailed calculations given in the Supplementary Information. The mass of nZVI injected would have yielded a maximum of 13.9 moles of reducing equivalents, making these available for reaction with target cVOCs, oxygen, water, and other reducible species (eg. nitrate and sulfate) (Liu et al. 2007, Reinsch et al. 2010). Reducing equivalents calculated from increased chloride concentrations are higher than the values calculated from changes in cVOC concentrations. As ethene, ethane, and methane were not measured, and therefore not included in the cVOC transformation calculations, the difference may be partly attributed to chloride produced from the production of these compounds. Sorption of cVOCs, both parent and degradation products is also not accounted for in the cVOC transformation calculations, nor is the estimate specific to a single reaction pathway as there is a mixture of compounds and the source cannot be confidently stated. Therefore the chloride data are considered the most reliable. In MW4 and MW9 many of the reducing equivalents estimates are negative, however, this is not possible given the environmental conditions on site. The negative estimate occurs when the reducing equivalents in the background (-1.2 days) are greater than the reducing

equivalents following injection, suggesting that there is a missing component in the mass balance. It is possible that the negative values are an artifact of injection fluid dilution. This missing component could be sorbed mass entering aqueous solution or perhaps back diffusion from a less permeable zone. These negative values are most likely the result of oversampling these wells despite efforts to maintain very low sampling rates, drawing sample from a catchment following injection that is not representative of the pre-injection conditions.

Table 4.1: Estimated electron equivalents (as a concentration, mol/L) from reaction following injection of nZVI/CMC.

Balance of electron reducing equivalents									
	Electron Reducing Equivalents								
	$\mu\text{mol/L}$								
Source	Δdhc	$\Delta c\text{VOCs}$				ΔCl			
Observation	2 days	2 days	3 days	10 days	21 days	2 days	3 days	10 days	21 Days
MW1	0.64	- 5.9	1.5	25	170	560	680	2000	5400
MW6	0.27	160	140	370	230	5900	3400	6300	7400
MW5	0.019	0.16	-17	17	39	- 620	- 820	890	1600
MW9	- 0.097	- 33	- 14	- 6.4	45	- 2600	1500	- 510	3200
MW4	- 0.025	32	- 3.7	30	28	- 750	- 1700	- 5000	- 5000
MW2	5.7	- 42	- 31	- 14	3.3	N/A	- 5500	- 4000	- 5000

Microbial reductive dechlorination of cVOCs also results in transformation of electron equivalents through metabolic organohalide respiration. Metabolic growth and reproduction of the microorganisms can be related to the reducing equivalents through the yield coefficient (Löffler et al. 2013) with the assumption that the environmental conditions for growth and activity can be extended to field application. Quantification of the *dhc* via qPCR allows for the calculation of the reducing equivalents involved in reductive dechlorination by microorganisms. Along flowpath #1, the elevated reducing equivalents suggest that there was microbial degradation occurring following injection, this is due to the increased microbial abundance. Along the adjacent flowpath #2 little change was observed compared to the background conditions. Similar to electron equivalents for cVOC degradation at 2 days, the electron equivalents calculated from increased microbial abundance are less than that of electron equivalents associated with Cl^- production. This could, in part, be attributable to a considerable amount of abiotic degradation in the 2 days following nZVI injection. However, it could also be due to a possible underestimation of the abundance of dechlorinating organisms. In this study, only suspended *dhc* were quantified. Other dechlorinating organisms

present at the site (ie. *dehalobacter*, *geobacter*) and any dechlorinating organisms attached to subsurface solids (Cápiro et al. 2014) would therefore not be included in the calculations. The extraction process for DNA is not 100% efficient, which may lead to underestimated DNA concentrations compared to the groundwater.

The biological component of degradation cannot be compared to the 21 day results because qPCR data was not available at day 21. However, the reducing equivalents utilization based on direct measurements (e.g., chloride evolution and cVOC transformation) during this time period suggests that there was significant degradation occurring. At some time during this period biotic degradation would have been expected to become the dominant degradation process as available Fe^0 would have been oxidized depleting reactivity of nZVI particles and limiting the long term extent of abiotic degradation. The reducing equivalent analysis suggests that greater dechlorination (i.e., chloride analysis) occurred than what was apparent from cVOC samples. It is important to note that microbial breakdown of CMC would also contribute to the reducing equivalents of the system, which is not accounted for in this analysis but should be quantified in further studies. Earlier investigation of CMC degradation suggested that 31% is digestible over a 4 day period in an anaerobic culture (Soundar et al. 1987), however, this result will vary widely depending on the environmental conditions. It is hypothesized that CMC would be metabolized to cellulose rapidly and used to support microbial reductive dechlorination *insitu*. nZVI likely provided a significant portion of the reducing equivalents initially in the system through the production of hydrogen gas, which may also be utilized biotically over an extended period of time as has been shown in other anaerobic systems (Zhu et al. 2012). It has been shown that nZVI can retain reactivity over a long period of time in the laboratory, with Fe^0 half-life as long as 160 days for crystalline nZVI (Liu et al. 2006). Oxidants such as contaminants and minerals are abundant in the subsurface which would constrain reaction longevity. The longevity of nZVI/CMC has yet to be well documented in literature.

4.5 Environmental Implications

The results show that the *dhc* population increased specifically in areas that were impacted by CMC stabilized nZVI injection, increasing cVOC degradation.. Along the nZVI flowpath, during the first two days following injection, organohalide-respiring organisms

increased by an order of magnitude. Increased abundance did not occur along the control flowpath, where degradation remained at a background level. One explanation for the increased abundance of organohalide-respiring microorganisms in the nZVI impacted flowpath is the cathodic production of H₂ from nZVI reaction with water. This has been previously reported for methanogenic, sulfur reducing, and organohalide-respiring microorganisms in lab studies (Weathers et al. 1997, Kirschling et al. 2010, Xiu et al. 2010, Jeon et al. 2013). Clearly the CMC polymer in this study and other stabilizing agents used in previous studies with nZVI can be an electron donor for microbial dechlorination. Nevertheless, few studies to date have evaluated the effects of nZVI injections on cVOC degrading microbial communities in the field. Positive remedial results were also reported following previous applications of nZVI long after nZVI would have oxidized, limiting abiotic degradation (Henn 2006, He et al. 2010). This suggests that biotic degradation was important following nZVI addition. In contrast, some laboratory studies suggest that nZVI inhibited microbial activity in mixed cultures containing *dhc* (Barnes et al. 2010, Xiu et al. 2010). Barnes et al (2010) reported that the rate of biological degradation decreases at about 0.1 g/L nZVI dose and is completely inhibited at approximately 0.3 g/L for Ni/Fe nanoparticles. Xiu et al (2010) found that bare nZVI down-regulated gene expression of specific dechlorinating reductive dehydrogenases *tceA* and *vcrA*, however this inhibition did not occur over a several day period when a polymer coating accompanied the nZVI. These lab studies may not adequately reproduce in situ conditions. In the current study, the increased *dhc* and *vcrA* abundance and the increase in cVOC daughter products suggest that the microbial communities were able to thrive following nZVI/CMC injection, most likely as a result of altered environmental conditions associated with the injection, rather than interaction with nZVI itself.

Recent publications have demonstrated the ability to deliver nZVI/CMC to the subsurface reliably, and this study demonstrates that a dose of 1 g/L nZVI can be effectively coupled with organohalide-respiring microorganisms in degrading cVOCs in-situ. This study presents evidence that microbial activity was significantly enhanced within two days of the injection of nZVI/CMC. The carboxymethyl cellulose polymer provides a biological substrate that appears to promote reductive dechlorination through organohalide-respiring organisms (eg. *dhc*). Furthermore, this study highlights the importance of detailed characterization to accurately assess site remediation goals using nZVI. Without delineating

the extent of nZVI transport in this study, the effectiveness of remediation could not have been accurately interpreted. Therefore, methods of evaluating nZVI transport on site must be investigated further and refined to complement the suite of analyses for cVOC degradation.

In summary nZVI application at this site resulted in considerable cVOC degradation, involving both abiotic and stimulated biotic degradation. This suggests that application of nZVI at contaminated field sites should not be considered solely on the basis of abiotic degradation but consideration should be given to the long term biotic degradation that is stimulated when designing remedial activities.

4.6 Acknowledgements

The authors acknowledge the sources of funding for this study including the Ontario Research Fund and Natural Science and Engineering Research Council, Dow Chemical, and CH2M HILL Canada Limited. The work would not have been possible without the hard work of Dr. Prabhakar Sharma and Dr. Nataphan Sakulchaicharoen during preparation and laboratory analysis as well as Chris Kuron for his integral role in data collection and field site coordination.

4.7 References

- Adeleye, A., A. Keller, R. Miller and H. Lenihan (2013). "Persistence of commercial nanoscaled zero-valent iron (nZVI) and by-products." Journal of Nanoparticle Research **15**(1): 1-18.
- Auffan, M., W. Achouak, J. Rose, M.-A. Roncato, C. Chaneï, D. T. Waite, A. Masion, J. C. Woicik, M. R. Wiesner and J.-Y. Bottero (2008). "Relation between the Redox State of Iron-Based Nanoparticles and Their Cytotoxicity toward *Escherichia coli*." Environmental Science & Technology **42**(17): 6730-6735.
- Barnes, R. J., O. Riba, M. N. Gardner, A. C. Singer, S. A. Jackman and I. P. Thompson (2010). "Inhibition of biological TCE and sulphate reduction in the presence of iron nanoparticles." Chemosphere **80**(5): 554-562.
- Bennett, P., F. He, D. Zhao, B. Aiken and L. Feldman (2010). "In Situ Testing of Metallic Iron Nanoparticle Mobility and Reactivity in a Shallow Granular Aquifer." Journal of Contaminant Hydrology **116**(1-4): 35-46.
- Bernhardt, E. S., B. P. Colman, M. F. Hochella, B. J. Cardinale, R. M. Nisbet, C. J. Richardson and L. Y. Yin (2010). "An Ecological Perspective on Nanomaterial Impacts in the Environment." Journal of Environmental Quality **39**(6): 1954-1965.
- Cápiro, N. L., Y. Wang, J. K. Hatt, C. A. Lebrón, K. D. Pennell and F. E. Löffler (2014). "Distribution of Organohalide-Respiring Bacteria between Solid and Aqueous Phases." Environmental Science & Technology **48**(18): 10878-10887.
- Chen, P.-J., W.-L. Wu and K. C.-W. Wu (2013). "The zerovalent iron nanoparticle causes higher developmental toxicity than its oxidation products in early life stages of medaka fish." Water Research **47**(12): 3899-3909.
- Comba, S., A. Di Molfetta and R. Sethi (2011). "A comparison between field applications of nano-, micro-, and millimetric zero-valent iron for the remediation of contaminated aquifers." Water, Air, and Soil Pollution **215**(1-4): 595-607.

Diao, M. and M. Yao (2009). "Use of zero-valent iron nanoparticles in inactivating microbes." Water Research **43**(20): 5243-5251.

Dunphy Guzman, K. A., M. R. Taylor and J. F. Banfield (2006). "Environmental Risks of Nanotechnology: National Nanotechnology Initiative Funding, 2000-2004." Environmental Science & Technology **40**(5): 1401-1407.

Elliott, D. (2010). nZVI Field Application Case Studies in the U.S. USEPA Clu-In Webinar: Field scale Remediation Experience using Iron Nanoparticles and Evolving Risk-Benefit Understanding.

Elliott, D. W. and W.-x. Zhang (2001). "Field Assessment of Nanoscale Bimetallic Particles for Groundwater Treatment." Environmental Science & Technology **35**(24): 4922-4926.

Fajardo, C., M. L. Saccà, M. Martinez-Gomariz, G. Costa, M. Nande and M. Martin (2013). "Transcriptional and proteomic stress responses of a soil bacterium *Bacillus cereus* to nanosized zero-valent iron (nZVI) particles." Chemosphere **93**(6): 1077-1083.

Gavaskar A., T. L., Condit W., (2005). Contract Report: Cost and Performance Report: nanoscale zerovalent iron technologies for source remediation. Port Huenema, CA, NAVFAC: Naval Facilities Engineering Command. **CR-05-007-ENV**.

Glazier, R., R. Venkatakrishnan, F. Gheorghiu, L. Walata, R. Nash and Z. Wei-xian (2003). "Nanotechnology Takes Root." Civil Engineering (08857024) **73**(5): 64.

Groster, A. and E. A. Edwards (2009). "Characterization of a Dehalobacter Coculture That Dechlorinates 1,2-Dichloroethane to Ethene and Identification of the Putative Reductive Dehalogenase Gene." Applied and Environmental Microbiology **75**(9): 2684-2693.

He, F. and D. Zhao (2005). "Preparation and Characterization of a New Class of Starch-Stabilized Bimetallic Nanoparticles for Degradation of Chlorinated Hydrocarbons in Water." Environmental Science & Technology **39**(9): 3314-3320.

He, F. and D. Zhao (2007). "Manipulating the Size and Dispersibility of Zerovalent Iron Nanoparticles by Use of Carboxymethyl Cellulose Stabilizers." Environmental Science & Technology **41**(17): 6216-6221.

- He, F., D. Zhao and C. Paul (2010). "Field assessment of carboxymethyl cellulose stabilized iron nanoparticles for in situ destruction of chlorinated solvents in source zones." Water Research **44**(7): 2360-2370.
- He, F. and D. Y. Zhao (2008). "Hydrodechlorination of trichloroethene using stabilized Fe-Pd nanoparticles: Reaction mechanism and effects of stabilizers, catalysts and reaction conditions." Applied Catalysis B-Environmental **84**(3-4): 533-540.
- Henn, K. W., Waddill, D.W. (2006). "Utilization of nanoscale zero-valent iron for source remediation - A case study." Remediation Journal **16**(2): 57-77.
- Husain, M. M., J. A. Cherry, S. Fidler and S. K. Frappe (1998). "On the long-term hydraulic gradient in the thick clayey aquitard in the Sarnia region, Ontario." Canadian Geotechnical Journal **35**(6): 986-1003.
- Jeon, J.-R., K. Murugesan, I.-H. Nam and Y.-S. Chang (2013). "Coupling microbial catabolic actions with abiotic redox processes: A new recipe for persistent organic pollutant (POP) removal." Biotechnology Advances **31**(2): 246-256.
- Johnson, R. L., J. T. Nurmi, G. S. O'Brien Johnson, D. Fan, R. L. O'Brien Johnson, Z. Shi, A. J. Salter-Blanc, P. G. Tratnyek and G. V. Lowry (2013). "Field-Scale Transport and Transformation of Carboxymethylcellulose-Stabilized Nano Zero-Valent Iron." Environmental Science & Technology **47**(3): 1573-1580.
- Karn, B., Kuiken, T., Otto, M. (2009). "Nanotechnology and in Situ Remediation: A Review of the Benefits and Potential Risks." Environ Health Perspect **117**(12): 1823-1831.
- Keller, A. A., K. Garner, R. J. Miller and H. S. Lenihan (2012). "Toxicity of Nano-Zero Valent Iron to Freshwater and Marine Organisms." PLoS ONE **7**(8): e43983.
- Kirschling, T. L., P. L. Golas, J. M. Unrine, K. Matyjaszewski, K. B. Gregory, G. V. Lowry and R. D. Tilton (2011). "Microbial Bioavailability of Covalently Bound Polymer Coatings on Model Engineered Nanomaterials." Environmental Science & Technology **45**(12): 5253-5259.

- Kirschling, T. L., K. B. Gregory, J. E. G. Minkley, G. V. Lowry and R. D. Tilton (2010). "Impact of Nanoscale Zero Valent Iron on Geochemistry and Microbial Populations in Trichloroethylene Contaminated Aquifer Materials." Environmental Science & Technology **44**(9): 3474-3480.
- Kocur, C. M., A. I. Chowdhury, N. Sakulchaicharoen, H. K. Boparai, K. P. Weber, P. Sharma, M. M. Krol, L. Austrins, C. Peace, B. E. Sleep and D. M. O'Carroll (2014). "Characterization of nZVI Mobility in a Field Scale Test." Environmental Science & Technology **48**(5): 2862-2869.
- Lee, C., J. Y. Kim, W. I. Lee, K. L. Nelson, J. Yoon and D. L. Sedlak (2008). "Bactericidal Effect of Zero-Valent Iron Nanoparticles on Escherichia coli." Environmental Science & Technology **42**(13): 4927-4933.
- Li, H., Q. Zhou, Y. Wu, J. Fu, T. Wang and G. Jiang (2009). "Effects of waterborne nano-iron on medaka (*Oryzias latipes*): Antioxidant enzymatic activity, lipid peroxidation and histopathology." Ecotoxicology and Environmental Safety **72**(3): 684-692.
- Li, Z. Q., K. Greden, P. J. J. Alvarez, K. B. Gregory and G. V. Lowry (2010). "Adsorbed Polymer and NOM Limits Adhesion and Toxicity of Nano Scale Zerovalent Iron to E. coli." Environmental Science & Technology **44**(9): 3462-3467.
- Lien, H.-L. and W.-x. Zhang (1999). "Transformation of Chlorinated Methanes by Nanoscale Iron Particles." Journal of Environmental Engineering **125**(11): 1042-1047.
- Lien, H.-L. and W.-x. Zhang (2001). "Nanoscale iron particles for complete reduction of chlorinated ethenes." Colloids and Surfaces A: Physicochemical and Engineering Aspects **191**(1-2): 97-105.
- Liu, Y. and G. V. Lowry (2006). "Effect of Particle Age (Fe⁰ Content) and Solution pH On NZVI Reactivity: H₂ Evolution and TCE Dechlorination." Environmental Science & Technology **40**(19): 6085-6090.

- Liu, Y., T. Phenrat and G. V. Lowry (2007). "Effect of TCE Concentration and Dissolved Groundwater Solutes on NZVI-Promoted TCE Dechlorination and H₂ Evolution." Environmental Science & Technology **41**(22): 7881-7887.
- Löffler, F. E., J. Yan, K. M. Ritalahti, L. Adrian, E. A. Edwards, K. T. Konstantinidis, J. A. Müller, H. Fullerton, S. H. Zinder and A. M. Spormann (2013). "Dehalococcoides mccartyi gen. nov., sp. nov., obligately organohalide-respiring anaerobic bacteria relevant to halogen cycling and bioremediation, belong to a novel bacterial class, Dehalococcoidia classis nov., order Dehalococcoidales ord. nov. and family Dehalococcoidaceae fam. nov., within the phylum Chloroflexi." International Journal of Systematic and Evolutionary Microbiology **63**(Pt 2): 625-635.
- Lowry, G. V., E. M. Hotze, E. S. Bernhardt, D. D. Dionysiou, J. A. Pedersen, M. R. Wiesner and B. S. Xing (2010). "Environmental Occurrences, Behavior, Fate, and Ecological Effects of Nanomaterials: An Introduction to the Special Series." Journal of Environmental Quality **39**(6): 1867-1874.
- Mace, C. (2006). "Controlling Groundwater VOCs: do nanoscale ZVI particles have any advantages over microscale ZVI of BNP." Pollution Engineering **38**(4): 24-28.
- Matheson, L. J. and P. G. Tratnyek (1994). "Reductive Dehalogenation of Chlorinated Methanes by Iron Metal." Environmental Science & Technology **28**(12): 2045-2053.
- Orth, W. S. and R. W. Gillham (1995). "Dechlorination of Trichloroethene in Aqueous Solution Using Fe⁰." Environmental Science & Technology **30**(1): 66-71.
- Phenrat, T., F. Fagerlund, T. Illangasekare, G. V. Lowry and R. D. Tilton (2011). "Polymer-Modified Fe⁰ Nanoparticles Target Entrapped NAPL in Two Dimensional Porous Media: Effect of Particle Concentration, NAPL Saturation, and Injection Strategy." Environmental Science & Technology **45**(14): 6102-6109.
- Phenrat, T., Y. Liu, R. D. Tilton and G. V. Lowry (2009). "Adsorbed Polyelectrolyte Coatings Decrease Fe⁰ Nanoparticle Reactivity with TCE in Water: Conceptual Model and Mechanisms." Environmental Science & Technology **43**(5): 1507-1514.

- Phenrat, T., T. C. Long, G. V. Lowry and B. Veronesi (2009). "Partial Oxidation ("Aging") and Surface Modification Decrease the Toxicity of Nanosized Zerovalent Iron." Environmental Science & Technology **43**(1): 195-200.
- Phenrat, T., N. Saleh, K. Sirk, H.-J. Kim, R. Tilton and G. Lowry (2008). "Stabilization of aqueous nanoscale zerovalent iron dispersions by anionic polyelectrolytes: adsorbed anionic polyelectrolyte layer properties and their effect on aggregation and sedimentation." Journal of Nanoparticle Research **10**(5): 795-814.
- Ponder, S. M., J. G. Darab, J. Bucher, D. Caulder, I. Craig, L. Davis, N. Edelstein, W. Lukens, H. Nitsche, L. Rao, D. K. Shuh and T. E. Mallouk (2001). "Surface Chemistry and Electrochemistry of Supported Zerovalent Iron Nanoparticles in the Remediation of Aqueous Metal Contaminants." Chemistry of Materials **13**(2): 479-486.
- Reinsch, B. C., B. Forsberg, R. L. Penn, C. S. Kim and G. V. Lowry (2010). "Chemical Transformations during Aging of Zerovalent Iron Nanoparticles in the Presence of Common Groundwater Dissolved Constituents." Environmental Science & Technology **44**(9): 3455-3461.
- Ritalahti, K. M., B. K. Amos, Y. Sung, Q. Wu, S. S. Koenigsberg and F. E. Löffler (2006). "Quantitative PCR targeting 16S rRNA and reductive dehalogenase genes simultaneously monitors multiple Dehalococcoides strains." Applied and Environmental Microbiology **72**(4): 2765-2774.
- Sakulchaicharoen, N., D. M. O'Carroll and J. E. Herrera (2010). "Enhanced stability and dechlorination activity of pre-synthesis stabilized nanoscale FePd particles." Journal of Contaminant Hydrology **118**(3-4): 117-127.
- Saleh, N., T. Phenrat, K. Sirk, B. Dufour, J. Ok, T. Sarbu, K. Matyjaszewski, R. D. Tilton and G. V. Lowry (2005). "Adsorbed Triblock Copolymers Deliver Reactive Iron Nanoparticles to the Oil/Water Interface." Nano Letters **5**(12): 2489-2494.
- Shin, K.-H. and D. K. Cha (2008). "Microbial reduction of nitrate in the presence of nanoscale zero-valent iron." Chemosphere **72**(2): 257-262.

- Simonet, B. M. and M. Valcarcel (2009). "Monitoring nanoparticles in the environment." Analytical and Bioanalytical Chemistry **393**(1): 17-21.
- Soundar, S. and T. S. Chandra (1987). "Cellulose degradation by a mixed bacterial culture." Journal of Industrial Microbiology **2**(5): 257-265.
- Taghavy, A., J. Costanza, K. D. Pennell and L. M. Abriola (2010). "Effectiveness of nanoscale zero-valent iron for treatment of a PCE-DNAPL source zone." Journal of Contaminant Hydrology **118**(3-4): 128-142.
- Waller, A. S., R. Krajmalnik-Brown, F. E. Löffler and E. A. Edwards (2005). "Multiple Reductive-Dehalogenase-Homologous Genes Are Simultaneously Transcribed during Dechlorination by Dehalococcoides-Containing Cultures." Applied and Environmental Microbiology **71**(12): 8257-8264.
- Wang, C.-B. and W.-x. Zhang (1997). "Synthesizing Nanoscale Iron Particles for Rapid and Complete Dechlorination of TCE and PCBs." Environmental Science & Technology **31**(7): 2154-2156.
- Weathers, L. J., G. F. Parkin and P. J. Alvarez (1997). "Utilization of Cathodic Hydrogen as Electron Donor for Chloroform Cometabolism by a Mixed, Methanogenic Culture." Environmental Science & Technology **31**(3): 880-885.
- Wei, Y. T., S. C. Wu, C. M. Chou, C. H. Che, S. M. Tsai and H. L. Lien (2010). "Influence of nanoscale zero-valent iron on geochemical properties of groundwater and vinyl chloride degradation: A field case study." Water Research **44**(1): 131-140.
- Wiesner, M. R., G. V. Lowry, P. Alvarez, D. Dionysiou and P. Biswas (2006). "Assessing the Risks of Manufactured Nanomaterials." Environmental Science & Technology **40**(14): 4336-4345.
- Xiu, Z.-m., K. B. Gregory, G. V. Lowry and P. J. J. Alvarez (2010). "Effect of Bare and Coated Nanoscale Zerovalent Iron on tceA and vcrA Gene Expression in Dehalococcoides spp." Environmental Science & Technology **44**(19): 7647-7651.

Xiu, Z.-m., Z.-h. Jin, T.-l. Li, S. Mahendra, G. V. Lowry and P. J. J. Alvarez (2010). "Effects of nano-scale zero-valent iron particles on a mixed culture dechlorinating trichloroethylene." Bioresource Technology **101**(4): 1141-1146.

Zhang, L. and A. Manthiram (1997). "Chains composed of nanosize metal particles and identifying the factors driving their formation." Applied Physics Letters **70**(18): 2469-2471.

Zhou, L., T. L. Thanh, J. Gong, J.-H. Kim, E.-J. Kim and Y.-S. Chang (2014). "Carboxymethyl cellulose coating decreases toxicity and oxidizing capacity of nanoscale zerovalent iron." Chemosphere **104**(0): 155-161.

Zhu, L., H.-z. Lin, J.-q. Qi, X.-y. Xu and H.-y. Qi (2012). "Effect of H₂ on reductive transformation of p-ClNB in a combined ZVI–anaerobic sludge system." Water Research **46**(19): 6291-6299.

Chapter 5

5 Long Term Dechlorination Following nZVI/CMC Injection and Impact on Microbial Communities, Including Organohalide-Respiring Microorganisms

Chris M.D. Kocur, Lomheim, L., Edwards, E.A., Weber, K.P., Sleep, B.E., Boparai, H.K., O'Carroll, D.M.

5.1 Abstract

The long term response of microbial communities were monitored along with the abundance of organohalide-respiring microorganisms during a two year period following the injection of nZVI/CMC. Enhanced dechlorination past cis-DCE was observed in the contaminated utility corridor in areas that were impacted by nZVI/CMC amendments. Dechlorination was sustained long after the Fe^0 content was expected to have oxidized. The abundance of *Dehalococcoides spp.* (*dhc*) and *vcrA* were monitored over the two year period using RT-qPCR, comparing the nZVI/CMC impacted wells to the less impacted control wells. It was discovered that the average *dhc* abundance in nZVI/CMC impacted wells increased an order of magnitude and remained at 1×10^8 gene copies/L after injection, while the less impacted wells remained at the background 7.6×10^6 gene copies/L. In addition to the biomarkers for dechlorination, the nZVI/CMC effect on the microbial community was also investigated. Next-generation amplicon pyrosequencing was used to obtain the genetic profile of all microbial species on site. More than 75% of the community in the background samples was identified from previously described organisms, and the community was uniform across the site. However, a drastic shift in microbial community took place during remediation, enriching phyla of anaerobic fermenters and creating a more diverse community than that initially observed with 50-70% relative abundance of Proteobacteria. *Chloroflexi*, and specifically *dhc* and *dehalogenimonas* (*dhg*) were enriched making up as much as 10.9 % and 3% relative abundance, respectively. The results suggest that nZVI/CMC played a major role in creating the microbial conditions on site.

5.2 Introduction

nZVI has become an attractive remediation alternative due to the wide range of contaminants that have undergone successful proof of concept degradation studies (He et al. 2005, Liu et al. 2005, Song et al. 2005, Kanel et al. 2006, Taghavy et al. 2010, Boparai et al. 2011). In addition laboratory results have advanced the understanding of nZVI/polymer mobility and reaction in well controlled systems (Kanel et al. 2008, Tiraferri et al. 2008, Comba et al. 2009, Tiraferri et al. 2009, Vecchia et al. 2009, Raychoudhury et al. 2010, Sakulchaicharn et al. 2010, Tosco et al. 2010, Phenrat et al. 2011, Wang et al. 2011, Comba

et al. 2012, Fagerlund et al. 2012, Raychoudhury et al. 2012, Raychoudhury et al. 2014). These studies have led to a range of field applications (Henn 2006, Bennett et al. 2010, He et al. 2010, Su et al. 2012, Johnson et al. 2013, Kocur et al. 2014). These studies found that nZVI with a polymeric coating is more mobile in the subsurface (He et al. 2009, Johnson et al. 2009, Phenrat et al. 2009, Phenrat et al. 2010, Wei et al. 2010, Kocur et al. 2013) than earlier generations of unstabilized nZVI (Elliott et al. 2001, Zhang 2003, Mace 2006). However challenges related to implementation of nZVI at the field scale still exist as the behavior of amendment injection cannot be easily predicted and is rarely monitored to ensure that emplacement is as expected, leading to difficulties in interpretation of degradation results.

In-situ bioremediation is now an accepted remediation technology for cVOC contaminated sites. This is because various groups of phylogenetically-distant anaerobic microorganisms couple reductive dechlorination of chlorinated organic compounds (e.g., chlorinated alkanes and alkenes) with oxidative phosphorylation, obtaining energy for growth in a process termed organohalide respiration (e.g., *Dehalococcoides*, *Desulfitobacterium*, *Dehalobacter*, *Sulfurospirillum*, *Desulfuromonas*, *Geobacter*, *Dehalogenimonas*) (Gerritse et al. 1996, Krumholz et al. 1997, Holliger et al. 1998, Luitjen et al. 2003, Sung et al. 2006, Moe et al. 2009). While chloroethene-respiring bacteria have been identified from multiple bacterial phyla, thus far critical dechlorination steps (i.e., DCE to VC to ethane) have only been shown for *Dehalococcoidales* in the Phylum *Chloroflexi* (Maymó-Gatell et al. 1997, Cupples et al. 2003, He et al. 2003, Duhamel et al. 2004, Sung et al. 2006, Manchester et al. 2012). The majority of the currently known organohalide-respiring bacteria carry multiple reductive dehalogenase genes and the complement of these genes confers dechlorinating ability.

nZVI field studies have used a dose as low as 0.3 g/L (Bennett et al. 2010) and as high as 30 g/L (PARS_Environmental 2003, Gavaskar A. 2005). Recent pilot scale studies have prepared and injected nZVI at 1 g/L (He et al. 2010, Johnson et al. 2013, Kocur et al. 2014). Mass of subsurface contaminant, natural reductant demand and nZVI reactive life are all important considerations when determining nZVI dose. nZVI dose typically applied in the field is often insufficient to stoichiometrically degrade all cVOCs with a single injection, whereas typical laboratory studies apply nZVI well in excess of that required based on stoichiometric considerations (Lien et al. 1999, Lien et al. 2001, Liu et al. 2005, Liu et al. 2007, He et al. 2008, Sakulchaicharoen et al. 2010). However there is considerable optimism that

microbially-mediated degradation, following nZVI treatment, will yield cVOC degradation beyond that expected based on stoichiometric considerations of the nZVI dose (He et al. 2010). The extent of microbially-mediated degradation, following nZVI treatment, has not, however, been quantified.

Microbially-mediated remediation requires that nZVI does not negatively impact organohalide-respiring microorganisms that exist on site. The impact of nanometals on microbial populations has been the subject of some debate in the literature, but microscale ZVI has shown synergistic degradation as an electron donor for *Dehalococcoides* (Rosenthal et al. 2004). Some studies suggest enhanced microbial activity following nZVI application as some zero valent iron oxidation products, including hydrogen gas and electrons, can be bioavailable as energy sources in anaerobic digestion (Zhu et al. 2012), nitrate reduction (Shin et al. 2008, Liu et al. 2014), as well as in the reduction of groundwater contaminants (Jeon et al. 2013). However, it has also been suggested that organohalide-respiration and abiotic nZVI-mediated degradation may not occur at the same time based on laboratory experiments (Barnes et al. 2010). Microcosms studies have also suggested that there is initially inhibition of microbial degradation occurs, but the organohalide-mediated degradation rates recover after a lag period (Xiu et al. 2010). Literature currently demonstrates many of the tradeoffs involved in nZVI implementation in laboratory scale tests, however, “a comprehensive assessment of the impacts of nZVI on soil geochemistry and microbiology under field conditions is difficult to obtain” (Yan et al. 2013). Numerous field studies have commented on active microbially-mediated dechlorination as a result of nZVI injection (Henn 2006, He et al. 2010, Man et al. 2013). A field study reported degradation of both parent and daughter cVOCs in the 3 weeks following nZVI/CMC injection (1 g/L) as well as an order of magnitude increase in *Dehalococcoides spp.* abundance 2 days after nZVI injection (Kocur et al 2015). Kocur *et al* (2015), in a study preceding this manuscript provide evidence that abiotic and biotic processes were operable during this time.

A limited number of studies have investigated the effect of nZVI on organohalide-respiring microorganisms (Cullen et al. 2011), especially under conditions representative of remedial nZVI application in the environment. Studies have shown that microbial inactivation (Lee et al. 2008, Diao et al. 2009, Marsalek et al. 2012, Tilston et al. 2013), increased stress response (Li et al. 2009, Fajardo et al. 2013), and inhibited gene expression will occur in the

presence of nZVI in aquatic systems (Jiang et al. 2013, Yang et al. 2013). Studies have reported cellular uptake of nZVI in mammalian cells (Phenrat et al. 2009), toxicity and oxidative stress in aquatic organisms (Auffan et al. 2008, Barnes et al. 2010, Sevcu et al. 2011, Kadar et al. 2012, Keller et al. 2012, Chen et al. 2013), soils (Saccà et al. 2014), soil dwelling organisms (El-Temsah et al. 2012, El-Temsah et al. 2013), and human tissue (Keenan et al. 2009). However impacts have been mitigated (e.g., effects of cellular uptake of nZVI, a decreased stress response, and lessened effects of cell wall oxidative stress) when polymeric coatings are included in the nanoparticle suspension and when the sample is in an environmental matrix (Li et al. 2010, Xiu et al. 2010, Chen et al. 2011, Pawlett et al. 2013, Zhou et al. 2014). Certainly, studies that have implemented nZVI in the field to date (with a polymer amendment or not) have not observed any negative effects on degradation (Henn 2006, Bennett et al. 2010, He et al. 2010, Wei et al. 2010, Köber et al. 2014). Nonetheless, process-level understanding of nZVI impact on microbial populations at active remediation field sites is needed given the contradictory results reported in the literature.

Remediation goals rely on microbial degradation to achieve site closure. Thus, biomarker development has led to primers for specific organohalide-respiring microorganisms including *Dehalococcoides spp* (Grostern et al. 2009) as well as compound specific reductive dehydrogenase genes (Waller et al. 2005). Microbiological profiling using next-generation sequencing has emerged as a tool for characterizing microbiological communities as techniques develop (Pilloni et al. 2012). Community based analysis of degrading cultures using pyrosequencing are now focusing on PCE and TCE degrading cultures (Ziv-El et al. 2012) in addition to broader concern of the entire chloroflexi phyla (Krzmarzick et al. 2012). Amplicon pyrosequencing methods can also be used to obtain the entire microbiological profile of organisms in aquifers (Pilloni et al. 2012, Kolb et al. 2013). To the authors' knowledge, this next-generation pyrosequencing has not been used to characterize the effects of remedial action at a field site to date.

Organohalide-respiring microorganism abundance, specifically *Dehalococcoides spp.* and phylum level microbial community composition is monitored following nZVI/CMC injection at a field site in Sarnia, Ontario. The field synthesized nZVI/CMC (He et al. 2010) was delineated and characterized in the subsurface following remedial injection and migration (Kocur et al. 2014). The objectives of this study were to (1) monitor the degradation of a

mixture of aqueous phase chlorinated volatile organic compounds (cVOCs) over a two year period. (2) Investigate the response of *Dehalococcoides* and *Dehalogenimonas* to nZVI/CMC injection under field scale conditions, comparing nZVI/CMC impacted zones to non-impacted zones. (3) Explore the impact of nZVI/CMC injection, and the site conditions that result, on the predominant microbial phyla on site including proteobacteria, bacteroidetes, and firmicutes. (4) Identify the environmental factors that lead to enriched in-situ organohalide-respiring microorganisms and strict anaerobic/fermenting conditions. Microcosm studies have demonstrated that ZVI can be an effective electron donor for *Dehalococcoides spp* (Rosenthal et al. 2004) and other field studies have observed enhanced degradation following nZVI/CMC injection (Bennett et al. 2010, He et al. 2010). This study presents the first field scale microbiological investigation following nZVI/CMC injection.

5.3 Methods

5.3.1 Site Background, Injection, and Sampling

The study was conducted at a cVOC impacted site in Sarnia, Ontario where nZVI/CMC was injected and monitored over a two year period. Site characterization included a pump test, slug tests, and a tracer test to evaluate hydraulic gradients, hydraulic conductivities, and hydraulic connection of the monitoring wells. Details have been previously described and summarized (Kocur et al. 2014)(Kocur et al 2015). The nZVI/CMC injection slurry was synthesized on site using a scaled up version of the He & Zhao (2005) method using 0.8% CMC polymer (Dai-ichi Kogyo, Japan). A total of 700L of 1 g/L nZVI was introduced into four wells on site (Figure 5.1), however the majority of the injected volume (330L) was injected into INJW over a 24 hour period.

5.3.2 cVOCs

The site was monitored over a 2 year period following nZVI/CMC amendment injection to quantify cVOC parent compound degradation and the formation of daughter compounds. Aqueous phase water samples containing cVOCs were collected prior to injection (-1 day) followed by 6 monitoring events over the two year monitoring period (at 10, 134,246,315,448, and 671 days). Detailed methods used in the analysis of chlorinated ethenes,

ethane, and methanes were previously described (Kocur 2015). Ethene and Ethane were measured for the 315, 448, and 671 day samples using a GS-Gaspro column (30 m x 0.32 mm) and an FID on an Agilent 7890A GC. GC vials with a 1mL aliquot of water sample were equilibrated prior to injection at 60°C for 10 mins.

5.3.3 DNA extraction

DNA extractions were done using the UltraClean® Soil DNA isolation kit (Mo Bio Laboratories Inc., Carlsbad, CA). One litre of groundwater was filtered from each well. Filters were removed from the filter casing, sliced into small pieces with a sterile surgical blade, and the filter pieces were transferred to the bead-beating tube. The DNA was extracted by following the manufacturer's protocol for maximum yields, except that DNA was eluted in 50µL sterile UltraPure distilled water (Invitrogen, Carlsbad, CA) rather than the eluent provided with the kit. The DNA concentration and quality were assessed using a NanoDrop ND-1000 spectrophotometer at a wavelength of 260 nm (NanoDrop Technologies, Wilmington, DE).

5.3.4 Quantitative PCR (qPCR) analyses

DNA samples were diluted 10 and 100 times with sterile UltraPure distilled water, and all subsequent sample manipulations were conducted in a PCR cabinet (ESCO Technologies, Gatboro, PA). Each qPCR reaction was run in duplicate. Two *Dehalococcoides* genes were targeted by qPCR: 1) the phylogenetic 16S rRNA gene and 2) the functional vinyl chloride reductase gene, *vcrA*. Each qPCR run was calibrated by constructing a standard curve using known concentrations of plasmid DNA containing the gene insert of interest. The standard curve was run with 8 concentrations, ranging from 10 to 10⁸ gene copies/µL. All qPCR analyses were conducted using a CFX96 real-time PCR detection system, with a C1000 Thermo Cycler (Bio-Rad Laboratories, Hercules, CA). Each 20 µL qPCR reaction was prepared in sterile UltraPure distilled water containing 10 µL of EvaGreen® Supermix (Bio-Rad Laboratories, Hercules, CA), 0.5 µL of each primer (forward and reverse, each from 10 µM stock solutions), and 2 µL of diluted template (DNA extract or standard plasmids). The thermocycling program was as follows: initial denaturation at 95°C for 2 min, followed by 40 cycles of denaturation at 98°C for 5s, annealing at 60°C and 61° C (for 16S rRNA and *vcrA* genes, respectively) for 10s. A final melting curve analysis was conducted at the end of the

program. The following primer sets were used: *Dehalococcoides* 16S rRNA Dhc1f (5'-GATGAACGCTAGCGGCG-3') and Dhc264r (5'-CCTCTCAGACCAGCTACCGATCGAA-3') (Grostern et al. 2009); and the vinyl chloride reductase gene vcrA_642f (GAAAGCTCAGCCGATGACTC-3') and vcrA_846r (5'-TGTTGAGGTAGGGTGAAGG-3') (Waller et al. 2005)

5.3.5 Pyrotag Sequencing

DNA samples were prepared for PCR in a PCR cabinet (ESCO Technologies, Gatboro, PA). 1 to 4 independent 100uL PCR amplification reactions were preformed per sample. Each PCR reaction was set up in sterile Ultra-Pure H₂O containing 50uL of PCR mix (Thermo Fisher Scientific, Waltham, MA), 2 µL of each primer (forward and reverse, each from 10 µM stock solutions), 10uL of a 3% BSA solution, and 4 µL of DNA extract. PCR reactions were run on a MJ Research PTC-200 Peltier Thermal Cycler (Bio-Rad Laboratories, Hercules, CA) with the following thermocycling program; 95 °C, 3 min; 25 cycles of 95 °C 30 s, 54 °C 45 s, 72 °C 90 s; 72 °C 10 min; final hold at 4 °C (modified from Ramos-Padron et al. (2011)). The universal primer set, 926f (5'-AAACTYAAAKGAATTGACGG-3') and 1392r (5'-ACGGGCGGTGTGTRC-3'), targeting the V8 variable region of the 16SrRNA gene from bacteria and archea, as well as the 18S rRNA gene in eukarya, were used (Engelbrektson et al. 2010). The forward and reverse primers included adaptors (926f: CCATCTCATCCCTGCGTGTCTCCGACTCAG and, 1392r: CCTATCCCCTGTGTGCCTTGGCAGTCTCAG), and the reverse primer also included 10bp multiplex identifier bar codes (MID) for distinguishing multiple samples pooled within one sequencing region. The PCR products were verified on a 2% agarose gel and replicates were combined and purified using GeneJET™ PCR Purification Kit (Fermentas), according to the manufacturer's instructions.

The concentration of the PCR products were determined using a NanoDrop ND-1000 Spectrophotometer at a wavelength of 260 nm (NanoDrop ND-1000; NanoDrop Technologies, Wilmington, DE). The concentrations and qualities of the final PCR products were also evaluated by loading them on 2% agarose gels, and comparing them with a serial dilution of ladders with known DNA concentrations.

The purified, barcoded amplicons were sent to McGill University and Genome Quebec Innovation Centre, where they were checked for quality, pooled and analyzed by unidirectional sequencing (i.e. Lib-1 chemistry) of the 16S gene libraries, using the Roche GS FLX Titanium technology (Roche Diagnostics Corporation).

The raw sequencing results were filtered, trimmed and processed using the Quantitative Insights Into Microbial Ecology (QIIME v1.8.0) pipeline (Caporaso et al. 2010) with default settings, unless stated otherwise. Only sequences between 300 and 500 bp, quality score above 25, and with homopolymer shorter than 8 bases were processed for downstream analysis. Sequences were clustered into individual OTUs using the UCLUST algorithm (Edgar 2010), and the GreenGenes database (release version) (DeSantis et al. 2006). The most abundant sequence within each OTU was chosen as the representative sequence for each OUT. Chimeric sequences were identified by ChimeraSlayer (Haas et al. 2011) and Decipher (Wright et al. 2012), and all sequences identified by both programs were removed from the data set. Taxonomy was assigned to each OTU by RDP classifier (Wang et al. 2007). Taxa were filtered out when the OTUs had average relative abundance <1% in any of the analyzed samples.

5.3.6 Nonmetric Dimensional Scaling

In order to investigate the impact of changing environmental parameters on the microbial population, redundancy analysis were conducted using the Vegan package (Dixon 2003, Oksanen et al. 2013) in the statistics software R (R Core Team, 2013). Rarefaction was conducted on the processed data set in order to remove sample heterogeneity and to standardize the sequencing data. A commonly used step size of 500 sequences per sample and a total run of 100 rarefactions were taken (Bowers et al. 2010, Agler et al. 2012). Nonmetric Multidimensional Scaling (NMDS) was done on the rarefied sample matrix using Bray-Curtis dissimilarity index (Bray 1957), and 27 environmental parameters were fitted.

Samples that have phylogenetically similar microbial populations will appear close together in the coordination plot. Clustering of data was used to test the significance of the microbial population similarity in the microbial communities. Microbial population similarity was tested in 2 different schemes to show the effects from nZVI/CMC introduction. The two assigned clustering groups were based on 1.) the sampling time in the monitoring wells creating 5 different clusters, and 2.) Previously determined exposure to nZVI/CMC (i.e., whether the

well was impacted by nZVI/CMC injection or not) creating 3 clusters including a background sampling cluster. The 95% confidence ellipses are plotted based on the permutation of samples within the coordination space showing the difference of the clustered groups. Vectors for the environmental parameters were fit on the microbial community ordination space using envfit in VEGAN. Gradients are plotted as vectors on the ordination space showing the environmental parameters with the highest correlation coefficients rankings. The 13 vectors shown were determined to be the most correlated parameters to the microbial community space.

Species were also plotted for both assigned and unassigned OTUs that were referenced in the greengenes database. The position of the species in the ordination plot corresponds to the same solution (i.e., the positions correspond to the sample positions) associating predominant species with sampling events and sample grouping. Similar to the fitted vectors in envfit, ordisurf was used to fit the ORP data to the ordination space as a contour plot. The non-linear surface of ORP on the microbial community space provides insight in how this environmental parameter affects the species.

5.4 Results

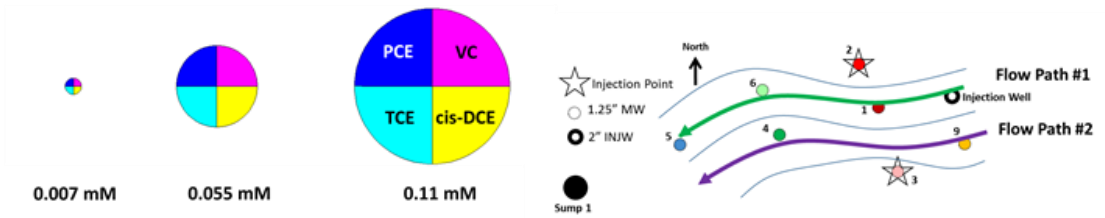
5.4.1 4.1 Degradation of cVOCs

In the wells immediately impacted by nZVI/CMC, such as those along flow path #1 (Figure 5.1), the parent compounds (PCE and TCE) were rapidly degraded and transformed into daughter cVOC products (eg. cis 1,2 DCE and VC). In MW1, PCE and TCE were degraded from 40% to 3 % within 3 weeks (Kocur 2015). In other wells that were impacted by amendment injection (i.e., MW 6 and 5) degradation continued, reducing the PCE and TCE composition to less than 3% of the total cVOCs within 134 days. At 10 days and 134 days it is apparent, that cVOCs in wells along flow path #1 are degraded to a greater extent than wells that were not impacted by amendment injection (i.e., MW9 and MW4) (Figure 5.1). Enhanced desorption of sorbed phase contaminants caused an increase in the cis-DCE and VC concentrations in wells impacted by nZVI/CMC in the 134 days following injection as parent compounds were degraded. Sustained degradation occurred over a 2 year period along flow path #1 (Figure 5.1). The same definitive decline in parent compound concentrations and limited decline of lesser chlorinated compounds does not occur in the less-impacted flow path. At later times (i.e., 314 and 447 days) considerable conversion of cVOCs past VC was

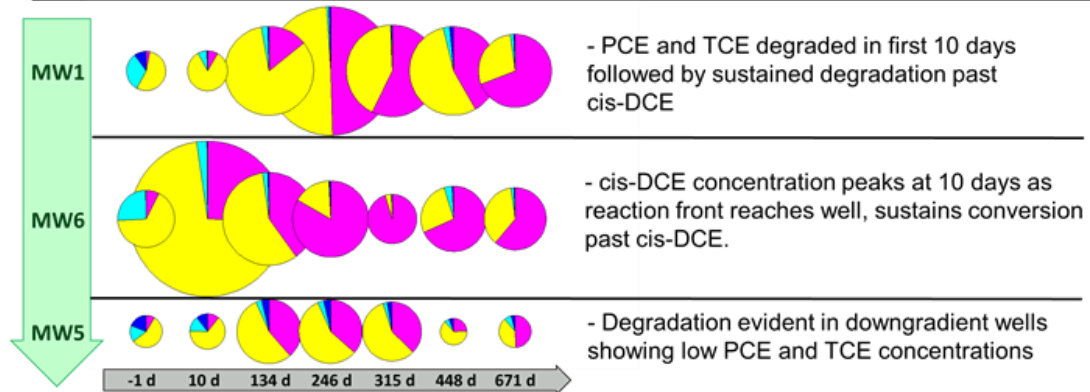
observed in wells impacted by nZVI/CMC amendment in contrast to degradation in the non-impacted wells. Ethene concentrations were only quantified for the 314, 447, and 671 day samples and typically represented the greatest proportion of degradation products in wells impacted by nZVI/CMC amendment (Appendix D.4). By comparison in MW4, a non-impacted well, parent compounds remained at background concentrations with only a moderate increase in cis-DCE concentrations. This progression from TCE to cis-DCE suggests that degradation was occurring in MW4, but likely occurring at pre-injection rates. The amount of ethene measured in MW4 made up less than 1% of the cVOC molar ratio 314 days after injection, compared to between 20% and 50% of the cVOC molar ratio in wells impacted by nZVI/CMC amendment. Similar behavior is also observed at MW9, a non-impacted well. At MW9 a delayed increase in degradation product concentrations after several months suggests that either amendment constituents or microbes that grew in the nearby injection well may have diffused into the well catchment area. Similar to the wells impacted by nZVI/CMC amendment this likely leads to enhanced desorption and degradation, causing total cVOC concentrations to exceed background concentration. The molar ratio of ethene after 314 days was only 13%, whereas after 671 days the ethene was equal to that of other impacted wells.

Chlorinated ethanes and methanes degradation patterns are similar to those observed for chlorinated ethenes. In wells impacted by nZVI/CMC amendment total ethanes decreased 30-60% over the 2 year monitoring period (Appendix D.1). Chlorinated methanes decreased to non-detectable concentrations in MW1 and MW6 within 134 and 315 days, respectively. Additionally chloroform concentrations degraded over time in all wells impacted by nZVI/CMC amendment injection. At MW9 degradation of chlorinated ethanes and methanes occurred slowly. Unlike other monitoring locations CF concentrations at MW4 increase during the monitoring period. It is possible that this may be due to enhanced desorption of chloroform in the vicinity of MW4, as observed for cis-DCE, due to the apparent increase in degradation products in the aqueous phase in MW6 due to increased byproduct solubility, compared to the parent compound (i.e. TCE). However, there is no indication, given the low ethene production, that injected amendments impacted MW4. Overall, the extent to which cis-DCE and VC were converted to ethene, even after 2 years, shows that there was considerably more degradation occurring within nZVI/CMC amendment impacted wells.

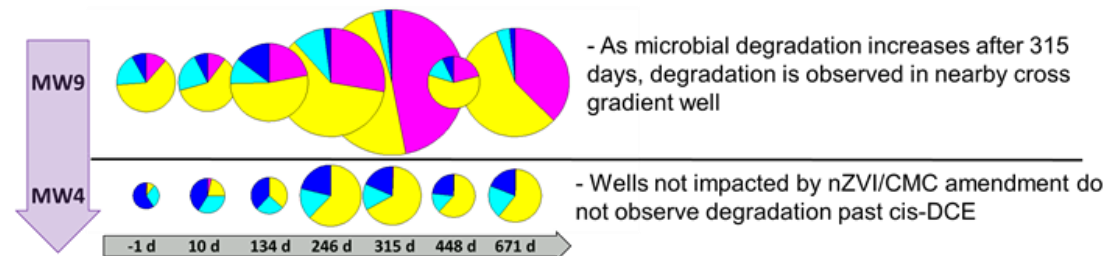
Legend



Flow Path #1



Flow Path #2



Injection Wells

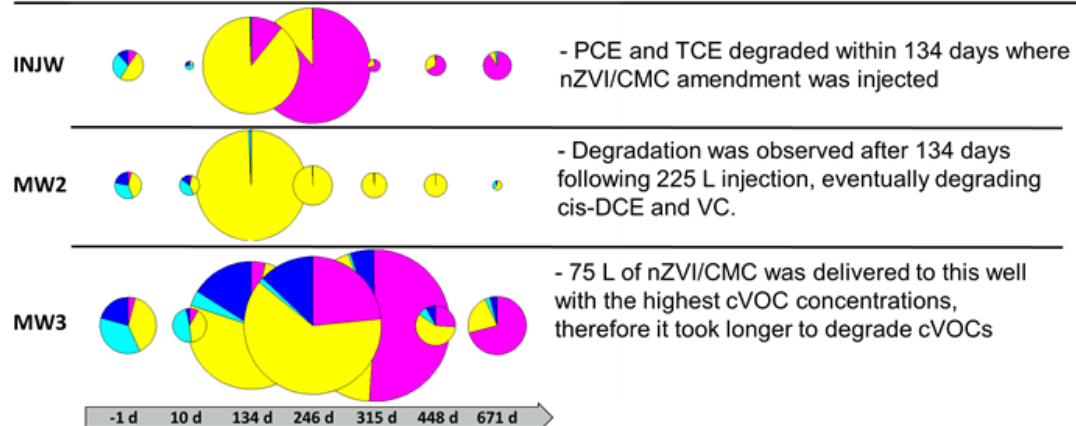


Figure 5.1: Degradation of chlorinated ethenes in monitoring wells over the two-year monitoring period. Pie charts show the composition of chlorinated ethenes in each

well. The radius of each pie illustrates the total concentration of all chlorinated ethenes in the well (mM). Three distinct groups of wells are shown; wells that were impacted by nZVI/CMC through injection or transport (Flow Path #1), wells that were less impacted by the injection (Flow Path #2), and injection wells.

5.4.2 Abundance of *Dehalococcoides* spp.

The abundance of *dhc* shows a distinct effect resulting from the injection of nZVI/CMC amendment (Figure 5.2). The average abundance of *dhc* (7×10^6 gene copies/L) in the background samples (i.e., before injection) was uniform across the site suggesting a large, healthy dechlorinator population was initially present. 1×10^7 gene copies/L is commonly used as a benchmark for a population of *dhc* associated with biodegradation (Wilson et al. 2007). In wells not impacted by nZVI/CMC amendment injection, no change in microbial abundance was observed during the monitoring period. The average abundance in MW4 and MW9 was 7.5×10^6 gene copies/L, similar to the initial abundance. Considered together as a group, the wells impacted by nZVI/CMC show a distinct change in the abundance of *dhc* after 8 months. The average for the wells impacted by the nZVI/CMC injection in Figure 5.2, is 1×10^8 gene copies/L, showing an order of magnitude increase in abundance compared to the background. Furthermore, the increase in abundance appeared to be an order of magnitude in each well regardless of how the amendment reached the well (i.e., as reactive nZVI or breakdown nZVI constituents at later times). Appendix D.5 shows the average and standard error about the mean for each sample grouping in Figure 5.2 showing that the nZVI/CMC impacted locations are statistically different than the other locations. *Dhc* abundance in MW2 and MW1, where measureable nZVI/CMC was immediately transported, increased by an order of magnitude immediately following injection (2 days). At these locations *dhc* abundance remained high throughout the 2 year monitoring period. MW5, located 3.5m downgradient of the primary injection site, showed an order of magnitude increase in *dhc* abundance and higher than baseline average *dhc* abundances for the remainder of the 2 year monitoring period, suggesting that the conditions created by the nZVI/CMC injection led to sustained degradation of cVOCs due to the high abundance of dechlorinating organisms.

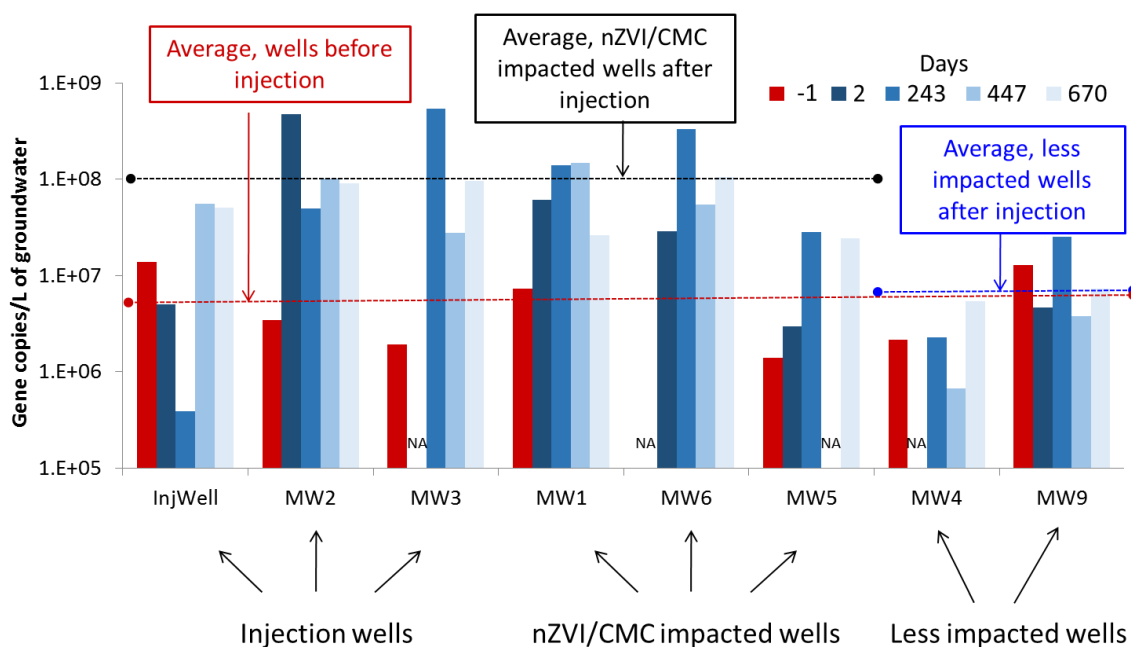


Figure 5.2: Concentration of *Dehalococcoides* genes in each well (gene copies/L) over a two year monitoring period following CMC-nZVI injection, determined by qPCR analysis. Prior to CMC-nZVI injection the average of all monitoring wells yielded *dhc* levels of 7×10^6 gene copies/L, which is above the level at which dechlorination is expected to occur at contaminated sites (Wilson et al. 2007). Compared to pre-injection conditions, the average of post injection *dhc* levels in all nZVI/CMC impacted wells increased by an order of magnitude while the average of the less impacted wells stayed the same.

5.4.3 Effects of dilution on *Dehalococcoides* spp. in injection wells.

The change in abundance of *dhc* in the injection well (INJW) at 2 and 243 days was opposite to that observed in another injection well (MW2) and monitoring wells (MW1 and MW6 in Figure 5.2). The nZVI/CMC injection well received the greatest volume of amendment, but did not result in the largest increase in *dhc* abundance. *Dhc* abundance declined following injection and only exceeded background abundance after 447 days. Several factors could have contributed to the decline of *dhc* abundance in INJW for the 2 and 243 day monitoring rounds. For example the large injection volume may have diluted cVOCs in the injection wells pushing aqueous cVOCs out of the treatment area. This is supported by the low cVOC concentrations in the injection well (Figure 5.1), and has been previously observed in

field injection studies (Bennett et al 2010, perhaps others). Lower cVOC concentrations in the vicinity of the injection wells would result in lower *dhc* abundance due to the lack of an energy source for obligate dehalorespiring microorganisms. It is noted that the redox potential at these injection well would be low and ample CMC substrate would have been available as a carbon source, similar to other wells. These results suggest that comparison of injection and monitoring well concentrations, as an indicator of remediation success, should be done with caution and only with careful characterization of each well to support results.

5.4.4 Microbial Composition

In addition to *dhc* abundance microbial community composition was quantified. Prior to injection the microbial composition was largely uniform across all sampling wells. Appendix D.2 shows the phylum level classification of the organisms in background samples where over 70% of the microorganisms were identified from previous classification entries in the NCBI database. Proteobacteria had the highest relative abundance, making up between 55% and 73% of the microbial community. The balance of identified organisms, between 20% and 35%, were bacteroidetes, firmicutes, and the OP11 Bacterial Phyla. These are phyla widely found in soils and environmental systems and they were also consistently and uniformly distributed across the monitoring area. Chloroflexi, particularly organisms in the *Dehalococcoidaceae* family, are of interest on this site and make up a small yet important phyla in the community due to members previously shown to degrade not only PCE and TCE, but also Cis-DCE and VC (Maymó-Gatell et al. 2000, Krajmalnik-Brown et al. 2004, Löffler et al. 2013). Chloroflexi make up between 1% and 4% of the microbial community in background samples. *Dehalococcoides* and *Dehalogenimonas*, the organisms within the chloroflexi phyla capable of organohalide-respiration, make up less than 1% of the relative abundance.

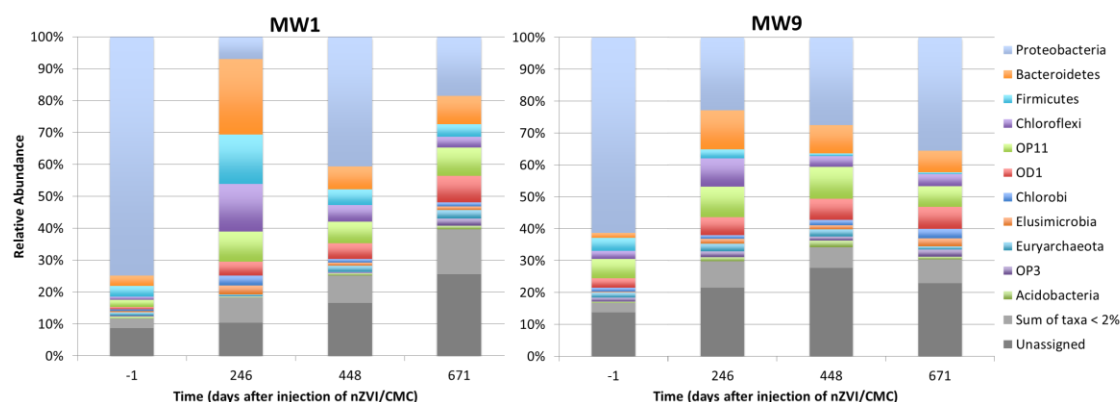


Figure 5.3: Phylogenetic composition of the microbial community in one monitoring well that was impacted (MW1), and one well that was less impacted (MW9) by the CMC-nZVI injection. Relative abundance of each phylum is represented for each monitoring well. Within the chloroflexi Phyla, more specific operational taxonomy units were identified for the dechlorinating species *Dehalococcoides*. and *Dehalogenimonas*.

Microbial community composition shifted following the nZVI/CMC amendment injection (Figure 5.3), primarily in wells that were impacted by amendment injection. Proteobacteria relative abundance decreased as relative abundance of other phyla associated with anaerobic and fermenting functions were enriched. The microbial diversity increased along with the change in relative abundance. In MW1 the relative abundance of the strict anaerobe phyla increased, notably Chloroflexi, Bacteroidetes, and Firmicutes. This shift in taxa results in a far greater diversity of phyla than in background samples and suggests that microbial community composition changed in response to nZVI/CMC amendment injection and associated changes in ORP, pH and carbon source (i.e., CMC). The shift in MW1 included an increase in Chloroflexi, increasing to 15% of the relative abundance, which is representative of the changes in the nZVI/CMC impacted wells. The relative abundance of the dechlorinators, *Dehalococcoides* and *Dehalogenimonas*, also increased after nZVI/CMC amendment injection, from less than 1% before injection to 10.9% for *Dehalococcoides* and up to 3% for *Dehalogenimonas*. Comparatively, the relative abundance of dechlorinators did not change after 2 days in MW9 (Figure 5.3). Eventually dechlorinator populations represented a greater proportion of the microbial community (i.e., after 246 days) in MW9 likely due to its proximity to the nZVI/CMC amendment injection, consistent with the discussion of *dhc* abundance at this location. The relative abundance of proteobacteria also decreased to 23% in MW9 after 246

days. Monitoring wells that were not impacted by the amendment injection had *Dehalococcoides* and *Dehalogenimonas* populations ranging from 0.5-3.2% and 0.4 - 2.6% of the microbial community, respectively, following amendment injection. This suggests a measureable change in microbial community composition in non-impacted wells however changes are to a lesser degree, and do not share the same change in dechlorinator abundance. As discussed in sections 4.1 and 4.2, microbial degradation did not occur to the same extent in non-impacted wells as in the impacted areas.

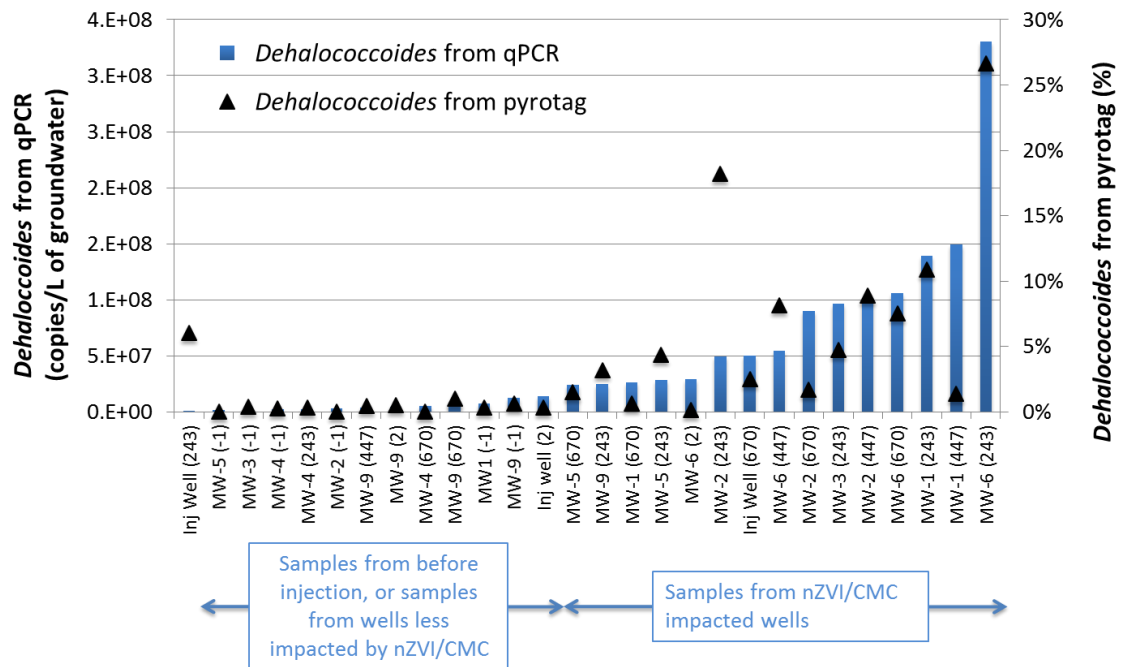


Figure 5.4: Relative abundance (%) and absolute abundance (gene copies/L) of *dhc* measured by amplicon pyrosequencing and qPCR, respectively. Wells impacted by CMC-nZVI show higher relative and absolute abundance compared to non-impacted wells that remain unchanged following injection.

The most enriched populations of *dhc* using both metrics (i.e., relative and absolute abundance) was in the group of wells that were impacted by the nZVI/CMC as illustrated in Figure 5.4. The distinction between impacted and less-impacted wells is apparent in this figure, with the results sorted by ascending absolute abundance of *dhc*, quantified by qPCR. All background (i.e., pre-injection) samples reside on the left side of the plot along with the non-impacted post-injection wells (e.g., control wells MW4 and MW9). Non-impacted wells, even at late times (e.g., MW4 after 670 days, and MW9 at 447 and 670 days) reside to the left

of the plot, whereas, the highest relative and absolute abundances associated with the impacted wells, reside on the right side of the plot (e.g., MW6 at 2 days and 670 days). Although the relative and absolute abundance cannot be directly compared, this plot shows that both amplicon pyrosequencing and the more widely used method for determining *dhc* (qPCR), detect the distinctive changes that occurred on site due to nZVI/CMC amendment injection. Both methods of evaluating *dhc* highlight the distinction between the impacted and non-impacted wells, showing that microbial community changes occurred in as little as 2 days.

5.4.5 Community evaluation using NMDS

The relationship between any single group of organisms and a given independent variable (e.g., another relative abundance, time, pH, ORP) is difficult to interpret given that many independent variables change together. As such a non-metric dimensional scaling technique was adopted. Ordination plots using NMDS show the results from background and 3 subsequent sampling events in Figure 5.5. Figure 5.5.a sampling events are grouped 95% confidence ellipses surrounding each respective sampling round and shows that the background samples occupy a distinct compact space in the northwest corner of the plot. Of note that all background samples are present in this area. 246 days following injection, the ellipse occupies space to the east due to changes in microbial community composition favoring more anaerobe fermenters compared to the proteobacteria that initially dominated the community. Most samples fall within these 95% ellipse, however the samples that were less impacted (MW9 and MW4) remain towards the west as they are dissimilar. The 95% ellipse grew in size following injection with similar characteristics at 448 days compared to 246 days as the community shifted further east in plot Figure 5.5.a. The 246 day and 448 day ellipses are elongated from northeast to southwest as injection of nZVI/CMC impacted sampling locations to different extents. The most impacted wells are to the northeast and samples thought to be background controls remained in the central and west (i.e., closer to background sample locations). The elongation was less apparent after 671 days of monitoring as it is hypothesized that the community may be starting to return to pre-injection conditions. This hypothesis was tested in Figure 5.5.b, where the 95% ellipses are separated for the groups of impacted and non-impacted locations showing that the parameter space in the northeast is only occupied by the nZVI/CMC impacted samples. The ellipses in Figure 5.5.b clearly separate the background, less-impacted and impacted groups of samples from each other.

In order to explore the impact of measured parameters on microbial community composition, envfit plot fits are represented as a vector on top of the ellipses for before and immediately after injection, less impacted wells and impacted wells (Figure 5.5.c). The magnitudes of the vectors show the relative influence of the parameter on the parameter space (e.g., VC magnitude is larger than pH, therefore the VC concentration has higher correlation to the microbial species), and the direction shows the trend within the dataset (e.g., TCE vector points in the direction of increasing TCE concentration). The vectors for *dhc* and *vcrA* point to the north-east showing that these qPCR derived abundances correlate with the microbial communities that are also associated with the nZVI/CMC impacted samples. Thus, an increase in *dhc* abundance is associated with the changes in microbial community due to the impact of the injection. The plot shows that samples that were not impacted by nZVI/CMC amendment injection have higher concentrations of cVOCs (e.g., PCE, TCE, as well as parent chlorinated ethane compounds), similar to the background samples. The south-west is also populated by samples with lower concentrations of vinyl chloride because there was less degradation of the parent compounds compared to the nZVI/CMC impacted wells. The time vector is also plotted and accounts for the southeast migration of the dataset, as shown in Figure 5.5.a, as the microbial communities change over time. Higher total iron and increases in pH, associated with nZVI injection, are also more prevalent in wells populating the north-east region.

to south-west of the parameter space, whereas, the north-east is populated with many of the strict anaerobes. Notably, *dhc* and several other dechlorinators are located in the north-east as such they are associated with the environmental conditions that are caused by the nZVI/CMC amendment injection. The ORP gradient is overlaid on top of the microbial community space (Figure 5.5.d). The strict anaerobic species in Figure 5.5.d are colored blue and predominantly populate the north-east parameter space. This further highlights the link between the nZVI/CMC injection and the shift in microbial community composition to strict anaerobe fermenters and dechlorinators (especially *dhc*). The north-east part of Figure 5.5.d is populated by the enriched dechlorinating species, *Dehalococcoides* (*dhc*) and *Dehalogenimonas* (*dhg*), within a surrounding community of predominantly strict anaerobes that sustained dechlorination. Figure 5.5.d also show that this position is also associated with reducing conditions (ORP < - 100 mV), and increased absolute abundances of *dhc* and *vcrA*. The results suggest that the conditions that were created following the delivery of nZVI/CMC led enriched dechlorinating species and strict anaerobes in the subsurface.

5.5 Environmental Implications

The results of this study clearly show that the nZVI/CMC amendment injection significantly impacted the microbial community composition and *dhc* abundance. The injection enriched the dechlorinating species on site leading to long term degradation of cVOCs due to microbially mediated processes. This also caused an increased relative and absolute abundance of *dhc* in the subsurface, which can only be caused by organohalide respiration. Previous field studies have suggested that organohalide-respiring microorganisms would be enhanced following nZVI/polymer application based on the cVOC degradation products that are observed (Elliott et al. 2001, He et al. 2010, Wei et al. 2010). This study demonstrates this link between the nZVI injection, geochemical conditions, and the microbial chlorinator species necessary for long term degradation. Sustained degradation of cVOCs occurred in the treatment area over the two year monitoring period. Initially, cVOCs were degraded by nZVI with nZVI also being consumed by dissolved oxygen and oxidized with water, forming hydrogen. These conditions create geochemical conditions that favored the strict anaerobic microbial species. These anaerobic conditions facilitated increased abundance of organohalide-respiring microorganisms which were sustained for two years. Within the nZVI impacted area enhanced desorption and degradation increased the byproduct concentrations

above background levels. Downstream monitoring is a necessity to avoid undesirable and dangerous high byproduct concentrations in downstream wells. Concerns related to the impact of nanoparticle in natural systems have become increasingly prevalent due to potential adverse effects. Reports of nZVI toxicity in environmental systems have been primarily evaluated on proteobacteria in aquatic organisms. This study used polymer coated nZVI that would have oxidized within a short period following injection and found that conditions that were not favorable for proteobacteria. In this study proteobacteria relative abundance decreased following nZVI/CMC amendment injection, as would be expected due to the creation of strongly reducing conditions. Changes to the community occurred, most likely, due to the rapidly altered geochemical conditions (especially ORP). The community shifted due to this disturbance to the surrounding conditions, but the community also increased in diversity, showing a natural response to changing conditions. The microbial community shifted from an aerobe - facultative anaerobe community to a strict anaerobic community over a short period of time, however, the community remained functional, and in fact thrived within the conditions that were created. This is shown in the fact that the community sustained organohalide-respiring conditions for 2 years.

5.6 References

- Agler, M. T., J. J. Werner, L. B. Iten, A. Dekker, M. A. Cotta, B. S. Dien and L. T. Angenent (2012). "Shaping Reactor Microbiomes to Produce the Fuel Precursor n-Butyrate from Pretreated Cellulosic Hydrolysates." Environmental Science & Technology **46**(18): 10229-10238.
- Auffan, M., W. Achouak, J. Rose, M.-A. Roncato, C. Chanei, D. T. Waite, A. Masion, J. C. Woicik, M. R. Wiesner and J.-Y. Bottero (2008). "Relation between the Redox State of Iron-Based Nanoparticles and Their Cytotoxicity toward *Escherichia coli*." Environmental Science & Technology **42**(17): 6730-6735.
- Barnes, R. J., O. Riba, M. N. Gardner, A. C. Singer, S. A. Jackman and I. P. Thompson (2010). "Inhibition of biological TCE and sulphate reduction in the presence of iron nanoparticles." Chemosphere **80**(5): 554-562.
- Barnes, R. J., C. J. van der Gast, O. Riba, L. E. Lehtovirta, J. I. Prosser, P. J. Dobson and I. P. Thompson (2010). "The impact of zero-valent iron nanoparticles on a river water bacterial community." Journal of Hazardous Materials **184**(1-3): 73-80.
- Bennett, P., F. He, D. Zhao, B. Aiken and L. Feldman (2010). "In Situ Testing of Metallic Iron Nanoparticle Mobility and Reactivity in a Shallow Granular Aquifer." Journal of Contaminant Hydrology **116**(1-4): 35-46.
- Boparai, H. K., M. Joseph and D. M. O'Carroll (2011). "Kinetics and thermodynamics of cadmium ion removal by adsorption onto nano zerovalent iron particles." Journal of Hazardous Materials **186**(1): 458-465.
- Bowers, J. R., D. M. Engelthaler, J. L. Ginther, T. Pearson, S. J. Peacock, A. Tuanyok, D. M. Wagner, B. J. Currie and P. S. Keim (2010). "BurkDiff: A Real-Time PCR Allelic Discrimination Assay for *Burkholderia Pseudomallei* and *B. mallei*." PLoS ONE **5**(11): e15413.
- Bray, R. J., Curtis, J.T., (1957). "An ordination of the upland forest communities of southern Wisconsin." Ecological Monographs **27**: 325-349.
- Caporaso, J. G., J. Kuczynski, J. Stombaugh, K. Bittinger, F. D. Bushman, E. K. Costello, N. Fierer, A. G. Pena, J. K. Goodrich, J. I. Gordon, G. A. Huttley, S. T. Kelley, D. Knights, J. E. Koenig, R. E. Ley, C. A. Lozupone, D. McDonald, B. D. Muegge, M. Pirrung, J. Reeder, J. R. Sevinsky, P. J. Turnbaugh, W. A. Walters, J. Widmann, T. Yatsunenko, J. Zaneveld and R. Knight (2010). "QIIME allows analysis of high-throughput community sequencing data." Nat Methods **7**(5): 335-336.
- Chen, J., Z. Xiu, G. V. Lowry and P. J. J. Alvarez (2011). "Effect of natural organic matter on toxicity and reactivity of nano-scale zero-valent iron." Water Research **45**(5): 1995-2001.
- Chen, P.-J., W.-L. Wu and K. C.-W. Wu (2013). "The zerovalent iron nanoparticle causes higher developmental toxicity than its oxidation products in early life stages of medaka fish." Water Research **47**(12): 3899-3909.

- Comba, S., D. Dalmazzo, E. Santagata and R. Sethi (2012). "Rheological characterization of xanthan suspensions of nanoscale iron for injection in porous media." Journal of Hazardous Materials **185**(2-3): 598-605.
- Comba, S. and R. Sethi (2009). "Stabilization of highly concentrated suspensions of iron nanoparticles using shear-thinning gels of xanthan gum." Water Research **43**(15): 3717-3726.
- Cullen, L. G., E. L. Tilston, G. R. Mitchell, C. D. Collins and L. J. Shaw (2011). "Assessing the impact of nano- and micro-scale zerovalent iron particles on soil microbial activities: Particle reactivity interferes with assay conditions and interpretation of genuine microbial effects." Chemosphere **82**(11): 1675-1682.
- Cupples, A. M., A. M. Spormann and P. L. McCarty (2003). "Growth of a Dehalococcoides-Like Microorganism on Vinyl Chloride and cis-Dichloroethene as Electron Acceptors as Determined by Competitive PCR." Applied and Environmental Microbiology **69**(2): 953-959.
- DeSantis, T. Z., P. Hugenholtz, N. Larsen, M. Rojas, E. L. Brodie, K. Keller, T. Huber, D. Dalevi, P. Hu and G. L. Andersen (2006). "Greengenes, a chimera-checked 16S rRNA gene database and workbench compatible with ARB." Appl Environ Microbiol **72**(7): 5069-5072.
- Diao, M. and M. Yao (2009). "Use of zero-valent iron nanoparticles in inactivating microbes." Water Research **43**(20): 5243-5251.
- Dixon, P. (2003). "VEGAN, a package of R functions for community ecology." Journal of Vegetation Science **14**(6): 927-930.
- Duhamel, M., K. Mo and E. A. Edwards (2004). "Characterization of a Highly Enriched Dehalococcoides-Containing Culture That Grows on Vinyl Chloride and Trichloroethene." Applied and Environmental Microbiology **70**(9): 5538-5545.
- Edgar, R. C. (2010). "Search and clustering orders of magnitude faster than BLAST." Bioinformatics **26**(19): 2460-2461.
- El-Temsah, Y. S. and E. J. Joner (2012). "Ecotoxicological effects on earthworms of fresh and aged nano-sized zero-valent iron (nZVI) in soil." Chemosphere **89**(1): 76-82.
- El-Temsah, Y. S. and E. J. Joner (2013). "Effects of nano-sized zero-valent iron (nZVI) on DDT degradation in soil and its toxicity to collembola and ostracods." Chemosphere **92**(1): 131-137.
- Elliott, D. W. and W.-x. Zhang (2001). "Field Assessment of Nanoscale Bimetallic Particles for Groundwater Treatment." Environmental Science & Technology **35**(24): 4922-4926.
- Engelbrektson, A., V. Kunin, K. C. Wrighton, N. Zvenigorodsky, F. Chen, H. Ochman and P. Hugenholtz (2010). "Experimental factors affecting PCR-based estimates of microbial species richness and evenness." ISME J **4**(5): 642-647.

- Fagerlund, F., T. H. Illangasekare, T. Phenrat, H. J. Kim and G. V. Lowry (2012). "PCE dissolution and simultaneous dechlorination by nanoscale zero-valent iron particles in a DNAPL source zone." Journal of Contaminant Hydrology **131**(1-4): 9-28.
- Fajardo, C., M. L. Saccà, M. Martinez-Gomariz, G. Costa, M. Nande and M. Martin (2013). "Transcriptional and proteomic stress responses of a soil bacterium *Bacillus cereus* to nanosized zero-valent iron (nZVI) particles." Chemosphere **93**(6): 1077-1083.
- Gavaskar A., T. L., Condit W., (2005). Contract Report: Cost and Performance Report: nanoscale zerovalent iron technologies for source remediation. Port Huenema, CA, NAVFAC: Naval Facilities Engineering Command. **CR-05-007-ENV**.
- Gerritse, J., V. Renard, T. M. Pedro Gomes, P. A. Lawson, M. D. Collins and J. C. Gottschal (1996). "Desulfitobacterium sp. strain PCE1, an anaerobic bacterium that can grow by reductive dechlorination of tetrachloroethene or ortho-chlorinated phenols." Archives of Microbiology **165**(2): 132-140.
- Groster, A. and E. A. Edwards (2009). "Characterization of a Dehalobacter Coculture That Dechlorinates 1,2-Dichloroethane to Ethene and Identification of the Putative Reductive Dehalogenase Gene." Applied and Environmental Microbiology **75**(9): 2684-2693.
- Haas, B. J., D. Gevers, A. M. Earl, M. Feldgarden, D. V. Ward, G. Giannoukos, D. Ciulla, D. Tabbaa, S. K. Highlander, E. Sodergren, B. Methe, T. Z. DeSantis, C. Human Microbiome, J. F. Petrosino, R. Knight and B. W. Birren (2011). "Chimeric 16S rRNA sequence formation and detection in Sanger and 454-pyrosequenced PCR amplicons." Genome Res **21**(3): 494-504.
- He, F., M. Zhang, T. Qian and D. Zhao (2009). "Transport of carboxymethyl cellulose stabilized iron nanoparticles in porous media: Column experiments and modeling." Journal of Colloid and Interface Science **334**(1): 96-102.
- He, F. and D. Zhao (2005). "Preparation and Characterization of a New Class of Starch-Stabilized Bimetallic Nanoparticles for Degradation of Chlorinated Hydrocarbons in Water." Environmental Science & Technology **39**(9): 3314-3320.
- He, F., D. Zhao and C. Paul (2010). "Field assessment of carboxymethyl cellulose stabilized iron nanoparticles for in situ destruction of chlorinated solvents in source zones." Water Research **44**(7): 2360-2370.
- He, F. and D. Y. Zhao (2008). "Hydrodechlorination of trichloroethene using stabilized Fe-Pd nanoparticles: Reaction mechanism and effects of stabilizers, catalysts and reaction conditions." Applied Catalysis B-Environmental **84**(3-4): 533-540.
- He, J., K. M. Ritalahti, M. R. Aiello and F. E. Löffler (2003). "Complete Detoxification of Vinyl Chloride by an Anaerobic Enrichment Culture and Identification of the Reductively Dechlorinating Population as a Dehalococcoides Species." Applied and Environmental Microbiology **69**(2): 996-1003.
- Henn, K. W., Waddill, D.W. (2006). "Utilization of nanoscale zero-valent iron for source remediation - A case study." Remediation Journal **16**(2): 57-77.

- Holliger, C., D. Hahn, H. Harmsen, W. Ludwig, W. Schumacher, B. Tindall, F. Vazquez, N. Weiss and A. J. B. Zehnder (1998). "Dehalobacter restrictus gen. nov. and sp. nov., a strictly anaerobic bacterium that reductively dechlorinates tetra- and trichloroethene in an anaerobic respiration." Archives of Microbiology **169**(4): 313-321.
- Jeon, J.-R., K. Murugesan, I.-H. Nam and Y.-S. Chang (2013). "Coupling microbial catabolic actions with abiotic redox processes: A new recipe for persistent organic pollutant (POP) removal." Biotechnology Advances **31**(2): 246-256.
- Jiang, C., Y. Liu, Z. Chen, M. Megharaj and R. Naidu (2013). "Impact of iron-based nanoparticles on microbial denitrification by *Paracoccus* sp. strain YF1." Aquatic Toxicology **142–143**(0): 329-335.
- Johnson, R. L., G. O. B. Johnson, J. T. Nurmi and P. G. Tratnyek (2009). "Natural Organic Matter Enhanced Mobility of Nano Zerovalent Iron." Environmental Science & Technology **43**(14): 5455-5460.
- Johnson, R. L., J. T. Nurmi, G. S. O'Brien Johnson, D. Fan, R. L. O'Brien Johnson, Z. Shi, A. J. Salter-Blanc, P. G. Tratnyek and G. V. Lowry (2013). "Field-Scale Transport and Transformation of Carboxymethylcellulose-Stabilized Nano Zero-Valent Iron." Environmental Science & Technology **47**(3): 1573-1580.
- Kadar, E., P. Rooks, C. Lakey and D. A. White (2012). "The effect of engineered iron nanoparticles on growth and metabolic status of marine microalgae cultures." Science of The Total Environment **439**(0): 8-17.
- Kanel, S. R., R. R. Goswami, T. P. Clement, M. O. Barnett and D. Zhao (2008). "Two Dimensional Transport Characteristics of Surface Stabilized Zero-valent Iron Nanoparticles in Porous Media." Environmental Science & Technology **42**(3): 896-900.
- Kanel, S. R., J.-M. Grenache and H. Choi (2006). "Arsenic(V) Removal from Groundwater Using Nano Scale Zero-Valent Iron as a Colloidal Reactive Barrier Material." Environmental Science & Technology **40**(6): 2045-2050.
- Keenan, C. R., R. Goth-Goldstein, D. Lucas and D. L. Sedlak (2009). "Oxidative Stress Induced by Zero-Valent Iron Nanoparticles and Fe(II) in Human Bronchial Epithelial Cells." Environmental Science & Technology **43**(12): 4555-4560.
- Keller, A. A., K. Garner, R. J. Miller and H. S. Lenihan (2012). "Toxicity of Nano-Zero Valent Iron to Freshwater and Marine Organisms." PLoS ONE **7**(8): e43983.
- Köber, R., H. Hollert, G. Hornbruch, M. Jekel, A. Kamptner, N. Klaas, H. Maes, K. M. Mangold, E. Martac, A. Matheis, H. Paar, A. Schäffer, H. Schell, A. Schiwy, K. R. Schmidt, T. J. Strutz, S. Thümmler, A. Tiehm and J. Braun (2014). "Nanoscale zero-valent iron flakes for groundwater treatment." Environmental Earth Sciences **72**(9): 3339-3352.
- Kocur, C. M., A. I. Chowdhury, N. Sakulchaicharoen, H. K. Boparai, K. P. Weber, P. Sharma, M. M. Krol, L. Austrins, C. Peace, B. E. Sleep and D. M. O'Carroll (2014). "Characterization of nZVI Mobility in a Field Scale Test." Environmental Science & Technology **48**(5): 2862-2869.
- Kocur, C. M., D. M. O'Carroll and B. E. Sleep (2013). "Impact of nZVI stability on mobility in porous media." Journal of Contaminant Hydrology **145**(0): 17-25.

Kolb, S. and A. Stacheter (2013). "Prerequisites for amplicon pyrosequencing of microbial methanol utilizors in the environment." Frontiers in Microbiology **4**(SEP).

Krajmalnik-Brown, R., T. Hölscher, I. N. Thomson, F. M. Saunders, K. M. Ritalahti and F. E. Löffler (2004). "Genetic Identification of a Putative Vinyl Chloride Reductase in Dehalococcoides sp. Strain BAV1." Applied and Environmental Microbiology **70**(10): 6347-6351.

Krumholz, L. R., J. P. McKinley, G. A. Ulrich and J. M. Suflita (1997). "Confined subsurface microbial communities in Cretaceous rock." Nature **386**(6620): 64-66.

Krzmarzick, M. J., B. B. Crary, J. J. Harding, O. O. Oyerinde, A. C. Leri, S. C. B. Myneni and P. J. Novak (2012). "Natural Niche for Organohalide-Respiring Chloroflexi." Applied and Environmental Microbiology **78**(2): 393-401.

Lee, C., J. Y. Kim, W. I. Lee, K. L. Nelson, J. Yoon and D. L. Sedlak (2008). "Bactericidal Effect of Zero-Valent Iron Nanoparticles on Escherichia coli." Environmental Science & Technology **42**(13): 4927-4933.

Li, H., Q. Zhou, Y. Wu, J. Fu, T. Wang and G. Jiang (2009). "Effects of waterborne nano-iron on medaka (Oryzias latipes): Antioxidant enzymatic activity, lipid peroxidation and histopathology." Ecotoxicology and Environmental Safety **72**(3): 684-692.

Li, Z. Q., K. Greden, P. J. J. Alvarez, K. B. Gregory and G. V. Lowry (2010). "Adsorbed Polymer and NOM Limits Adhesion and Toxicity of Nano Scale Zerovalent Iron to E. coli." Environmental Science & Technology **44**(9): 3462-3467.

Lien, H.-L. and W.-x. Zhang (1999). "Transformation of Chlorinated Methanes by Nanoscale Iron Particles." Journal of Environmental Engineering **125**(11): 1042-1047.

Lien, H.-L. and W.-x. Zhang (2001). "Nanoscale iron particles for complete reduction of chlorinated ethenes." Colloids and Surfaces A: Physicochemical and Engineering Aspects **191**(1-2): 97-105.

Liu, Y., H. Choi, D. Dionysiou and G. V. Lowry (2005). "Trichloroethene Hydrodechlorination in Water by Highly Disordered Monometallic Nanoiron." Chemistry of Materials **17**(21): 5315-5322.

Liu, Y., S. Li, Z. Chen, M. Megharaj and R. Naidu (2014). "Influence of zero-valent iron nanoparticles on nitrate removal by Paracoccus sp." Chemosphere **108**(0): 426-432.

Liu, Y., S. A. Majetich, R. D. Tilton, D. S. Sholl and G. V. Lowry (2005). "TCE Dechlorination Rates, Pathways, and Efficiency of Nanoscale Iron Particles with Different Properties." Environmental Science & Technology **39**(5): 1338-1345.

Liu, Y., T. Phenrat and G. V. Lowry (2007). "Effect of TCE Concentration and Dissolved Groundwater Solutes on NZVI-Promoted TCE Dechlorination and H₂ Evolution." Environmental Science & Technology **41**(22): 7881-7887.

Löffler, F. E., J. Yan, K. M. Ritalahti, L. Adrian, E. A. Edwards, K. T. Konstantinidis, J. A. Müller, H. Fullerton, S. H. Zinder and A. M. Spormann (2013). "Dehalococcoides mccartyi gen. nov., sp. nov., obligately organohalide-respiring anaerobic bacteria relevant to halogen cycling and bioremediation, belong to a novel bacterial class, Dehalococcoidia

classis nov., order Dehalococcoidales ord. nov. and family Dehalococcoidaceae fam. nov., within the phylum Chloroflexi." International Journal of Systematic and Evolutionary Microbiology **63**(Pt 2): 625-635.

Luijten, M. L. G. C., J. de Weert, H. Smidt, H. T. S. Boschker, W. M. de Vos, G. Schraa and A. J. M. Stams (2003). "Description of *Sulfurospirillum halorespirans* sp. nov., an anaerobic, tetrachloroethene-respiring bacterium, and transfer of *Dehalospirillum multivorans* to the genus *Sulfurospirillum* as *Sulfurospirillum multivorans* comb. nov." International Journal of Systematic and Evolutionary Microbiology **53**(3): 787-793.

Mace, C. (2006). "Controlling Groundwater VOCs: do nanoscale ZVI particles have any advantages over microscale ZVI of BNP." Pollution Engineering **38**(4): 24-28.

Man, Z. and Z. Dongye (2013). In Situ Dechlorination in Soil and Groundwater Using Stabilized Zero-Valent Iron Nanoparticles: Some Field Experience on Effectiveness and Limitations. Novel Solutions to Water Pollution, American Chemical Society. **1123**: 79-96.

Manchester, M. J., L. A. Hug, M. Zarek, A. Zila and E. A. Edwards (2012). "Discovery of a trans-Dichloroethene-Respiring *Dehalogenimonas* Species in the 1,1,2,2-Tetrachloroethane-Dechlorinating WBC-2 Consortium." Applied and Environmental Microbiology **78**(15): 5280-5287.

Marsalek, B., D. Jancula, E. Marsalkova, M. Mashlan, K. Safarova, J. Tucek and R. Zboril (2012). "Multimodal action and selective toxicity of zerovalent iron nanoparticles against cyanobacteria." Environmental Science and Technology **46**(4): 2316-2323.

Maymó-Gatell, X., Y.-t. Chien, J. M. Gossett and S. H. Zinder (1997). "Isolation of a Bacterium That Reductively Dechlorinates Tetrachloroethene to Ethene." Science **276**(5318): 1568-1571.

Maymó-Gatell, X., I. Nijenhuis and S. H. Zinder (2000). "Reductive Dechlorination of cis-1,2-Dichloroethene and Vinyl Chloride by "Dehalococcoides ethenogenes". " Environmental Science & Technology **35**(3): 516-521.

Moe, W. M., J. Yan, M. F. Nobre, M. S. da Costa and F. A. Rainey (2009). "*Dehalogenimonas lykanthroporepellens* gen. nov., sp. nov., a reductively dehalogenating bacterium isolated from chlorinated solvent-contaminated groundwater." International Journal of Systematic and Evolutionary Microbiology **59**(11): 2692-2697.

Oksanen, J., F. Blanchet and R. Kindt (2013). "Vegan: community ecology package. 2013." R package version: 2.0-7.

PARS_Environmental (2003). Pilot Test Final Report: Bimetallic Nanoscale Particle of Groundwater at Area 1. **1**.

Pawlett, M., K. Ritz, R. A. Dorey, S. Rocks, J. Ramsden and J. A. Harris (2013). "The impact of zero-valent iron nanoparticles upon soil microbial communities is context dependent." Environmental Science and Pollution Research International **20**(2): 1041-1049.

Phenrat, T., F. Fagerlund, T. Illangasekare, G. V. Lowry and R. D. Tilton (2011). "Polymer-Modified Fe⁰ Nanoparticles Target Entrapped NAPL in Two Dimensional Porous

Media: Effect of Particle Concentration, NAPL Saturation, and Injection Strategy." Environmental Science & Technology **45**(14): 6102-6109.

Phenrat, T., H.-J. Kim, F. Fagerlund, T. Illangasekare, R. D. Tilton and G. V. Lowry (2009). "Particle Size Distribution, Concentration, and Magnetic Attraction Affect Transport of Polymer-Modified Fe₀ Nanoparticles in Sand Columns." Environmental Science & Technology **43**(13): 5079-5085.

Phenrat, T., H. J. Kim, F. Fagerlund, T. Illangasekare and G. V. Lowry (2010). "Empirical correlations to estimate agglomerate size and deposition during injection of a polyelectrolyte-modified Fe-0 nanoparticle at high particle concentration in saturated sand." Journal of Contaminant Hydrology **118**(3-4): 152-164.

Phenrat, T., T. C. Long, G. V. Lowry and B. Veronesi (2009). "Partial Oxidation ("Aging") and Surface Modification Decrease the Toxicity of Nanosized Zerovalent Iron." Environmental Science & Technology **43**(1): 195-200.

Pilloni, G., M. S. Granitsiotis, M. Engel and T. Lueders (2012). "Testing the Limits of 454 Pyrotag Sequencing: Reproducibility, Quantitative Assessment and Comparison to T-RFLP Fingerprinting of Aquifer Microbes." PLoS ONE **7**(7): e40467.

Ramos-Padron, E., S. Bordenave, S. Lin, I. M. Bhaskar, X. Dong, C. W. Sensen, J. Fournier, G. Voordouw and L. M. Gieg (2011). "Carbon and sulfur cycling by microbial communities in a gypsum-treated oil sands tailings pond." Environ Sci Technol **45**(2): 439-446.

Raychoudhury, T., G. Naja and S. Ghoshal (2010). "Assessment of transport of two polyelectrolyte-stabilized zero-valent iron nanoparticles in porous media." Journal of Contaminant Hydrology **118**(3-4): 143-151.

Raychoudhury, T., N. Tufenkji and S. Ghoshal (2012). "Aggregation and deposition kinetics of carboxymethyl cellulose-modified zero-valent iron nanoparticles in porous media." Water Research **46**(6): 1735-1744.

Raychoudhury, T., N. Tufenkji and S. Ghoshal (2014). "Straining of polyelectrolyte-stabilized nanoscale zero valent iron particles during transport through granular porous media." Water Research **50**(0): 80-89.

Rosenthal, H., L. Adrian and M. Steiof (2004). "Dechlorination of PCE in the presence of Fe₀ enhanced by a mixed culture containing two Dehalococcoides strains." Chemosphere **55**(5): 661-669.

Saccà, M. L., C. Fajardo, G. Costa, C. Lobo, M. Nande and M. Martin (2014). "Integrating classical and molecular approaches to evaluate the impact of nanosized zero-valent iron (nZVI) on soil organisms." Chemosphere **104**(0): 184-189.

Sakulchaicharoen, N., D. M. O'Carroll and J. E. Herrera (2010). "Enhanced stability and dechlorination activity of pre-synthesis stabilized nanoscale FePd particles." Journal of Contaminant Hydrology **118**(3-4): 117-127.

Sevcu, Alena, Y. S. El-Temsah, E. J. Joner and M. Cernik (2011). "Oxidative Stress Induced in Microorganisms by Zero-valent Iron Nanoparticles." Microbes and Environments **26**(4): 271-281.

Shin, K.-H. and D. K. Cha (2008). "Microbial reduction of nitrate in the presence of nanoscale zero-valent iron." Chemosphere **72**(2): 257-262.

Song, H. and E. R. Carraway (2005). "Reduction of Chlorinated Ethanes by Nanosized Zero-Valent Iron: Kinetics, Pathways, and Effects of Reaction Conditions." Environmental Science & Technology **39**(16): 6237-6245.

Su, C., R. W. Puls, T. A. Krug, M. T. Watling, S. K. O'Hara, J. W. Quinn and N. E. Ruiz (2012). "A two and half-year-performance evaluation of a field test on treatment of source zone tetrachloroethene and its chlorinated daughter products using emulsified zero valent iron nanoparticles." Water Research **46**(16): 5071-5084.

Sung, Y., K. E. Fletcher, K. M. Ritalahti, R. P. Apkarian, N. Ramos-Hernández, R. A. Sanford, N. M. Mesbah and F. E. Löffler (2006). "Geobacter lovleyi sp. nov. Strain SZ, a Novel Metal-Reducing and Tetrachloroethene-Dechlorinating Bacterium." Applied and Environmental Microbiology **72**(4): 2775-2782.

Sung, Y., K. M. Ritalahti, R. P. Apkarian and F. E. Löffler (2006). "Quantitative PCR confirms purity of strain GT, a novel trichloroethene-to- ethene-respiring Dehalococcoides isolate." Applied and Environmental Microbiology **72**(3): 1980-1987.

Taghavy, A., J. Costanza, K. D. Pennell and L. M. Abriola (2010). "Effectiveness of nanoscale zero-valent iron for treatment of a PCE-DNAPL source zone." Journal of Contaminant Hydrology **118**(3-4): 128-142.

Tilston, E. L., C. D. Collins, G. R. Mitchell, J. Princivalle and L. J. Shaw (2013). "Nanoscale zerovalent iron alters soil bacterial community structure and inhibits chloroaromatic biodegradation potential in Aroclor 1242-contaminated soil." Environmental Pollution **173**(0): 38-46.

Tiraferrri, A., K. L. Chen, R. Sethi and M. Elimelech (2008). "Reduced aggregation and sedimentation of zero-valent iron nanoparticles in the presence of guar gum." Journal of Colloid and Interface Science **324**(1-2): 71-79.

Tiraferrri, A. and R. Sethi (2009). "Enhanced transport of zerovalent iron nanoparticles in saturated porous media by guar gum." Journal of Nanoparticle Research **11**(3): 635-645.

Tosco, T. and R. Sethi (2010). "Transport of Non-Newtonian Suspensions of Highly Concentrated Micro- And Nanoscale Iron Particles in Porous Media: A Modeling Approach." Environmental Science & Technology **44**(23): 9062-9068.

Vecchia, E. D., M. Luna and R. Sethi (2009). "Transport in Porous Media of Highly Concentrated Iron Micro- and Nanoparticles in the Presence of Xanthan Gum." Environmental Science & Technology.

Waller, A. S., R. Krajmalnik-Brown, F. E. Löffler and E. A. Edwards (2005). "Multiple reductive-dehalogenase-homologous genes are simultaneously transcribed during dechlorination by Dehalococcoides-containing cultures." Appl Environ Microbiol **71**(12): 8257-8264.

Waller, A. S., R. Krajmalnik-Brown, F. E. Löffler and E. A. Edwards (2005). "Multiple Reductive-Dehalogenase-Homologous Genes Are Simultaneously Transcribed

during Dechlorination by Dehalococcoides-Containing Cultures." Applied and Environmental Microbiology **71**(12): 8257-8264.

Wang, Q., G. M. Garrity, J. M. Tiedje and J. R. Cole (2007). "Naive Bayesian classifier for rapid assignment of rRNA sequences into the new bacterial taxonomy." Appl Environ Microbiol **73**(16): 5261-5267.

Wang, Y., D. Zhou, Y. Wang, X. Zhu and S. Jin (2011). "Humic acid and metal ions accelerating the dechlorination of 4-chlorobiphenyl by nanoscale zero-valent iron." Journal of Environmental Sciences **23**(8): 1286-1292.

Wei, Y. T., S. C. Wu, C. M. Chou, C. H. Che, S. M. Tsai and H. L. Lien (2010). "Influence of nanoscale zero-valent iron on geochemical properties of groundwater and vinyl chloride degradation: A field case study." Water Research **44**(1): 131-140.

Wilson, J. T. and X. Lu (2007). Relationship between Dehalococcoides DNA in groundwater and natural attenuation of chlorinated solvents. Battelle Press - 9th International In Situ and On-Site Bioremediation Symposium 2007.

Wright, E. S., L. S. Yilmaz and D. R. Noguera (2012). "DECIPHER, a search-based approach to chimera identification for 16S rRNA sequences." Appl Environ Microbiol **78**(3): 717-725.

Xiu, Z.-m., K. B. Gregory, G. V. Lowry and P. J. J. Alvarez (2010). "Effect of Bare and Coated Nanoscale Zerovalent Iron on tceA and vcrA Gene Expression in Dehalococcoides spp." Environmental Science & Technology **44**(19): 7647-7651.

Xiu, Z.-m., Z.-h. Jin, T.-l. Li, S. Mahendra, G. V. Lowry and P. J. J. Alvarez (2010). "Effects of nano-scale zero-valent iron particles on a mixed culture dechlorinating trichloroethylene." Bioresource Technology **101**(4): 1141-1146.

Yan, W., H.-L. Lien, B. E. Koel and W.-x. Zhang (2013). "Iron nanoparticles for environmental clean-up: recent developments and future outlook." Environmental Science: Processes & Impacts **15**(1): 63-77.

Yang, Y., J. Guo and Z. Hu (2013). "Impact of nano zero valent iron (NZVI) on methanogenic activity and population dynamics in anaerobic digestion." Water Research **47**(17): 6790-6800.

Zhang, W.-x. (2003). "Nanoscale Iron Particles for Environmental Remediation: An Overview." Journal of Nanoparticle Research **5**(3): 323-332.

Zhou, L., T. L. Thanh, J. Gong, J.-H. Kim, E.-J. Kim and Y.-S. Chang (2014). "Carboxymethyl cellulose coating decreases toxicity and oxidizing capacity of nanoscale zerovalent iron." Chemosphere **104**(0): 155-161.

Zhu, L., H.-z. Lin, J.-q. Qi, X.-y. Xu and H.-y. Qi (2012). "Effect of H₂ on reductive transformation of p-ClNB in a combined ZVI-anaerobic sludge system." Water Research **46**(19): 6291-6299.

Ziv-El, M., S. C. Popat, P. Parameswaran, D.-W. Kang, A. Polasko, R. U. Halden, B. E. Rittmann and R. Krajmalnik-Brown (2012). "Using electron balances and molecular

techniques to assess trichloroethene-induced shifts to a dechlorinating microbial community." Biotechnology and Bioengineering **109**(9): 2230-2239.

Chapter 6

6 Conclusions and Recommendation

6.1 Summary

This thesis presents a comprehensive field scale evaluation of nZVI/CMC as a remediation alternative for the treatment of chlorinated solvents. Three manuscripts were prepared for this thesis exploring important aspects of field scale nZVI application.

Mobility of nZVI/CMC in natural porous media at the field scale, and therefore delivery to the target in situ treatment area, had not been clearly demonstrated prior to this work, therefore the first manuscript set out with the goal of monitoring nZVI mobility at an active field site. Delivery of nZVI/CMC into a contaminated utility corridor was tracked during gravity feed injection. Although consultants and practitioners may assert nZVI mobility at the field scale, when the first manuscript in this thesis was published it was among the most demonstration of nZVI field scale mobility in literature. What made this work impactful was sample preservation for improved nZVI characterization during transport. A systematic approach to monitoring nZVI parameters was able to definitively link the geochemical indicators that have been previously used to delineate nZVI injection (e.g., Total Fe, ORP, Fe₀ content) to the analytical evidence from TEM, EDS, and DLS.

The strong evidence of nZVI/CMC delineation in the subsurface was the first of its kind at a field site, allowing for improved interpretation of degradation resulting from injection in the second study. cVOC degradation from abiotic and biotic sources was the focus of the second paper as it was known that nZVI had travelled along a primary flow path and this could be compared to an adjacent flow path where nZVI/CMC was not detected. Degradation was monitored and observed to be high along the nZVI/CMC flow path, compared to the adjacent flowpath suggesting that the enhanced degradation that occurred was attributable to nZVI/CMC injection. The abundance of *Dehalococcoides* along the nZVI/CMC flowpath was also determined to be higher than background levels on site. In previous studies the longevity of nZVI reaction has been called into question as reports suggest that the Fe₀ content is completely oxidized in less than a week in the subsurface. Limited reaction longevity would

weaken the benefits of nZVI (i.e, increased surface area and rapid contaminant degradation) over other treatment options. The implication that nZVI/CMC enhanced the microbially mediated degradation on site, however, introduces a yet to be quantified net benefit of the introduction of nZVI/CMC. Different methods of estimating electron equivalents from environmental parameters were explored along the two flow paths providing further evidence that the nZVI/CMC enhanced degradation over an unexpectedly short period of time.

The third study used the knowledge of nZVI/CMC delineation in the first paper to present the first field scale study of microbiological community response to nZVI/CMC remedial injection. In addition to the qPCR methods presented in the second study, that are more regularly implemented in monitoring natural attenuation or enhanced bioremediation at contaminated sites, next generation amplicon pyrosequencing was used on a selected sample group. This genomic information was used to identify the entire microbiological community present on the site for a two year monitoring period following nZVI/CMC injection. Drastic changes in the community resulted in enrichment of strict anaerobes and fermenters in locations that were originally impacted and sustained dechlorination persisted throughout the monitoring period due nZVI/CMC injection.

6.2 Conclusions

The major conclusions that were drawn from these studies are as follows:

Characterization of nZVI Mobility in a Field Scale Test

- nZVI/CMC synthesized in the field is a viable method of scalable application that creates laboratory quality particles. Injection into direct-push wells are able to deliver nZVI into clayey-sand. For other subsurface material pilot tests should be undertaken to similarly demonstrate injection capabilities.
- Definitive proof of nZVI/CMC transport was achieved through rigorous and thoughtful sample collection and preparation. Sophisticated laboratory techniques were successfully used to evaluate nZVI field samples.
- Characterization of nZVI particles definitively showed that nanoparticles were transmitted through the subsurface and retrieved from a monitoring well. Size

analysis determined that the particles were similar upon arrival at the well and elemental composition of the particles was the same as that injected.

- A link was established between many of the geochemical parameters that have been used to infer mobility of polymer stabilized nZVI and the confirmed mobility in this study.

Contributions of Abiotic and Biotic Dechlorination Following Carboxymethyl Cellulose Stabilized Nanoscale Zero Valent Iron Injection

- nZVI/CMC significantly impacts the dechlorinating microorganism *Dehalococcoides (dhc)* in-situ immediately following injection. Absolute abundance of *dhc* increases within days of nZVI/CMC injection.
- Clarifies concerns over bactericidal effects of nZVI on microorganisms in the context of contaminated site remediation.
- Enhanced degradation is observed downgradient of the nZVI/CMC injection. Parent compound degradation is immediate, however, a longer time period (i.e., further downgradient) was required for degradation of lesser chlorinated compounds.
- Corroborates earlier studies that suggest that nZVI enhances microbially mediated degradation in the subsurface.

Long term dechlorination following ZVI/CMC injection and impact on microbial communities, including organohalide-respiring microorganisms

- There was a long term decline in parent cVOC compound concentrations in the nZVI impacted wells and large increases in lesser chlorinated compound concentrations followed by degradation past cis-DCE. The same definitive decline in parent compound concentrations does not occur in the non-impacted wells, nor does the peak and decline of lesser chlorinated compounds.
- In wells less-impacted by nZVI/CMC injection, no change in *dhc* abundance was observed during the monitoring period (i.e., average abundance at MW4 and MW9 was 7.5×10^6 gene copies/L, similar to background *dhc* abundance). The average for the wells affected by the nZVI/CMC injection, is

1x10⁸ gene copies/L, showing an order of magnitude increase in abundance compared to the wells that were less-impacted by the injection.

- The microbial community on site prior to amendment activities is largely uniform, consisting of a high relative abundance of proteobacteria and other phyla that have been previously characterized. Looking beyond the phylum level revealed that dechlorinators are abundant in background samples throughout the site. The relative abundance for *dhc* increased following amendment activities and remain elevated for a two year period suggesting that the injection activities enriched *dhc* on site
- Following the injection of nZVI/CMC the microbial community shifted with a large increase in relative abundance of anaerobes and fermenters, and a decline in the relative abundance of proteobacteria.
- The most enriched populations of *dhc* using both metrics (relative and absolute abundance) are associated with the group of wells that were impacted by the nZVI/CMC injection highlighting the distinction between the impacted and less impacted wells using two measured abundances of *dhc*.
- The microbial ecology significantly changed on site during the monitoring period. These changes were the result of the changes associated with the injection activities on the site as there is a clear distinction between the nZVI/CMC impacted and non-impacted wells in the ordination space.
- Wells that were impacted by the injection share the following similarities:
 - they have lower parent compound concentrations and higher concentrations of degradation products
 - they have higher absolute abundances of *dhc* and *vcrA* from qPCR
 - they have a higher pH and a lower ORP
- The predominant organohalide-respiring species *Dehalococcoides* (*dhc*) and *Dehalogenimonas* (*dhg*) occupy the same ordination space as the nZVI/CMC impacted wells. Thus, the microbial ecology that has resulted from the injection has enriched these species.

6.3 Implications

- nZVI/CMC injection follows preferential paths in the subsurface and is likely only mobile while a sufficiently high hydraulic gradient is applied or exists naturally.
- The effect of abiotic and biotic degradation is detectable in the first three weeks following injection where the nZVI/CMC is detected. Without delineating the extend of nZVI injection, subsequent interpretation of cVOC degradation becomes somewhat speculative.
- Abundances of *Dehalococcoides spp.* increased over a very short period of time reaching levels that were unexpectedly high. Such levels are specifically targeted by enhanced bioremediation or bio-augmentation efforts that use enriched inoculated cultures.
- Sustained degradation conditions were created on site as a result of a relatively low dose of nZVI (1 g/L) and CMC (0.8% wt). Considering the immediate effect that nZVI/CMC had on the dechlorinating species, nZVI/CMC may be explored and specifically designed as a method of initiating enhanced bioremediation.
- Microbial communities that are not suited to anaerobic reducing conditions do not persist during remedial activities following nZVI/CMC injection. Enriched organohalide-respiring and supporting microbial communities are enriched during remediation using nZVI/CMC

6.4 Future Outlook and Research Needs

- Established techniques and approaches in site characterization have been shown to improve the conceptual understanding of chlorinated solvent remediation. However, these techniques are undervalued and often overlooked in the beginning phases of site management leading to repercussions during remediation.
- Field methods and techniques are needed to the determination of nZVI concentration and reactive content in-situ. Aqueous based methods for analyzing nZVI result in oxidation which impacts the results. Aqueous

sampling in the field also may not accurately represent the nZVI that is attached or otherwise immobile in the subsurface.

- The reactivity of mobilized and immobilized nZVI insitu and the reaction longevity under remediation relevant conditions has not been explored. Experimental conditions for nZVI reactivity with chlorinated solvents have most often been reported at Fe^0 loadings that would most accurately reflect PRB plume remediation conditions. Few studies have investigated multicomponent chlorinated solvent systems and lower Fe^0 loadings.
- Mechanisms have been proposed showing reactive site blocking and diffusive barriers to product and reactants due to polymer surface coatings in microcosm experiments. The implications of such mechanisms and the resulting deviation from established reaction mechanisms for ZVI surfaces have not been explored in macroscopic studies. Thus, the consequences on scaled up experiments is not known. This may be, in part, due to difficulty in mass balance closure in nZVI/CMC systems.
- The use of empirical correlation for the predictive modelling of nZVI/CMC mobility and reactivity has been presented from a bottom up approach, building empirical relationships from a theoretical basis. There is a need to include relevant environmental parameters acquired from a top down approach from field investigation.
- The introduction and fate of nZVI into the subsurface through remedial injection is becoming more clearly acceptable from an ecotoxicity perspective. Studies show that the nZVI is oxidizes relatively quickly, posing far less risk in its “aged” state. More studies are needed to evaluate remediation relevant conditions and microorganisms that are expected to be exposed to such conditions. There are significant challenges, but a great need for recreating field conditions in controlled manner that does not disrupt microorganism behavior.

Appendices

7 Appendix A: NANOSCALE ZERO VALENT IRON AND BIMETALLIC PARTICLES FOR CONTAMINATED SITE REMEDIATION

Denis O'Carroll^{a,b,*}, Brent Sleep^c, Magdalena Krol^a, Hardiljeet Boparai^a and Christopher Kocur^a

^aCivil and Environmental Engineering, The University of Western Ontario, 1151 Richmond Street, London, ON, Canada, N6A 5B9

^bWater Research Laboratory, Civil and Environmental Engineering, University of New South Wales, 110 King Street, Manly Vale, NSW, Australia

^cCivil Engineering, University of Toronto, 35 St. George St.; Toronto, ON, Canada, M5S 1A4

7.1 Abstract:

Since the late 1990s, the use of nano zero valent iron (nZVI) for groundwater remediation has been investigated for its potential to reduce subsurface contaminants such as PCBs, chlorinated solvents, and heavy metals. nZVI shows tremendous promise in the environmental sector due to its high reactivity and as such, numerous laboratory and field studies have been performed to assess its effectiveness. This paper reviews the current knowledge of nZVI/bimetallic technology as it pertains to subsurface remediation of chlorinated solvents and heavy metals. The manuscript provides background on the technology, summarizing nZVI reactions with chlorinated solvents and metals, and examines the factors affecting nZVI reactivity. Studies on subsurface transport of bare and coated nZVI particles are also reviewed and challenges with field implementation are discussed. This manuscript offers a comprehensive review of nZVI technology and highlights the work still needed to optimize it for subsurface remediation.

7.2 Introduction

In the past, liquid wastes were disposed through direct pumping into the ground, migrated into the ground from leaky storage ponds and through surface spills, with no recognition of the likelihood that these wastes could persist in the subsurface for decades, potentially contaminating drinking water sources. Effluent slurries with high heavy metal content and non-aqueous phase liquids (NAPLs) are two common waste liquids that have been frequently disposed of improperly following a variety of industrial processes. Both heavy metals and chlorinated solvents, a particularly persistent NAPL contaminant, can contaminate water sources for decades and are one of the more common contaminants at brownfield and industrialized sites. Although a number of innovative remediation technologies have been developed, such as steam and density modified displacement, stabilization/solidification and *in situ* redox manipulation (e.g. She et al. 1999, Fruchter et al. 2000, USEPA 2000, Ramsburg et al. 2002), existing technologies are rarely able to achieve clean up goals in contaminated

aquifers at the completion of remedial activities. The problem relates to the inability of existing remedial technologies to remove, sequester or convert sufficient contaminant mass in the subsurface to significantly reduce aqueous phase concentrations and contaminant flux. The decisions related to site remediation are therefore still subject to considerable debate despite over two decades of active research and development (Sale et al. 2001, NSF 2004). The development of new and innovative remediation technologies is, therefore, crucial to achieve clean up goals at contaminated sites and ensure an abundant source of safe water for future generations.

The use of nanometals for subsurface remediation of chlorinated compound and heavy metal contaminated sites has received significant attention in part due to the ability of nanometals to rapidly transform contaminants in controlled laboratory experiments. Nanometals used for these purposes include nano iron and zinc, however nanoscale zero valent iron (nZVI) is most commonly used. In addition, other metals such as palladium or nickel have been added to increase the reduction rate. This combination of nZVI with a noble metal is referred to as a bimetallic nanometal. The reactivity and the availability of existing technology to precisely design and synthesize nanometals make nanometals particularly attractive for the remediation of subsurface contaminants. This remediation technology involves a series of steps for nanometals:

1. Transport, in the aqueous phase (or other delivery fluid), to the contaminated zone;
2. Attachment to soils in the contaminated zone or partitioning to the NAPL/aqueous phase;
3. Reaction with the target contaminant to form less toxic or less mobile products.

Nanometals have potential for use in remediation of a wide range of priority pollutants as indicated by a number of controlled laboratory experiments (e.g. Lien et al. 2001, Liu et al. 2005, Song et al. 2005, Karabelli et al. 2008, Li et al. 2008, Liu et al. 2010, Sarathy et al. 2010,

Boparai et al. 2011, Hwang et al. 2011). However, further work is necessary to address the complexities associated with nanometal application at the field scale. For example, nanometals may react with various naturally occurring groundwater constituents decreasing the reducing equivalents available for reaction with the target contaminants. Another problem that has hampered the widespread implementation of nanometals is poor subsurface mobility. Due to strong attractive interparticle forces, primarily magnetic, nZVI, the typical nanometal used for remediation, tends to agglomerate to micron size particles, which have limited mobility in porous media. To overcome this problem, various polymers, and other coatings, have been used to stabilize nZVI particles, with varying degrees of success (e.g. He et al. 2005, Saleh et al. 2005, He et al. 2007, Sun et al. 2007, Phenrat et al. 2008, Zhan et al. 2009, He et al. 2010, Phenrat et al. 2010, Sakulchaicharoen et al. 2010). A number of field trials have been conducted to evaluate nZVI mobility and the impact of nZVI on chlorinated solvent contaminant mass and flux. However, several field scale applications have suffered from poor nZVI mobility (Quinn et al. 2005, Bennett et al. 2010). Other studies have inferred good nZVI mobility but these mobility evaluations were based on measurements of contaminant reductions or total iron (i.e., including dissolved iron species) in wells downgradient of the injection well (Elliott et al. 2001, Zhang 2003), rather than direct measurement of Fe^0 concentrations. Given these limited studies, additional work is required to assess field mobility and performance of nZVI/bimetallic nanometals at the field scale.

The goal of this review is to present the current state of knowledge related to the use of nZVI/bimetallic nanometals for the *in situ* remediation of chlorinated solvents and heavy metals. This work is divided into six main sections: nanometal reactivity with chlorinated compounds; reactivity with heavy metal target contaminants; factors affecting nZVI reactivity; nanometal mobility in controlled laboratory experiments; the current state of modeling nZVI subsurface transport; and outcomes of a series of nanometal field trials and lessons learned. Although nanometals have been used for the remediation of a variety of priority pollutants this work focuses on two classes (heavy metals and chlorinated solvents) that are of particular concern. Throughout this work, additional research needs and unresolved challenges are highlighted providing a comprehensive review as well as a look to the future of nZVI/bimetallic subsurface remediation.

7.3 Background

7.3.1 Development of Zero Valent Metals for Remediation

Although environmental nanotechnology for remediation applications was mainly developed in the last decade following the seminal work of Wang and Zhang (1997), larger micron and millimeter size metals for contaminant destruction have been employed for some time. The first use of zero valent metals for degradation of chlorinated compounds in the environment was studied by Sweeney and Fischer (1972) who used metallic zinc for the degradation of halogenated organic compounds. Subsequently, iron powder was used for the removal of chlorinated compounds from wastewater (Senzaki et al. 1988, Senzaki et al. 1989) as well as contaminated groundwater (Gillham et al. 1994, Orth et al. 1996, Baciocchi et al. 2003).

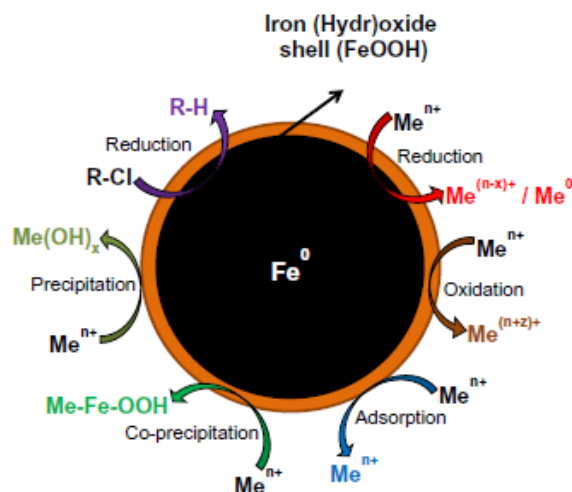
Gillham and O'Hannesin (1994) were the first to show the effectiveness of zero valent iron (ZVI) for chlorinated ethane, ethene and methane degradation with normalized (to 1 m²/ml) contaminant half-lives ranging from 0.013 to 20 hrs based on a series batch tests with ZVI. Matheson and Tratnyek (1994) also reported rapid dehalogenation of carbon tetrachloride (CT) and chloroform using iron particles. In addition, ZVI was found to be effective for the remediation of a variety of priority pollutants, including metals, (Gould 1982, Cantrell et al. 1995, Blowes et al. 2000, Su et al. 2001, Nikolaidis et al. 2003, Lien et al. 2005, Moraci et al. 2010), polychlorinated biphenyls (PCBs) (Chuang et al. 1995, Wai et al. 1999), chlorinated pesticides (Sayles et al. 1997, Satapanajaru et al. 2006, Comfort et al. 2009), nitro aromatic compounds (Agrawal et al. 1996, Hundal et al. 1997, Bandstra et al. 2005) and nitrates (Young et al. 1964, Cheng et al. 1997).

These studies, along with others (Johnson et al. 1996, Tratnyek 1996, Arnold et al. 2000), have resulted in application of ZVI, mostly in the form of permeable reactive barriers (PRBs) (Blowes et al. 2000, Baciocchi et al. 2003, Wilkin et al. 2005, Henderson et al. 2007, Higgins et al. 2009, Gillham 2010, Phillips et al. 2010). Although PRBs are effective at limiting off site migration of contaminants, they do not specifically target contaminant source zone remediation and have limited applications due to construction restrictions (i.e. depth of wall). Wang and Zhang (Wang et al. 1997) reported a method of synthesizing nanoscale ZVI (nZVI).

This breakthrough was important for two reasons: the nZVI particles have a very high surface area to weight ratio, resulting in higher reactivity rates than micron scale ZVI when normalized to mass (Orth et al. 1996, Wang et al. 1997, Liu et al. 2005, Nurmi et al. 2005, Li 2006, Rivero-Huguet et al. 2009) and nZVI particles are smaller than most porous media pore throats. As a result, nZVI particles could theoretically be transported through the subsurface to a contaminant source zone. Since 1997, many studies have shown that nanometals are able to rapidly degrade a wide variety of priority pollutants (e.g. Liu et al. 2005, Song et al. 2005, Li et al. 2007, Li et al. 2008, Liu et al. 2010, Sarathy et al. 2010, Hwang et al. 2011). Bimetallic nanoparticles and stabilizers have also been investigated and have been shown to enhance the reactivity and mobility of nanoparticles, respectively (Elliott et al. 2001, Lien et al. 2001, Schrick et al. 2002, He et al. 2005, Barnes et al. 2010, Sakulchaicharoen et al. 2010).

7.3.2 nZVI Particle Structure

Bare nZVI particles are typically less than 100 nm in diameter. In aqueous solutions, all nZVI particles react with water and oxygen to form an outer iron (hydr)oxide layer. As a result, nZVI particles have a core-shell structure (Nurmi et al. 2005, Sun et al. 2006, Li et al. 2007) (Appendix A.1). The thin and distorted oxide layer allows electron transfer from the metal (1) directly through defects such as pits or pinholes, (2) indirectly via the oxide conduction band, impurity or localized band, and (3) from sorbed or structural Fe^{2+} , thus sustaining the capacity of the particles for reduction of contaminants (Li 2006). The outer (hydr)oxide layer may also act as an efficient adsorbent for various contaminants, including metals, as will be discussed in Section 4.



Appendix A. 1: Core-shell structure of nZVI depicting various mechanisms for the removal of metals and chlorinated compounds. Adapted from Li et al [62].

nZVI can be synthesized by a number of methods, including the sonochemical method, the electrochemical method, the gas phase reduction method, and the liquid phase reduction method (Grinstaff et al. 1993, Glavee et al. 1995, Wang et al. 1997, Uegami et al. 2003, Yoo et al. 2007). Among these, gas phase reduction and liquid phase reduction are the most common methods for synthesizing nZVI for remediation purposes. nZVI particles synthesized by these methods rapidly develop a core-shell structure due to reaction with air or water, but may differ in particle size, surface area, degree of crystallinity, and thickness and composition of oxide shell (Signorini et al. 2003, Liu et al. 2005, Nurmi et al. 2005). Reactive nanoscale iron particles (RNIP), commercially available from Toda Kogyo Corp., are produced by reducing goethite and hematite particles at high temperatures with hydrogen gas (Uegami et al. 2003, Nurmi et al. 2005). These particles are made up of a relatively large α -Fe core and an outer magnetite (Fe_3O_4) shell (Liu et al. 2005, Nurmi et al. 2005, Phenrat et al. 2007), with reported particle diameters of 40-70 nm (Liu et al. 2005, Liu et al. 2005, Nurmi et al. 2005, Phenrat et al. 2007, Phenrat et al. 2009). α -Fe can be defined as an allotropic form of pure iron having a body centered cubic (bcc) crystal structure (Kakani et al. 2004). Synthesizing nZVI using sodium borohydride (Fe^{BH}) results in amorphous particles with an α -Fe core and an outer shell consisting of iron (hydr)oxides (Nurmi et al. 2005, Li 2006, Yan et al. 2010). These particles are typically 10-100 nm in diameter (Wang et al. 1997, Liu et al. 2005, e.g. Liu et al. 2005, Nurmi et al. 2005, Song et al. 2005). Although Wang and Zhang (1997) identified a “periodic

arrangement of iron atoms” using XRD analysis, which is indicative of crystal structures, Fe^{BH} nanoparticles have typically been characterized as amorphous (Liu et al. 2006). This may be because even though Fe^{BH} particles have a crystalline core, the core diameters for Fe^{BH} are much smaller in size (< 1.5 nm) than RNIP core diameters (30 nm) (Nurmi et al. 2005). XRD studies also showed that Fe^{BH} cores were less ordered than RNIP cores (Liu et al. 2005). These differences in nZVI structural properties strongly influence particle reactivity and the aging of particles, and therefore the particle efficiency (fraction of added Fe⁰ in nZVI particles that is used in degrading contaminant) (Liu et al. 2005, Liu et al. 2005, Nurmi et al. 2005). Liu et al. (2005) examined the reductive dechlorination rates of Fe^{BH} when the Fe⁰ core was poorly ordered/amorphous and the Fe⁰ had been crystallized through annealing. The amorphous Fe^{BH} produced a greater reaction rate and extent of dechlorination of TCE with ethane as major end product when H₂ was externally supplied. In contrast, the rates of TCE dechlorination for the crystalline Fe^{BH} were similar in the presence and absence of externally supplied H₂. These results indicate that the amorphous Fe⁰ in Fe^{BH} can catalyze the reaction of H₂ with chlorinated solvents, while the crystalline forms of Fe⁰, such as in RNIP (Liu et al. 2005) would not have this catalytic effect. The crystallization of these particles resulted in less H₂ activation and slower TCE dechlorination, with acetylene as the major end product. Liu et al. (2005) also found that Fe^{BH} efficiency was much higher than RNIP (92% to 52% respectively) with some inaccessible Fe⁰ remaining in the RNIP particles but not in the Fe^{BH} particles. These studies show that the reactivity and efficiency of nanoparticles is dependent on particle characteristics and is an important consideration for remediation activities.

7.4 Reaction of Chlorinated Solvents with Nanometals

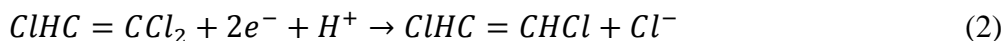
As a strong reductant (i.e., reduction potential of -0.440 V (Bard et al. 1985)) iron reduces chlorinated compounds by reductive dehalogenation while being oxidized:



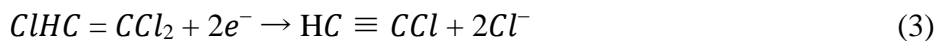
Arnold and Roberts (2000) and Li and Farrell (2000) describe reductive dehalogenation via two reactive pathways: hydrogenolysis, and reductive elimination (dihaloelimination).

Arnold and Roberts (2000) note that reductive dehalogenation can occur via more than one pathway simultaneously in the same system.

Hydrogenolysis of chlorinated compounds, such as trichloroethene, involves replacement of a chlorine atom by a hydrogen atom and requires an electron donor as well as a proton donor (hydrogen) (Roberts et al. 1996). The general equation for reduction of chlorinated compounds by hydrogenolysis is (Matheson et al. 1994, Orth et al. 1996):

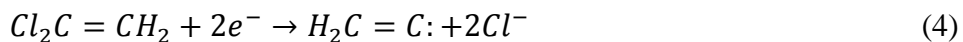


In reductive elimination (α or β), chlorine atoms are released by the chlorinated compound without addition of hydrogen. β -elimination releases chlorine atoms, resulting in the decrease in the degree of saturation of the carbon-carbon bond. Equation 3 is an example of β -elimination of a chlorinated ethene (such as TCE to chloroacetylene):



β -elimination can also occur with chlorinated ethanes, such as 1,2-DCA to vinyl chloride.

α -elimination can also lead to dehalogenation of chlorinated compounds. This pathway is typically associated with compounds that have both chlorine atoms located on the same carbon and results in the formation of a carbene radical that can react rapidly to form ethene, avoiding the formation of vinyl chloride (Arnold et al. 2000):



Another reaction that is pertinent to systems undergoing reductive dechlorination is hydrogenation, which involves the addition of hydrogen across a double or triple carbon-carbon bond, converting alkynes to alkenes (acetylene to ethene for example) and alkenes to alkanes (ethene to ethane for example). This is often the last reaction after α or β -elimination and is often catalyzed with another metal or atomic hydrogen (Matheson et al. 1994, Yu et al. 1997, Liu et al. 2005).

Iron can also react with water producing hydrogen gas (Orth et al. 1996, Liu et al. 2005):



This can lead to the formation of iron (hydr)oxide precipitates (e.g. $\text{Fe}(\text{OH})_2$) resulting in the formation of a surface layer on nZVI particles (Matheson et al. 1994, Cook 2009, Gillham 2010).

Irrespective of the reductive pathway, electrons needed for reductive dehalogenation can be donated via three different mechanisms as described in Matheson and Tratnyek (1994). Direct oxidation of elemental iron at the metal surface transfers electrons to the reduced compound (Eq. 1) and allows for dehalogenation of chlorinated compounds. The reduction of water (Eq. 5) leads to the formation of hydrogen gas which can act as a reductant (Liu et al. 2005). Dehalogenation with hydrogen as direct electron donor often requires a catalyst as H_2 alone is not a good reductant (Matheson et al. 1994). Fe^{2+} can also be oxidized to Fe^{3+} producing reducing equivalents for dehalogenation. This is a slow process and often requires the presence of ligands (Matheson et al. 1994).

One significant concern of any remediation technology is the formation of daughter products that are more toxic than the parent compounds. Although hydrogenolysis can be an important dehalogenation pathway for many chlorinated solvents, the formation of vinyl chloride (VC) following the hydrogenolysis of PCE, TCE and cis-DCE is undesirable. In contrast, VC is not formed in the β -elimination of TCE (Arnold et al. 2000). However, Su and Puls (1999) reported that TCE may be degraded by ZVI through both reaction pathways. Reductive dehalogenation studies with micro-sized ZVI suggest that the reduction of TCE and PCE using ZVI typically results in ethene and ethane with VC typically less than 10% of the daughter products (Orth et al. 1996, Li et al. 2000), which may be an indication that β -elimination is the major pathway, or that any VC formed is rapidly degraded in the presence of ZVI. Arnold and Roberts (2000) showed that β -elimination is much more common with chlorinated ethenes that possess α,β -pairs of chlorine atoms (e.g., TCE and PCE). Dehalogenation of chlorinated alkynes and carbon tetrachloride (CT) have been reported to follow hydrogenolysis (Matheson et al. 1994, Arnold et al. 2000). Arnold and Roberts (2000) propose that the reduction of 1,1-DCE to ethylene occurs via α -elimination (Eq. 4), also avoiding the formation of VC.

These aforementioned studies investigating reductive dehalogenation pathways used micro-scale zero valent iron. Limited work has been completed examining the pathways

associated with nZVI and the reductive degradation of chlorinated compounds although there is some evidence that the pathways are similar to the ones taken by larger ZVI particles. However, the pathway also seems to be dependent on the type of nanoparticle used (Liu et al. 2005, Elsner et al. 2008), as well as, the type of compound under investigation (Song et al. 2005). For example, similar to Arnold and Roberts (2000), who used microscale ZVI, Song and Carraway (2005) reported that chlorinated alkanes that possess α,β -pairs of chlorine atoms (i.e., each chlorine atom is on a different carbon atom such as hexachlorethane and perchloroethane) will undergo β -elimination when reduced by Fe^{BH} , while hydrogenolysis and α -elimination can both occur for compounds with all chlorine atoms on the same carbon (e.g., 1,1-DCA, 1,1,1-TCA). Liu et al. (2005) compared the pathways for RNIP and Fe^{BH} nanoparticles under high and low TCE concentrations and found that the governing pathway was β -elimination for RNIP (as indicated by acetylene production) and primarily hydrogenolysis for Fe^{BH} particles. Reaction with Fe^{BH} also resulted in higher amounts of ethane than with RNIP. Only trace amounts of chlorinated by-products, such as cis-DCE and VC, were observed after reaction with both Fe^{BH} and RNIP in spite of the different dominant pathways. Fe^{BH} particles also increased dechlorination rates (higher k_{sa} - surface area normalized rate constant, Lm^2/min) with both high and low TCE concentrations. Liu et al. (2005) suggest that this is due to the catalysis of the reaction between TCE and H_2 that occurs with Fe^{BH} . Elsner et al. (2008) also compared the reactivity of Fe^{BH} and RNIP with chlorinated ethenes using isotope analysis. Their conclusions are consistent with previous findings (Liu et al. 2005), that Fe^{BH} produced greater reaction rates than RNIP and that Fe^{BH} reduced chlorinated ethenes primarily through hydrogenolysis while RNIP reduced chlorinated ethenes primarily via β -elimination. Unlike microscale iron, where the compound plays a controlling factor in the pathway (Arnold et al. 2000), nZVI studies suggest that pathways also depend on the form of zero valent iron in the particles.

Aqueous solution	Half reactions	E^0 (V)
Chromium (Cr)	$\text{CrO}_4^{2-} + 8\text{H}^+ + 3\text{e}^- \leftrightarrow \text{Cr}^{3+} + 4\text{H}_2\text{O}$	1.51
Chromium (Cr)	$\text{Cr}_2\text{O}_7^{2-} + 14\text{H}^+ + 6\text{e}^- \leftrightarrow 2\text{Cr}^{3+} + 7\text{H}_2\text{O}$	1.36
Platinum (Pt)	$\text{Pt}^{2+} + 2\text{e}^- \leftrightarrow \text{Pt}$	1.19
Palladium(P)	$\text{Pd}^{2+} + 2\text{e}^- \leftrightarrow \text{Pd}$	0.92
Mercury (Hg)	$\text{Hg}^{2+} + 2\text{e}^- \leftrightarrow \text{Hg}$	0.86
Silver (Ag)	$\text{Ag}^+ + \text{e}^- \leftrightarrow \text{Ag}$	0.80
Arsenic (As^{V})	$\text{H}_3\text{AsO}_4 + 2\text{H}^+ + 2\text{e}^- \leftrightarrow \text{HAsO}_2 + 4\text{H}_2\text{O}$	0.56
Copper (Cu)	$\text{Cu}^{2+} + 2\text{e}^- \leftrightarrow \text{Cu}$	0.34
Uranium (U)	$\text{UO}_2^{2+} + 4\text{H}^+ + 2\text{e}^- \leftrightarrow \text{U}^{4+} + 2\text{H}_2\text{O}$	0.27
Arsenic (As^{III})	$\text{H}_3\text{AsO}_3 + 3\text{H}^+ + 3\text{e}^- \leftrightarrow \text{As} + 3\text{H}_2\text{O}$	0.24
Copper (Cu^+)	$\text{Cu}^{2+} + \text{e}^- \leftrightarrow \text{Cu}^+$	0.16
Lead (Pb)	$\text{Pb}^{2+} + 2\text{e}^- \leftrightarrow \text{Pb}$	-0.13
Nickel (Ni)	$\text{Ni}^{2+} + 2\text{e}^- \leftrightarrow \text{Ni}$	-0.25
Cadmium (Cd)	$\text{Cd}^{2+} + 2\text{e}^- \leftrightarrow \text{Cd}$	-0.40
Iron (Fe)	$\text{Fe}^{2+} + 2\text{e}^- \leftrightarrow \text{Fe}$	-0.44
Zinc (Zn)	$\text{Zn}^{2+} + 2\text{e}^- \leftrightarrow \text{Zn}$	-0.76
Barium (Ba)	$\text{Ba}^{2+} + 2\text{e}^- \leftrightarrow \text{Ba}$	-2.92
1,2-Dichloroethane	$\text{ClH}_2\text{C}-\text{CH}_2\text{Cl} + 2\text{e}^- \leftrightarrow \text{H}_2\text{C}=\text{CH}_2 + 2\text{Cl}^-$	0.74
Carbon tetrachloride (CT)	$\text{CCl}_4 + \text{H}^+ + 2\text{e}^- \leftrightarrow \text{CHCl}_3 + \text{Cl}^-$	0.67
Tetrachloroethylene (PCE)	$\text{Cl}_2\text{C}=\text{CCl}_2 + \text{H}^+ + 2\text{e}^- \leftrightarrow \text{Cl}_2\text{C}=\text{CHCl} + \text{Cl}^-$	0.57
Trichloroethylene (TCE)	$\text{Cl}_2\text{C}=\text{CHCl} + \text{H}^+ + 2\text{e}^- \leftrightarrow \text{Cl}_2\text{C}=\text{CH}_2 + \text{Cl}^-$	0.53
Vinyl chloride (VC)	$\text{ClHC}=\text{CH}_2 + \text{H}^+ + 2\text{e}^- \leftrightarrow \text{H}_2\text{C}=\text{CH}_2 + \text{Cl}^-$	0.45
1,1-Dichloroethene (1,1- DCE)	$\text{Cl}_2\text{C}=\text{CH}_2 + \text{H}^+ + 2\text{e}^- \leftrightarrow \text{ClHC}=\text{CH}_2 + \text{Cl}^-$	0.42

Appendix A. 2: Standard redox potentials (E^0) in aqueous solution at 25 °C [80, 220]

Biodegradation of chlorinated ethenes (PCE and TCE) can also occur via hydrogenolysis. However, biodegradation of chlorinated ethenes can lead to production of substantial concentrations of VC. For example, *Dehalococcoides (dhc)* strain 195 degrades VC cometabolically (Mattes et al. 2010), leading to accumulation of VC in the biodegradation of PCE and TCE (DiStefano et al. 1991, He et al. 2003). Isalou et al. (1998) measured VC concentrations of 35.9 mg/L in columns with *dhc* Strain 195 degrading 100 mg/L of PCE while Hood et al. (2008) reported VC concentrations of approximately 60 mg/L after bioremediation activities at a TCE contaminated site. Other *dhc* strains can biodegrade VC metabolically, and therefore produce lower peak VC concentrations. For example, Morrill et al. (2009) used KB-1 (a mixed microbial culture that includes two strains of *dhc*) in a bioaugmentation lab test and reduced TCE concentration to ethene, with final VC concentrations up to 8.9 mg/L. In studies of reductive degradation of TCE and PCE by nZVI, VC is consistently found only in trace amounts or non-detect (Li et al. 2000, Lien et al. 2001, Liu et al. 2005), much lower than from biodegradation, likely due to the dominance of the β -elimination pathway with nZVI.

With nZVI injection the redox potential may be decreased substantially, leading to a potential increase in anaerobic microbial activity and biodegradation. In addition, microbes that dehalogenate chlorinated ethenes may use the H_2 produced from nZVI reaction with water. However, when Xiu et al. (2010) examined the use of nZVI (RNIP) with a *dhc* containing culture, they found that nZVI increased methanogenesis due to the production of H_2 , and a temporary inhibition of TCE dechlorination was observed. The onset of accelerated TCE dechlorination and growth of dechlorinators was hypothesized to be due to passivation of nZVI. Xiu et al. (2010) suggested that coating the nZVI particles with a copolymer could minimize the inhibitory effect on biodechlorination of chlorinated ethenes.

The addition of a second noble metal (e.g., Pd, Pt, Ni, Ag, or Cu) to the surface of nZVI particles yields bimetallic nanoparticles. Palladium is by far the most widely used metal for dehalogenation (Alonso et al. 2002) and has been shown to act as a catalyst, greatly enhancing rates of reaction with nZVI (e.g. Lien et al. 2001, Lien et al. 2004, Lien et al. 2007, Zhu et al. 2007, He et al. 2008, Sakulchaicharoen et al. 2010). Bimetallic nanoparticles are further discussed in Section 5.6.

7.5 Reaction of Heavy Metals with Nanometals

Nanometals have been proposed for use in the remediation of a variety of contaminants, including heavy metals. The transformation, solubility, mobility, and consequently toxicity, of heavy metals in the environment are governed by redox reactions, precipitation/dissolution reactions, and adsorption/desorption phenomena. Water treatment strategies for removal of metal contaminants typically involve manipulating these mechanisms to control the availability and toxicity of metal contaminants to biota. The solubility, mobility and toxicity of metals of environmental concern are strongly dependent upon their oxidation states. For example, at its higher oxidation state chromium (Cr^{6+}) is very toxic, whereas Cr^{3+} , an essential nutrient, is relatively non-reactive but can be toxic in large doses. Moreover, Cr^{6+} is highly soluble and mobile in soils whereas Cr^{3+} forms relatively insoluble oxide and hydroxide compounds (Jacobs et al. 2005). Given the strong dependence of Cr mobility and toxicity on its redox state, remediation technologies that reduce Cr^{6+} , such as a reduction by Fe^0 , are of significant interest.

The specific removal mechanisms involved in treatment of heavy metal contamination with ZVI depend on the standard redox potential (E^0) of the metal contaminant (Appendix A.2). Metals that have an E^0 that is more negative than, or similar to, that of Fe^0 , (e.g., Cd and Zn) are removed purely by adsorption to the iron (hydr)oxide shell. Metals with E^0 much more positive than Fe^0 (e.g., Cr, As, Cu, U, and Se) are preferentially removed by reduction and precipitation (Li et al. 2007). Metals with slightly more positive E^0 than Fe^0 , (e.g., Pb and Ni) can be removed by both reduction and adsorption. Oxidation and co-precipitation by iron oxides are the other possible reaction mechanisms depending upon the prevailing geochemical conditions such as pH, Eh and initial concentration and speciation of contaminant metals (Appendix A.1). A group of metals (i.e., Pd, Pt, Ni, Cu) exhibiting catalytic properties, if present in oxidized forms in solution, can be reduced by nZVI to create bimetallic nanoparticles (Fe^0/M^0) enhancing the rate of reaction of contaminants (see Section 5.6). A variety of surface analysis techniques, including X-ray photoelectron spectroscopy (XPS), extended X-ray absorption spectroscopy (EXAFS), X-ray absorption near edge structure spectroscopy (XANES), X-ray diffraction (XRD) and scanning transmission electron microscopy (STEM) with energy dispersive X-ray (EDX), can be used to investigate the metal removal mechanisms associated with nZVI.

The metal-nZVI interactions for various metals can be categorized as:

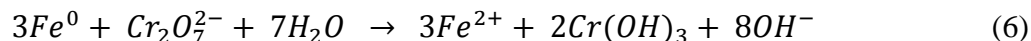
1. Reduction – Cr, As, Cu, U, Pb, Ni, Se, Co, Pd, Pt, Hg, Ag
2. Adsorption – Cr, As, U, Pb, Ni, Se, Co, Cd, Zn, Ba
3. Oxidation/Reoxidation – As, U, Se, Pb
4. Co-precipitation – Cr, As, Ni, Se
5. Precipitation – Cu, Pb, Cd, Co, Zn

Some of the metals that can react with nZVI by more than one mechanism are reviewed here in detail.

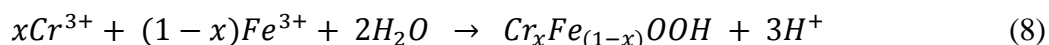
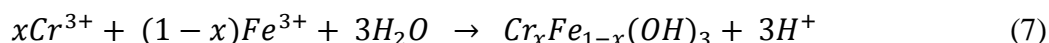
Chromium (Cr) is a common pollutant at industrial waste sites and can be present in both trivalent (Cr^{3+}) and hexavalent (Cr^{6+}) states. The carcinogenic, soluble and mobile Cr^{6+} may be reduced to less toxic Cr^{3+} by nZVI and immobilized by precipitation as $\text{Cr}(\text{OH})_3$ or by incorporation into the iron (hydr)oxide shell forming alloy-like Cr^{3+} - Fe^{3+} hydroxides (Ponder et al. 2000, Manning et al. 2007, Li et al. 2008). Some Cr^{6+} will also directly adsorb on the

hydr(oxide) shell of nZVI. These removal mechanisms have been confirmed by XPS, XANES and EXAFS analyses (Manning et al. 2007, Li et al. 2008). Relevant reactions between Cr and nZVI include (Li et al. 2008):

(A) Reduction of Cr^{6+} to Cr^{3+} :

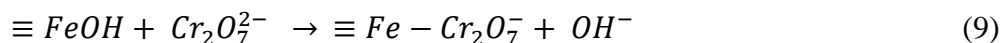


(B) Formation of mixed Cr^{3+} - Fe^{3+} hydroxides:



The Cr to Fe atomic ratio in mixed Cr^{3+} - Fe^{3+} hydroxides varies depending on the reaction conditions including pH and Cr^{6+} concentration.

(C) Adsorption of Cr^{6+} :



The formation of mixed Cr^{3+} - Fe^{3+} hydroxides on the oxidized nZVI surface layer may inhibit further electron transfer from the Fe^0 core to Cr^{6+} at later reaction times, favoring adsorption of Cr^{6+} on the nZVI surface, especially at high Cr^{VI} concentrations (Li et al. 2008, Hu et al. 2010). This self-inhibition of the reduction reaction can be overcome using bimetallic nanoparticles (e.g., Cu^0/Fe^0 and Pd^0/Fe^0) to increase both the rate and extent of Cr^{6+} removal by reductive precipitation (Rivero-Huguet et al. 2009, Hu et al. 2010). Though these short-term studies demonstrate an effective removal of Cr^{6+} by nZVI via reductive precipitation and co-precipitation, additional research is needed to further explore the overall efficiency of nZVI for remediation of Cr^{6+} contaminated groundwater where the prevailing geochemical conditions can influence these removal mechanisms.

Arsenic (As), a confirmed carcinogen, is present as arsenate (As^{5+}) and arsenite (As^{3+}) in groundwater throughout the world. As^{3+} is much more toxic and generally more mobile than As^{5+} (Korte et al. 1991). As^{5+} can be reduced by nZVI to either As^0 or As^{3+} as confirmed by the XPS analysis (Ramos et al. 2009). Any remaining As^{5+} is adsorbed onto iron oxides in the

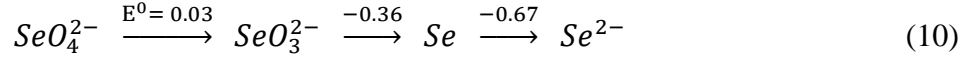
outer layer of the iron nanoparticles (Kanel et al. 2006, Ramos et al. 2009). As^{3+} , thus formed, is either adsorbed or co-precipitated at the iron nanoparticle surface (Ramos et al. 2009, Yan et al. 2010). Some As^{3+} is also reported to be oxidized to As^{5+} either by hydroxyl radicals or by iron oxides (both formed during oxidation of Fe^0) via formation of iron oxide- As^{3+} surface complexes (Kanel et al. 2005, Ramos et al. 2009, Yan et al. 2010). Adsorption of both As^{3+} and As^{5+} on iron nanoparticles occurs by forming inner-sphere complexes with the (hydr)oxide shell of nZVI (Jegadeesan 2005, Kanel et al. 2005, Kanel et al. 2007).

While studying the removal of As^{3+} by nZVI, 51% of the total As^{3+} was found as surface bound As^{3+} whereas 14 and 35% was transformed to As^{5+} by iron oxides and As^0 by Fe^0 respectively, indicating that nZVI exhibits broad functionality with the Fe^0 core having reduction capability and the (hydr)oxide layer promoting oxidation and adsorption/co-precipitation (Ramos et al. 2009, Yan et al. 2010). These studies suggest that under most common geochemical conditions there will be a mechanism by which application of nZVI will lead to treatment of As, leading to a potential for development of a robust nZVI *in situ* treatment technology for subsurface As contamination.

Uranium (U) is the most common radionuclide contaminant found at many nuclear waste sites. It is mainly detected in contaminated groundwater as highly soluble and mobile U^{6+} (Cao et al. 2010) and can be remediated by reducing it to insoluble U^{4+} oxides by various reductants (Yan et al. 2010). Reduction of U^{6+} to U^{4+} by ZVI is thermodynamically favorable (Fiedor et al. 1998). U^{6+} will be predominantly removed by nZVI via reductive precipitation of UO_2 (U^{4+}) with minor precipitation of $\text{UO}_3 \cdot 2\text{H}_2\text{O}$ (U^{6+}) as confirmed by the XPS and XRD analyses (Riba et al. 2008, Dickinson et al. 2010, Yan et al. 2010, Crane et al. 2011). U^{4+} may slowly reoxidize and redissolve as U^{6+} with concurrent reduction of Fe^{3+} to Fe^{2+} . The reoxidized U^{VI} may be removed via sorption onto the surfaces of iron (hydr)oxides (Dickinson et al. 2010). This suggests that the formation of iron hydr(oxides) during oxidation of Fe^0 also plays an important role in removing U especially after reoxidation of U^{4+} .

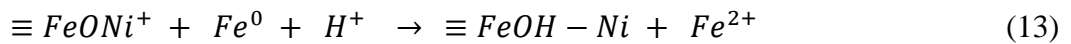
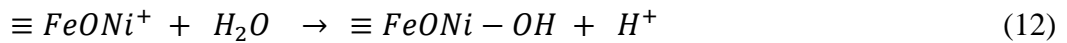
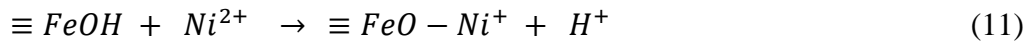
Selenium enters the environment naturally from weathering of minerals and anthropogenically from mining, agricultural, petrochemical and industrial operations. The toxicity and solubility of Se depends on the redox conditions. The formation of soluble selenate (SeO_4^{2-} or Se^{6+}) and selenite (SeO_3^{2-} or Se^{4+}) is favored under oxidizing conditions,

and formation of insoluble elemental Se (Se^0) and selenide (Se^{2-}) is favored under reducing conditions (Scheinost et al. 2008). The reduction of Se^{6+} to Se^{2-} can be written as (Bard et al. 1985):



The reduction of soluble Se^{6+} to insoluble Se^0 by nZVI is thermodynamically favorable, but further reduction to Se^{2-} is not. Se^{6+} removal is quite complex with a variety of removal mechanisms possible (e.g., reduction, complex formation, adsorption and reoxidation). These removal mechanisms have been shown to occur through investigation by SEM-EDX, XANES and EXAFS (Mondal et al. 2004, Olegario et al. 2010). For example, Se^{6+} can be reduced to Se^{2-} via formation of Se^{4+} and Se^0 which can then either complex with Fe^0 oxidation products forming iron selenide ($FeSe$) or reoxidize to Se^0 and Se^{4+} . The Se^{4+} can be immobilized by strongly binding to iron (hydr)oxides via inner-sphere adsorption (Olegario et al. 2010). This indicates that nZVI is capable of removing various Se species even after oxidizing to iron hydr(oxides). More research is needed to investigate the long term stability of various Se species formed after interaction with nZVI as these can be impacted by groundwater chemistry.

Nickel (Ni^{2+}) and Lead (Pb^{2+}), common pollutants of electroplating industry, may be removed by nZVI via reduction to Ni^0 and Pb^0 and by adsorption as Ni^{2+} and Pb^{2+} (Ponder et al. 2000, Sun et al. 2006, Li et al. 2007, Efecan et al. 2009, Xi et al. 2010). While reacting with nZVI, Pb^{2+} also precipitates as $Pb(OH)_2$ and oxidizes as α - PbO_2 as confirmed by the XRD analysis (Ponder et al. 2000, Lien et al. 2007). Detailed XPS analysis shows that Ni^{2+} is initially bound to the nZVI surface by physical sorption, then binds strongly by chemisorption and finally reduced to Ni^0 as described here (Sun et al. 2006):



Other metals of environmental importance, including Cu^{2+} , Hg^{2+} and Ag^{2+} may be sequestered via chemical reduction to their elemental forms (Li et al. 2007, Lien et al. 2007, Karabelli et al. 2008, Uzum 2009, Yan et al. 2010). Cu^{2+} may also be reduced to Cu^+ by nZVI

resulting in the formation of Cu_2O (Lien et al. 2007, Karabelli et al. 2008). However, the sorption of these metals on the oxidized nZVI surface prior to their reduction cannot be ignored as the (hydr)oxide layer on the nZVI surface has high sorption affinity for metal cations (Li et al. 2007, Yan et al. 2010). Metals with E^0 more negative or close to that of Fe^0 (e.g., Co, Cd, Zn and Ba) will be removed by sorption and/or precipitation (Celebi 2007, Li et al. 2007, Üzüüm et al. 2008, Uzun 2009, Yan et al. 2010, Boparai et al. 2011). The addition of nZVI to aqueous systems usually increases the pH to 8.0-8.2 due to generation of OH^- from reduction of water by Fe^0 , resulting in the immobilization of metals by precipitation as hydroxides. Zn and Co may also be removed by precipitation on the oxidized nZVI surface as $\text{Zn}(\text{OH})_2$ and $\text{Co}(\text{OH})_2$ (Üzüüm et al. 2008, Yan et al. 2010). These studies suggest that other metal contaminants with more negative redox potentials than Fe^0 (e.g., Be, Ra, Th, Pu, Sr, Mn, Cs) may be removed by adsorption and precipitation on the nZVI surface.

Metal catalysts (e.g. Pd, Pt, Ni, and Cu) with E^0 more positive than Fe^0 may be reduced by nZVI to form bimetallic iron nanoparticles (Fe^0/Pd^0 , Fe^0/Pt^0 , Fe^0/Ni^0 and Fe^0/Cu^0). A small amount of metal catalyst deposited on the nZVI surface increases contaminant transformation rates significantly (Schrack et al. 2002, Lien et al. 2007, Hu et al. 2010). These metal catalysts, existing as co-contaminants at mixed waste sites, can be manipulated to form *in situ* bimetallic iron nanoparticles, enhancing the remediation process (Lien et al. 2007). For example, Cr^{6+} removal is significantly enhanced using bimetallics (e.g., Fe^0/Cu^0 , Fe^0/Pd^0 and Fe^0/Ni^0) (Rivero-Huguet et al. 2009, Hu et al. 2010, Liu et al. 2010). Bimetallic iron nanoparticles play an important role in overcoming the self-inhibition of metal removal reactions by preventing oxide formation on the nZVI surface. More research using bimetallics is needed for the metals like U and Se, which get reoxidized or redissolved at later times of reaction with nZVI.

A large number of metals can be removed by adsorption. As such a detailed understanding of adsorption kinetics and thermodynamics is important to design for the optimal pathway (e.g., chemisorption versus physisorption) and sorption mechanism (e.g. surface versus intraparticle diffusion) to maximize adsorption rates and adsorptive capacity of nZVI for specific metals. Few studies have investigated adsorption kinetics and thermodynamics of metal removal by nZVI (Kanel et al. 2005, Kanel et al. 2006, Celebi 2007, Liu et al. 2009, Zhu et al. 2009, Boparai et al. 2011). Arsenic (As^{3+} and As^{5+}) adsorption exhibited a pseudo-first-order rate and could be fitted well with both Freundlich and Langmuir

isotherm models (Kanel et al. 2005, Kanel et al. 2006). The kinetics and thermodynamics of cadmium adsorption on nZVI provide evidence that Cd removal by nZVI occurs via chemisorption with surface diffusion as the rate-limiting step (Boparai et al. 2011). More research is needed to investigate adsorption mechanisms, kinetics, and thermodynamics for other metals that may be removed by adsorption to nZVI particles.

7.6 Factors Affecting Reactivity of nZVI with Metals and Chlorinated Solvents

As shown by several studies, there are many factors impacting nZVI reactivity with chlorinated compounds and metals. In addition to the degree of crystallinity of the Fe^0 core, which was discussed in Section 2, factors affecting nZVI reactivity include surface area (Nurmi et al. 2005, Song et al. 2005, Kanel et al. 2006, Tratnyek et al. 2006, Rivero-Huguet et al. 2009), age of the nanoparticle (Liu et al. 2006, Sarathy et al. 2008, Reinsch et al. 2010), aqueous phase pH (Matheson et al. 1994, Li et al. 2000, Chen et al. 2001, Mondal et al. 2004, Tamara et al. 2004, Song et al. 2005, Kanel et al. 2006, Liu et al. 2006), nZVI stabilizers (He et al. 2005, Phenrat et al. 2009, Phenrat et al. 2009, He et al. 2010, Sakulchaicharoen et al. 2010), and concentrations of contaminants and other reactive groundwater constituents (Liu et al. 2005, Song et al. 2005, Liu et al. 2007, Lim et al. 2008). These effects will be discussed in greater detail in the following sections.

7.6.1 Surface Area

Gillham and O'Hannesin (1994) were the first to report that greater ZVI surface area resulted in greater rates of dehalogenation of chlorinated compounds. This helped spur interest in nano-scale ZVI, since smaller particles have a much higher surface area to mass ratio. For example, nZVI surface area can be in excess of $40 \text{ m}^2/\text{g}$ for stabilized particles (He et al. 2005, Sakulchaicharoen et al. 2010, Wang et al. 2010) and $15\text{-}34 \text{ m}^2/\text{g}$ for bare particles, with Fe^{BH} having greater surface area than RNIP particles (e.g. Wang et al. 1997, Nurmi et al. 2005, Phenrat et al. 2009, Wang et al. 2010). Catalyst metals like Ni have been reported to further increase the surface area of bimetallic particles (Fe^0/Ni^0) when they are added to the iron precursor prior to the borohydride reduction step (Schrack et al. 2002, Tee et al. 2005). Micron scale ZVI has a surface area on the order of $< 1 \text{ m}^2/\text{g}$ (Matheson et al. 1994, Wang et al. 1997,

Nurmi et al. 2005). Nurmi et al. (Nurmi et al. 2005) showed that nanoparticles (both RNIP and Fe^{BH}) exhibited greater reactivity than micro-sized iron particles for reduction of CT on a per mass basis. However, when normalized to surface area the rate constants were similar for both nano and micro-sized particles suggesting that a nano-effect may not exist. The presence of a larger number of reactive sites on nZVI particles, as compared to mZVI particles may enhance nZVI reactivity (Nurmi et al. 2005, Tratnyek et al. 2006). The larger surface area of nZVI than mZVI also provides greater density of reactive sites for reduction and adsorption of metals thus increasing the removal rate and capacity of nZVI. Kanel et al. (2006) found the k_{sa} (surface area normalized rate constant, Lm^2/min) of arsenic removal by nZVI to be 1-3 orders of magnitude larger than that of microscale ZVI. Similarly, Rivero-Huguet and Marshall (2009) reported enhanced removal of Cr^{6+} by nano iron due to the increased specific surface area and higher surface reactivity of the nano iron. Since nanoparticles tend to aggregate (due to magnetic and van der Waals forces), it is unclear whether the reactivity of nZVI will change due to the decrease in surface area/unit mass or remain unchanged from the original reactivity of the individual nanoparticles (Nurmi et al. 2005, Tratnyek et al. 2006).

7.6.2 Aging

nZVI rapidly oxidizes in aqueous solutions by reacting with oxygen or water or through reaction with naturally occurring subsurface constituents. When nZVI is exposed to water several processes can occur. The original oxide shell can break down due to reaction with water (Hoerle et al. 2004) or autoreduction (reduction of the oxide shell by underlying Fe^0), allowing for the freshly formed Fe^0 to oxidize, coupled with the reduction of electron acceptors in the water. In addition, the particles can aggregate and a new, mixed-valence ($\text{Fe}^{2+}\text{-Fe}^{3+}$) oxide layer can form (Sarathy et al. 2008). nZVI aging/oxidation results in a loss of Fe^0 content (Liu et al. 2005, Liu et al. 2006, Sarathy et al. 2008), decreasing the reducing equivalents available for reaction with the target contaminant. Due to the time elapsed between nZVI synthesis and nZVI arrival at the target source zone, this loss should be accounted for in determining the required amount of nZVI for contaminant transformation. At present there is limited ability to predict the additional nZVI requirements to account for the loss of Fe^0 content in various subsurface environments.

A number of studies have investigated the impact of aging on nZVI reactivity. Sarathy et al. (2008) reported a decrease in Fe^0 content after exposing RNIP to water for six months. They observed an initial (2 day) increase in the CT mass-normalized, first-order, degradation rate constant (k_M) followed by a gradual decrease in k_M . Kim et al. (Kim et al. 2010) observed a similar trend for TCE degradation rates, using shell-modified RNIP exposed to air or water. This change in rate constants with aging was attributed to depassivation of particles initially followed by repassivation upon prolonged exposure (Sarathy et al. 2008, Kim et al. 2010). Wang et al. (2010) also reported decrease in reactivity of Fe^{BH} that was stabilized with inert gas and then exposed to air .

Liu and Lowry (2006) also studied reactivity changes with aging of RNIP. Although they observed a significant initial decrease (for the first 10 days) in TCE reaction rate constants, the TCE reaction rate remained nearly the same or increased slightly for the rest of the study period. They reported nearly the same reaction rate constants (at day 20), irrespective of the Fe^0 content, and concluded that the TCE reaction is zero-order with respect to the Fe^0 content of RNIP. Similarly, Liu et al. (2005) reported that the partial oxidation of Fe^{BH} particles did not significantly affect the maximum Fe^0 -normalized reaction rate of TCE or the reaction product distribution , although partially oxidized particles were reported to have longer periods of lower reactivity when compared to fresh Fe^{BH} particles.

Differences in results in these various studies might be due to differences in reaction conditions such as pH, initial contaminant concentration, method of nZVI synthesis/stabilization, exposure time, and medium for oxidation (air or water). For example, aging of shell-modified RNIP in water resulted in formation of a goethite surface layer whereas exposure to air yielded wüstite, hematite and maghemite surface layers in addition to pre-existing magnetite (Kim et al. 2010). Although the thickness of the oxide layer is reported to be constant with aging, the composition may change (Sohn et al. 2006, Sarathy et al. 2008). Any changes to the iron oxide surface characteristics could affect reactivity, as adsorbed Fe^{2+} is capable of mediating reductive transformation of chlorinated solvents and metal contaminants (Danielsen et al. 2004, Kim et al. 2008, Boland et al. 2011)

Catalysts are commonly used to increase reaction rates by decreasing the activation energy; however they can also affect the aging process and consequently the reactivity of

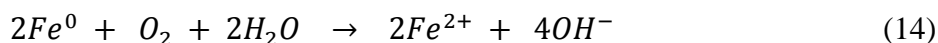
bimetallic nZVI particles. Yan et al. (2010) deposited Pd⁰ on the surface of fresh nZVI particles. After aging for 24 hours no Pd was detected on the nZVI surface, indicating that it may have become embedded under the oxide shell. No metallic iron was detected by XPS suggesting that particles had undergone severe oxidation upon aging. Reactivity of the Pd-nZVI with TCE, aged in water for 24 hours, decreased by 80% compared to that of the fresh Pd-nZVI particles. Similar results were found by Zhu and Lim (2007) for aged Pd-nZVI (in water for 24 hours) and 1,2,4-Trichlorobenzene. This decrease was attributed to detachment of Pd from iron and its encapsulation in iron oxides formed during nZVI oxidation. These studies suggest that the decreased reactivity of aged bimetallic nanoparticles is due to their oxidation and is similar to uncatalyzed nZVI.

nZVI oxidation can also have a significant impact on heavy metal removal rates and mechanisms. The reduction of metals by nZVI can be slowed or inhibited due to the oxidation of nZVI particles. Metals (e.g., U and Se) that are initially reduced by Fe⁰ can be partly reoxidized with reduction of iron oxides in the iron nanoparticles (Dickinson et al. 2010, Olegario et al. 2010). As most metal contaminants can be removed by adsorption at the iron oxide surface, adsorption may become the dominant removal mechanism after oxidation of nZVI particles. Although nZVI aging has been identified as a significant issue impacting reactivity, limited work has been completed in this area and more research is needed.

7.6.3 pH

pH strongly influences the redox reactions occurring at the ZVI surface by accelerating corrosion at low pH (Eq. 1) and passivating the iron surface at high pH through the formation of iron hydr(oxides) (Matheson et al. 1994, Song et al. 2005).

The oxidation of Fe⁰ in aqueous systems releases OH⁻ ions, increasing the pH of the system (>8.0) as shown in Equation 5 and in the following reaction:



Given these reactions, the high iron mass ratio (10-50 wt%) (i.e., ratio of iron mass to iron plus water mass in a given volume) of micro and granular iron used in PRBs can buffer groundwater pH at 8-9 resulting in iron passivation (Liu et al. 2006). However, the iron mass ratio of nZVI in injection suspensions is much lower (0.2-0.5 wt%), favoring corrosion at a

prevailing near neutral pH. Thus, iron longevity/efficiency can differ for micro- and nano- iron particles under the same field conditions.

A number of studies have reported an increase in reaction rates with decreasing pH for reductive dehalogenation of chlorinated compounds by RNIP and Fe^{BH} (Song et al. 2005, Liu et al. 2006, Song et al. 2006, Satapanajaru et al. 2008, Zhu et al. 2010). This may be attributed to greater availability of electrons from the Fe^0 core due to dissolution of the oxide layer at low pH. pH not only affects reaction rates but also the dominant reaction pathways.

Liu and Lowry (2006) studied the effect of pH on H_2 evolution rates (k_{H_2}) of RNIP. Decreasing the pH resulted in an increased k_{H_2} and TCE reaction rates (k_{obs}), and the increase in k_{H_2} was an order of magnitude greater than k_{obs} over the same pH range. A fitted linear relationship between pH and k_{obs} had a weak dependence, indicating that TCE dechlorination does not strongly depend on pH. H_2 evolution had little effect on TCE dechlorination rates by RNIP, while Liu et al. (Liu et al. 2005) showed that addition of H_2 to systems with Fe^{BH} resulted in higher rates of dechlorination. Evolution of H_2 can also positively impact microbial degradation of contaminants (Freedman et al. 1989). In this case, addition of nZVI to the subsurface may have prolonged remediation benefits if microbial dechlorination is stimulated.

Outer ZVI shell characteristics (Chen et al. 2001, Liu et al. 2006) may be affected by pH. The extent to which pH affects the formation of the oxide layer at the nanoscale ZVI surface is not fully understood. Liu and Lowry (2006) suggest that different Fe-oxides phases may exist on RNIP particles at different pH while Song and Carraway (2005) propose that Fe^{BH} is less passivated than microscale ZVI as they observed a smaller effect of pH on the reaction rate constant for nanoscale nZVI than microscale ZVI (Matheson et al. 1994).

The impact of pH on metal removal by nZVI depends on the oxidation state of the metal and the removal mechanism. Passivation of the nZVI surface at high pH hinders electron transfer from the Fe^0 core, thus, decreasing the removal of metal contaminants by reductive precipitation. For example, Se^{VI} removal by nZVI decreased from 91 to 11% with increase in pH from 3.5 to 11 (Mondal et al. 2004). High pH also decreases adsorption of metal anions due to electrostatic repulsion caused by the negative nZVI surface charge above the pH of 7.8 (Kanel et al. 2005, Kanel et al. 2006). However, this negatively charged nZVI surface is favorable for adsorption of metal cations. Some metals are immobilized via precipitation by

hydrolyzing as metal hydroxides at high pH (e.g., Cd, Zn, Co, Cu). More research is needed to study the effect of pH on metal removal by nZVI to determine the specific impact on each removal mechanism.

7.6.4 Coatings/Stabilizers

Numerous reports have shown that nZVI particles quickly aggregate, decreasing surface area for reaction and limiting mobility (see section 6.1). Therefore, different coatings/stabilizers have been used to stabilize nanoparticles in the subsurface (Schrack et al. 2004, He et al. 2005, Saleh et al. 2005, He et al. 2007, Sun et al. 2007, Zhan et al. 2008, Zheng et al. 2008, e.g. Bishop et al. 2010, Sakulchaicharoen et al. 2010) providing higher surface area for reaction (He et al. 2007). These coatings include guar gum, carboxymethyl cellulose (CMC), poly-styrene-sulphonate (PSS) and poly(methyl)methacryl and can be applied by: 1. physically absorbing polymer coatings on existing nZVI particles in a post-synthesis process (e.g. Saleh et al. 2005, Tiraferri et al. 2008, Cirtiu et al. 2011); 2. synthesizing nZVI in the presence of polymer which concurrently stabilizes the particles (e.g. He et al. 2005, He et al. 2007, Sun et al. 2007). There are also emerging techniques to synthesize nanoparticles that incorporate ZVI into a matrix (Huang et al. 2008, Zhan et al. 2008, Zheng et al. 2008, Zhan et al. 2009, Zhan et al. 2011) or membrane (Xu et al. 2005).

It is important to distinguish between the methods of coating nZVI with polymer as the different processes affect particle structure (see Section 2.2), as well as colloidal stability (see Section 6.2). Literature studies have reported conflicting reactivity results that likely depend on the stabilization approach and the type of stabilizer. The post-synthesis stabilization approach has been shown to decrease reactivity (Phenrat et al. 2009) whereas the pre-synthesis approach has improved reactivity and significantly increased surface area (He et al. 2005). In the case of the post-synthesis process, decreased reactivity has been attributed to a number of mechanisms, including reaction sites on the surface of nZVI being blocked by the polymer, the diffusion of aqueous phase contaminant to the surface being inhibited. The slow diffusion of reaction products away from the surface may inhibit desorption from reactive sites (Phenrat et al. 2009). The dominant process will depend on the concentration of the polymer on the surface (Phenrat et al. 2009) and may differ depending on the properties of the polymer coating. Wang et al. (Wang et al. 2010) showed that there is competition for contaminant between the reactive

sites on the nZVI and sorption sites on the polymer coating. However, the loss of reactivity was not significant and must be weighed against benefits provided by the polymer coating. In addition, it has been suggested that several polymer coatings are readily available for biological degradation (He et al. 2010, Kirschling et al. 2010), and in some cases natural polymers (i.e., humic and fulvic acids) can act as co-reactants or electron donors with nZVI to degrade chlorinated compounds (Kang et al. 2009, Wang et al. 2011).

As nZVI migrates through the subsurface and approaches the source zone, nZVI surface charge and interfacial tension will impact interactions between nZVI and the contaminant, and hence the reaction rate (Saleh et al. 2007, Bishop et al. 2010). Enhancing interaction and reaction at the NAPL/water interface requires that nZVI particles exhibit some hydrophobicity, a characteristic not intrinsic to nZVI. Surface coatings can be designed to provide this hydrophobicity, increasing affinity for nZVI to partition to the NAPL-water interface where all reactants are present for contaminant destruction. To reduce the impact of these potential rate-limiting steps recent work has focused on developing nZVI in oil-in-water emulsions such that nZVI degrades NAPL contaminants within the NAPL phase (Berge et al. 2010, Taghavy et al. 2010).

Although some studies have observed a decrease in nZVI reactivity with the addition of a coating (Phenrat et al. 2009, Wang et al. 2010), colloidal stability and mobility of nZVI depend upon polymer coating or other form of stabilizers (He et al. 2007, He et al. 2009). Thus, injection of nZVI for remediation should consider reactivity as well as the benefits of coatings for mobility in order to optimize the exposure of nZVI to contaminants.

7.6.5 Impact of Natural Groundwater Constituents and Initial Chlorinated Solvent Concentrations

Typical groundwater contains many dissolved electron acceptors (e.g., nitrate or sulfate) that can react with nZVI surface and produce iron surface passivation. The effect of both contaminant and solute concentrations on nZVI performance has been investigated in several studies.

Nitrate (NO_3^-) can strongly influence nZVI reactivity. Liu et al. (2007) reported inhibition of TCE reduction by RNIP at high nitrate concentrations (≥ 3 mM) whereas TCE

reduction was slightly enhanced at $[\text{NO}_3^-] \leq 1$ mN. The decreased nZVI reactivity at high NO_3^- concentrations was attributed to competition between NO_3^- and TCE for reactive sites and electrons, and passivation of the nZVI surface due to formation of iron (hydr)oxides. H_2 evolution was also inhibited at high NO_3^- concentrations as Fe^0 preferentially reduced NO_3^- . Reinsch et al. (Reinsch et al. 2010) also reported passivation of RNIP surface at nitrate concentrations of 10^{-4} to 10^{-1} mN, which prevented further oxidation of the Fe^0 for over 6 months.

The effect of other anions such as Cl^- , HCO_3^- , SO_4^{2-} and HPO_4^{2-} on RNIP reactivity was also explored by Liu et al. (2007). Unlike nitrate, these anions had no measureable effect on H_2 evolution. However, they decreased the TCE reduction rate in increasing order of $\text{Cl}^- < \text{SO}_4^{2-} < \text{HCO}_3^- < \text{HPO}_4^{2-}$ which is consistent with their affinity to form complexes with iron oxides. This suggests the decreased TCE dehalogenation may be attributed to passivation of the nZVI surface by formation of Fe-anion complexes.

In a study of the effects of anions on dechlorination of 1,2,4-trichlorobenzene by Pd/Fe^{BH} , Lim and Zhu (2008) reported a loss in reactivity of Pd/Fe^{BH} with 1,2,4-TCB with the presence of carbonate, nitrate, phosphate, nitrite, sulfite, and sulfide (in increasing order of loss) and with higher concentrations further decreasing reaction rates. Based on the nature of inhibitory effect, the anions were classified as (1) adsorption-precipitation passivating species (phosphate, carbonate), (2) redox-active species (nitrate, nitrite, perchlorate), and catalyst poisons (sulfide, sulfite). The sulfite and sulfide acted as catalyst poisons by diffusing into the bulk of the Pd metal and sorbing onto the Pd sites (also suggested by Lowry and Reinhard (2000)).

Heavy metals remediated by nZVI are also influenced by the presence of competitive ions in groundwater. Competitive anions such as sulfates, nitrates and nitrites inhibit metal removal by competing for electrons whereas anions like phosphates and carbonates compete for adsorption sites. Arsenite and arsenate removal by Fe^{BH} decreased significantly in the presence of high concentrations of bicarbonates and phosphates (Jegadeesan 2005, Kanel et al. 2005, Kanel et al. 2006). Similarly, U^{VI} reduction decreased by 90% in the presence of 1 mM HCO_3^- (Yan et al. 2010). Given the complexity of the interaction of groundwater constituents

with nZVI, more research is needed to investigate the mechanisms associated with inhibition of removal of heavy metals by nZVI in the presence of various anions.

A number of studies have examined the effect of contaminant concentrations on rates of reaction with nZVI. Higher initial contaminant concentrations increased effective half life values of micro-scale ZVI with time due to surface passivation and saturation of reaction sites (Farrell et al. 2000). For RNIP, Liu et al. (2007) showed that lower reaction rates at later times were observed but only for higher initial TCE concentrations. Liu et al. (2005) showed that RNIP particles resulted in lower reaction rates under iron limited conditions (high TCE concentrations) while Fe^{BH} particles shift from pseudo-first order kinetics at low concentrations to zero-order at high TCE concentrations. Liu et al. (2005) postulated that either the outer shell on the Fe^{BH} particles remains reactive or that the particles are dissolving leading to exposure of fresh active sites on the Fe^0 surface. In contrast, RNIP particles showed signs of deactivation when TCE concentration increased, likely due to the growth of the Fe_3O_4 shell.

Liu et al. (2007) also reported a decrease in RNIP reactive lifetime with higher initial TCE concentrations. The higher TCE concentrations also decreased the total amount of H_2 evolved at the end of the particle's reactive lifetime signifying that RNIP is reducing TCE rather than H^+ . Thus, at higher TCE concentrations, most of Fe^0 was used for transforming TCE rather than for forming H_2 by reducing water. This suggests that the application of RNIP particles to NAPL source zones with high TCE concentrations could increase the efficiency of the nanoparticles (as opposed to applying RNIP in low concentration plumes) leading to rapid degradation.

Heavy metals combined with chlorinated solvents are often found as mixed wastes at hazardous sites around the world. The metal co-contaminants undergoing redox reactions may enhance or hinder the removal of chlorinated solvents by nZVI. Some heavy metals (e.g., As, Cr, U) can decrease reactivity by either competing for electrons or precipitating as metal (hydr)oxides on nZVI surface causing passivation. On the other hand, metals like Cu, Ni exhibiting catalytic properties may enhance the nZVI reactivity by forming bimetallic nanoparticles (Schrack et al. 2002, Lien et al. 2007). Although extensive research has

investigated the effect of metal catalysts on nZVI reactivity, no work has investigated the effect of metal contaminants like As, Cr, or U on nZVI reactivity towards chlorinated solvents.

7.6.6 Bimetallic Nanoparticles

As with monometallic nZVI, bimetallic particles were first used with micro scale iron (e.g. Grittini et al. 1995, Muftikian et al. 1996, Lowry et al. 1999). Bimetallic particles are composed of a corrosive metal such as iron or zinc along with a noble metal such as palladium (Pd), platinum (Pt), nickel (Ni), silver (Ag) or copper (Cu). The noble metal is a catalyst and increases the rate of reduction.

Bimetallic nanoparticles can be synthesized in variety of different ways. Wang and Zhang (Wang et al. 1997) prepared their particles by soaking fresh nZVI particles in an ethanol solution containing a noble metal (Pd, Pt, Ni, Ag, or Cu). Alternatively, the noble metal can be added through a water-based approach (He et al. 2005, He et al. 2007) where a small amount of salt containing the noble metal is used (e.g., K_2PdCl_6 for Pd). Irrespective of the method of synthesis, the iron reduces the noble metal and the metal deposits onto the iron surface:



The resulting nanoparticle has a thin discontinuous layer of the noble metal on top of the Fe^0 surface (Elliott et al. 2001, Barnes et al. 2010).

Palladium is the most common reductive dehalogenation catalyst used with nZVI for remediation purposes (e.g. Lien et al. 2001, He et al. 2005, Lien et al. 2007, Sakulchaicharoen et al. 2010). The addition of a noble metal lowers the activation energy of the reaction, allowing more interactions between the compounds to result in reactions, thus increasing the reaction rate. As a result, bimetallic nanoparticles have been used to catalyze dechlorination of compounds which typically have very slow reaction rates with nZVI (e.g. aromatics and polychlorinated biphenyls (PCBs)) (e.g. Wang et al. 1997, Lien et al. 1999, Lien et al. 2001, He et al. 2005, Zhu et al. 2007).

The reaction rates of nZVI particles enhanced with Pd (FePd) and Ni (FeNi) have been reported to be much higher than those of monometallic nZVI. Tee et al. (2005) reported the

reaction rate (k_{sa}) of FeNi particles to be almost two orders of magnitude higher than monometallic nZVI for degradation of TCE, similar to Schrick et al. (2002) who reported degradation rates for FePd nanoparticles over an order of magnitude faster than nZVI and 9 times faster than the FeNi particles for the reduction of TCE. Schrick et al. (2002) also noticed that Ni was cathodically protected by the iron, but no long term study was performed to examine whether Ni would be oxidized once all the Fe was depleted. Similarly to Schrick et al. (2002), Barnes et al. (2010) reported no oxidized species of Pd were observed suggesting that the catalyst remains unchanged during the reaction. Lien and Zhang (2004) noted that these increased degradation rates (k_{obs}) only occurred when the particles were 1-5% wt Pd. If the weight was greater than 5%, no increase in reactivity was observed. This is consistent with Barnes et al. (2010) who reported 3.2% Ni as the optimum Ni/Fe ratio for maximum dehalogenation of TCE, while Tee et al. (2005) reports 20% wt Ni would obtain the highest degradation rate (k_{sa}). Application of nZVI suspensions with significant fractions of catalysts at field sites is unlikely given the toxicity of the noble catalysts.

End products following reduction of TCE by bimetallic nanoparticles are typically ethane and ethene. Elliott and Zhang (2001) reported complete reduction of TCE in 12 hrs using FePd nanoparticles with ethene and ethane as the major end products, while with non palladized nZVI, ethene was the end product. Lien and Zhang (2001) observed complete dechlorination of PCE in 90 min with FePd, with ethane as the major end product, while TCE degradation resulted in both ethane and ethene production.

The reason for the increased rate of reaction of bimetallic nanoparticles has been debated by several authors. Lowry and Reinhard (2000) reported that the second metal (in this case AlPd) catalyzes the dehalogenation reaction, resulting in complete conversion of chlorinated ethenes to ethane at the metal surface without any trace of intermediate compounds (i.e. VC). Elliott and Zhang (2001) proposed the creation of galvanic cells on the iron surface, where iron is the anode, and the noble metal acts as a cathode. Li and Farrell (Li et al. 2000) suggested that the increased ethene and ethane production (as compared to monometallic nZVI) is due to bimetallic nanoparticles reducing the contaminants (in this case TCE) through β -elimination. Lien and Zhang (2005) proposed that a transition state species produced in β -elimination is behind dehalogenation of chlorinated ethanes, similar to (Arnold et al. 2000). Conversely, Schrick et al. (2002) proposed that the mechanism for TCE degradation with FeNi

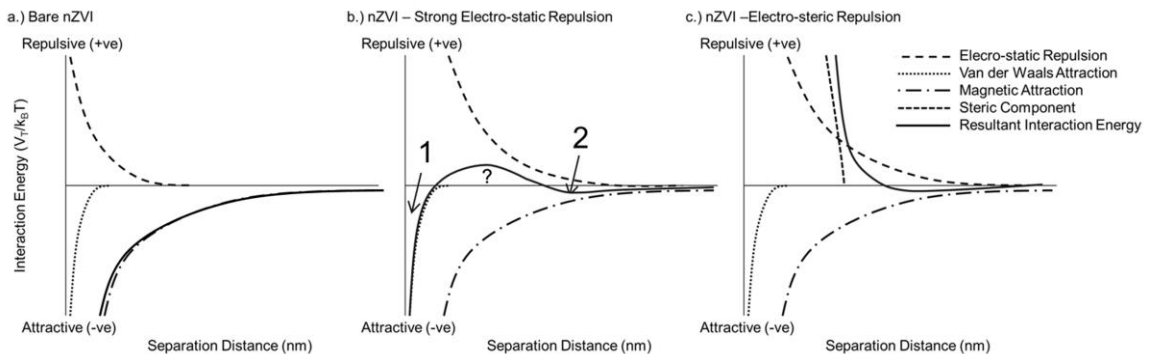
nanoparticles involves the transfer of electrons to the Ni which breaks the Cl-C bond and replaces the halogen with a hydrogen atom (in other words, hydrogenolysis). Lien and Zhang (2007) suggest that atomic hydrogen is formed on the noble metal surface and acts as the reducing agent for chlorinated compounds. Tee et al. (2005) also hypothesized that the addition of a noble metal leads to the enhancement of hydrogenation (of unsaturated compounds to saturated compounds) due to the presence of atomic hydrogen on the noble metal. This may explain the higher concentrations of ethane as the end product in comparison to when non-bimetallic nZVI is used. Given that all the studies with bimetallic nanoparticles to date use Fe^{BH} particles, and these particles can support hydrogenolysis (unlike RNIP particles where β -elimination governs, Section 3), it is likely that enhanced hydrogenation as well as hydrogen production is the main cause for increased reaction rates. However, given the numerous theories put forward with respect to bimetallic nanoparticles, further studies are needed to address these discrepancies.

The disadvantage of using bimetallic nanoparticles is their potentially short lifetimes in the subsurface due to surface passivation (Schrack et al. 2002). In addition, FePd bimetallic nanoparticles show significant structural changes leading to decreased reactivity (Section 5.2) (Zhu et al. 2007, Yan et al. 2010). Zhu and Lim (2007) recommend that Pd be introduced to the nZVI at the time of use, rather than preparing the FePd particles a priori and storing them in order to achieve the highest reactivity. Another disadvantage of bimetallic nanoparticles is the added environmental risk associated with injecting another metal into the subsurface, especially when using FeNi nanoparticles (Schrack et al. 2002, Liu et al. 2005).

7.7 Stability and Mobility of Unstabilized nZVI

Laboratory batch studies have shown that nZVI has significant potential for use in remediating chlorinated compound and heavy metal contaminated sites. One significant obstacle limiting wider application of nZVI is the tendency of nZVI particles to rapidly aggregate and settle out of aqueous suspensions. Agglomeration on a timescale of 2-15 minutes is common for unstabilized nZVI with rapid settling for the following 30 minutes, resulting in a more than one order of magnitude decrease in suspended nZVI particle concentrations within one hour (He et al. 2005, Saleh et al. 2005, Phenrat et al. 2007). Classical Derjaguin, Landau, Verwey and Overbeek (DLVO) theory predicts the interaction energy (i.e., sum of van der

Waals attractive forces and electrostatic repulsion forces) between two identical colloids (Appendix A.3). As the separation distance between two colloids decreases, attractive (negative by convention) van der Waals forces act on a given colloid. These forces are counteracted by repulsive (positive by convention) electrostatic forces which form an energy barrier when they are larger than attractive forces (Appendix A.3.b). At close separation distances, the attractive forces exceed the electrostatic forces, creating a primary energy minimum well in which particles become irreversibly attached. Phenrat et al. (2007) showed that attractive interactions between nZVI particles are dominated by magnetic attractive forces when colloid separation distance decreases (e.g. Shown in Appendix A.3.a). This study also showed that magnetic attraction between nZVI particles increases proportionally to particle Fe^0 content and particle radius to the 6th power (Phenrat et al. 2007). These studies provide insight into particle aggregation but not mobility. Hong et al. (Hong et al. 2009) examined various iron oxide particles and demonstrated that nanoparticles with high magnetic moments exhibit poor mobility in porous media due to rapid particle aggregation. Limiting particle aggregation and settling is a prerequisite for enhanced migration.



Appendix A. 3: Conceptual Model of DLVO interaction forces for nZVI particles with different surface properties. a.) Bare nZVI b.) nZVI with strong electro-static repulsion c.) nZVI with both electro-static and steric repulsion. Points 1 and 2 refer to the primary and secondary minimum, respectively.

Many nZVI studies were conducted at relatively low nZVI concentrations (lower than would be expected during field applications) (Berge et al. 2009). Increasing nZVI concentration (volume fraction) results in closer range interaction forces between particles, increasing aggregation (Phenrat et al. 2007). It has been suggested that above 0.015 g/L

aggregation is expected to play a role in nZVI stability (Rosicka et al. 2011), which is consistent with stability observations (Phenrat et al. 2007). A recent study suggests large aggregates play a strong inhibitory role in nZVI colloidal stability due to the very long range of magnetic forces in solution (Rosicka et al. 2011).

Poor stability and mobility has been observed in column experiments that evaluate unstabilized nZVI transport (Schrack et al. 2004, Saleh et al. 2007) due to the absence of a sufficient electro-static energy barrier to prevent large aggregates from forming and depositing (Tiraferri et al. 2009). These experiments were performed at relatively low concentration (0.1-0.3 g/L) nZVI. Delivering nZVI through porous media becomes more challenging when higher concentrations are used and aggregation becomes more rapid. Field applications of nZVI typically have used over an order of magnitude higher concentration (1.0-30.0 g/L) (Gavaskar A. 2005, Quinn et al. 2005, Bennett et al. 2010, He et al. 2010, Krug 2010, Wei et al. 2010) and have encountered problems with limited nZVI mobility likely due to extensive nanoparticle aggregation and retention.

7.7.1 Improved Colloidal Stability

Recognizing the strong interaction between nZVI particles, researchers have devoted considerable effort to the development of surface modifications to minimize aggregation and settling, thereby increasing nZVI mobility in porous media. To this end, desirable characteristics of nZVI slurries include: 1) particles that do not rapidly aggregate, thus are a stable size and do not settle; 2) particles that contain enough zero valent content and surface area for reaction upon delivery; 3) stabilizer characteristics that do not negatively affect injection or reactivity while providing stability and mobility in porous media.

There are two widely adopted methods for stabilization of nZVI particles: nZVI stabilization following synthesis, or inclusion of a stabilizer in the suspension during nZVI synthesis, as discussed in section 3.4. There is a large body of literature focused on characterizing and stabilizing nZVI particles that have been previously synthesized and allowed to aggregate (Schrack et al. 2004, Saleh et al. 2005, Hydutsky et al. 2007, Kanel et al. 2007, Tiraferri et al. 2008, Johnson et al. 2009). This technique uses ultra-sonic probes and baths to apply a sufficiently high energy to dis-aggregate nZVI particles. Stabilizing agents are then physically adsorbed to the surface via mixing. Many polymers have been successfully

used to stabilize nZVI using this technique, the most successful of which are high molecular weight anionic polyelectrolytes (e.g., poly-styrene sulfonate, polyvinyl pyrrolidone) (Saleh et al. 2008). Naturally occurring organic matter may serve the same stabilizing function (Johnson et al. 2009). The polymer provides a “brush” that both provides electro-static repulsion due to the charge on the polymer and physically inhibits permanent aggregation upon intra-particle interaction due to steric repulsion (Phenrat et al. 2008). Appendix A.3.c shows the DLVO and magnetic force considerations for nZVI as well as the physical mechanisms of intra-particle repulsion afforded by polymer coating, including electro-static and steric repulsion. The main advantage of the post-synthesis stabilization methodology is that unstabilized nZVI is a more economical choice. nZVI that is re-suspended has a passivated oxide shell which protects the zero valent iron core from further oxidation, allowing reasonable shipping and holding times (Kim et al. 2009). The disadvantages are that, in addition to the laborious and lengthy process of stabilizing particles, a large fraction (by weight) of the nZVI particles cannot be effectively stabilized (Phenrat et al. 2009). Dense surface polymers necessary to stabilize re-suspended nZVI inhibit reaction with contaminants (Phenrat et al. 2009).

Similar post-synthesis stabilization methods have been tested for other polymers. Guar gum was investigated as an alternative polymer (Tiraferri et al. 2008, Tiraferri et al. 2009) providing similar stability to previously studied anionic polymers. Commonly used as an additive in drilling and hydraulic fracturing, guar gum molecules do not have charged functional groups to contribute to electro-static repulsion, but provide steric repulsion. This shows that the electro-static interaction is less important for screening magnetic attraction forces for post-synthesis stabilized nZVI than steric repulsion. Shear thinning polymers like Xanthan Gum (Xg), previously used for the delivery of micro-scale ZVI for remedial purposes (Cantrell et al. 1997), have also been suggested as a suitable stabilizer (Comba et al. 2009). This approach produces very stable nZVI particles (on the order of weeks without agglomeration and settling) due to the creation of gelling (or networking) between individual particles that inhibit interaction (Vecchia et al. 2009). This approach is advantageous when very high concentrations of nZVI need to be injected (> 15 g/L nZVI). However, due to the high polymer content (0.3- 0.6% wt Xg) the injection solution can be very viscous (approaching 1000 cP at shear rates below 1 s^{-1}) complicating injection conditions due to large pressure required for injection. Adsorption of hydrophilic carbon, another variation of post-

synthesis stabilization, has also been reported (Schrack et al. 2004, Hoch et al. 2008) and shown to improve stability and mobility of nZVI compared to bare nZVI.

The second method for nZVI stabilization involves a modified chemical precipitation process in which the presence of the polymer stabilizes nZVI particles as they are precipitated from solution (presynthesis). This method, developed by researchers at Auburn University (He et al. 2005), has been most widely used with CMC. This polymer controls nZVI nucleation limiting aggregation during synthesis (He et al. 2007, He et al. 2007, Sakulchaicharoen et al. 2010). The presynthesis stabilization process has been shown to yield very stable nZVI solutions for select anionic polymers (Sakulchaicharoen et al. 2010) that can provide electro-steric repulsive interactions. In addition, the process facilitates manipulation of particle size (He et al. 2007). Enhanced ultra-sonic mixing techniques during synthesis in the presence of a high molecular weight polyvinyl acid can be used to control particle size, breaking up large particles (Sun et al. 2007). This additional step produced very small nZVI particles that were reportedly stable in solution for months. Composite nanoparticles containing zero valent iron (i.e. nZVI in a silica matrix) have also been synthesized as a delivery vehicle (Zhan et al. 2008, Zhan et al. 2009). nZVI particles, grown on stabilizing media have also been presented (Huang et al. 2008) to improve PRBs. An extension of this is the incorporation of nZVI particles into reactive membranes (Xu et al. 2005) with potential applications in industrial water and wastewater treatment.

The use of nZVI emulsions have also been presented as a method of limiting particle-particle and particle-soil interactions (Quinn et al. 2005, Berge et al. 2009). Using this modified post-synthesis approach, nano or micro scale iron particles can be stabilized through their encapsulation in biodegradable oil with the aid of a surfactant. The EZVI process effectively encapsulates nZVI slurry in an oil phase utilizing viscosity and surface tension to prevent particle settling (Quinn et al. 2005). One concern with this approach is that nZVI emulsions have a very high viscosity (>1000cP) and would necessitate elevated injection pressures. Recognizing this problem, in a more recent study the highly viscous vegetable oil in the emulsion was replaced with oleic acid, producing less viscous nZVI emulsion slurries (Berge et al. 2009). This oil in water emulsion method separates nZVI and water in the emulsion, preventing oxidation. An important consideration with using emulsions to transport nZVI is the integrity of the emulsion droplets under high shear conditions present at the well screen,

which could potentially destroy the effective mechanism of nZVI stability. In addition consideration of the droplet sizes is important to avoid pore straining which would negatively impact mobility (i.e., emulsion droplets must remain smaller than the pores to be mobile) (Berge et al. 2009).

7.7.2 Bench scale experiments investigating nZVI mobility

In order to make nZVI economically feasible a considerable amount of the injected nZVI mass must reach the contaminated source zone. Small scale column tests are commonly used to evaluate nZVI mobility under a range of representative subsurface conditions. Such experiments have been used to study the transport of numerous environmental colloids (e.g. Logan et al. 1995, Ryan et al. 1996, Tufenkji et al. 2004), as well as other engineered nanoparticles (Lecoanet et al. 2004), nC₆₀ particles, (Li et al. 2008) and carbon nanotubes (Liu et al. 2009).

Several column experiments have been conducted with unstabilized nZVI; however mobility was limited (Schrack et al. 2004, Johnson et al. 2009, Tiraferri et al. 2009). Subsequent studies showed that mobility can be improved when the nZVI surface is modified to provide electro-steric repulsion (Hydutsky et al. 2007, Kanel et al. 2007, Hoch et al. 2008, Phenrat et al. 2008, Saleh et al. 2008, Zhan et al. 2008, Johnson et al. 2009, Kim et al. 2009). Phenrat et al. (Phenrat et al. 2008) measured the steric layer properties of several polymers adsorbed to nZVI and demonstrated that the same steric repulsion that limits aggregation also increases nZVI transport through porous media by limiting particle-soil interactions. Very high mobility has also been reported in column experiments performed with nZVI prepared using a presynthesis stabilization technique with CMC polymer that provides electro-steric repulsion (He et al. 2009). It has also been demonstrated in transport experiments that both methods of providing electro-steric stabilization (pre and post synthesis) still provide good stabilization even in solutions of high ionic strength and divalent cations (Saleh et al. 2008, He et al. 2009). Studies also show that naturally occurring organic matter subsurface constituents may act in a similar fashion to surface modifications, potentially increasing the mobility of nZVI (Johnson et al. 2009) as with other colloids (Kretzschmar et al. 1995).

Although significant advances have been made in improving nZVI mobility in porous media, many early transport studies were conducted using conditions that did not adequately

represent subsurface conditions. Experiments were typically conducted at unrealistically high pore velocities. Another limitation of these early studies is the low nZVI concentrations (less than 0.25 g/L) that were used. According to the USEPA voluntary database of past and future nZVI field injections; concentrations on the order of 1 to 30 g/L are utilized in the field (Varadhi 2005, Bennett et al. 2010). Results from column experiments conducted at low nZVI concentrations may not be directly applicable to field application scenarios using much higher nZVI concentrations. More recent column experiments have been conducted at higher concentration injections, providing more relevant information for nZVI application. Phenrat et al. (Phenrat et al. 2009) demonstrated that higher concentrations of post-synthesis stabilized nZVI could be transported through porous media, although transport was limited by aggregation of nZVI more than nZVI interaction with the porous media. At high nZVI concentrations nZVI particles collide more frequently and are attracted to one another, depositing in the secondary energy minimum, forming larger aggregates. Particles trapped in a secondary minimum (Point 2 in Appendix A.3.b) are weakly attached as opposed to those in primary minimum that are irreversibly removed from solution (Point 1 in Appendix A.3.a). nZVI particles deposited in the secondary minimum can detach/disaggregate due to fluid shear or diffusion (Phenrat et al. 2009). Low concentration nZVI suspensions have higher particle diffusion resulting in disaggregation rates that can approach aggregation rates. To limit nZVI deposition in the secondary minimum and hence limit aggregation, polymers should be chosen to maximize long range electro-steric screening resulting in only a shallow secondary minimum (e.g. Appendix A.3.c).

Another important design consideration for optimal mobility is particle size. Elliot and Zhang (Elliott et al. 2001) suggested particle diameters of between 100 and 200nm (Elliott et al. 2001) to optimize mobility at typical groundwater velocities and limit nZVI retention in porous media due to physicochemical filtration (Bai et al. 1996, Tufenkji et al. 2004). Mobility is limited by deposition due to diffusion when particles are smaller than this range and gravity deposition becomes limiting for mobility when particles are larger than this range. In addition, the particle size in this case is not necessarily the individual initial nZVI particle size if particles are growing to form stable aggregates (Hong et al. 2009). However, many other factors affect this optimal range including injection velocity, porous media grain size, and solution viscosity, and should thus be included in design considerations along with particle size.

One of the main limitations of many column studies to date is the range of velocities used. Typical groundwater velocities range on the order of 0.1 m/day under natural conditions to 10 m/day in a typical remediation scenario with an imposed hydraulic gradient (Elliott et al. 2001, Berge et al. 2009). Subsurface heterogeneity results in significant variation in hydraulic conductivity (K), resulting in low permeability zones where groundwater velocity will be even lower than 0.1 m/day, limiting nZVI mobility. Column experiment pore velocities ranging from 15-35 m/day (Hydutsky et al. 2007, He et al. 2009, Phenrat et al. 2009) up to 260 m/day have been reported (Zhan et al. 2008, Vecchia et al. 2009, Tosco et al. 2010). Although these experiments are quicker to complete, they are not representative of nZVI transport at field sites. There have been several recent column studies reporting high concentration nZVI injection at realistic pore velocities. Berge and Ramsburg (Berge et al. 2009) reported column experiments showing good mobility of nZVI emulsions at velocities of 0.4 m/day, a velocity that could occur within a few meters of an injection well (Berge et al. 2009). Their nZVI suspension viscosity was 2.4-9.3 cP which would be within an acceptable range for field injection. Mobility has varied at low pore velocities in other studies. Post-synthesis stabilized nZVI (using guar gum) had limited mobility as velocities decreased to 2 m/day (Tiraferri et al. 2009) whereas, presynthesis stabilized nZVI (using CMC polymer) was reported to be mobile at low velocities (0.1 - 2 m/day), and at higher concentrations (3 g/L) (Raychoudhury et al. 2011).

Previous studies that utilized high pore water velocities for nanometal delivery typically did not consider the prohibitively large injection pressures required to achieve these velocities. Vecchia et al. (Vecchia et al. 2009) studied the transport of shear thinning polymers for nZVI delivery and recorded pressures exceeding 60 kPa in column (46 cm long) experiments using highly viscous injections. Berge and Ramsburg (Berge et al. 2009) discussed the effects of viscosity on injection and the need to minimize solution viscosity, optimize velocity and minimize pressure during field scale injection, discussed in Section 8.2. Recent work has also suggested that the high shear in column experiments, believed to encourage disaggregation (or re-suspend nZVI deposited in a shallow secondary energy minimum), may not occur when multidimensional experiments are conducted due to the additional flow paths provided (Phenrat et al. 2010). Although column studies are unable to replicate all of the complex phenomena occurring at the field scale they are an important step in building and validating conceptual models for the prediction of nZVI transport. Ultimately,

these experiments will aid in the design nZVI injection at field sites, especially when they are performed under representative subsurface conditions.

7.7.3 NAPL Targeting

Limiting interactions between nZVI and porous media is desirable to maximize nZVI mobility. However, once nZVI has reached the target contaminated zone, sufficient residence time is required to allow completion of reactions with contaminants. This can occur due to deposition of nZVI on soil in the contaminated zone, or due to partitioning of nZVI to the NAPL-water interface. As nZVI is typically stabilized in an aqueous phase it has a limited affinity for NAPL. Several studies have investigated the ability of surface modifiers to “target” NAPL, or preferentially interact with non-polar species. EZVI was designed to surround ZVI by an oil-liquid membrane that will absorb free phase NAPL bringing nZVI and NAPL into proximity (Quinn et al. 2005). Reductive dechlorination associated with nZVI requires that water (or another proton donor) be present. Thus, nZVI will be the most reactive at the interface of NAPL and water. Partitioning of nZVI to the NAPL-water interface has been achieved using hydrophilic and hydrophobic polymers adsorbed to the nZVI, reducing the energy of this surface. These formulations had an increased affinity for hydrophobic coated sand grains (Saleh et al. 2007). A study evaluating the targeting tendencies of more widely used and inexpensive polymers (e.g., PAA, CMC) (Bishop et al. 2010) suggested that ideal polymers would maintain low interaction with soils to enhance transport and exhibit slight hydrophobicity to increase affinity for NAPL. Berge and Ramsburg (Berge et al. 2009) developed an nZVI emulsion that was hydrophobic, and could partition to NAPL. They were able to achieve reductive dechlorination within a NAPL using an nZVI emulsion. Consideration of the potentially negative impacts of DNAPL mobilization and subsequent sinking, especially when using high injection pressures, surfactants, and high viscosity solutions, need to be considered when using any of these NAPL targeting techniques (Berge et al. 2009).

7.8 Simulation of nZVI Transport

Numerical models can be valuable tools for design of remediation schemes at contaminated sites. Once validated, these models can reduce the need for costly treatability studies and avoid costly errors such as the implementation of inappropriate or ineffective

remediation methods. To date, no comprehensive numerical model has been developed for the prediction of nanoparticle transport and remediation. The limited model development to simulate nanoparticle transport and reactivity completed to date has been predominantly applied to small batch experiments or one-dimensional column experiments (Schrack et al. 2004, Liu et al. 2005, Zhan et al. 2008, Barnes et al. 2010).

Many of the models developed are based on colloid filtration theory (CFT), which was originally developed for water treatment (Yao et al. 1971) and has been widely used to describe physicochemical filtration in porous media. The colloid filtration process is incorporated into the advection-dispersion equation as a first order attachment term:

$$\frac{\partial C}{\partial t} = D_H \frac{\partial^2 C}{\partial x^2} - v_p \frac{\partial C}{\partial x} - K_{Att} C \quad (16)$$

where C is the nZVI concentration in the solution (M/L^3), D_H is the hydrodynamic dispersion (L^2/T), v_p is the pore water velocity (L/T), t is time (T), K_{Att} is the rate at which nZVI attaches or is deposited on available collector sites ($1/T$).

$$K_{Att} = \frac{3(1 - \theta_w)}{2d_{50}} \alpha \eta_o v_p \quad (17)$$

where d_{50} is the median collector grain size (L), θ_w is the volumetric water content (-) and η_o is the theoretical collision efficiency (-). η_o is defined as the ratio of particles striking a collector to those approaching the collector. It is calculated by considering the cumulative effects of diffusion (i.e., Brownian motion), interception, and gravity on the particle as it passes by an ideal collector (e.g. Yao et al. 1971, Bai et al. 1996, Tufenkji et al. 2004). The dimensionless parameter α is the sticking efficiency (-), which is the ratio of colloids that stick to the collector to those that strike the collector. η_o can be estimated using a variety of approaches (Yao et al. 1971, Bai et al. 1996, Tufenkji et al. 2004, Nelson et al. 2011) whereas α is typically a fitting parameter. Many researchers use the steady state analytical solution to Equation 17 to quantify the sticking efficiency in nanoparticle mobility studies:

$$\alpha = -\frac{2}{3} \frac{d_{50}}{(1-\theta)L\eta_o} \ln(C/C_0) \quad (18)$$

where L is the length of porous media (L), and C/C_0 is the maximum normalized effluent concentration.

A number of studies have used CFT to interpret results from column studies and extrapolate to maximum nZVI travel distance in the field (calculated as the distance needed for nZVI concentration to reduce to 0.1% of the initial concentration). Column studies have used bare nZVI (Schrack et al. 2004, Johnson et al. 2009, Tiraferri et al. 2009), postsynthesis stabilized nZVI (Schrack et al. 2004, Saleh et al. 2007, Johnson et al. 2009, Phenrat et al. 2009, Tiraferri et al. 2009, Vecchia et al. 2009) as well as presynthesis stabilized nZVI (He et al. 2009, Raychoudhury et al. 2011). One common method to compare experimental results has been to compare the sticking coefficient fitted using Equation 18. Fitted sticking coefficients have ranged from 0.1 to 1.0 for bare nZVI, 0.002 to 0.07 for postsynthesis stabilized nZVI and 0.0003 to 0.0023 for presynthesis stabilized nZVI (Schrack et al. 2004, He et al. 2009, Johnson et al. 2009, Phenrat et al. 2009). Application of Equation 17 assumes that nZVI particles are stable in suspension (i.e., no aggregation or settling). A number of studies have found that this is not the case. At high nZVI concentrations (above 1 g/L), aggregation and deposition can become a dominant removal mechanism in comparison to particle-soil interactions, due to the increased number of particle/particle interactions (Phenrat et al. 2009). Given that CFT does not account for particle-particle interactions, it should be used with caution for the prediction or interpretation of unstable nZVI transport (Phenrat et al. 2009). It should be noted, however, that studies have been able to interpret some nZVI transport experiments using CFT since nZVI was colloidally stable in these studies (He et al. 2009).

A goal of several studies has been to improve the understanding of particle aggregation or temporal changes in aggregate size, with an ultimate goal of modifying Equation 17 to incorporate particle aggregation. A recent study shows that consideration of nZVI size change with time improves interpretation of nZVI transport in column experiments (Raychoudhury et al. 2011). Hong et al. (Hong et al. 2009) observed that stable aggregates formed in proportion to the total magnetic interaction and proposed that use of the stable aggregate size, as opposed to the individual nZVI particle size, would be more appropriate for the estimation of the

collector efficiency (η_0). A study of iron oxide nanoparticles indicated that the size of particles during aggregation and disaggregation can be mathematically described using an exponential decay function (Baalousha 2009). This work supports earlier experimental work by Phenrat et al. (Phenrat et al. 2007) who showed that unstabilized nZVI quickly aggregated and settled in time resolved UV-light absorption experiments. Models based on the solution of Equation 17 can utilize this relationship, updating η_0 to reflect the aggregating particle size in time. It has also been shown that the aggregation rate increased with larger initial particle size (Rosicka et al. 2011).

Phenrat et al. (Phenrat et al. 2010) developed an empirical correlation for changes in nZVI aggregate size during transport in porous media. However, this correlation requires specification of a large number of system parameters (e.g., geologic, hydrologic, and geochemical) in addition to a number of small scale parameters that can vary widely depending on subsurface conditions. Given that this correlation was calibrated for a reasonably small range of the parameters, model prediction would likely only be valid within the calibration range. Another study has proposed a statistical approach to account for bimodal particle size distributions requiring solution of the CFT equation for each particle size subpopulation (Chatterjee et al. 2009). More research is needed to develop more fundamental understanding of the nZVI aggregation processes.

Not all studies have applied CFT to predict nZVI transport. Kanel et al. (Kanel et al. 2008) successfully used SEAWAT (Langevin et al. 2006) to predict the downward migration of nZVI, due to density contrasts, observed in 2-D sandbox experiments. However, SEAWAT simulates density effects associated with dissolved salts, not suspensions of particles. Other variations of the nZVI technology that will require a novel modeling approach include the simulation of viscosity changes associated with shear thinning fluids in the stabilization suspension (Tosco et al. 2010). Prediction of nZVI transport, whether or not in the framework of CFT, must also account for particle-particle as well as particle-collector interactions.

Although many studies have simulated nZVI transport in controlled laboratory experiments, there are currently no published modeling studies of nZVI transport at the field scale. Before nZVI fate and transport models can be confidently used in design of field scale remediation, the models need to be validated using data from well monitored field

investigations. Given the complex redox reactions involved in nZVI remediation, it is likely that there will be a need for the development of models that will go well beyond simple application of CFT and include particle-particle interactions, particle-soil interactions, and reactions with contaminants and other groundwater constituents.

7.9 nZVI Field Applications

The first field scale injections of nZVI used unstabilized nZVI leading to limited mobility (Elliott et al. 2001). More recent field scale studies have utilized a variety of stabilizers, improving nZVI transport (Henn et al. 2006, Bennett et al. 2010, He et al. 2010, Wei et al. 2010). Although nZVI has been injected at a number of sites, many of the test sites reported in a recent EPA database (26 in total) do not have associated publications or technical reports (Otto 2010). Details from 8 studies have been presented in academic journals and limited information has been provided for 13 others in the form of conference papers, conference presentations, reports, and other technical reports that have been made publically available but not peer-reviewed. According to a recent report published by the National Institute of Environmental Health Sciences there have been 44 sites worldwide where nano-materials have been injected into the subsurface for remediation purposes (Karn 2009). With the growing number of bench scale feasibility studies reporting mobile nZVI, this number is likely to grow.

7.9.1 Early Studies of nZVI in the Field

Initial nZVI field studies used unstabilized nZVI (Elliott et al. 2001, Zhang 2003) that has since been shown to rapidly aggregate and settle out of suspension (Phenrat et al. 2007). In the field, this translates into rapid deposition of nZVI within the wellbore, limiting mobility. In one field study nZVI was injected at 1.5 g/L; however, only 10-20 mg/L (expressed as total Fe) reached monitoring wells at a distance of 1.5 m (Elliott et al. 2001). Poor mobility on the order of a few inches to a few feet was believed to be due to clogging of the well screen by nZVI aggregates (Sun et al. 2007). Discrete nZVI particles, present as zero valent iron, were not distinguished from soluble iron corrosion products. It is likely that much of the downstream iron quantified was soluble iron corrosion products that dissolved near the injection well screen

and flowed to the monitoring location. In a subsequent study nZVI was injected into a highly conductive fractured bedrock with a reported estimated radius of influence from the injection to be 6-11 m based on ORP readings, although the ORP readings outside the injection well rebounded shortly after injection (Glazier et al. 2003, Zhang 2003). Recent work has questioned the interpretation of ORP data as evidence of successful nZVI emplacement during field application, suggesting that the highly complex redox response indicates nZVI corrosion and transport of these corrosion products and not transport of the nZVI particles themselves (Shi et al. 2011). Early studies evaluating nZVI injection only briefly address mobility and delivery, primarily focusing on reaction of target contaminants. Target VOC removal efficiencies were reported to be 36-96% (Glazier et al. 2003, Zhang 2003), where removal efficiency is defined to be the observed aqueous phase VOC concentrations normalized to the baseline concentration. These removal efficiencies were sustained for three months, although the most successful results were observed in the injection well.

To effectively monitor remediation, more rigorous monitoring will be required as concentrations within the injection well are not an accurate indication of formation contaminant concentrations. In many studies nZVI likely deposited in the well screen, and monitoring VOC degradation at the injection well may only have been measuring degradation through the well screen, which effectively acted as a PRB. In one study (Glazier et al. 2003), VOC concentrations in the monitoring well 6m down gradient continued to decrease for two months after injection, although the contributions of up gradient reaction with nZVI and biological activity, followed by transport of degradation products downstream, is not discussed. The evaluation of the success of nZVI delivery in field scale applications is further complicated by widely spaced monitoring well locations and the inability to directly identify nanoparticles, relying instead on indirect evidence of nanoparticle transport (e.g., ORP).

These first studies were reported as successes with limited discussion addressing challenges associated with nZVI application at the field scale (Elliott et al. 2001, Glazier et al. 2003, Zhang 2003). There is a significant need for field studies that demonstrate rigorous site characterization, optimization of on-site injection infrastructure, design of injection fluid properties, and reporting methods in order to reduce the uncertainty associated with nZVI delivery.

7.9.2 Improvements to Field Scale nZVI Delivery

Rapid nZVI aggregation in early field studies likely caused nZVI to travel less than a metre upon injection (Sun et al. 2007), partially contributing to nZVI not being widely accepted in the remediation community. Several field scale studies have been conducted to evaluate the use of stabilized nZVI, with promising results in comparison to early studies (Henn et al. 2006, Bennett et al. 2010, He et al. 2010, Wei et al. 2010). These studies have used nZVI injection concentrations ranging from 0.2 – 30 g/L (Gavaskar A. 2005, Quinn et al. 2005, Bennett et al. 2010, He et al. 2010, Krug 2010, Wei et al. 2010). However, field studies to date lack definitive evidence of nZVI mobility at the intended radius of influence and uniform nZVI spreading within the treatment zone.

Henn et al. (Henn et al. 2006) observed “black stained” water, a color indicative of nZVI, in a monitoring well 1.06 m from an injection point. Post-injection slug tests confirmed that the injection wells were not significantly impacted by well clogging, suggesting the nZVI was mobile. However, at other monitoring points, located between 0.75 - 1.5 m from injection wells, no black color was observed. Other studies report lower than expected travel distances using postsynthesis stabilized nZVI (e.g. PARS_Environmental 2003, Gavaskar A. 2005) and nonuniform travel to target monitoring wells (e.g. Varadhi 2005). A recent study reported that stabilized nZVI was mobile in a field test traveling 3 m to a monitoring well, aided by a very high 20 L/min injection rate (Wei et al. 2010). However, nZVI was not well distributed throughout the targeted depth of contamination. Most of the nZVI appears to have traveled through a preferential pathway comprised of coarse sand due to a 15 m screened interval in the injection well.

In the case of He et al. (He et al. 2010), high mobility of presynthesis stabilized nZVI was demonstrated during a field study using two injection conditions. Using gravity feed and pressurized injections nZVI was observed in a monitoring well 1.5 m down gradient at breakthrough concentrations of 37% and 70% respectively (when normalized to the tracer) (He et al. 2010). Use of tracers is important for the validation of nanoparticle transport models and in the determination of nZVI deposition in the subsurface. Their study also reported that nZVI was not detected in a monitoring well 3 m down gradient. However, this well was screened at a depth 1.5 m above the injection well, suggesting that the nZVI may have moved vertically

as it traveled horizontally. In summary, stabilized nZVI has been visually confirmed to travel 1 m from an injection well, although evidence suggests that maximum travel distances of up to 2 -3 m may be achieved in high permeability formations.

Careful control of the hydraulic conditions, and therefore groundwater velocity, is essential for delivery of nZVI. There is evidence to suggest that under ambient groundwater conditions even the most stable nZVI is effectively immobile. Bennett et al. (Bennett et al. 2010), performing a push-pull field test, observed a significant loss of mobility after a 13 hour lag period (i.e., no applied gradient resulting in a pore water velocity < 0.3 m/d) (Bennett et al. 2010). This nZVI formulation has been shown to be highly mobile in column experiments (He et al. 2009) and exhibited good mobility in two other push pull tests in this field study (Bennett et al. 2010), suggesting that groundwater recirculation and other methods to promote nZVI spreading in previous studies (Gavaskar A. 2005, Henn et al. 2006) may be a necessity for nZVI delivery.

The addition of stabilizers to nZVI suspensions can result in colloiddally stable nZVI that can be transmitted through porous media; however the addition of stabilizer also affects fluid properties (e.g. viscosity, interfacial tension) of the injection fluid. Solution viscosity has been reported in very few studies, but can range from slightly above water (e.g. 5-20 cP) to much higher viscosities (e.g. 1942 cP (Quinn et al. 2005)), having a significant impact on injection. Increased solution viscosity resulting from stabilizers can increase the head in the injection well, at constant injection rates, or reduce injection velocities given a constant injection head. Reported injection pressures during field studies have ranged from low to moderate (e.g. < 34.5 kPa (He et al. 2010) to 137.9 kPa (Varadhi 2005)) in some injections, but have reached higher pressures (e.g. 344.7 kPa (Krug 2010)) when the viscosity of the nZVI suspension is greater.

Highly viscous suspensions can be advantageous to mitigate against viscous fingering during pressurized injection and have been demonstrated to emplace EZVI with a reported radius of influence of 2.13 m (Krug 2010) compared to 0.45 m using gravity feed. However, it has also been suggested that highly viscous nZVI suspensions are capable of mobilizing NAPL even at moderate injection velocities (Berge et al. 2009), which should be considered in the hydraulic design of the injection. Another consideration in manipulating the flow field

is the depth of injection and potential daylighting (Krug 2010), which renders the injection well unusable for subsequent injection. Recent nZVI injections have been successful in comparison to early field injections which had limited nZVI mobility due to aggregation. However, unpredictable mobility and inconsistent subsurface distribution continue to pose problems upon injection.

7.9.3 Tracking Remediation Following nZVI Injection

Many nZVI field trials have been reported as successes but direct comparison of these studies is challenging, as data reporting is inconsistent. As was the case with comparison of bench scale column experiments, comparing pilot scale studies is complicated due to the use of different types of nZVI, different stabilizers, different injection conditions (e.g., injection pressure and rate, injection well screen length) as well as injection into different geologies (e.g., fractured rock, sandy aquifer material, and low permeability media). It is important to develop metrics of nZVI injection success as well as remediation to facilitate a comparison between field studies and provide an impartial assessment of this remediation technology.

There are many uncertainties associated with field scale application of nZVI. One significant need is for methods to directly identify and quantify nZVI (among other nanoparticles (Simonet et al. 2009)) in environmental systems. Knowledge of the extent of nZVI migration is required to determine if the injected nZVI is reaching the target treatment zone. Currently, nZVI transport is often tracked by observing changes in aqueous geochemistry caused by nZVI reactions (Elliott et al. 2001, He et al. 2010, Wei et al. 2010). ORP, pH, total iron, suspended solids, total solids, and dissolved oxygen (DO) have all been suggested as indicators of nZVI at field sites. However, none of these parameters alone directly confirm the presence of nZVI particles. The problem with these indirect indicators of nZVI presence is that they do not distinguish between nZVI particles and dissolved corrosion species and associated geochemical changes. Due to the significant iron corrosion and dissolution this becomes important at the field scale. Separation of dissolved iron species and nZVI particles is problematic as stable nZVI particles (e.g. 20 nm) have been reported to pass filters (e.g. 0.45 μm) commonly used to distinguish dissolved and total iron (Bennett et al. 2010). This suggests that methods must be improved to distinguish dissolved iron species from stable nZVI particles in field samples.

Changes in ORP have been commonly used to indicate the presence of nZVI in field studies (Elliott et al. 2001, Glazier et al. 2003, Zhang 2003, Wei et al. 2010, Zhu et al. 2010) as it becomes strongly negative following application of nZVI due to iron oxidation (e.g. decreasing to -360 mV and -700 mV in the injection well following nZVI injection). However, one study (Gavaskar A. 2005) observed no change in ORP after injection, likely because a highly concentrated nZVI solution was diluted with tap water that had a high dissolved oxygen content so that the surface of the iron would have been oxidized prior to injection and no further iron oxidation occurred *in situ*. In some cases ORP response has been interpreted as successful delivery of nZVI (He et al. 2010, Wei et al. 2010). However, a recent study investigating the temporal evolution of ORP impact from nZVI has reported that even low concentrations of nZVI (e.g. <50 mg/L) can lead to significant reductions in measured ORP (Shi et al. 2011). The study reports that at low nZVI concentrations ORP readings are a mixture of contributions from nZVI as well as dissolved reaction products (e.g. H₂ and Fe²⁺) (Shi et al. 2011) which will have different transport characteristics. They also found that with increasing nZVI concentration, ORP readings were influenced by the adsorption of nZVI to the ORP probe (Shi et al. 2011). This implies that presence of nZVI in environmental samples should not be based solely on ORP but on multiple lines of evidence.

Other geochemical parameters that have been associated with the presence of nZVI in field samples include pH and DO. Oxidation of nZVI in aqueous solution increases aqueous phase pH (Eq. 6 and 7) and can lead to the consumption of oxidants (e.g. dissolved oxygen). Several field studies have noted pH increases following nZVI injection (Elliott et al. 2001, Glazier et al. 2003, Zhang 2003), and in some cases has been suggested as an indicator of the nZVI migration front (Henn et al. 2006, Wei et al. 2010). However, two nZVI field injections resulted in no significant pH change after injection (Gavaskar A. 2005, Henn et al. 2006). It is difficult to draw conclusions from these conflicting reports, as groundwater chemistry can vary widely (e.g. buffering capacity, oxidant species), and there are other compounding reactions in the subsurface that can influence pH. Decreases in DO have been observed following nZVI injection in several field studies (Elliott et al. 2001, Gavaskar A. 2005, Henn et al. 2006, He et al. 2010). However, similar to the discussion related to ORP, low DO measurements may be the result of upstream nZVI corrosion and subsequent downstream migration. As such they may not indicate the presence of nZVI.

Success in remediation studies is often based on decrease in total aqueous VOC concentrations, with reported decreases greater than 90% in injection wells (Mace 2006), in some cases persisting for months after injection. Other studies have reported similarly high target contaminant removal efficiencies (e.g. 50-99% removal of vinyl chloride (Wei et al. 2010)) and have gone so far as to declare site closure or recourse to monitored natural attenuation following nZVI injection (e.g. Varadhi 2005). However, aqueous phase contaminants can be displaced by the injection fluid, pushing contamination out of the treatment area (Henn et al. 2006, Bennett et al. 2010). These studies imply that earlier studies that report aqueous VOC removal within monitoring and injection wells need to account for the transfer or displacement of contaminated groundwater out of the study area after injection. This displaced water with high VOC concentrations can flow back to the treatment zone under ambient flow conditions, resulting in rebounding VOC levels as observed by Mace (Mace 2006). For this reason it has been suggested that nZVI is best utilized when the majority of contamination exists in a stationary phase (NAPL or sorbed phase contamination, not aqueous phase (Bennett et al. 2010)).

Another uncertainty in evaluating remediation of chlorinated solvents using nZVI is determining the contributions from abiotic and biotic degradation. nZVI injection creates reducing conditions in the subsurface that are favorable for bioremediation (Elliott et al. 2001, Henn et al. 2006, Mace 2006, He et al. 2010, Wei et al. 2010). Injection suspensions commonly contain a polymer (or other substrate) that is readily biodegradable. Rapid decreases in VOC concentrations are typically associated with abiotic degradation (Quinn et al. 2005, Henn et al. 2006, He et al. 2010). However with time concentrations may rebound over an intermediate period (Henn et al. 2006, Mace 2006, He et al. 2010) prior to the onset of biodegradation (He et al. 2010). Other studies report similar long term declining VOC trends and increases of reaction products, confirming that some remediation occurs up to 19 months after nZVI injection (Quinn et al. 2005). There is a need to better distinguish abiotic and biotic degradation and to determine the impact of nZVI on biological activity to assess the utility of applying nZVI over some other type of biostimulation technology.

There are many groundwater constituents that interact with nZVI; however many of these interactions are not well understood or otherwise cannot be individually isolated in natural systems. The presence of naturally occurring groundwater species (e.g. nitrate, nitrite,

sulfate) are examples that may affect nZVI reaction. Interpretation of data in the field is further complicated by reaction products from bioremediation (Quinn et al. 2005, Henn et al. 2006, He et al. 2010) as well as processes that dilute and disperse groundwater constituents. Due to the complexity of subsurface biogeochemistry, analysis of dissolved light hydrocarbons (e.g. methane), anions (e.g. nitrate, sulfate), volatile fatty acids, as well as total organic carbon, have become common baseline analytes to evaluate bioremediation in field studies utilizing nZVI (Krug 2010). This is in addition to analysis of VOCs, anions, ORP, pH, total iron, suspended solids, total solids, and DO. No supporting studies to date have presented evidence to suggest that application of nZVI will elicit a predictable and reliable response from any of these parameters, given pre-injection biogeochemistry.

To draw conclusions about remediation, an extensive monitoring plan is often used employing many of the aforementioned parameters. Field studies have sampled daily to weekly to evaluate abiotic remediation (Henn et al. 2006, Bennett et al. 2010, He et al. 2010, Wei et al. 2010), and quarterly to biannually to evaluate nZVI induced bioremediation (Quinn et al. 2005, Henn et al. 2006, He et al. 2010, Krug 2010, Wei et al. 2010). Though with relatively few supporting lab studies that investigate the complex effects of nZVI with constituents in the subsurface (e.g. Shi et al. 2011), it is difficult to conclusively evaluate nZVI performance. Future nZVI pilot projects should complement field monitoring with supporting bench scale experiments and investigations to fill the knowledge gaps in nZVI implementation including the effect of nZVI on pH, DO, ORP, dissolved Fe, and other groundwater constituents. There is also a need for field investigations to demonstrate the technology using established field techniques in order to develop definitive metrics of success for field scale injection. These studies would aid in informing practitioners of effective methods to monitor and apply nZVI in the field, leading to successful remediation.

7.10 Summary and Outlook

Significant potential has been demonstrated for the application of nanometals for the remediation of a wide range of priority pollutants in controlled laboratory experiments. However, nanometal technology has not achieved widespread commercial application for a number of reasons. Rapid aggregation and settling of nZVI, leading to poor subsurface

mobility has been a problem. In addition, reaction of nZVI with a number of natural groundwater constituents has led to decreases of the reducing equivalents available for reaction with the target contaminants.. These problems pose the greatest challenge to the nZVI technology, resulting in ineffective delivery of nZVI particles to the contaminants and reducing the effectiveness of nZVI. Another issue is the high cost associated with synthesis of nanometals for field application. This cost continues to decrease as new sources of nanometal raw materials are found (e.g., new suppliers, alternative raw materials). Lastly, displacement of dilute contaminant plumes upon nZVI injection has been observed at some sites, suggesting that nZVI technology may be better suited to source zones rather than dilute plumes.

Additional research is needed at all scales (i.e., nanoscale to field scale) to improve the understanding of the potential of nanometals for remediation. At the nanoscale, an improved understanding of the governing chemical reactions and physical mechanisms governing transport will ultimately translate into success at the field scale. More field applications are required with detailed characterization before and after nZVI injection to assess nZVI mobility and the extent of contaminant destruction. All of this information will aid in the development and validation of numerical models that can be used to predict remediation at a wide range of field sites.

The research and development to date highlights the significant promise of nanometal technology for contaminated site remediation. Future research in nanotechnology is expected to lead to new advances in bimetallic particles, improved stabilizers, and improved formulations for enhancing partitioning of nZVI to NAPL.

7.11 References

- Abriola, L. R., A., Pennell, K. (2011). Final Report: Development and Optimization of Targeted Nanoscale Iron Delivery Methods for Treatment of NAPL Source Zones. Strategic Environmental Research and Development Program, Tufts University.
- Acar, Y. B. and A. N. Alshawabkeh (1993). "Principles of electrokinetic remediation." Environmental Science & Technology **27**(13): 2638-2647.
- Adeleye, A., A. Keller, R. Miller and H. Lenihan (2013). "Persistence of commercial nanoscaled zero-valent iron (nZVI) and by-products." Journal of Nanoparticle Research **15**(1): 1-18.

Agler, M. T., J. J. Werner, L. B. Iten, A. Dekker, M. A. Cotta, B. S. Dien and L. T. Angenent (2012). "Shaping Reactor Microbiomes to Produce the Fuel Precursor n-Butyrate from Pretreated Cellulosic Hydrolysates." Environmental Science & Technology **46**(18): 10229-10238.

Agrawal, A. and P. G. Tratnyek (1996). "Reduction of nitro aromatic compounds by zero-valent iron metal." Environ Sci Technol **30**(1): 153-160.

Alonso, F., I. P. Beletskaya and M. Yus (2002). "Metal-mediated reductive hydrodehalogenation of organic halides." Chemical Reviews **102**(11): 4009-4091.

Annable, M. D., J. W. Jawitz, P. S. C. Rao, D. P. Dai, H. Kim and A. L. Wood (1998). "Field evaluation of interfacial and partitioning tracers for characterization of effective NAPL-water contact areas." Ground Water **36**(3): 495-502.

Arnason, J. G., M. Harkness and B. Butler-Veytia (2014). "Evaluating the Subsurface Distribution of Zero-Valent Iron Using Magnetic Susceptibility." Groundwater Monitoring & Remediation **34**(2): 96-106.

Arnold, W. A. and A. L. Roberts (2000). "Pathways and Kinetics of Chlorinated Ethylene and Chlorinated Acetylene Reaction with Fe(0) Particles." Environmental Science & Technology **34**(9): 1794-1805.

Auffan, M., W. Achouak, J. Rose, M.-A. Roncato, C. Chaneï, D. T. Waite, A. Masion, J. C. Woicik, M. R. Wiesner and J.-Y. Bottero (2008). "Relation between the Redox State of Iron-Based Nanoparticles and Their Cytotoxicity toward Escherichia coli." Environmental Science & Technology **42**(17): 6730-6735.

Baalousha, M. (2009). "Aggregation and disaggregation of iron oxide nanoparticles: Influence of particle concentration, pH and natural organic matter." Science of the Total Environment **407**(6): 2093-2101.

Baciacchi, R., M. R. Boni and L. D'Aprile (2003). "Characterization and performance of granular iron as reactive media for TCE degradation by permeable reactive barriers." Water Air Soil Poll **149**(1-4): 211-226.

Bai, R. and C. Tien (1996). "A New Correlation for the Initial Filter Coefficient under Unfavorable Surface Interactions." Journal of Colloid and Interface Science **179**(2): 631-634.

Bai, R. and C. Tien (1999). "Particle Deposition under Unfavorable Surface Interactions." Journal of Colloid and Interface Science **218**(2): 488-499.

Bandstra, J. Z., R. Miehr, R. L. Johnson and P. G. Tratnyek (2005). "Reduction of 2,4,6-trinitrotoluene by iron metal: Kinetic controls on product distributions in batch experiments." Environmental Science & Technology **39**(1): 230-238.

Bard, A. J., R. Parsons and J. Jordan, Eds. (1985). Standard potentials in aqueous solution. New York, Marcel Dekker, Inc.

Barnes, R. J., O. Riba, M. N. Gardner, T. B. Scott, S. A. Jackman and I. P. Thompson (2010). "Optimization of nano-scale nickel/iron particles for the reduction of high concentration chlorinated aliphatic hydrocarbon solutions." Chemosphere **79**(4): 448-454.

Barnes, R. J., O. Riba, M. N. Gardner, A. C. Singer, S. A. Jackman and I. P. Thompson (2010). "Inhibition of biological TCE and sulphate reduction in the presence of iron nanoparticles." Chemosphere **80**(5): 554-562.

Barnes, R. J., C. J. van der Gast, O. Riba, L. E. Lehtovirta, J. I. Prosser, P. J. Dobson and I. P. Thompson (2010). "The impact of zero-valent iron nanoparticles on a river water bacterial community." Journal of Hazardous Materials **184**(1-3): 73-80.

Bennett, P., F. He, D. Zhao, B. Aiken and L. Feldman (2010). "In Situ Testing of Metallic Iron Nanoparticle Mobility and Reactivity in a Shallow Granular Aquifer." Journal of Contaminant Hydrology.

Bennett, P., F. He, D. Zhao, B. Aiken and L. Feldman (2010). "In Situ Testing of Metallic Iron Nanoparticle Mobility and Reactivity in a Shallow Granular Aquifer." Journal of Contaminant Hydrology **116**(1-4): 35-46.

Benson, R. C. (2005). Remote Sensing and Geophysical Methods for Evaluation of Subsurface Conditions. Practical Handbook of Environmental Site Characterization and Ground-Water Monitoring, Second Edition, CRC Press: 249-295.

Berge, N. D. and C. A. Ramsburg (2009). "Oil-in-Water Emulsions for Encapsulated Delivery of Reactive Iron Particles." Environmental Science & Technology **43**(13): 5060-5066.

Berge, N. D. and C. A. Ramsburg (2010). "Iron-mediated trichloroethene reduction within nonaqueous phase liquid." Journal of Contaminant Hydrology **118**(3-4): 105-116.

Bernhardt, E. S., B. P. Colman, M. F. Hochella, B. J. Cardinale, R. M. Nisbet, C. J. Richardson and L. Y. Yin (2010). "An Ecological Perspective on Nanomaterial Impacts in the Environment." Journal of Environmental Quality **39**(6): 1954-1965.

Bishop, E. J., D. E. Fowler, J. M. Skluzacek, E. Seibel and T. E. Mallouk (2010). "Anionic Homopolymers Efficiently Target Zerovalent Iron Particles to Hydrophobic Contaminants in Sand Columns." Environmental Science & Technology **44**(23): 9069-9074.

Blowes, D. W., C. J. Ptacek, S. G. Benner, C. W. T. McRae, T. A. Bennett and R. W. Puls (2000). "Treatment of inorganic contaminants using permeable reactive barriers." Journal of Contaminant Hydrology **45**(1-2): 123-137.

Boland, D. D., R. N. Collins, T. E. Payne and T. D. Waite (2011). "Effect of Amorphous Fe(III) Oxide Transformation on the Fe(II)-Mediated Reduction of U(VI)." Environmental Science & Technology **45**(4): 1327-1333.

Boparai, H. K., M. Joseph and D. M. O'Carroll (2011). "Kinetics and thermodynamics of cadmium ion removal by adsorption onto nano zerovalent iron particles." Journal of Hazardous Materials **186**(1): 458-465.

Boparai, H. K., M. Joseph and D. M. O'Carroll (2011). "Kinetics and thermodynamics of cadmium ion removal by adsorption onto nanozerovalent iron particles." Journal of Hazardous Materials **186**(1): 458-465.

Bowers, J. R., D. M. Engelthaler, J. L. Ginther, T. Pearson, S. J. Peacock, A. Tuanyok, D. M. Wagner, B. J. Currie and P. S. Keim (2010). "BurkDiff: A Real-Time PCR Allelic Discrimination Assay for *Burkholderia Pseudomallei* and *B. mallei*." PLoS ONE **5**(11): e15413.

Bray, R. J., Curtis, J.T., (1957). "An ordination of the upland forest communities of southern Wisconsin." Ecological Monographs **27**: 325-349.

Buchau, A., W. M. Rucker, C. V. De Boer and N. Klaas (2010). "Inductive detection and concentration measurement of nano sized zero valent iron in the subsurface." IET Science, Measurement and Technology **4**(6): 289-297.

Butler, J. J. (1997). The Design, Performance, and Analysis of Slug Tests, Taylor & Francis.

Cantrell, K. J., D. I. Kaplan and T. J. Gilmore (1997). "Injection of Colloidal Fe₀ Particles in Sand with Shear-Thinning Fluids." Journal of Environmental Engineering **123**(8): 786-791.

Cantrell, K. J., D. I. Kaplan and T. J. Gilmore (1997). "Injection of colloidal Fe-0 particles in sand with shear-thinning fluids." Journal of Environmental Engineering-Asce **123**(8): 786-791.

Cantrell, K. J., D. I. Kaplan and T. J. Gilmore (1997). "Injection of colloidal size particles of Fe₀ in porous media with shear thinning fluids as a method to emplace a permeable reactive zone." Land Contamination and Reclamation **5**(3): 253-257.

Cantrell, K. J., D. I. Kaplan and T. W. Wietsma (1995). "Zero-Valent Iron for the in-Situ Remediation of Selected Metals in Groundwater." Journal of Hazardous Materials **42**(2): 201-212.

Cantrell, K. J., D. I. Kaplan and T. W. Wietsma (1995). "Zero-valent iron for the in situ remediation of selected metals in groundwater." Journal of Hazardous Materials **42**(2): 201-212.

Cao, B., B. Ahmed and H. Beyenal (2010). Immobilization of uranium in groundwater using biofilms. Emerging environmental technologies Volume II. V. Shah. New York, Springer: 1-37.

Cápiro, N. L., Y. Wang, J. K. Hatt, C. A. Lebrón, K. D. Pennell and F. E. Löffler (2014). "Distribution of Organohalide-Respiring Bacteria between Solid and Aqueous Phases." Environmental Science & Technology **48**(18): 10878-10887.

Caporaso, J. G., J. Kuczynski, J. Stombaugh, K. Bittinger, F. D. Bushman, E. K. Costello, N. Fierer, A. G. Pena, J. K. Goodrich, J. I. Gordon, G. A. Huttley, S. T. Kelley, D. Knights, J. E. Koenig, R. E. Ley, C. A. Lozupone, D. McDonald, B. D. Muegge, M. Pirrung, J. Reeder, J. R. Sevinsky, P. J. Turnbaugh, W. A. Walters, J. Widmann, T. Yatsunenko, J. Zaneveld and R. Knight (2010). "QIIME allows analysis of high-throughput community sequencing data." Nat Methods **7**(5): 335-336.

Celebi, O., C. Uzum, T. Shahwan, H. N. Erten (2007). "A radiotracer study of the adsorption behavior of aqueous Ba²⁺ ions on nanoparticles of zero-valent iron." J. Hazard. Mater. **148**(3): 761-767.

Chang, M. C. and H. Y. Kang (2009). "Remediation of pyrene-contaminated soil by synthesized nanoscale zero-valent iron particles." Journal of Environmental Science and Health, Part A **44**(6): 576-582.

Chatterjee, J. and S. K. Gupta (2009). "An Agglomeration-Based Model for Colloid Filtration." Environmental Science & Technology **43**(10): 3694.

Chen, J., Z. Xiu, G. V. Lowry and P. J. J. Alvarez (2011). "Effect of natural organic matter on toxicity and reactivity of nano-scale zero-valent iron." Water Research **45**(5): 1995-2001.

Chen, J. L., S. R. Al-Abed, J. A. Ryan and Z. B. Li (2001). "Effects of pH on dechlorination of trichloroethylene by zero-valent iron." J Hazard Mater **83**(3): 243-254.

Chen, P.-J., W.-L. Wu and K. C.-W. Wu (2013). "The zerovalent iron nanoparticle causes higher developmental toxicity than its oxidation products in early life stages of medaka fish." Water Research **47**(12): 3899-3909.

Cheng, I. F., R. Muftikian, Q. Fernando and N. Korte (1997). "Reduction of nitrate to ammonia by zero-valent iron." Chemosphere **35**(11): 2689-2695.

Chowdhury, A. I. A., D. M. O'Carroll, Y. Xu and B. E. Sleep (2012). "Electrophoresis enhanced transport of nano-scale zero valent iron." Advances in Water Resources **40**(0): 71-82.

Chuang, F. W., R. A. Larson and M. S. Wessman (1995). "Zero-valent iron-promoted dechlorination of polychlorinated-biphenyls." Environ Sci Technol **29**(9): 2460-2463.

CIDNews (2000). "E. coli O157:H7 outbreak in Walkerton, Ontario." Clinical Infectious Diseases **31**(2): i-iii.

Cirtiu, C. M., T. Raychoudhury, S. Ghoshal and A. Moores (2011). "Systematic comparison of the size, surface characteristics and colloidal stability of zero valent iron nanoparticles pre- and post-grafted with common polymers." Colloid Surface A **390**(1-3): 95-104.

Comba, S., D. Dalmazzo, E. Santagata and R. Sethi (2012). "Rheological characterization of xanthan suspensions of nanoscale iron for injection in porous media." Journal of Hazardous Materials **185**(2-3): 598-605.

Comba, S., A. Di Molfetta and R. Sethi (2011). "A comparison between field applications of nano-, micro-, and millimetric zero-valent iron for the remediation of contaminated aquifers." Water, Air, and Soil Pollution **215**(1-4): 595-607.

Comba, S. and R. Sethi (2009). "Stabilization of highly concentrated suspensions of iron nanoparticles using shear-thinning gels of xanthan gum." Water Research **43**(15): 3717-3726.

Comfort, S. D., M. Waria, S. Onanong, T. Satapanajaru, H. Boparai, C. Harris, D. D. Snow and D. A. Cassada (2009). "Field-Scale Cleanup of Atrazine and Cyanazine Contaminated Soil with a Combined Chemical-Biological Approach." Journal of Environmental Quality **38**(5): 1803-1811.

Cook, S. M. (2009). Assessing the Use and Application of Zero-Valent Iron Nanoparticle Technology for Remediation at Contaminated Sites. Washington, DC, Office of Solid Waste and Emergency Response; Office of Superfund Remediation and Technology Innovation.

Crane, R. A., M. Dickinson, I. C. Popescu and T. B. Scott (2011). "Magnetite and zero-valent iron nanoparticles for the remediation of uranium contaminated environmental water." Water Research **45**(9): 2931-2942.

Cullen, L. G., E. L. Tilston, G. R. Mitchell, C. D. Collins and L. J. Shaw (2011). "Assessing the impact of nano- and micro-scale zerovalent iron particles on soil microbial activities: Particle reactivity interferes with assay conditions and interpretation of genuine microbial effects." Chemosphere **82**(11): 1675-1682.

Cupples, A. M., A. M. Spormann and P. L. McCarty (2003). "Growth of a Dehalococcoides-Like Microorganism on Vinyl Chloride and cis-Dichloroethene as Electron Acceptors as Determined by Competitive PCR." Applied and Environmental Microbiology **69**(2): 953-959.

Danielsen, K. M. and K. F. Hayes (2004). "PH dependence of carbon tetrachloride reductive dechlorination by magnetite." Environmental Science & Technology **38**(18): 4745-4752.

Davis, R. E., E. Bromels and C. L. Kibby (1962). "Boron Hydrides. III. Hydrolysis of Sodium Borohydride in Aqueous Solution." Journal of the American Chemical Society **84**(6): 885-892.

DeSantis, T. Z., P. Hugenholtz, N. Larsen, M. Rojas, E. L. Brodie, K. Keller, T. Huber, D. Dalevi, P. Hu and G. L. Andersen (2006). "Greengenes, a chimera-checked 16S rRNA gene database and workbench compatible with ARB." Appl Environ Microbiol **72**(7): 5069-5072.

Diao, M. and M. Yao (2009). "Use of zero-valent iron nanoparticles in inactivating microbes." Water Research **43**(20): 5243-5251.

Dickinson, M. and T. B. Scott (2010). "The application of zero-valent iron nanoparticles for the remediation of a uranium-contaminated waste effluent." Journal of Hazardous Materials **178**(1-3): 171-179.

DiStefano, T. D., J. M. Gossett and S. H. Zinder (1991). "Reductive dechlorination of high concentrations of tetrachloroethene to ethene by an anaerobic enrichment culture in the absence of methanogenesis." Applied and Environmental Microbiology **57**(8): 2287-2292.

Dixon, P. (2003). "VEGAN, a package of R functions for community ecology." Journal of Vegetation Science **14**(6): 927-930.

Duhamel, M., K. Mo and E. A. Edwards (2004). "Characterization of a Highly Enriched Dehalococcoides-Containing Culture That Grows on Vinyl Chloride and Trichloroethene." Applied and Environmental Microbiology **70**(9): 5538-5545.

Dukhin, A. S., P. J. Goetz and S. Truesdail (2001). "Titration of concentrated dispersions using electroacoustic ζ -potential probe." Langmuir **17**(4): 964-968.

Dunphy Guzman, K. A., M. R. Taylor and J. F. Banfield (2006). "Environmental Risks of Nanotechnology: National Nanotechnology Initiative Funding, 2000-2004." Environmental Science & Technology **40**(5): 1401-1407.

Edgar, R. C. (2010). "Search and clustering orders of magnitude faster than BLAST." Bioinformatics **26**(19): 2460-2461.

Edwards, E. A. (2014). "Breathing the unbreathable." Science **346**(6208): 424-425.

Efecan, N., T. Shahwan, A. E. Eroglu and I. Lieberwirth (2009). "Characterization of the uptake of aqueous Ni²⁺ ions on nanoparticles of zero-valent iron (nZVI)." Desalination **249**(3): 1048-1054.

Einarson, M. (2005). Multilevel Ground-Water Monitoring. Practical Handbook of Environmental Site Characterization and Ground-Water Monitoring, Second Edition, CRC Press: 807-848.

El-Temsah, Y. S. and E. J. Joner (2012). "Ecotoxicological effects on earthworms of fresh and aged nano-sized zero-valent iron (nZVI) in soil." Chemosphere **89**(1): 76-82.

El-Temsah, Y. S. and E. J. Joner (2013). "Effects of nano-sized zero-valent iron (nZVI) on DDT degradation in soil and its toxicity to collembola and ostracods." Chemosphere **92**(1): 131-137.

Elliott, D. (2010). nZVI Field Application Case Studies in the U.S. USEPA Clu-In Webinar: Field scale Remediation Experience using Iron Nanoparticles and Evolving Risk-Benefit Understanding.

Elliott, D. W. and W.-x. Zhang (2001). "Field Assessment of Nanoscale Bimetallic Particles for Groundwater Treatment." Environmental Science & Technology **35**(24): 4922-4926.

Elsner, M., M. Chartrand, N. VanStone, G. Lacrampe Couloume and B. Sherwood Lollar (2008). Identifying Abiotic Chlorinated Ethene Degradation: Characteristic Isotope Patterns in Reaction Products with Nanoscale Zero-Valent Iron. **42**: 5963-5970.

Engelbrektsen, A., V. Kunin, K. C. Wrighton, N. Zvenigorodsky, F. Chen, H. Ochman and P. Hugenholtz (2010). "Experimental factors affecting PCR-based estimates of microbial species richness and evenness." ISME J **4**(5): 642-647.

EPA, U. S. (2008). EPA Fact Sheet: Nanotechnology for site remediation. S. W. a. E. Response. Washington DC, US.EPA. **EPA 542-F-08-009**.

Eykholt, G. R. and D. T. Davenport (1998). "Dechlorination of the Chloroacetanilide Herbicides Alachlor and Metolachlor by Iron Metal." Environmental Science & Technology **32**(10): 1482-1487.

Fagerlund, F., T. H. Illangasekare, T. Phenrat, H. J. Kim and G. V. Lowry (2012). "PCE dissolution and simultaneous dechlorination by nanoscale zero-valent iron particles in a DNAPL source zone." Journal of Contaminant Hydrology **131**(1-4): 9-28.

Fajardo, C., M. L. Saccà, M. Martinez-Gomariz, G. Costa, M. Nande and M. Martin (2013). "Transcriptional and proteomic stress responses of a soil bacterium *Bacillus cereus* to nanosized zero-valent iron (nZVI) particles." Chemosphere **93**(6): 1077-1083.

Farrell, J., M. Kason, N. Melitas and T. Li (2000). "Investigation of the long-term performance of zero-valent iron for reductive dechlorination of trichloroethylene." Environmental Science & Technology **34**(3): 514-521.

Fernandez-Sanchez, J. M., E. J. Sawvel and P. J. J. Alvarez (2004). "Effect of Fe⁰ quantity on the efficiency of integrated microbial-Fe⁰ treatment processes." Chemosphere **54**(7): 823-829.

Fetter, C. W. (2001). Applied Hydrogeology. Upper Saddle River, NJ, Prentice-Hall, Inc.

Fiedor, J. N., W. D. Bostick, R. J. Jarabek and J. Farrell (1998). "Understanding the mechanism of uranium removal from groundwater by zero-valent iron using X-ray photoelectron spectroscopy." Environmental Science & Technology **32**(10): 1466-1473.

Freedman, D. L. and J. M. Gossett (1989). "Biological reductive dechlorination of tetrachloroethylene and trichloroethylene to ethylene under methanogenic conditions." Applied and Environmental Microbiology **55**(9): 2144-2151.

Fruchter, J. S., C. R. Cole, M. D. Williams, V. R. Vermeul, J. E. Amonette, J. E. Szecsody, J. D. Istok and M. D. Humphrey (2000). "Creation of a subsurface permeable treatment zone for aqueous chromate contamination using in situ redox manipulation." Ground Water Monit R **20**(2): 66-77.

Gavaskar, A., Tatar L., Condit W., (2005). Contract Report: Cost and Performance Report: nanoscale zerovalent iron technologies for source remediation. Port Huenema, CA, NAVFAC: Naval Facilities Engineering Command. **CR-05-007-ENV**.

Gavaskar A., T. L., Condit W., (2005). Contract Report: Cost and Performance Report: nanoscale zerovalent iron technologies for source remediation. Port Huenema, CA, NAVFAC: Naval Facilities Engineering Command. **CR-05-007-ENV**.

Gerritse, J., V. Renard, T. M. Pedro Gomes, P. A. Lawson, M. D. Collins and J. C. Gottschal (1996). "Desulfitobacterium sp. strain PCE1, an anaerobic bacterium that can grow by reductive dechlorination of tetrachloroethene or ortho-chlorinated phenols." Archives of Microbiology **165**(2): 132-140.

Gillham, R., Vogan, J., Gui, L., Duchene, M., Son, J., (2010). Iron Barrier Walls for Chlorinated Solvent Remediation. In Situ Remediation of Chlorinated Solvent Plumes. H. F. Stroo, Ward, C.H.,. New York, Springer Science Media: 537-571.

Gillham, R. W. and S. F. O'Hannesin (1994). "Enhanced Degradation of Halogenated Aliphatics by Zero-Valent Iron." Ground Water **32**(6): 958-967.

Gillham, R. W. and S. F. Ohannesin (1994). "Enhanced degradation of halogenated aliphatics by zero valent iron." Ground Water **32**(6): 958-967.

Glavee, G. N., K. J. Klabunde, C. M. Sorensen and G. C. Hadjipanayis (1995). "Chemistry of Borohydride Reduction of Iron(Ii) and Iron(Iii) Ions in Aqueous and Nonaqueous Media - Formation of Nanoscale Fe, Fe₂, and Fe₂b Powders." Inorganic Chemistry **34**(1): 28-35.

Glazier, R., R. Venkatakrishnan, F. Gheorghiu, L. Walata, R. Nash and Z. Wei-xian (2003). "Nanotechnology Takes Root." Civil Engineering (08857024) **73**(5): 64.

Gould, J. P. (1982). "The Kinetics of Hexavalent Chromium Reduction by Metallic Iron." Water Research **16**(6): 871-877.

Grinstaff, M. W., M. B. Salamon and K. S. Suslick (1993). "Magnetic-Properties of Amorphous Iron." Physical Review B **48**(1): 269-273.

Grittini, C., M. Malcomson, Q. Fernando and N. Korte (1995). "Rapid dechlorination of polychlorinated biphenyls on the surface of a Pd/Fe bimetallic system." Environmental Science and Technology **29**(11): 2898-2900.

Groster, A. and E. A. Edwards (2009). "Characterization of a Dehalobacter Coculture That Dechlorinates 1,2-Dichloroethane to Ethene and Identification of the Putative Reductive Dehalogenase Gene." Applied and Environmental Microbiology **75**(9): 2684-2693.

Haas, B. J., D. Gevers, A. M. Earl, M. Feldgarden, D. V. Ward, G. Giannoukos, D. Ciulla, D. Tabbaa, S. K. Highlander, E. Sodergren, B. Methe, T. Z. DeSantis, C. Human Microbiome, J. F. Petrosino, R. Knight and B. W. Birren (2011). "Chimeric 16S rRNA sequence formation and detection in Sanger and 454-pyrosequenced PCR amplicons." Genome Res **21**(3): 494-504.

Harr, J. (1996). A Civil Action, Vintage Books.

- Haselow, J. S., R. L. Siegrist, M. Crimi and T. Jarosch (2003). "Estimating the total oxidant demand for in situ chemical oxidation design." Remediation Journal **13**(4): 5-16.
- He, F., M. Zhang, T. Qian and D. Zhao (2009). "Transport of carboxymethyl cellulose stabilized iron nanoparticles in porous media: Column experiments and modeling." Journal of Colloid and Interface Science **334**(1): 96-102.
- He, F. and D. Zhao (2005). "Preparation and Characterization of a New Class of Starch-Stabilized Bimetallic Nanoparticles for Degradation of Chlorinated Hydrocarbons in Water." Environmental Science & Technology **39**(9): 3314-3320.
- He, F. and D. Zhao (2007). "Manipulating the Size and Dispersibility of Zerovalent Iron Nanoparticles by Use of Carboxymethyl Cellulose Stabilizers." Environmental Science & Technology **41**(17): 6216-6221.
- He, F., D. Zhao, J. Liu and C. B. Roberts (2007). "Stabilization of Fe-Pd Nanoparticles with Sodium Carboxymethyl Cellulose for Enhanced Transport and Dechlorination of Trichloroethylene in Soil and Groundwater." Industrial & Engineering Chemical Research **46**(1): 29-34.
- He, F., D. Zhao and C. Paul (2010). "Field assessment of carboxymethyl cellulose stabilized iron nanoparticles for in situ destruction of chlorinated solvents in source zones." Water Research **44**(7): 2360-2370.
- He, F. and D. Y. Zhao (2008). "Hydrodechlorination of trichloroethene using stabilized Fe-Pd nanoparticles: Reaction mechanism and effects of stabilizers, catalysts and reaction conditions." Applied Catalysis B-Environmental **84**(3-4): 533-540.
- He, J., K. M. Ritalahti, M. R. Aiello and F. E. Löffler (2003). "Complete detoxification of vinyl chloride by an anaerobic enrichment culture and identification of the reductively dechlorinating population as a Dehalococcoides species." Applied and Environmental Microbiology **69**(2): 996-1003.
- He, J., K. M. Ritalahti, M. R. Aiello and F. E. Löffler (2003). "Complete Detoxification of Vinyl Chloride by an Anaerobic Enrichment Culture and Identification of the Reductively Dechlorinating Population as a Dehalococcoides Species." Applied and Environmental Microbiology **69**(2): 996-1003.
- Henderson, A. D. and A. H. Demond (2007). "Long-term performance of zero-valent iron permeable reactive barriers: A critical review." Environ Eng Sci **24**(4): 401-423.
- Henn, K. W. and D. W. Waddill (2006). "Utilization of Nanoscale Zero-Valent Iron for Source Remediation—A Case Study." Remediation: 57-76.
- Henn, K. W., Waddill, D.W. (2006). "Utilization of nanoscale zero-valent iron for source remediation - A case study." Remediation Journal **16**(2): 57-77.
- Higgins, M. R. and T. M. Olson (2009). "Life-cycle case study comparison of permeable reactive barrier versus pump-and-treat remediation." Environ Sci Technol **43**(24): 9432-9438.
- Hoch, L. B., E. J. Mack, B. W. Hydutsky, J. M. Hershman, J. M. Skluzacek and T. E. Mallouk (2008). "Carbothermal Synthesis of Carbon-supported Nanoscale Zero-valent Iron Particles for the Remediation of Hexavalent Chromium." Environmental Science & Technology **42**(7): 2600-2605.
- Hoerle, S., F. Mazaudier, P. Dillmann and G. Santarini (2004). "Advances in understanding atmospheric corrosion of iron. II. Mechanistic modelling of wet-dry cycles." Corrosion Science **46**(6): 1431-1465.
- Holliger, C., D. Hahn, H. Harmsen, W. Ludwig, W. Schumacher, B. Tindall, F. Vazquez, N. Weiss and A. J. B. Zehnder (1998). "Dehalobacter restrictus gen. nov. and sp. nov., a strictly

anaerobic bacterium that reductively dechlorinates tetra- and trichloroethene in an anaerobic respiration." Archives of Microbiology **169**(4): 313-321.

Hong, Y. S., R. J. Honda, N. V. Myung and S. L. Walker (2009). "Transport of Iron-Based Nanoparticles: Role of Magnetic Properties." Environmental Science & Technology **43**(23): 8834-8839.

Hood, E. D., D. W. Major, J. W. Quinn, W. S. Yoon, A. Gavaskar and E. A. Edwards (2008). "Demonstration of enhanced bioremediation in a TCE source area at Launch Complex 34, Cape Canaveral Air Force Station." Ground Water Monitoring and Remediation **28**(2): 98-107.

Hu, C. Y., S. L. Lo, Y. H. Liou, Y. W. Hsu, K. Shih and C. J. Lin (2010). "Hexavalent chromium removal from near natural water by copper-iron bimetallic particles." Water Research **44**(10): 3101-3108.

Huang, Q., X. Shi, R. A. Pinto, E. J. Petersen and W. J. Weber (2008). "Tunable Synthesis and Immobilization of Zero-Valent Iron Nanoparticles for Environmental Applications." Environmental Science & Technology **42**(23): 8884-8889.

Hug, L. A., F. Maphosa, D. Leys, F. E. Löffler, H. Smidt, E. A. Edwards and L. Adrian (2013). "Overview of organohalide-respiring bacteria and a proposal for a classification system for reductive dehalogenases." Philosophical Transactions of the Royal Society B: Biological Sciences **368**(1616).

Hundal, L. S., J. Singh, E. L. Bier, P. J. Shea, S. D. Comfort and W. L. Powers (1997). "Removal of TNT and RDX from water and soil using iron metal." Environmental Pollution **97**(1-2): 55-64.

Husain, M. M., J. A. Cherry, S. Fidler and S. K. Frape (1998). "On the long-term hydraulic gradient in the thick clayey aquitard in the Sarnia region, Ontario." Canadian Geotechnical Journal **35**(6): 986-1003.

Hwang, Y. H., D. G. Kim and H. S. Shin (2011). "Mechanism study of nitrate reduction by nano zero valent iron." Journal of Hazardous Materials **185**(2-3): 1513-1521.

Hydutsky, B. W., E. J. Mack, B. B. Beckerman, J. M. Skluzacek and T. E. Mallouk (2007). "Optimization of Nano- and Microiron Transport through Sand Columns Using Polyelectrolyte Mixtures." Environmental Science & Technology **41**(18): 6418-6424.

Isalou, M., B. E. Sleep and S. N. Liss (1998). "Biodegradation of high concentrations of tetrachloroethene in a continuous flow column system." Environmental Science and Technology **32**(22): 3579-3585.

ITRC, I. T. R. C. (2011). Integrated DNAPL Site Strategy. Washington, D.C, Interstate Technology & Regulatory Council, Integrated DNAPL Site Strategy Team.

Jacobs, J. A. and S. M. Testa (2005). Overview of chromium(VI) in the environment: Background and history. Chromium(VI) handbook. J. Guertin, J. A. Jacobs and C. P. Avakian. New York, CRC Press: 1-21.

Jegadeesan, G., K. Mondal, S. B. Lalvani (2005). "Arsenate remediation using nanosized modified zerovalent iron particles." Environ. Prog. **24**(3): 289-296.

Jeon, J.-R., K. Murugesan, I.-H. Nam and Y.-S. Chang (2013). "Coupling microbial catabolic actions with abiotic redox processes: A new recipe for persistent organic pollutant (POP) removal." Biotechnology Advances **31**(2): 246-256.

Jiang, C., Y. Liu, Z. Chen, M. Megharaj and R. Naidu (2013). "Impact of iron-based nanoparticles on microbial denitrification by *Paracoccus* sp. strain YF1." Aquatic Toxicology **142-143**(0): 329-335.

Johnson, R. L., G. O. Johnson, J. T. Nurmi and P. G. Tratnyek (2009). "Natural Organic Matter Enhanced Mobility of Nano Zerovalent Iron." Environmental Science & Technology **43**(14): 5455-5460.

Johnson, R. L., G. O. B. Johnson, J. T. Nurmi and P. G. Tratnyek (2009). "Natural Organic Matter Enhanced Mobility of Nano Zerovalent Iron." Environmental Science & Technology **43**(14): 5455-5460.

Johnson, R. L., J. T. Nurmi, G. S. O'Brien Johnson, D. Fan, R. L. O'Brien Johnson, Z. Shi, A. J. Salter-Blanc, P. G. Tratnyek and G. V. Lowry (2013). "Field-Scale Transport and Transformation of Carboxymethylcellulose-Stabilized Nano Zero-Valent Iron." Environmental Science & Technology **47**(3): 1573-1580.

Johnson, T. L., M. M. Scherer and P. G. Tratnyek (1996). "Kinetics of halogenated organic compound degradation by iron metal." Environ Sci Technol **30**(8): 2634-2640.

Johnson, T. L., M. M. Scherer and P. G. Tratnyek (1996). "Kinetics of Halogenated Organic Compound Degradation by Iron Metal." Environmental Science & Technology **30**(8): 2634-2640.

Jones, B. D. and J. D. Ingle Jr (2001). "Evaluation of immobilized redox indicators as reversible, in situ redox sensors for determining Fe(III)-reducing conditions in environmental samples." Talanta **55**(4): 699-714.

Jones, B. D. and J. D. Ingle Jr (2005). "Evaluation of redox indicators for determining sulfate-reducing and dechlorinating conditions." Water Research **39**(18): 4343-4354.

Joyce, R. A., D. R. Glaser, D. D. Werkema and E. A. Atekwana (2012). "Spectral induced polarization response to nanoparticles in a saturated sand matrix." Journal of Applied Geophysics **77**: 63-71.

Kadar, E., P. Rooks, C. Lakey and D. A. White (2012). "The effect of engineered iron nanoparticles on growth and metabolic status of marine microalgae cultures." Science of The Total Environment **439**(0): 8-17.

Kakani, S. L. and A. Kakani (2004). Material Science. New Delhi, New Age International Publishers.

Kanel, S., D. Nepal, B. Manning and H. Choi (2007). "Transport of surface-modified iron nanoparticles in porous media and application to arsenic(III) remediation." Journal of Nanoparticle Research **9**(5): 725-735.

Kanel, S. R., R. R. Goswami, T. P. Clement, M. O. Barnett and D. Zhao (2008). "Two Dimensional Transport Characteristics of Surface Stabilized Zero-valent Iron Nanoparticles in Porous Media." Environmental Science & Technology **42**(3): 896-900.

Kanel, S. R., J.-M. Grenèche and H. Choi (2006). "Arsenic(V) Removal from Groundwater Using Nano Scale Zero-Valent Iron as a Colloidal Reactive Barrier Material." Environmental Science & Technology **40**(6): 2045-2050.

Kanel, S. R., J.-M. Grenache and H. Choi (2006). "Arsenic(V) Removal from Groundwater Using Nano Scale Zero-Valent Iron as a Colloidal Reactive Barrier Material." Environmental Science & Technology **40**(6): 2045-2050.

Kanel, S. R., B. Manning, L. Charlet and H. Choi (2005). "Removal of Arsenic(III) from Groundwater by Nanoscale Zero-Valent Iron." Environmental Science & Technology **39**(5): 1291-1298.

Kang, S.-H. and W. Choi (2009). "Oxidative Degradation of Organic Compounds Using Zero-Valent Iron in the Presence of Natural Organic Matter Serving as an Electron Shuttle." Environmental Science & Technology **43**(3): 878-883.

Kaplan, D. I., K. J. Cantrell, T. W. Wietsma and M. A. Potter (1996). "Retention of Zero-Valent Iron Colloids by Sand Columns: Application to Chemical Barrier Formation." Journal of Environmental Quality **25**(5): 1086-1094.

Karabelli, D., Ç. Üzümlü, T. Shahwan, A. E. Eroğlu, T. B. Scott, K. R. Hallam and I. Lieberwirth (2008). "Batch removal of aqueous Cu^{2+} ions using nanoparticles of zero-valent iron: A study of the capacity and mechanism of uptake." Industrial & Engineering Chemistry Research **47**(14): 4758-4764.

Karn, B., Kuiken, T., Otto, M. (2009). "Nanotechnology and *in Situ* Remediation: A Review of the Benefits and Potential Risks." Environ Health Perspect **117**(12).

Karn, B., Kuiken, T., Otto, M. (2009). "Nanotechnology and *in Situ* Remediation: A Review of the Benefits and Potential Risks." Environ Health Perspect **117**(12): 1823-1831.

Keenan, C. R., R. Goth-Goldstein, D. Lucas and D. L. Sedlak (2009). "Oxidative Stress Induced by Zero-Valent Iron Nanoparticles and Fe(II) in Human Bronchial Epithelial Cells." Environmental Science & Technology **43**(12): 4555-4560.

Keller, A. A., K. Garner, R. J. Miller and H. S. Lenihan (2012). "Toxicity of Nano-Zero Valent Iron to Freshwater and Marine Organisms." PLoS ONE **7**(8): e43983.

Kim, H. J., T. Phenrat, R. D. Tilton and G. V. Lowry (2009). "Fe-0 Nanoparticles Remain Mobile in Porous Media after Aging Due to Slow Desorption of Polymeric Surface Modifiers." Environmental Science & Technology **43**(10): 3824-3830.

Kim, H. S., J. Y. Ahn, K. Y. Hwang, I. K. Kim and I. Hwang (2010). "Atmospherically Stable Nanoscale Zero-Valent Iron Particles Formed under Controlled Air Contact: Characteristics and Reactivity." Environmental Science & Technology **44**(5): 1760-1766.

Kim, H. S., W. H. Kang, M. Kim, J. Y. Park and I. Hwang (2008). "Comparison of hematite/Fe(II) systems with cement/Fe(II) systems in reductively dechlorinating trichloroethylene." Chemosphere **73**(5): 813-819.

Kirschling, T. L., P. L. Golas, J. M. Unrine, K. Matyjaszewski, K. B. Gregory, G. V. Lowry and R. D. Tilton (2011). "Microbial Bioavailability of Covalently Bound Polymer Coatings on Model Engineered Nanomaterials." Environmental Science & Technology **45**(12): 5253-5259.

Kirschling, T. L., K. B. Gregory, E. G. Minkley, G. V. Lowry and R. D. Tilton (2010). "Impact of Nanoscale Zero Valent Iron on Geochemistry and Microbial Populations in Trichloroethylene Contaminated Aquifer Materials." Environmental Science & Technology **44**(9): 3474-3480.

Kirschling, T. L., K. B. Gregory, J. E. G. Minkley, G. V. Lowry and R. D. Tilton (2010). "Impact of Nanoscale Zero Valent Iron on Geochemistry and Microbial Populations in Trichloroethylene Contaminated Aquifer Materials." Environmental Science & Technology **44**(9): 3474-3480.

Köber, R., H. Hollert, G. Hornbruch, M. Jekel, A. Kamptner, N. Klaas, H. Maes, K. M. Mangold, E. Martac, A. Matheis, H. Paar, A. Schäffer, H. Schell, A. Schiwy, K. R. Schmidt, T. J. Strutz, S. Thümmel, A. Tiehm and J. Braun (2014). "Nanoscale zero-valent iron flakes for groundwater treatment." Environmental Earth Sciences **72**(9): 3339-3352.

Kocur, C. M., A. I. Chowdhury, N. Sakulchaicharoen, H. K. Boparai, K. P. Weber, P. Sharma, M. M. Krol, L. Austrins, C. Peace, B. E. Sleep and D. M. O'Carroll (2014). "Characterization of nZVI Mobility in a Field Scale Test." Environmental Science & Technology **48**(5): 2862-2869.

Kocur, C. M., D. M. O'Carroll and B. E. Sleep (2013). "Impact of nZVI stability on mobility in porous media." Journal of Contaminant Hydrology **145**(0): 17-25.

- Kolb, S. and A. Stacheter (2013). "Prerequisites for amplicon pyrosequencing of microbial methanol utilizers in the environment." Frontiers in Microbiology **4**(SEP).
- Korte, N. E. and Q. Fernando (1991). "A Review of Arsenic(III) in Groundwater." Critical Reviews in Environmental Control **21**(1): 1-39.
- Krajmalnik-Brown, R., T. Hölscher, I. N. Thomson, F. M. Saunders, K. M. Ritalahti and F. E. Löffler (2004). "Genetic Identification of a Putative Vinyl Chloride Reductase in *Dehalococcoides* sp. Strain BAV1." Applied and Environmental Microbiology **70**(10): 6347-6351.
- Kram, M. L. (2005). Dnapi Characterization Methods and Approaches. Practical Handbook of Environmental Site Characterization and Ground-Water Monitoring, Second Edition, CRC Press: 473-515.
- Kretzschmar, R., W. P. Robarge and A. Amoozegar (1995). "Influence of natural organic matter on colloid transport through saprolite." Water Resources Research **31**(3): 435-445.
- Krol, M. M., A. J. Oleniuk, C. M. Kocur, B. E. Sleep, P. Bennett, X. Zhong and D. M. O'Carroll (2013). "A Field-Validated Model for In Situ Transport of Polymer-Stabilized nZVI and Implications for Subsurface Injection." Environmental Science & Technology **47**(13): 7332-7340.
- Krug, T., O'Hara, S., Watling, M., Quinn, J., (2010). Final Report: Emulsified Zero-Valent Nano-Scale Iron Treatment of Chlorinated
- Solvent DNAPL Source Areas ESTCP Project ER-0431, Environmental Security Technology Certification Program.
- Krug, T., O'Hara, S., Watling, M., Quinn, J., (2010). Emulsified Zero-Valent Nano-scale Iron Treatment of Chlorinated Solvent NAPL Source Zones, Geosyntec Consultants.
- Krumholz, L. R., J. P. McKinley, G. A. Ulrich and J. M. Suflita (1997). "Confined subsurface microbial communities in Cretaceous rock." Nature **386**(6620): 64-66.
- Krzmarzick, M. J., B. B. Crary, J. J. Harding, O. O. Oyerinde, A. C. Leri, S. C. B. Myneni and P. J. Novak (2012). "Natural Niche for Organohalide-Respiring Chloroflexi." Applied and Environmental Microbiology **78**(2): 393-401.
- Kueper, B. H. (2014). Chlorinated Solvent Source Zone Remediation, Springer.
- Lampron, K. J., P. C. Chiu and D. K. Cha (1998). "Biological reduction of trichloroethene supported by Fe(0)." Bioremediation Journal **2**(3-4): 175-181.
- Lampron, K. J., P. C. Chiu and D. K. Cha (2001). "Reductive Dehalogenation of Chlorinated Ethenes with Elemental Iron: The Role of Microorganisms." Water Research **35**(13): 3077-3084.
- Langevin, C. D. and W. Guo (2006). "MODFLOW/MT3DMS-based simulation of variable-density ground water flow and transport." Ground Water **44**(3): 339-351.
- Laumann, S., V. Micić, G. V. Lowry and T. Hofmann (2013). "Carbonate minerals in porous media decrease mobility of polyacrylic acid modified zero-valent iron nanoparticles used for groundwater remediation." Environmental Pollution **179**(0): 53-60.
- Lecoanet, H. F., J.-Y. Bottero and M. R. Wiesner (2004). "Laboratory Assessment of the Mobility of Nanomaterials in Porous Media." Environmental Science & Technology **38**(19): 5164-5169.
- Lee, C., J. Y. Kim, W. I. Lee, K. L. Nelson, J. Yoon and D. L. Sedlak (2008). "Bactericidal Effect of Zero-Valent Iron Nanoparticles on *Escherichia coli*." Environmental Science & Technology **42**(13): 4927-4933.

Lee, M., E. Wells, Y. K. Wong, J. Koenig, L. Adrian, H. H. Richnow and M. Manefield (2015). "Relative Contributions of Dehalobacter and Zerovalent Iron in the Degradation of Chlorinated Methanes." Environmental Science & Technology **49**(7): 4481-4489.

Lee, S., X. Bi, R. B. Reed, J. F. Ranville, P. Herckes and P. Westerhoff (2014). "Nanoparticle Size Detection Limits by Single Particle ICP-MS for 40 Elements." Environmental Science & Technology **48**(17): 10291-10300.

Li, H., Q. Zhou, Y. Wu, J. Fu, T. Wang and G. Jiang (2009). "Effects of waterborne nano-iron on medaka (*Oryzias latipes*): Antioxidant enzymatic activity, lipid peroxidation and histopathology." Ecotoxicology and Environmental Safety **72**(3): 684-692.

Li, L., M. Fan, R. C. Brown, J. Van Leeuwen, J. Wang, W. Wang, Y. Song and P. Zhang (2006). "Synthesis, Properties, and Environmental Applications of Nanoscale Iron-Based Materials: A Review." Critical Reviews in Environmental Science and Technology **36**(5): 405 - 431.

Li, T. and J. Farrell (2000). "Reductive dechlorination of trichloroethene and carbon tetrachloride using iron and palladized-iron cathodes." Environmental Science & Technology **34**(1): 173-179.

Li, X.-q. and W.-x. Zhang (2007). "Sequestration of metal cations with zerovalent iron nanoparticles - A study with high resolution X-ray photoelectron spectroscopy (HR-XPS)." Journal of Physical Chemistry C **111**(19): 6939-6946.

Li, X. Q., J. S. Cao and W. X. Zhang (2008). "Stoichiometry of Cr(VI) immobilization using nanoscale zerovalent iron (nZVI): A study with high-resolution X-ray photoelectron Spectroscopy (HR-XPS)." Industrial & Engineering Chemistry Research **47**(7): 2131-2139.

Li, X. q., Elliot, D.W., Zhang, W.x. (2006). "Zero-Valent Iron Nanoparticles for Abatement of Environmental Pollutants: Materials and Engineering Aspects." Critical Reviews in Environmental Science and Technology **31**: 111-122.

Li, X. Q. and W. X. Zhang (2007). "Sequestration of metal cations with zerovalent iron nanoparticles - A study with high resolution X-ray photoelectron spectroscopy (HR-XPS)." Journal of Physical Chemistry C **111**(19): 6939-6946.

Li, Y., Y. Wang, K. D. Pennell and L. M. Abriola (2008). "Investigation of the Transport and Deposition of Fullerene (C60) Nanoparticles in Quartz Sands under Varying Flow Conditions." Environmental Science & Technology **42**(19): 7174-7180.

Li, Z. Q., K. Greden, P. J. J. Alvarez, K. B. Gregory and G. V. Lowry (2010). "Adsorbed Polymer and NOM Limits Adhesion and Toxicity of Nano Scale Zerovalent Iron to E. coli." Environmental Science & Technology **44**(9): 3462-3467.

Liang, L., N. Korte, J. D. Goodlaxson, J. Clausen, Q. Fernando and R. Muftikian (1997). "Byproduct Formation During the Reduction of TCE by Zero-Valence Iron and Palladized Iron." Ground Water Monitoring & Remediation **17**(1): 122-127.

Lien, H.-L. and W.-x. Zhang (1999). "Transformation of Chlorinated Methanes by Nanoscale Iron Particles." Journal of Environmental Engineering **125**(11): 1042-1047.

Lien, H.-L. and W.-x. Zhang (2001). "Nanoscale iron particles for complete reduction of chlorinated ethenes." Colloids and Surfaces A: Physicochemical and Engineering Aspects **191**(1-2): 97-105.

Lien, H.-L. and W. Zhang (2004). "Effect of palladium on the reductive dechlorination of chlorinated ethylenes with nanoscale Pd/Fe particles." Water Science and Technology: Water Supply **4**(5-6): 297-303.

Lien, H. L., Y. S. Jhuo and L. H. Chen (2007). "Effect of heavy metals on dechlorination of carbon tetrachloride by iron nanoparticles." Environmental Engineering Science **24**(1): 21-30.

- Lien, H. L. and R. T. Wilkin (2005). "High-level arsenite removal from groundwater by zero-valent iron." Chemosphere **59**(3): 377-386.
- Lien, H. L. and W. X. Zhang (2001). "Nanoscale iron particles for complete reduction of chlorinated ethenes." Colloids and Surfaces a-Physicochemical and Engineering Aspects **191**(1-2): 97-105.
- Lien, H. L. and W. X. Zhang (2005). "Hydrodechlorination of chlorinated ethanes by nanoscale Pd/Fe bimetallic particles." Journal of Environmental Engineering-Asce **131**(1): 4-10.
- Lien, H. L. and W. X. Zhang (2007). "Nanoscale Pd/Fe bimetallic particles: Catalytic effects of palladium on hydrodechlorination." Applied Catalysis B-Environmental **77**(1-2): 110-116.
- Lim, T. T. and B. W. Zhu (2008). "Effects of anions on the kinetics and reactivity of nanoscale Pd/Fe in trichlorobenzene dechlorination." Chemosphere **73**(9): 1471-1477.
- Liu, C. C., D. H. Tseng and C. Y. Wang (2006). "Effects of ferrous ions on the reductive dechlorination of trichloroethylene by zero-valent iron." Journal of Hazardous Materials **136**(3): 706-713.
- Liu, P., W. Cai, Z. Li, H. Zeng and J. Hu (2010). "Optical Study of the Reduction of Hexavalent Chromium by Iron-Based Nanoparticles." Journal of Nanoscience and Nanotechnology **10**(8): 5389-5392.
- Liu, Q. Y., Y. L. Bei and F. Zhou (2009). "Removal of lead(II) from aqueous solution with amino-functionalized nanoscale zero-valent iron." Cent. Eur. J. Chem. **7**(1): 79-82.
- Liu, X., D. M. O'Carroll, E. J. Petersen, Q. Huang and C. L. Anderson (2009). "Mobility of Multiwalled Carbon Nanotubes in Porous Media." Environmental Science & Technology **43**(21): 8153-8158.
- Liu, Y., H. Choi, D. Dionysiou and G. V. Lowry (2005). "Trichloroethene Hydrodechlorination in Water by Highly Disordered Monometallic Nanoiron." Chemistry of Materials **17**(21): 5315-5322.
- Liu, Y., S. Li, Z. Chen, M. Megharaj and R. Naidu (2014). "Influence of zero-valent iron nanoparticles on nitrate removal by *Paracoccus* sp." Chemosphere **108**(0): 426-432.
- Liu, Y. and G. V. Lowry (2006). "Effect of Particle Age (Fe₀ Content) and Solution pH On NZVI Reactivity: H₂ Evolution and TCE Dechlorination." Environmental Science & Technology **40**(19): 6085-6090.
- Liu, Y., S. A. Majetich, R. D. Tilton, D. S. Sholl and G. V. Lowry (2005). "TCE Dechlorination Rates, Pathways, and Efficiency of Nanoscale Iron Particles with Different Properties." Environmental Science & Technology **39**(5): 1338-1345.
- Liu, Y., T. Phenrat and G. V. Lowry (2007). "Effect of TCE Concentration and Dissolved Groundwater Solutes on NZVI-Promoted TCE Dechlorination and H₂ Evolution." Environmental Science & Technology **41**(22): 7881-7887.
- Liu, Z. G. and F. S. Zhang (2010). "Nano-zerovalent iron contained porous carbons developed from waste biomass for the adsorption and dechlorination of PCBs." Bioresource Technology **101**(7): 2562-2564.
- Löffler, F. E., J. Yan, K. M. Ritalahti, L. Adrian, E. A. Edwards, K. T. Konstantinidis, J. A. Müller, H. Fullerton, S. H. Zinder and A. M. Spormann (2013). "Dehalococcoides mccartyi gen. nov., sp. nov., obligately organohalide-respiring anaerobic bacteria relevant to halogen cycling and bioremediation, belong to a novel bacterial class, Dehalococcoidia classis nov., order Dehalococcoidales ord. nov. and family Dehalococcoidaceae fam. nov., within the phylum Chloroflexi." International Journal of Systematic and Evolutionary Microbiology **63**(Pt 2): 625-635.

- Logan, B. E., D. G. Jewett, R. G. Arnold, E. J. Bouwer and C. R. O'Melia (1995). "Clarification of clean-bed filtration models." Journal of Environmental Engineering **121**(12): 869-873.
- Lowry, G. V., E. M. Hotze, E. S. Bernhardt, D. D. Dionysiou, J. A. Pedersen, M. R. Wiesner and B. S. Xing (2010). "Environmental Occurrences, Behavior, Fate, and Ecological Effects of Nanomaterials: An Introduction to the Special Series." Journal of Environmental Quality **39**(6): 1867-1874.
- Lowry, G. V. and M. Reinhard (1999). "Hydrodehalogenation of 1-to 3-carbon halogenated organic compounds in water using a palladium catalyst and hydrogen gas." Environ Sci Technol **33**(11): 1905-1910.
- Lowry, G. V. and M. Reinhard (2000). "Pd-catalyzed TCE dechlorination in groundwater: Solute effects, biological control, and oxidative catalyst regeneration." Environ Sci Technol **34**(15): 3217-3223.
- Luijten, M. L. G. C., J. de Weert, H. Smidt, H. T. S. Boschker, W. M. de Vos, G. Schraa and A. J. M. Stams (2003). "Description of *Sulfurospirillum halorespirans* sp. nov., an anaerobic, tetrachloroethene-respiring bacterium, and transfer of *Dehalospirillum multivorans* to the genus *Sulfurospirillum* as *Sulfurospirillum multivorans* comb. nov." International Journal of Systematic and Evolutionary Microbiology **53**(3): 787-793.
- Luna, M., F. Gastone, T. Tosco, R. Sethi, M. Velimirovic, J. Gemoets, R. Muysshondt, H. Sapon, N. Klaas and L. Bastiaens (2015). "Pressure-controlled injection of guar gum stabilized microscale zerovalent iron for groundwater remediation." Journal of Contaminant Hydrology.
- Mace, C. (2006). "Controlling Groundwater VOCs: do nanoscale ZVI particles have any advantages over microscale ZVI of BNP." Pollution Engineering **38**(4): 24-28.
- Makeig, K. S., Nielsen, D.M., (2005). Regulatory Mandates for Ground-Water Monitoring. Practical Handbook of Environmental Site Characterization and Ground-Water Monitoring, Second Edition, CRC Press: 1-34.
- Man, Z. and Z. Dongye (2013). In Situ Dechlorination in Soil and Groundwater Using Stabilized Zero-Valent Iron Nanoparticles: Some Field Experience on Effectiveness and Limitations. Novel Solutions to Water Pollution, American Chemical Society. **1123**: 79-96.
- Manchester, M. J., L. A. Hug, M. Zarek, A. Zila and E. A. Edwards (2012). "Discovery of a trans-Dichloroethene-Respiring Dehalogenimonas Species in the 1,1,2,2-Tetrachloroethane-Dechlorinating WBC-2 Consortium." Applied and Environmental Microbiology **78**(15): 5280-5287.
- Manning, B. A., J. R. Kiser, H. Kwon and S. R. Kanel (2007). "Spectroscopic investigation of Cr(III)- and Cr(VI)-treated nanoscale zerovalent iron." Environmental Science & Technology **41**(2): 586-592.
- Mao, X., J. Wang, A. Ciblak, E. E. Cox, C. Riis, M. Terkelsen, D. B. Gent and A. N. Alshawabkeh (2012). "Electrokinetic-enhanced bioaugmentation for remediation of chlorinated solvents contaminated clay." Journal of Hazardous Materials **213-214**(0): 311-317.
- Marsalek, B., D. Jancula, E. Marsalkova, M. Mashlan, K. Safarova, J. Tucek and R. Zboril (2012). "Multimodal action and selective toxicity of zerovalent iron nanoparticles against cyanobacteria." Environmental Science and Technology **46**(4): 2316-2323.
- Martel, K. E., R. Martel, R. Lefebvre and P. J. Gélinas (1998). "Laboratory Study of Polymer Solutions Used for Mobility Control During In Situ NAPL Recovery." Ground Water Monitoring & Remediation **18**(3): 103-113.

Martin, T. D., Brockhoff, C.A., Creed, J.T. (1994). Determination of metals and trace elements in water and wastes by inductively coupled plasma - atomic emission spectrometry Cincinnati, OH, U.S EPA National Exposure Research Laboratory: 58.

Matheson, L. J. and P. G. Tratnyek (1994). "Reductive dehalogenation of chlorinated methanes by iron metal." Environmental Science and Technology **28**(12): 2045-2045.

Matheson, L. J. and P. G. Tratnyek (1994). "Reductive Dehalogenation of Chlorinated Methanes by Iron Metal." Environmental Science & Technology **28**(12): 2045-2053.

Mattes, T. E., A. K. Alexander and N. V. Coleman (2010). "Aerobic biodegradation of the chloroethenes: Pathways, enzymes, ecology, and evolution." FEMS Microbiology Reviews **34**(4): 445-475.

Maymó-Gatell, X., Y.-t. Chien, J. M. Gossett and S. H. Zinder (1997). "Isolation of a Bacterium That Reductively Dechlorinates Tetrachloroethene to Ethene." Science **276**(5318): 1568-1571.

Maymó-Gatell, X., I. Nijenhuis and S. H. Zinder (2000). "Reductive Dechlorination of cis-1,2-Dichloroethene and Vinyl Chloride by "Dehalococcoides ethenogenes"." Environmental Science & Technology **35**(3): 516-521.

Moe, W. M., J. Yan, M. F. Nobre, M. S. da Costa and F. A. Rainey (2009). "Dehalogenimonas lykanthroporepellens gen. nov., sp. nov., a reductively dehalogenating bacterium isolated from chlorinated solvent-contaminated groundwater." International Journal of Systematic and Evolutionary Microbiology **59**(11): 2692-2697.

Mondal, K., G. Jegadeesan and S. B. Lalvani (2004). "Removal of selenate by Fe and NiFe nanosized particles." Industrial & Engineering Chemistry Research **43**(16): 4922-4934.

Moraci, N. and P. S. Calabro (2010). "Heavy metals removal and hydraulic performance in zero-valent iron/pumice permeable reactive barriers." Journal of Environmental Management **91**(11): 2336-2341.

Morrill, P. L., B. E. Sleep, D. J. Seepersad, M. L. McMaster, E. D. Hood, C. LeBron, D. W. Major, E. A. Edwards and B. Sherwood Lollar (2009). "Variations in expression of carbon isotope fractionation of chlorinated ethenes during biologically enhanced PCE dissolution close to a source zone." Journal of Contaminant Hydrology **110**(1-2): 60-71.

Mueller, N. C., J. Braun, J. Bruns, M. Cernik, P. Rissing, D. Rickerby and B. Nowack (2012). "Application of nanoscale zero valent iron (NZVI) for groundwater remediation in Europe." Environmental Science and Pollution Research **19**(2): 550-558.

Muftikian, R., K. Nebesny, Q. Fernando and N. Korte (1996). "X-ray photoelectron spectra of the palladium - Iron bimetallic surface used for the rapid dechlorination of chlorinated organic environmental contaminants." Environmental Science and Technology **30**(12): 3593-3596.

Mulligan, C. N., R. N. Yong and B. F. Gibbs (2001). "Remediation technologies for metal-contaminated soils and groundwater: an evaluation." Engineering Geology **60**(1-4): 193-207.

Murdoch, L. and W. Slack (2002). "Forms of Hydraulic Fractures in Shallow Fine-Grained Formations." Journal of Geotechnical and Geoenvironmental Engineering **128**(6): 479-487.

Nelson, K. E. and T. R. Ginn (2011). "New collector efficiency equation for colloid filtration in both natural and engineered flow conditions." Water Resources Research **47**.

Němeček, J., O. Lhotský and T. Cajthaml (2014). "Nanoscale zero-valent iron application for in situ reduction of hexavalent chromium and its effects on indigenous microorganism populations." Science of The Total Environment **485-486**(0): 739-747.

Nikolaidis, N. P., G. M. Dobbs and J. A. Lackovic (2003). "Arsenic removal by zero-valent iron: field, laboratory and modeling studies." Water Research **37**(6): 1417-1425.

Nowlan, L. (2007). Out of Sight, Out of Mind? Taking Canada's Groundwater for Granted. Eau Canada: The Future of Canada's Water. K. Bakker, UBC Press: 4.

NSF (2004). Contaminants in the Subsurface: Source Zone Assessment and Remediation. Washington, DC, National Academies Press.

Nurmi, J. T., P. G. Tratnyek, V. Sarathy, D. R. Baer, J. E. Amonette, K. Pecher, C. Wang, J. C. Linehan, D. W. Matson, R. L. Penn and M. D. Driessen (2005). "Characterization and Properties of Metallic Iron Nanoparticles: Spectroscopy, Electrochemistry, and Kinetics." Environmental Science & Technology **39**(5): 1221-1230.

Nurmi, J. T., P. G. Tratnyek, V. Sarathy, D. R. Baer, J. E. Amonette, K. Pecher, C. M. Wang, J. C. Linehan, D. W. Matson, R. L. Penn and M. D. Driessen (2005). "Characterization and properties of metallic iron nanoparticles: Spectroscopy, electrochemistry, and kinetics." Environmental Science and Technology **39**(5): 1221-1230.

O'Carroll, D., B. Sleep, M. Krol, H. Boparai and C. Kocur (2013). "Nanoscale zero valent iron and bimetallic particles for contaminated site remediation." Advances in Water Resources **51**: 104-122.

O'Connor, H. D. R. (2002). Report of the Walkerton Inquiry.

O'Hara, S., T. Krug, J. Quinn, C. Clausen and C. Geiger (2006). "Field and laboratory evaluation of the treatment of DNAPL source zones using emulsified zero-valent iron." Remediation Journal **16**(2): 35-56.

Oksanen, J., F. Blanchet and R. Kindt (2013). "Vegan: community ecology package. 2013." R package version: 2.0-7.

Olegario, J. T., N. Yee, M. Miller, J. Sczepaniak and B. Manning (2010). "Reduction of Se(VI) to Se(-II) by zerovalent iron nanoparticle suspensions." Journal of Nanoparticle Research **12**(6): 2057-2068.

Oostrom, M., T. W. Wietsma, M. A. Covert and V. R. Vermeul (2007). "Zero-valent iron emplacement in permeable porous media using polymer additions." Ground Water Monitoring and Remediation **27**(1): 122-130.

Orth, W. S. and R. W. Gillham (1995). "Dechlorination of Trichloroethene in Aqueous Solution Using Fe⁰." Environmental Science & Technology **30**(1): 66-71.

Orth, W. S. and R. W. Gillham (1996). "Dechlorination of trichloroethene in aqueous solution using Fe-O." Environmental Science & Technology **30**(1): 66-71.

Otto, M. (2010). Use of Nanoscale Zero-Valent Iron for Site Remediation. Field scale Remediation Experience using Iron Nanoparticles and Evolving Risk-Benefit Understanding, Webinar, Clu.In

PARS_Environmental (2003). Pilot Test Final Report: Bimetalic Nanoscale Particle of Groundwater at Area 1. **1**.

Pawlett, M., K. Ritz, R. A. Dorey, S. Rocks, J. Ramsden and J. A. Harris (2013). "The impact of zero-valent iron nanoparticles upon soil microbial communities is context dependent." Environmental Science and Pollution Research International **20**(2): 1041-1049.

Pennell, K. D., M. Jin, L. M. Abriola and G. A. Pope (1994). "Surfactant enhanced remediation of soil columns contaminated by residual tetrachloroethylene." Journal of Contaminant Hydrology **16**(1): 35-53.

Petosa, A. R., D. P. Jaisi, I. R. Quevedo, M. Elimelech and N. Tufenkji (2010). "Aggregation and Deposition of Engineered Nanomaterials in Aquatic Environments: Role of Physicochemical Interactions." Environmental Science & Technology **44**(17): 6532-6549.

Phenrat, T., A. Cihan, H.-J. Kim, M. Mital, T. Illangasekare and G. V. Lowry (2010). "Transport and Deposition of Polymer-Modified Fe⁰ Nanoparticles in 2-D Heterogeneous

Porous Media: Effects of Particle Concentration, Fe⁰ Content, and Coatings." Environmental Science & Technology **44**(23): 9086-9093.

Phenrat, T., F. Fagerlund, T. Illangasekare, G. V. Lowry and R. D. Tilton (2011). "Polymer-Modified Fe⁰ Nanoparticles Target Entrapped NAPL in Two Dimensional Porous Media: Effect of Particle Concentration, NAPL Saturation, and Injection Strategy." Environmental Science & Technology **45**(14): 6102-6109.

Phenrat, T., H.-J. Kim, F. Fagerlund, T. Illangasekare, R. D. Tilton and G. V. Lowry (2009). "Particle Size Distribution, Concentration, and Magnetic Attraction Affect Transport of Polymer-Modified Fe⁰ Nanoparticles in Sand Columns." Environmental Science & Technology **43**(13): 5079-5085.

Phenrat, T., H. J. Kim, F. Fagerlund, T. Illangasekare and G. V. Lowry (2010). "Empirical correlations to estimate agglomerate size and deposition during injection of a polyelectrolyte-modified Fe-0 nanoparticle at high particle concentration in saturated sand." Journal of Contaminant Hydrology **118**(3-4): 152-164.

Phenrat, T., H. J. Kim, F. Fagerlund, T. Illangasekare, R. D. Tilton and G. V. Lowry (2009). "Particle Size Distribution, Concentration, and Magnetic Attraction Affect Transport of Polymer-Modified Fe-0 Nanoparticles in Sand Columns." Environmental Science & Technology **43**(13): 5079-5085.

Phenrat, T., Y. Liu, R. D. Tilton and G. V. Lowry (2009). "Adsorbed Polyelectrolyte Coatings Decrease Fe⁰ Nanoparticle Reactivity with TCE in Water: Conceptual Model and Mechanisms." Environmental Science & Technology **43**(5): 1507-1514.

Phenrat, T., T. C. Long, G. V. Lowry and B. Veronesi (2009). "Partial Oxidation ("Aging") and Surface Modification Decrease the Toxicity of Nanosized Zerovalent Iron." Environmental Science & Technology **43**(1): 195-200.

Phenrat, T., N. Saleh, K. Sirk, H.-J. Kim, R. Tilton and G. Lowry (2008). "Stabilization of aqueous nanoscale zerovalent iron dispersions by anionic polyelectrolytes: adsorbed anionic polyelectrolyte layer properties and their effect on aggregation and sedimentation." Journal of Nanoparticle Research **10**(5): 795-814.

Phenrat, T., N. Saleh, K. Sirk, R. D. Tilton and G. V. Lowry (2007). "Aggregation and Sedimentation of Aqueous Nanoscale Zerovalent Iron Dispersions." Environmental Science & Technology **41**(1): 284-290.

Phillips, D. H., T. Van Nooten, L. Bastiaens, M. I. Russell, K. Dickson, S. Plant, J. M. E. Ahad, T. Newton, T. Elliot and R. M. Kalin (2010). "Ten Year Performance Evaluation of a Field-Scale Zero-Valent Iron Permeable Reactive Barrier Installed to Remediate Trichloroethene Contaminated Groundwater." Environmental Science & Technology **44**(10): 3861-3869.

Pilloni, G., M. S. Granitsiotis, M. Engel and T. Lueders (2012). "Testing the Limits of 454 Pyrotag Sequencing: Reproducibility, Quantitative Assessment and Comparison to T-RFLP Fingerprinting of Aquifer Microbes." PLoS ONE **7**(7): e40467.

Pinder, G. F., Celia, M.A. (2006). Subsurface Hydrology. Hoboken, NJ, John Wiley & Sons, Inc.

Ponder, S. M., J. G. Darab, J. Bucher, D. Caulder, I. Craig, L. Davis, N. Edelstein, W. Lukens, H. Nitsche, L. Rao, D. K. Shuh and T. E. Mallouk (2001). "Surface Chemistry and Electrochemistry of Supported Zerovalent Iron Nanoparticles in the Remediation of Aqueous Metal Contaminants." Chemistry of Materials **13**(2): 479-486.

Ponder, S. M., J. G. Darab and T. E. Mallouk (2000). "Remediation of Cr(VI) and Pb(II) Aqueous Solutions Using Supported, Nanoscale Zero-valent Iron." Environmental Science & Technology **34**(12): 2564-2569.

Preslo, L. M., Nielsen, G.L., Nielsen, D.M., (2005). Environmental Site Characterization. Practical Handbook of Environmental Site Characterization and Ground-Water Monitoring, Second Edition, CRC Press: 35-205.

Puls, R. W. and M. J. Barcelona (1996). Ground water issue: Low-flow (minimal drawdown) ground-water sampling procedures. Other Information: DN: See also PB--95-269643; PBD: Apr 1996; Medium: P; Size: 14 p.

Quinn, J., C. Geiger, C. Clausen, K. Brooks, C. Coon, S. O'Hara, T. Krug, D. Major, W.-S. Yoon, A. Gavaskar and T. Holdsworth (2005). "Field Demonstration of DNAPL Dehalogenation Using Emulsified Zero-Valent Iron." Environmental Science & Technology **39**(5): 1309-1318.

Ramos-Padron, E., S. Bordenave, S. Lin, I. M. Bhaskar, X. Dong, C. W. Sensen, J. Fournier, G. Voordouw and L. M. Gieg (2011). "Carbon and sulfur cycling by microbial communities in a gypsum-treated oil sands tailings pond." Environ Sci Technol **45**(2): 439-446.

Ramos, M. A. V., W. Yan, X. Q. Li, B. E. Koel and W. X. Zhang (2009). "Simultaneous oxidation and reduction of arsenic by zero-valent iron nanoparticles: Understanding the significance of the core-shell structure." Journal of Physical Chemistry C **113**(33): 14591-14594.

Ramsburg, C. A. and K. D. Pennell (2002). "Density-modified displacement for DNAPL source zone remediation: Density conversion and recovery in heterogeneous aquifer cells." Environ Sci Technol **36**(14): 3176-3187.

Raychoudhury, T., G. Naja and S. Ghoshal (2010). "Assessment of transport of two polyelectrolyte-stabilized zero-valent iron nanoparticles in porous media." Journal of Contaminant Hydrology **118**(3-4): 143-151.

Raychoudhury, T., G. Naja and S. Ghoshal (2011). "Assessment of transport of two polyelectrolyte-stabilized zero-valent iron nanoparticles in porous media." Journal of Contaminant Hydrology **118**(3-4): 143-151.

Raychoudhury, T., N. Tufenkji and S. Ghoshal (2012). "Aggregation and deposition kinetics of carboxymethyl cellulose-modified zero-valent iron nanoparticles in porous media." Water Research **46**(6): 1735-1744.

Raychoudhury, T., N. Tufenkji and S. Ghoshal (2014). "Straining of polyelectrolyte-stabilized nanoscale zero valent iron particles during transport through granular porous media." Water Research **50**(0): 80-89.

Reinsch, B. C., B. Forsberg, R. L. Penn, C. S. Kim and G. V. Lowry (2010). "Chemical Transformations during Aging of Zerovalent Iron Nanoparticles in the Presence of Common Groundwater Dissolved Constituents." Environmental Science & Technology **44**(9): 3455-3461.

Riba, O., T. B. Scott, K. V. Ragnarsdottir and G. C. Allen (2008). "Reaction mechanism of uranyl in the presence of zero-valent iron nanoparticles." Geochimica Et Cosmochimica Acta **72**(16): 4047-4057.

Ritalahti, K. M., B. K. Amos, Y. Sung, Q. Wu, S. S. Koenigsberg and F. E. Löffler (2006). "Quantitative PCR targeting 16S rRNA and reductive dehalogenase genes simultaneously monitors multiple Dehalococcoides strains." Applied and Environmental Microbiology **72**(4): 2765-2774.

Rivero-Huguet, M. and W. D. Marshall (2009). "Reduction of hexavalent chromium mediated by micro- and nano-sized mixed metallic particles." J Hazard Mater **169**(1-3): 1081-1087.

Rivero-Huguet, M. and W. D. Marshall (2009). "Reduction of hexavalent chromium mediated by micro- and nano-sized mixed metallic particles." Journal of Hazardous Materials **169**(1-3): 1081-1087.

Rivero-Huguet, M. and W. D. Marshall (2009). "Reduction of hexavalent chromium mediated by micron- and nano-scale zero-valent metallic particles." J Environ Monit **11**(5): 1072-1079.

Roberts, A. L., L. A. Totten, W. A. Arnold, D. R. Burris and T. J. Campbell (1996). "Reductive elimination of chlorinated ethylenes by zero valent metals." Environmental Science & Technology **30**(8): 2654-2659.

Rosenthal, H., L. Adrian and M. Steiof (2004). "Dechlorination of PCE in the presence of Fe⁰ enhanced by a mixed culture containing two Dehalococcoides strains." Chemosphere **55**(5): 661-669.

Rosicka, D. and J. Sembera (2011). "Assessment of Influence of Magnetic Forces on Aggregation of Zero-valent Iron Nanoparticles." Nanoscale Res Lett **6**(1): 10.

Ryan, J. N. and M. Elimelech (1996). "Colloid mobilization and transport in groundwater." Colloids and Surfaces A: Physicochemical and Engineering Aspects **107**: 1-56.

Saccà, M. L., C. Fajardo, G. Costa, C. Lobo, M. Nande and M. Martin (2014). "Integrating classical and molecular approaches to evaluate the impact of nanosized zero-valent iron (nZVI) on soil organisms." Chemosphere **104**(0): 184-189.

Sakulchaicharn, N., D. M. O'Carroll and J. E. Herrera (2010). "Enhanced stability and dechlorination activity of pre-synthesis stabilized nanoscale FePd particles." Journal of Contaminant Hydrology **118**(3-4): 117-127.

Sale, T. C. and D. B. McWhorter (2001). "Steady state mass transfer from single-component dense nonaqueous phase liquids in uniform flow fields." Water Resour Res **37**(2): 393-404.

Saleh, N., H.-J. Kim, T. Phenrat, K. Matyjaszewski, R. D. Tilton and G. V. Lowry (2008). "Ionic Strength and Composition Affect the Mobility of Surface-Modified Fe⁰ Nanoparticles in Water-Saturated Sand Columns." Environmental Science & Technology **42**(9): 3349-3355.

Saleh, N., T. Phenrat, K. Sirk, B. Dufour, J. Ok, T. Sarbu, K. Matyjaszewski, R. D. Tilton and G. V. Lowry (2005). "Adsorbed Triblock Copolymers Deliver Reactive Iron Nanoparticles to the Oil/Water Interface." Nano Letters **5**(12): 2489-2494.

Saleh, N., K. Sirk, Y. Liu, T. Phenrat, B. Dufour, K. Matyjaszewski, R. D. Tilton and G. V. Lowry (2007). "Surface Modifications Enhance Nanoiron Transport and NAPL Targeting in Saturated Porous Media." Environmental Engineering Science **24**(1): 45-57.

Sarathy, V., A. J. Salter, J. T. Nurmi, G. O. Johnson, R. L. Johnson and P. G. Tratnyek (2010). "Degradation of 1,2,3-Trichloropropane (TCP): Hydrolysis, Elimination, and Reduction by Iron and Zinc." Environmental Science & Technology **44**(2): 787-793.

Sarathy, V., P. G. Tratnyek, J. T. Nurmi, D. R. Baer, J. E. Amonette, C. L. Chun, R. L. Penn and E. J. Reardon (2008). "Aging of Iron Nanoparticles in Aqueous Solution: Effects on Structure and Reactivity." The Journal of Physical Chemistry C **112**(7): 2286-2293.

Satapanajaru, T., P. Anurakpongsatorn, P. Pengthamkeerati and H. Boparai (2008). "Remediation of atrazine-contaminated soil and water by nano zerovalent iron." Water, Air and Soil Pollution **192**(1-4): 349-359.

Satapanajaru, T., P. Anurakpongsatorn, A. Songsasen, H. Boparai and J. Park (2006). "Using low-cost iron byproducts from automotive manufacturing to remediate DDT." Water Air and Soil Pollution **175**(1-4): 361-374.

Sayles, G. D., G. R. You, M. X. Wang and M. J. Kupferle (1997). "DDT, DDD, and DDE dechlorination by zero-valent iron." Environmental Science & Technology **31**(12): 3448-3454.

Scheinost, A. C., R. Kirsch, D. Banerjee, A. Fernandez-Martinez, H. Zaenker, H. Funke and L. Charlet (2008). "X-ray absorption and photoelectron spectroscopy investigation of selenite reduction by Fe(II)-bearing minerals." Journal of Contaminant Hydrology **102**(3-4): 228-245.

Schlesinger, H. I., H. C. Brown, A. E. Finholt, J. R. Gilbreath, H. R. Hoekstra and E. K. Hyde (1953). "Sodium Borohydride, Its Hydrolysis and its Use as a Reducing Agent and in the Generation of Hydrogen1." Journal of the American Chemical Society **75**(1): 215-219.

Schrack, B., J. L. Blough, A. D. Jones and T. E. Mallouk (2002). "Hydrodechlorination of trichloroethylene to hydrocarbons using bimetallic nickel-iron nanoparticles." Chemistry of Materials **14**(12): 5140-5147.

Schrack, B., B. W. Hydutsky, J. L. Blough and T. E. Mallouk (2004). "Delivery Vehicles for Zerovalent Metal Nanoparticles in Soil and Groundwater." Chemistry of Materials **16**(11): 2187-2193.

Senzaki, T. and Y. Kumagai (1988). "Removal of chlorinated organic compounds from waterwater by reduction process: Treatment of 1,1,2,2-tetrachloroethane with iron powder." Kogyo Yosui **357**: 2-7.

Senzaki, T. and Y. Kumagai (1989). "Removal of chlorinated organic compounds from waterwater by reduction process: Treatment of trichloroethylene with iron powder." Kogyo Yosui **369**: 19-25.

Sevcu, Alena, Y. S. El-Temsah, E. J. Joner and M. Cernik (2011). "Oxidative Stress Induced in Microorganisms by Zero-valent Iron Nanoparticles." Microbes and Environments **26**(4): 271-281.

She, H. Y. and B. E. Sleep (1999). "Removal of perchloroethylene from a layered soil system by steam flushing." Ground Water Monit Remed **19**(2): 70-77.

Shi, Z., D. Fan, R. L. Johnson, P. G. Tratnyek, J. T. Nurmi, Y. Wu and K. H. Williams (2015). "Methods for Characterizing the Fate and Effects of Nano Zerovalent Iron during Groundwater Remediation." Journal of Contaminant Hydrology(0).

Shi, Z., J. T. Nurmi and P. G. Tratnyek (2011). "Effects of Nano Zero-Valent Iron on Oxidation Reduction Potential." Environmental Science & Technology **45**(4): 1586-1592.

Shi, Z. Q., J. T. Nurmi and P. G. Tratnyek (2011). "Effects of Nano Zero-Valent Iron on Oxidation-Reduction Potential." Environmental Science & Technology **45**(4): 1586-1592.

Shin, K.-H. and D. K. Cha (2008). "Microbial reduction of nitrate in the presence of nanoscale zero-valent iron." Chemosphere **72**(2): 257-262.

Shrubsole, D., Draper, D. (2007). On Guard for Thee? Water (Ab)uses and Management in Canada Eau Canada: The Future of Canada's Water. K. Bakker, UBC Press: 3.

Signorini, L., L. Pasquini, L. Savini, R. Carboni, F. Boscherini, E. Bonetti, A. Giglia, M. Pedio, N. Mahne and S. Nannarone (2003). "Size-dependent oxidation in iron/iron oxide core-shell nanoparticles." Physical Review B **68**(19).

Simonet, B. M. and M. Valcarcel (2009). "Monitoring nanoparticles in the environment." Analytical and Bioanalytical Chemistry **393**(1): 17-21.

Slater, L. and A. Binley (2003). "Evaluation of permeable reactive barrier (PRB) integrity using electrical imaging methods." GEOPHYSICS **68**(3): 911-921.

Slater, L. D., J. Choi and Y. Wu (2005). "Electrical properties of iron-sand columns: Implications for induced polarization investigation and performance monitoring of iron-wall barriers." Geophysics **70**(4): G87-G94.

Sohn, K., S. W. Kang, S. Ahn, M. Woo and S. K. Yang (2006). "Fe(0) nanoparticles for nitrate reduction: Stability, reactivity, and transformation." Environmental Science & Technology **40**(17): 5514-5519.

Song, H. and E. R. Carraway (2005). "Reduction of chlorinated ethanes by nanosized zero-valent iron: Kinetics, pathways, and effects of reaction conditions." Environmental Science & Technology **39**(16): 6237-6245.

Song, H. and E. R. Carraway (2005). "Reduction of Chlorinated Ethanes by Nanosized Zero-Valent Iron: Kinetics, Pathways, and Effects of Reaction Conditions." Environmental Science & Technology **39**(16): 6237-6245.

Song, H. and E. R. Carraway (2006). "Reduction of chlorinated methanes by nano-sized zero-valent iron. Kinetics, pathways, and effect of reaction conditions." Environmental Engineering Science **23**(2): 272-284.

Song, H. and E. R. Carraway (2008). "Catalytic hydrodechlorination of chlorinated ethenes by nanoscale zero-valent iron." Applied Catalysis B: Environmental **78**(1–2): 53-60.

Soundar, S. and T. S. Chandra (1987). "Cellulose degradation by a mixed bacterial culture." Journal of Industrial Microbiology **2**(5): 257-265.

Stookey, L. L. (1970). "Ferrozine - A New Spectrophotometric Reagent for Iron." Analytical Chemistry **42**(7).

Su, C. and R. W. Puls (1999). "Kinetics of trichloroethene reduction by zerovalent iron and tin: Pretreatment effect, apparent activation energy, and intermediate products." Environmental Science and Technology **33**(1): 163-168.

Su, C., R. W. Puls, T. A. Krug, M. T. Watling, S. K. O'Hara, J. W. Quinn and N. E. Ruiz (2012). "A two and half-year-performance evaluation of a field test on treatment of source zone tetrachloroethene and its chlorinated daughter products using emulsified zero valent iron nanoparticles." Water Research **46**(16): 5071-5084.

Su, C. M. and R. W. Puls (2001). "Arsenate and arsenite removal by zerovalent iron: Kinetics, redox transformation, and implications for in situ groundwater remediation." Environmental Science & Technology **35**(7): 1487-1492.

Su, Y., A. S. Adeleye, X. Zhou, C. Dai, W. Zhang, A. A. Keller and Y. Zhang (2014). "Effects of nitrate on the treatment of lead contaminated groundwater by nanoscale zerovalent iron." Journal of Hazardous Materials **280**: 504-513.

Sun, J., S. Wang, D. Zhao, F. H. Hun, L. Weng and H. Liu (2011). "Cytotoxicity, permeability, and inflammation of metal oxide nanoparticles in human cardiac microvascular endothelial cells: Cytotoxicity, permeability, and inflammation of metal oxide nanoparticles." Cell Biology and Toxicology **27**(5): 333-342.

Sun, Q., A. J. Feitz, J. Guan and T. D. Waite (2008). "Comparison of the reactivity of nanosized zero-valent iron (nZVI) particles produced by borohydride and dithionite reduction of iron salts." Nano **3**(5): 341-349.

Sun, Y.-P., X.-q. Li, J. Cao, W.-x. Zhang and H. P. Wang (2006). "Characterization of zero-valent iron nanoparticles." Advances in Colloid and Interface Science **120**(1-3): 47-56.

Sun, Y.-P., X.-Q. Li, W.-X. Zhang and H. P. Wang (2007). "A method for the preparation of stable dispersion of zero-valent iron nanoparticles." Colloids and Surfaces A: Physicochemical and Engineering Aspects **308**(1-3): 60-66.

Sun, Y. P., X. Q. Li, J. S. Cao, W. X. Zhang and H. P. Wang (2006). "Characterization of zero-valent iron nanoparticles." Advances in Colloid and Interface Science **120**(1-3): 47-56.

Sun, Y. P., X. Q. Li, W. X. Zhang and H. P. Wang (2007). "A method for the preparation of stable dispersion of zero-valent iron nanoparticles." Colloids and Surfaces a-Physicochemical and Engineering Aspects **308**(1-3): 60-66.

Sung, Y., K. E. Fletcher, K. M. Ritalahti, R. P. Apkarian, N. Ramos-Hernández, R. A. Sanford, N. M. Mesbah and F. E. Löffler (2006). "Geobacter lovleyi sp. nov. Strain SZ, a

Novel Metal-Reducing and Tetrachloroethene-Dechlorinating Bacterium." Applied and Environmental Microbiology **72**(4): 2775-2782.

Sung, Y., K. M. Ritalahti, R. P. Apkarian and F. E. Löffler (2006). "Quantitative PCR confirms purity of strain GT, a novel trichloroethene-to- ethene-respiring Dehalococcoides isolate." Applied and Environmental Microbiology **72**(3): 1980-1987.

Sweeney, K. H. and J. R. Fischer (1972). Reductive Degradation of Halogenated Pesticides. U. S. Patent. **3,640,821**.

Szecsody, J. E., J. S. Fruchter, M. D. Williams, V. R. Vermeul and D. Sklarew (2004). "In situ chemical reduction of aquifer sediments: Enhancement of reactive iron phases and TCE dechlorination." Environmental Science and Technology **38**(17): 4656-4663.

Taghavy, A., J. Costanza, K. D. Pennell and L. M. Abriola (2010). "Effectiveness of nanoscale zero-valent iron for treatment of a PCE-DNAPL source zone." J Contam Hydrol **118**(3-4): 128-142.

Taghavy, A., J. Costanza, K. D. Pennell and L. M. Abriola (2010). "Effectiveness of nanoscale zero-valent iron for treatment of a PCE-DNAPL source zone." Journal of Contaminant Hydrology **118**(3-4): 128-142.

Tamara, M. L. and E. C. Butler (2004). "Effects of Iron Purity and Groundwater Characteristics on Rates and Products in the Degradation of Carbon Tetrachloride by Iron Metal." Environmental Science and Technology **38**(6): 1866-1876.

Tee, Y. H., E. Grulke and D. Bhattacharyya (2005). "Role of Ni/Fe nanoparticle composition on the degradation of trichloroethylene from water." Industrial & Engineering Chemistry Research **44**(18): 7062-7070.

Tilston, E. L., C. D. Collins, G. R. Mitchell, J. Princiville and L. J. Shaw (2013). "Nanoscale zerovalent iron alters soil bacterial community structure and inhibits chloroaromatic biodegradation potential in Aroclor 1242-contaminated soil." Environmental Pollution **173**(0): 38-46.

Tiraferrri, A., K. L. Chen, R. Sethi and M. Elimelech (2008). "Reduced aggregation and sedimentation of zero-valent iron nanoparticles in the presence of guar gum." Journal of Colloid and Interface Science **324**(1-2): 71-79.

Tiraferrri, A. and R. Sethi (2009). "Enhanced transport of zerovalent iron nanoparticles in saturated porous media by guar gum." Journal of Nanoparticle Research **11**(3): 635-645.

Tosco, T. and R. Sethi (2010). "Transport of Non-Newtonian Suspensions of Highly Concentrated Micro- And Nanoscale Iron Particles in Porous Media: A Modeling Approach." Environmental Science & Technology **44**(23): 9062-9068.

Tratnyek, P. G. (1996). "Putting corrosion to use: Remediating contaminated groundwater with zero-valent metals." Chemistry and Industry (London)(13): 499.

Tratnyek, P. G., Johnson R.L., Lowry, G.V., Brown, R.A. (2014). In Situ Chemical Reduction for Source Remediation, Springer.

Tratnyek, P. G. and R. L. Johnson (2006). "Nanotechnologies for environmental cleanup." Nano Today **1**(2): 44-48.

Tratnyek, P. G., T. Reilkoff, A. Lemon, M. Scherer, B. Balko, L. Feik and B. Henegar (2001). "Visualizing Redox Chemistry: Probing Environmental Oxidation–Reduction Reactions with Indicator Dyes." The Chemical Educator **6**(3): 172-179.

Truex, M. J., T. W. Macbeth, V. R. Vermeul, B. G. Fritz, D. P. Mendoza, R. D. Mackley, T. W. Wietsma, G. Sandberg, T. Powell, J. Powers, E. Pitre, M. Michalsen, S. J. Ballock-Dixon, L. Zhong and M. Oostrom (2011). "Demonstration of Combined Zero-Valent Iron and Electrical Resistance Heating for In Situ Trichloroethene Remediation." Environmental Science & Technology **45**(12): 5346-5351.

Truex, M. J., V. R. Vermeul, D. P. Mendoza, B. G. Fritz, R. D. Mackley, M. Oostrom, T. W. Wietsma and T. W. Macbeth (2011). "Injection of Zero-Valent Iron into an Unconfined Aquifer Using Shear-Thinning Fluids." Ground Water Monitoring and Remediation **31**(1): 50-58.

Tufenkji, N. and M. Elimelech (2004). "Correlation Equation for Predicting Single-Collector Efficiency in Physicochemical Filtration in Saturated Porous Media." Environmental Science & Technology **38**(2): 529-536.

Uegami, M., J. Kawano, T. Okita, Y. Fujii, K. Okinaka, K. Kakuyua and S. Yatagai (2003). Iron particles for purifying contaminated soil or ground water. Process for producing the iron particles, purifying agent comprising the iron particles, process for producing the purifying agent and method of purifying contaminated soil or ground water. Toda Kogyo Corp., U.S. Patent Application 2003/0217974 A1.

USEPA (2000). Solidification/stabilization use at superfund sites, United States Environmental Protection Agency, Cincinnati, OH. EPA-542-R-00-010.
http://www.epa.gov/tio/download/remed/ss_sfund.pdf.

Üzü, Ç., T. Shahwan, A. E. Eroğlu, I. Lieberwirth, T. B. Scott and K. R. Hallam (2008). "Application of zero-valent iron nanoparticles for the removal of aqueous Co^{2+} ions under various experimental conditions." Chemical Engineering Journal **144**(2): 213-220.

Uzum, C., T. Shahwan, A. E. Eroglu, K. R. Hallam, T. B. Scott, I. Lieberwirth (2009). "Synthesis and characterization of kaolinite-supported zero-valent iron nanoparticles and their application for the removal of aqueous Cu^{2+} and Co^{2+} ions." Appl. Clay Sci. **43**(2): 172-181.

Varadhi, S. N., Gill, H., Apoldo, L.J., Blackman, R.A., Wittman, W.K., (2005). Full-scale Nanoiron Injection for Treatment of Groundwater Contaminated with Chlorinated Hydrocarbons. Natural Gas Technologies Conf. Orlando. FLA.

Vecchia, E. D., M. Luna and R. Sethi (2009). "Transport in Porous Media of Highly Concentrated Iron Micro- and Nanoparticles in the Presence of Xanthan Gum." Environmental Science & Technology.

Velimirovic, M., T. Tosco, M. Uyttebroek, M. Luna, F. Gastone, C. De Boer, N. Klaas, H. Sapon, H. Eisenmann, P.-O. Larsson, J. Braun, R. Sethi and L. Bastiaens (2014). "Field assessment of guar gum stabilized microscale zerovalent iron particles for in-situ remediation of 1,1,1-trichloroethane." Journal of Contaminant Hydrology **164**(0): 88-99.

Viollier, E., P. W. Inglett, K. Hunter, A. N. Roychoudhury and P. Van Cappellen (2000). "The ferrozine method revisited: Fe(II)/Fe(III) determination in natural waters." Applied Geochemistry **15**(6): 785-790.

Wai, C. M., H. K. Yak, B. W. Wenclawiak, I. F. Cheng and J. G. Doyle (1999). "Reductive dechlorination of polychlorinated biphenyls by zerovalent iron in subcritical water." Environmental Science & Technology **33**(8): 1307-1310.

Waller, A. S., R. Krajmalnik-Brown, F. E. Löffler and E. A. Edwards (2005). "Multiple reductive-dehalogenase-homologous genes are simultaneously transcribed during dechlorination by Dehalococcoides-containing cultures." Appl Environ Microbiol **71**(12): 8257-8264.

Waller, A. S., R. Krajmalnik-Brown, F. E. Löffler and E. A. Edwards (2005). "Multiple Reductive-Dehalogenase-Homologous Genes Are Simultaneously Transcribed during Dechlorination by Dehalococcoides-Containing Cultures." Applied and Environmental Microbiology **71**(12): 8257-8264.

Wang, C.-B. and W.-x. Zhang (1997). "Synthesizing Nanoscale Iron Particles for Rapid and Complete Dechlorination of TCE and PCBs." Environmental Science & Technology **31**(7): 2154-2156.

Wang, Q., G. M. Garrity, J. M. Tiedje and J. R. Cole (2007). "Naive Bayesian classifier for rapid assignment of rRNA sequences into the new bacterial taxonomy." Appl Environ Microbiol **73**(16): 5261-5267.

Wang, Q., S. Lee and H. Choi (2010). "Aging study on the structure of Fe(0)-nanoparticles: Stabilization, characterization, and reactivity." J Phys Chem C **114**(5): 2027-2033.

Wang, W., M. Zhou, Z. Jin and T. Li (2010). "Reactivity characteristics of poly(methyl methacrylate) coated nanoscale iron particles for trichloroethylene remediation." Journal of Hazardous Materials **173**(1-3): 724-730.

Wang, Y., D. Zhou, Y. Wang, X. Zhu and S. Jin (2011). "Humic acid and metal ions accelerating the dechlorination of 4-chlorobiphenyl by nanoscale zero-valent iron." Journal of Environmental Sciences **23**(8): 1286-1292.

Weathers, L. J., G. F. Parkin and P. J. Alvarez (1997). "Utilization of Cathodic Hydrogen as Electron Donor for Chloroform Cometabolism by a Mixed, Methanogenic Culture." Environmental Science & Technology **31**(3): 880-885.

Wei, Y. T., S. C. Wu, C. M. Chou, C. H. Che, S. M. Tsai and H. L. Lien (2010). "Influence of nanoscale zero-valent iron on geochemical properties of groundwater and vinyl chloride degradation: A field case study." Water Research **44**(1): 131-140.

Wiesner, M. R., G. V. Lowry, P. Alvarez, D. Dionysiou and P. Biswas (2006). "Assessing the Risks of Manufactured Nanomaterials." Environmental Science & Technology **40**(14): 4336-4345.

Wilkin, R. T., C. M. Su, R. G. Ford and C. J. Paul (2005). "Chromium-removal processes during groundwater remediation by a zerovalent iron permeable reactive barrier." Environmental Science & Technology **39**(12): 4599-4605.

Wilson, J. T. and X. Lu (2007). Relationship between Dehalococcoides DNA in groundwater and natural attenuation of chlorinated solvents. Battelle Press - 9th International In Situ and On-Site Bioremediation Symposium 2007.

Wright, E. S., L. S. Yilmaz and D. R. Noguera (2012). "DECIPHER, a search-based approach to chimera identification for 16S rRNA sequences." Appl Environ Microbiol **78**(3): 717-725.

Wu, Y., L. Slater, R. Versteeg and D. LaBrecque (2008). "A comparison of the low frequency electrical signatures of iron oxide versus calcite precipitation in granular zero valent iron columns." Journal of Contaminant Hydrology **95**(3-4): 154-167.

Wu, Y., L. D. Slater and N. Korte (2005). "Effect of precipitation on low frequency electrical properties of zerovalent iron columns." Environmental Science and Technology **39**(23): 9197-9204.

Wu, Y., L. D. Slaters and N. Korte (2006). "Low frequency electrical properties of corroded iron barrier cores." Environmental Science and Technology **40**(7): 2254-2261.

Wu, Y., R. Versteeg, L. Slater and D. LaBrecque (2009). "Calcite precipitation dominates the electrical signatures of zero valent iron columns under simulated field conditions." Journal of Contaminant Hydrology **106**(3-4): 131-143.

Xi, Y. F., M. Mallavarapu and R. Naidu (2010). "Reduction and adsorption of Pb²⁺ in aqueous solution by nano-zero-valent iron-A SEM, TEM and XPS study." Materials Research Bulletin **45**(10): 1361-1367.

Xiu, Z.-m., K. B. Gregory, G. V. Lowry and P. J. J. Alvarez (2010). "Effect of Bare and Coated Nanoscale Zerovalent Iron on tceA and vcrA Gene Expression in Dehalococcoides spp." Environmental Science & Technology **44**(19): 7647-7651.

Xiu, Z.-m., Z.-h. Jin, T.-l. Li, S. Mahendra, G. V. Lowry and P. J. J. Alvarez (2010). "Effects of nano-scale zero-valent iron particles on a mixed culture dechlorinating trichloroethylene." Bioresource Technology **101**(4): 1141-1146.

Xiu, Z. M., K. B. Gregory, G. V. Lowry and P. J. J. Alvarez (2010). "Effect of bare and coated nanoscale zerovalent iron on tceA and vcrA gene expression in Dehalococcoides spp." Environmental Science and Technology **44**(19): 7647-7651.

Xiu, Z. m., Z. h. Jin, T. l. Li, S. Mahendra, G. V. Lowry and P. J. J. Alvarez (2010). "Effects of nano-scale zero-valent iron particles on a mixed culture dechlorinating trichloroethylene." Bioresource Technology **101**(4): 1141-1146.

Xu, J., A. Dozier and D. Bhattacharyya (2005). "Synthesis of nanoscale bimetallic particles in polyelectrolyte membrane matrix for reductive transformation of halogenated organic compounds." Journal of Nanoparticle Research **7**(4-5): 449-467.

Yan, S., B. Hua, Z. Y. Bao, J. Yang, C. X. Liu and B. L. Deng (2010). "Uranium(VI) Removal by Nanoscale Zerovalent Iron in Anoxic Batch Systems." Environ Sci Technol **44**(20): 7783-7789.

Yan, W., A. A. Herzing, C. J. Kiely and W.-x. Zhang (2010). "Nanoscale zero-valent iron (nZVI): Aspects of the core-shell structure and reactions with inorganic species in water." Journal of Contaminant Hydrology **118**(3-4): 96-104.

Yan, W., A. A. Herzing, X. Q. Li, C. J. Kiely and W. X. Zhang (2010). "Structural evolution of Pd-doped nanoscale zero-valent iron (nZVI) in aqueous media and implications for particle aging and reactivity." Environmental Science and Technology **44**(11): 4288-4294.

Yan, W., H.-L. Lien, B. E. Koel and W.-x. Zhang (2013). "Iron nanoparticles for environmental clean-up: recent developments and future outlook." Environmental Science: Processes & Impacts **15**(1): 63-77.

Yan, W. L., A. A. Herzing, C. J. Kiely and W. X. Zhang (2010). "Nanoscale zero-valent iron (nZVI): Aspects of the core-shell structure and reactions with inorganic species in water." Journal of Contaminant Hydrology **118**(3-4): 96-104.

Yan, W. L., M. A. V. Ramos, B. E. Koel and W. X. Zhang (2010). "Multi-tiered distributions of arsenic in iron nanoparticles: Observation of dual redox functionality enabled by a core-shell structure." Chemical Communications **46**(37): 6995-6997.

Yang, Y., J. Guo and Z. Hu (2013). "Impact of nano zero valent iron (NZVI) on methanogenic activity and population dynamics in anaerobic digestion." Water Research **47**(17): 6790-6800.

Yao, K.-M., M. T. Habibian and C. R. O'Melia (1971). "Water and waste water filtration. Concepts and applications." Environmental Science & Technology **5**(11): 1105-1112.

Yoo, B. Y., S. C. Hernandez, B. Koo, Y. Rheem and N. V. Myung (2007). "Electrochemically fabricated zero-valent iron, iron-nickel, and iron-palladium nanowires for environmental remediation applications." Water Science and Technology **55**(1-2): 149-156

544.

Young, G. K., H. R. Bungay, L. M. Brown and W. A. Parsons (1964). "Chemical Reduction of Nitrate in Water." Journal Water Pollution Control Federation **36**(3): 395-398.

Yu, Z. B., M. H. Qiao, H. X. Li and J. F. Deng (1997). "Preparation of amorphous Ni-Co-B alloys and the effect of cobalt on their hydrogenation activity." Applied Catalysis A: General **163**(1-2): 1-13.

Zhan, J., T. Zheng, G. Piringer, C. Day, G. L. McPherson, Y. Lu, K. Papadopoulos and V. T. John (2008). "Transport Characteristics of Nanoscale Functional Zerovalent Iron/Silica Composites for in Situ Remediation of Trichloroethylene." Environmental Science & Technology **42**(23): 8871-8876.

Zhan, J. J., I. Kolesnichenko, B. Sunkara, J. B. He, G. L. McPherson, G. Piringer and V. T. John (2011). "Multifunctional Iron-Carbon Nanocomposites through an Aerosol-Based Process for the In Situ Remediation of Chlorinated Hydrocarbons." Environmental Science & Technology **45**(5): 1949-1954.

Zhan, J. J., B. Sunkara, L. Le, V. T. John, J. B. He, G. L. McPherson, G. Piringer and Y. F. Lu (2009). "Multifunctional colloidal particles for in situ remediation of chlorinated hydrocarbons." Environ Sci Technol **43**(22): 8616-8621.

Zhang, L. and A. Manthiram (1997). "Chains composed of nanosize metal particles and identifying the factors driving their formation." Applied Physics Letters **70**(18): 2469-2471.

Zhang, W.-x. (2003). "Nanoscale Iron Particles for Environmental Remediation: An Overview." Journal of Nanoparticle Research **5**(3): 323-332.

Zheng, T. H., J. J. Zhan, J. B. He, C. Day, Y. F. Lu, G. L. Mcpherson, G. Piringer and V. T. John (2008). "Reactivity characteristics of nanoscale zerovalent iron-silica composites for trichloroethylene remediation." Environmental Science & Technology **42**(12): 4494-4499.

Zhong, L., M. Oostrom, T. W. Wietsma and M. A. Covert (2008). "Enhanced remedial amendment delivery through fluid viscosity modifications: Experiments and numerical simulations." Journal of Contaminant Hydrology **101**(1&4): 29-41.

Zhou, L., T. L. Thanh, J. Gong, J.-H. Kim, E.-J. Kim and Y.-S. Chang (2014). "Carboxymethyl cellulose coating decreases toxicity and oxidizing capacity of nanoscale zerovalent iron." Chemosphere **104**(0): 155-161.

Zhu, B. W. and T. T. Lim (2007). "Catalytic reduction of chlorobenzenes with Pd/Fe nanoparticles: Reactive sites, catalyst stability, particle aging, and regeneration." Environmental Science and Technology **41**(21): 7523-7529.

Zhu, H., Y. Jia, X. Wu and H. Wang (2009). "Removal of arsenic from water by supported nano zero-valent iron on activated carbon." J. Hazard. Mater. **172**: 1591-1596.

Zhu, L., H.-z. Lin, J.-q. Qi, X.-y. Xu and H.-y. Qi (2012). "Effect of H₂ on reductive transformation of p-CINB in a combined ZVI-anaerobic sludge system." Water Research **46**(19): 6291-6299.

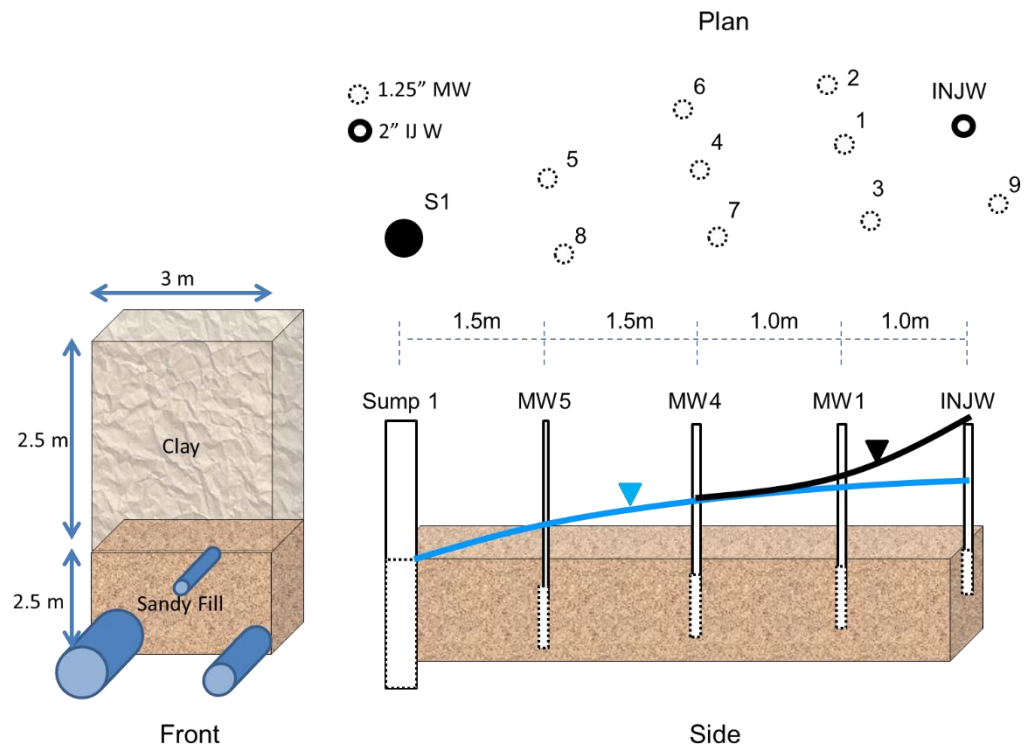
Zhu, L., H. Lin, J. Qi and X. Xu (2013). "Enhanced transformation and dechlorination of p-chloronitrobenzene in the combined ZVI-anaerobic sludge system." Environmental Science and Pollution Research **20**(9): 6119-6127.

Zhu, N. R., H. W. Luan, S. H. Yuan, J. Chen, X. H. Wu and L. L. Wang (2010). "Effective dechlorination of HCB by nanoscale Cu/Fe particles." Journal of Hazardous Materials **176**(1-3): 1101-1105.

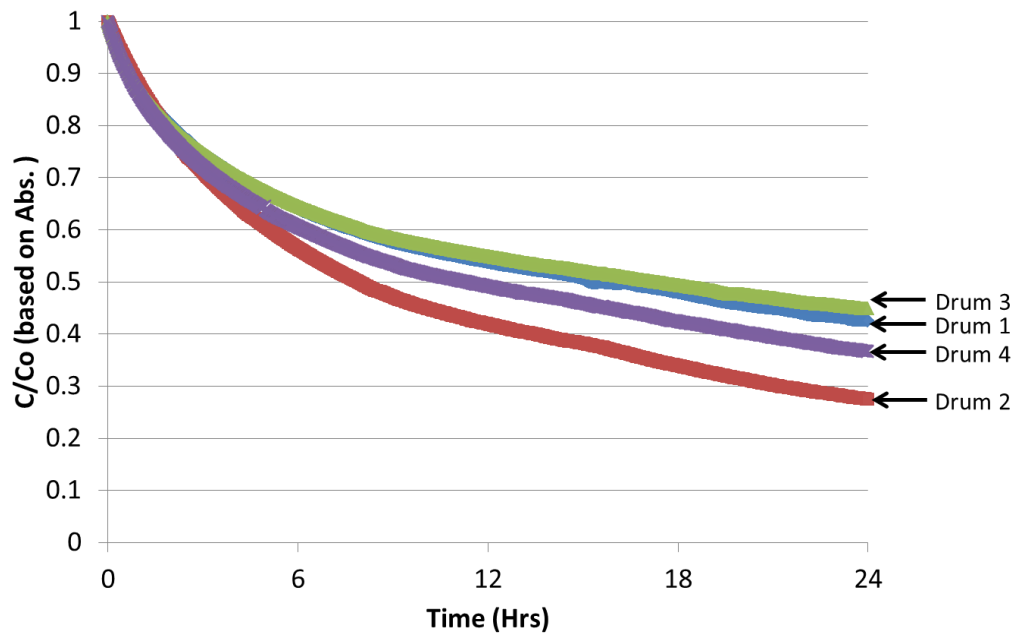
Ziv-El, M., S. C. Popat, P. Parameswaran, D.-W. Kang, A. Polasko, R. U. Halden, B. E. Rittmann and R. Krajmalnik-Brown (2012). "Using electron balances and molecular techniques to assess trichloroethene-induced shifts to a dechlorinating microbial community." Biotechnology and Bioengineering **109**(9): 2230-2239.

8 Appendix B: Supporting Information for Chapter 3 Characterization of nZVI mobility in a field scale test.

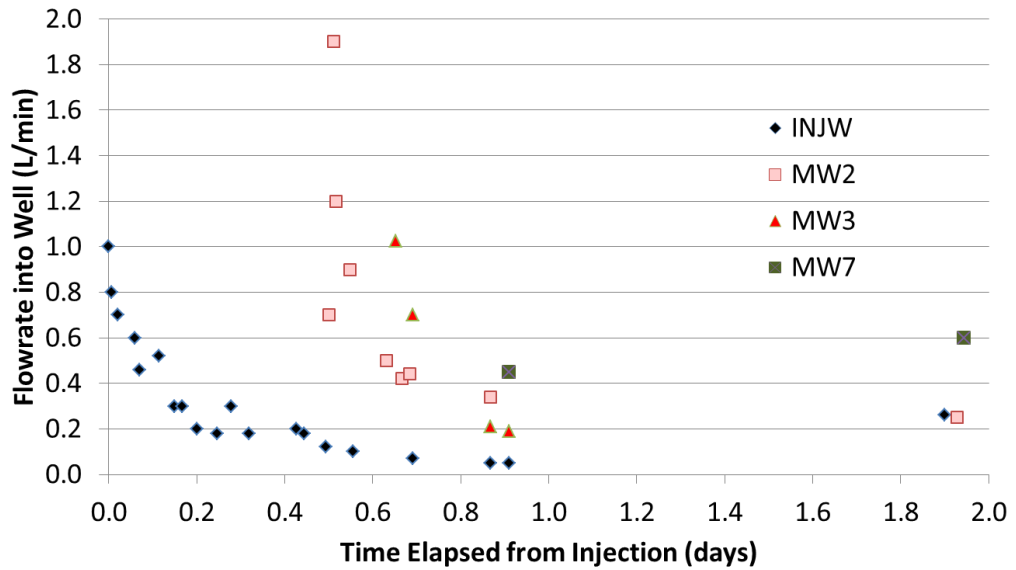
Appendix B. 1: 3-Dimensional conceptual model of the utility corridor showing the existing utilities (blue cylinders), as well as, the installed monitoring well field and a representation of the engineered hydraulic gradient used during nZVI injection.



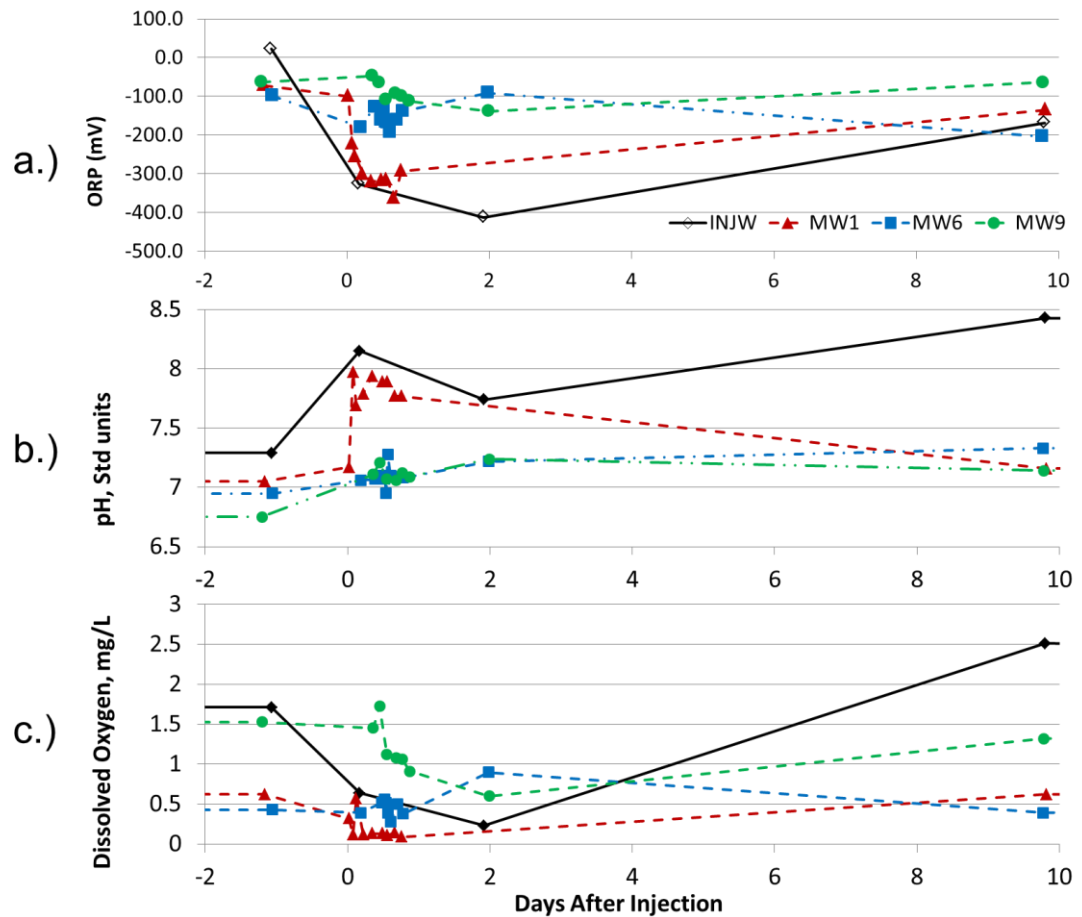
Appendix B. 2: Stability curves for 1 g/L nZVI stabilized with 0.8% CMC polymer sampled from field synthesis drums prior to injection into the subsurface. Samples were diluted 10x in de-ionized de-oxygenated water prior to analysis using UV-vis spectrophotometry at $\lambda = 504\text{nm}$. $t = 0$ for the stability curve corresponds to $t = 16\text{ hr}$ for the injection due to the sample travel time to the laboratory.



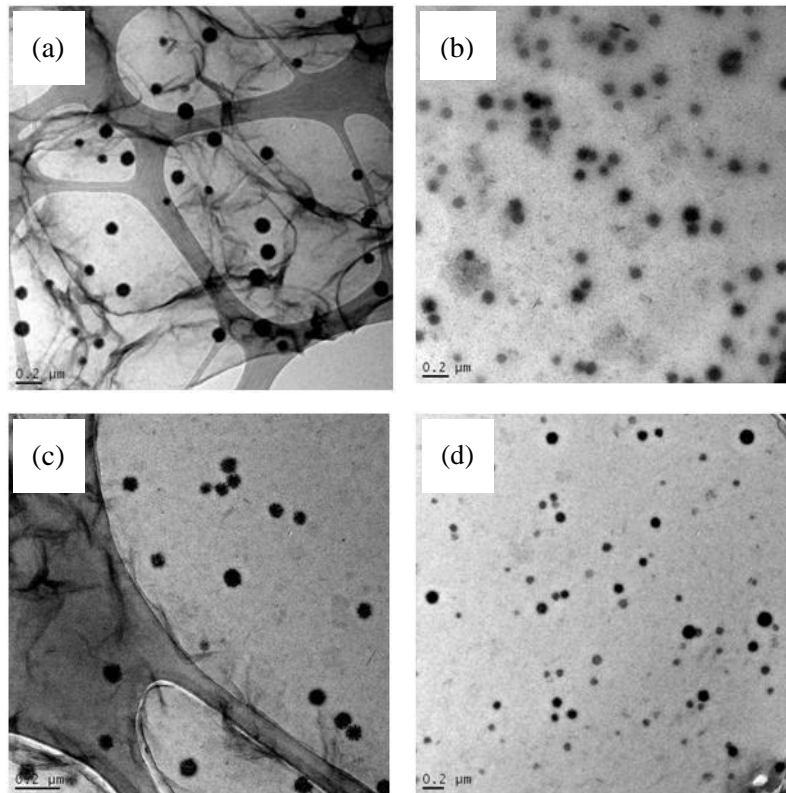
Appendix B. 3: Flow rates measured during gravity feed (constant well head) injection of 1.0 g/L nZVI stabilized with 0.8% CMC into sandy media. Injection proceeded over a 24 hr period in the primary injection well (INJW) and over shorter periods in secondary injection wells. The well productivity was observed to decrease in all cases as the viscous fluid traveled from the injection well.



Appendix B. 4: a) Redox Potential (ORP), b) pH, c) Dissolved oxygen (DO) plotted for the primary injection well (INJW) and other significant monitoring wells cross gradient (MW9) and down gradient (MW6) of the nZVI detection and characterization area (MW1).



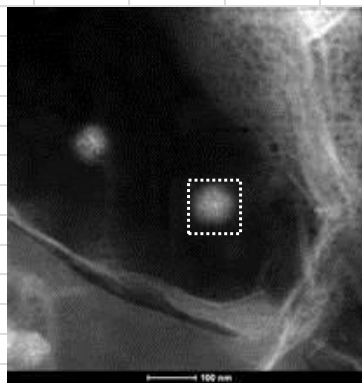
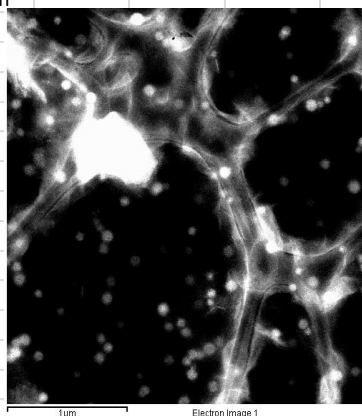
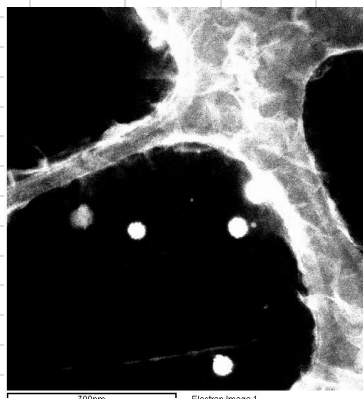
Appendix B. 5: Transmission electron micrographs of nZVI particles a.) freshly synthesized in suspension, b) retrieved from MW1 1 hr after injection began, c) 12 hr after injection began, d) 24 hr after injection began.

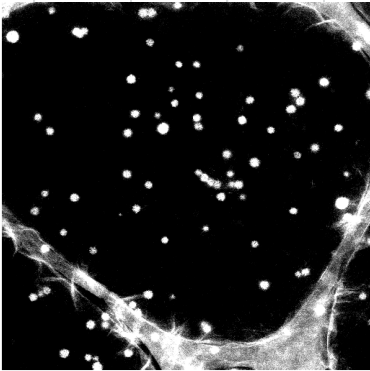
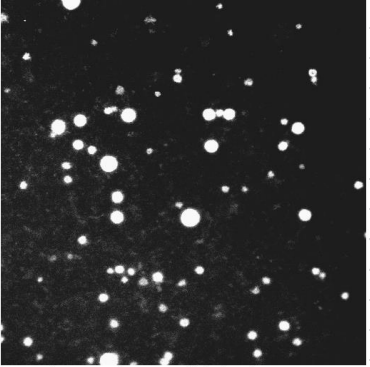


Appendix B. 6: Energy dispersive X-ray spectroscopy (EDS) results showing micrographs and corresponding elemental composition for nZVI particles a) freshly synthesized in Drum 1, b) collected from MW1 – 1 hr after injection, c) from MW1 isolated under high magnification, d) collected from MW1 – 12 hrs after injection

began, e) collected from MW1 – 24 hrs after injection began. The results confirm that nanoparticles that traveled to MW1 are composed of Fe.

Sample a.)		Synthesis Batch - Drum #1				
Sample Date		5:30pm Nov 31.10				
Analysis Date		4/28/2011				
Analysis Time		11:11				
Magnification		1.5 um x 1.5 um				
Analytical Area		1.5 um x 1.5 um				
Element		Weight%	Atomic%			
Na K		32.45	51.33			
S K		9.99	11.33			
Cl K		0.62	0.64			
Fe K		55.02	35.83			
Br L		1.93	0.88			
Totals		100				
Sample b.)		EDS Sample A - MW1 - 1hr following injection				
Sample Date		5:30pm Nov 31.10				
Analysis Date		4/28/2011				
Analysis Time		10:56				
Magnification		3 um x 3 um				
Analytical Area		3 um x 3 um				
Element		Weight%	Atomic%			
Na K		25.91	49.45			
S K		2.62	3.59			
Cl K		4.21	5.22			
Fe K		20.29	15.95			
Br L		46.96	25.79			
Totals		100				
Sample c.)		EDS Sample A - MW1 - 1hr following injection				
Sample Date		5:30pm Nov 31.10				
Analysis Date		4/28/2011				
Analysis Time		10:59				
Magnification		780nm x 780nm				
Analytical Area		90nm x 90nm				
Element		Weight%	Atomic%			
Na K		9.51	20.68			
S K		2.99	4.66			
Cl K		1.83	2.58			
Fe K		68.59	61.4			
Br L		17.08	10.69			
Totals		100				



Sample d.)		EDS Sample C - MW1 - 12hr after injection					
Sample Date	3:20am Dec 1.10						
Analysis Date	4/28/2011						
Anaylsis Time	11:19						
Magnification	3um x 3um						
Analytical Area	3um x 3um						
Element	Weight%	Atomic%					
Na K	34.17	52.17					
S K	15.2	16.63					
Cl K	1.53	1.51					
Fe K	42.9	26.96					
Br L	6.2	2.72					
Totals	100						
				 <p>Electron Image 1</p>			
Sample e.)		EDS Sample E - MW1 - 24hr after injection					
Sample Date	3:25pm Dec 1.10						
Analysis Date	4/28/2011						
Anaylsis Time	11:07						
Magnification	3um x 3um						
Analytical Area	3um x 3um						
Element	Weight%	Atomic%					
Na K	18.07	34.26					
S K	5.24	7.12					
Cl K	0.48	0.6					
Fe K	69.94	54.6					
Br L	6.27	3.42					
Totals	100						
				 <p>Electron Image 1</p>			

Appendix B. 7: Results of slug testing prior to nZVI injection for all monitoring wells and 10 days following nZVI injection for injection wells. Results show that there was a slight increase in the hydraulic conductivity of the injection wells following injection.

Well	Slug Test Results K (m/day)	
	Before Injection	After Injection
Injw	0.11	0.55
MW1	0.11	
MW2	0.43	0.88
MW3	0.08	0.46
MW4	0.02	
MW5	0.30	
MW6	0.46	
MW7	0.11	0.47
MW8	0.13	
MW9	0.02	

Appendix B. 8: Estimates of hydraulic conductivity (K), pore velocity (v_P), and arrival times were performed using theoretical, laboratory, and field methods. Laboratory analysis resulted in higher estimated K due to the specific targeting of sandy samples for analysis due to the assumption that nZVI will travel preferentially through these zones.

	Laboratory Testing Results		Pore Velocity (calculated- m/day)		Calc. Arrival Time at MW1 from INJW (Days)	
			During nZVI Inj.	Natural Gradient	During nZVI Inj.	Natural Gradient
	K (m/day)		0.0540	0.0002	0.0540	0.0002
Hazen Calculation ^a	7.8		1.3122	0.0049	0.8	205.8
Kozeny-Carmen ^b	2.7		0.4520	0.0017	2.2	597.4
Laboratory Testing ^c	5.1		0.8674	0.0032	1.2	311.3
Slug Tests	Before Injection	After Injection				
Geometric Mean	0.11	0.57	0.01874	0.000069	53.4	14407.6
Max (MW6)	0.46		0.07810	0.000289	12.8	3456.7
Min (MW9)	0.015		0.00253	0.000009	393.9	106360.3

^a based on the grain size distribution from recovered soils (D10).

^b based on the grain size distribution from recovered soils (D60).

^c constant head testing of recovered soils.

Appendix B. 9: Results of quantitative characterization of nZVI particles prior to injection and following transport through the subsurface

	Particle Diameter - Individual Particle (TEM)	Particle Diameter – Hydrodynamic (DLS)	Zeta Potential	ZVI Content in Particle
Injection Slurry	86.0 +/- 12 nm (n=182)	624.8 +/- 47.6 nm	-49.2 +/- 1.5 mV	55.4 %
MW1 (1hr)	80.2 +/- 15 nm (n=132)	562.9 +/- 212.7 nm	-48.3 +/- 2.3 mV	17.8 %

8.1.1 Calculations of nanoparticle filtration in soil

Two calculations were completed to determine if the mobility observed in the field is similar to the mobility in column experiments. These calculations rely on several assumptions that are outlined below. These calculations act as a parameter comparison.

Assumptions:

porosity - $n = 0.32$

Collector diameter - $d_c = 0.300\text{mm}$ from grain size distribution.

Particle Diameter - $d_p = 625\text{ nm}$ from DLS

Particle Density = 7850 kg/m^3

Fluid Density = 1000 kg/m^3

Viscosity = 7 cP (the viscosity of the injection fluid)

Pore Water Velocity – $v_p = 0.87\text{ m/day} = 0.00001\text{ m/s}$ (from slug testing & hydraulic gradient during injection)

Hamaker Constant – $A = 1\text{e-}19\text{ J}$ (from previous studies (Chowdhury et al. 2012, Kocur et al. 2013))

Length to MW1 from injection = 1m

Calculated Collector efficiency – $\eta_o = 0.028$

Assuming a typical value of α from column studies $\alpha = 0.016$ (From Kocur et al 2013))

Maximum Travel Distance in Soil (L_{Max}) for 99% of particles based on literature parameters

$$L_{Max} = -\frac{2}{3} \frac{d_c}{(1-n)\alpha\eta_o} \ln\left(\frac{C}{C_o}\right) = -\frac{2}{3} \frac{\frac{0.0003\text{m}}{s}}{(1-.32)0.016 * 0.028} \ln(0.01) = \mathbf{2.99m}$$

Based on Field parameters

For $L = 1\text{ m}$ at MW1, $C/C_o = 0.54$

Then $\eta = \alpha\eta_o$ for the field scenario is ...

$$\eta = -\frac{2}{3} \frac{d_c}{(1-n)L} \ln \frac{C}{C_o} = -\frac{2}{3} \frac{0.0003m}{(1-.32)1m} \ln 0.54 = \mathbf{0.00018}$$

Compared to $\alpha \cdot \eta_o = 0.016 \cdot 0.028 = 0.000448$ for the literature values.

Maximum Travel Distance in Soil (L_{Max}) for 99% of particles based on field parameters

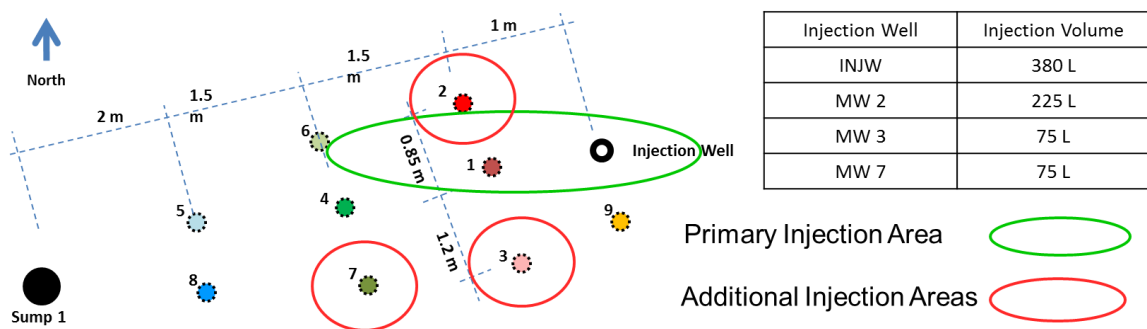
$$L_{Max} = -\frac{2}{3} \frac{d_c}{(1-n)\eta} \ln \left(\frac{C}{C_o} \right) = -\frac{2}{3} \frac{0.0003}{(1-.32)0.00018} \ln(0.01) = \mathbf{7.52m}$$

References

- Chowdhury, A. I. A., D. M. O'Carroll, Y. Xu and B. E. Sleep (2012). "Electrophoresis enhanced transport of nano-scale zero valent iron." *Advances in Water Resources* 40(0): 71-82.
- Kocur, C. M., D. M. O'Carroll and B. E. Sleep (2013). "Impact of nZVI stability on mobility in porous media." *Journal of Contaminant Hydrology* 145(0): 17-25.

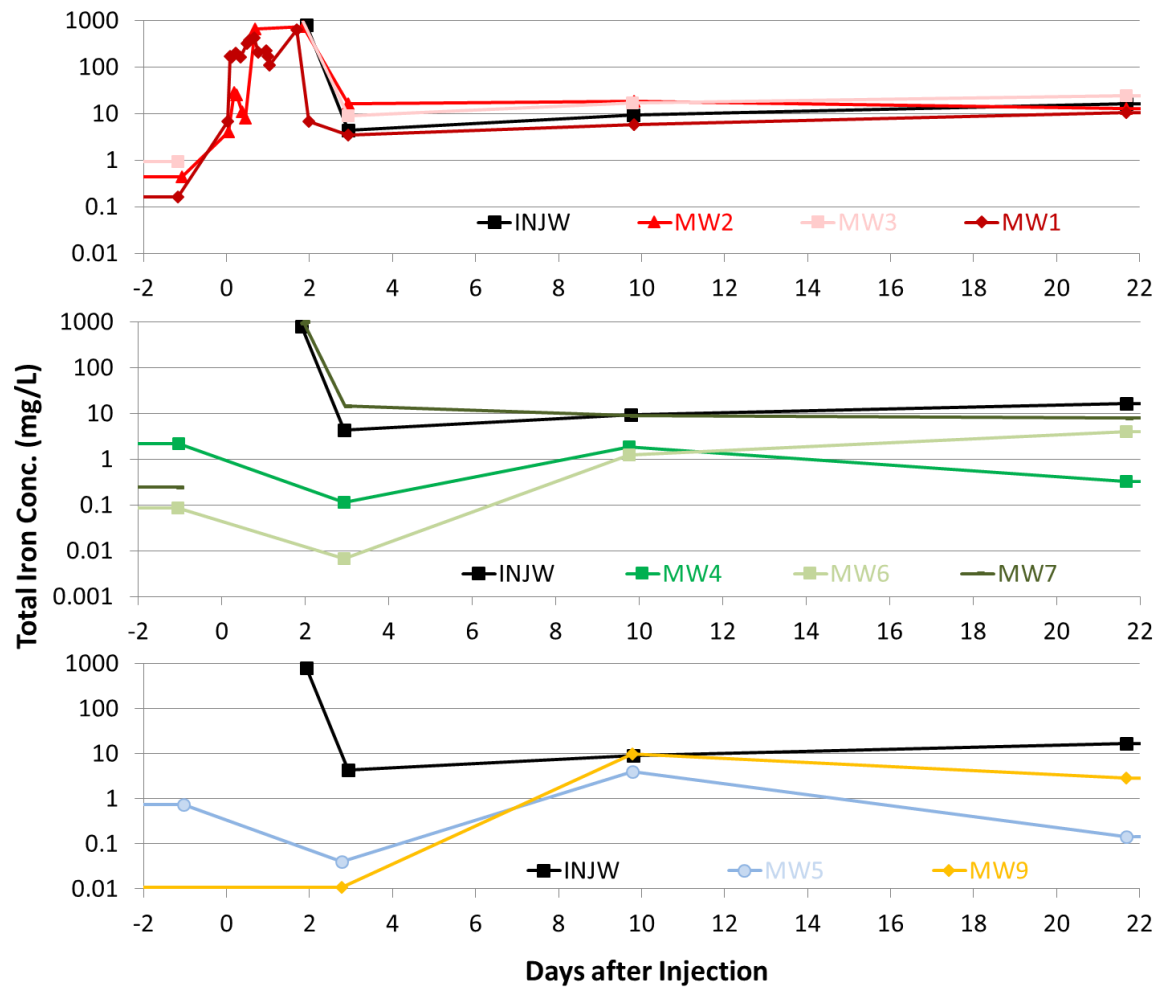
9 Appendix C: Supplemental Information for Chapter 4: Contributions of Abiotic and Biotic Dechlorination Following Carboxymethyl Cellulose Stabilized Nanoscale Zero Valent Iron Injection

Appendix C. 1: Schematic of the injection and monitoring wells on site showing the estimated spatial distribution of nZVI from each injected volume

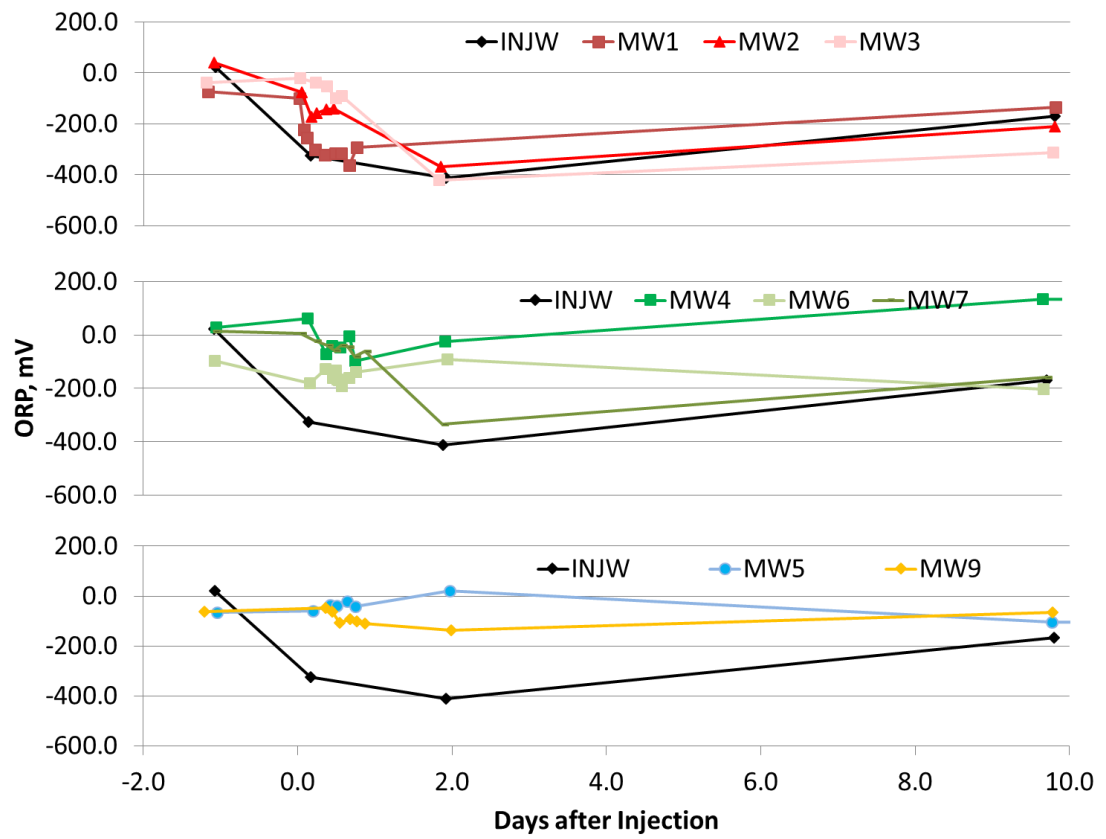


Appendix C. 2: Geochemical data showing a.) total Fe, b.) ORP, c.) pH, d.) Chloride in the monitoring wells

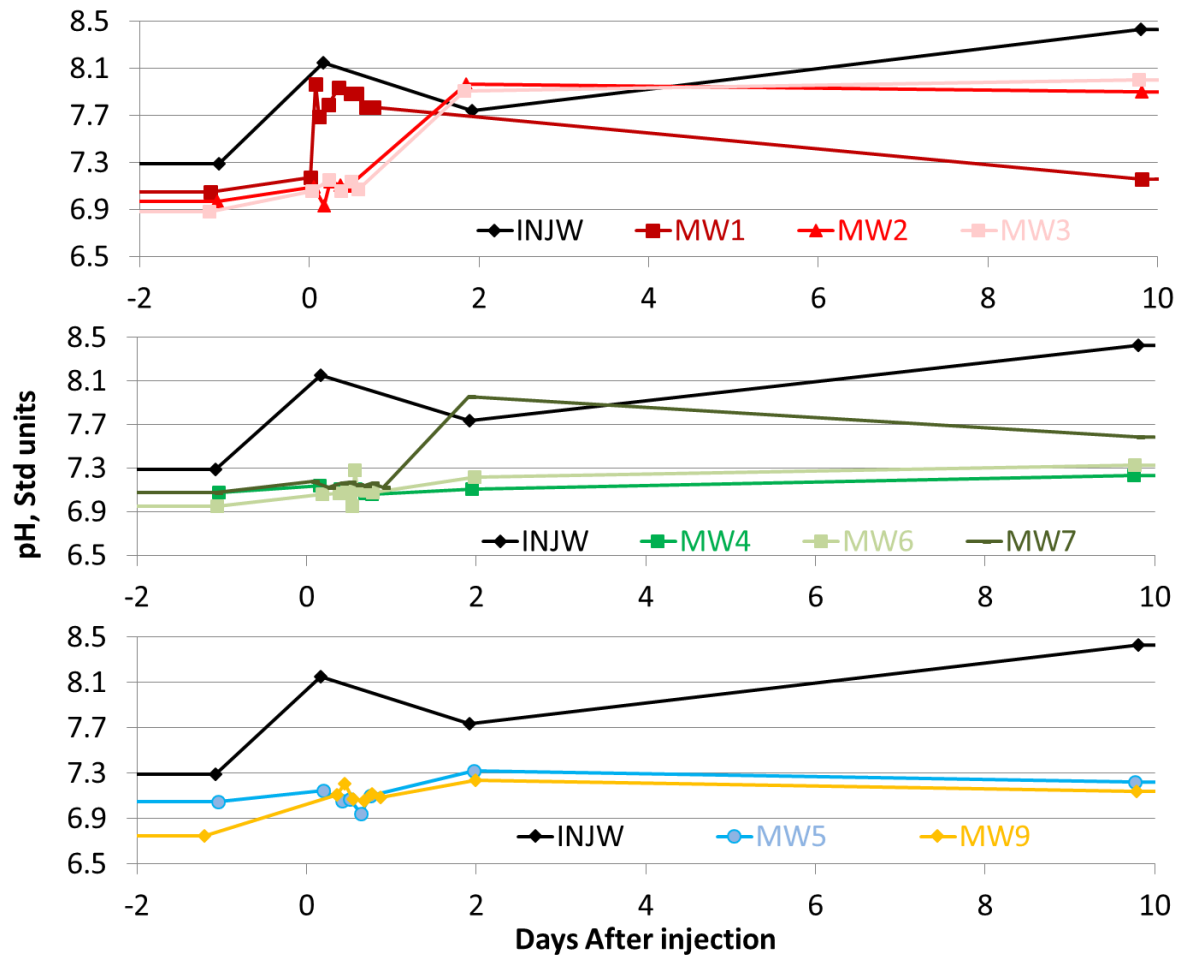
a.)



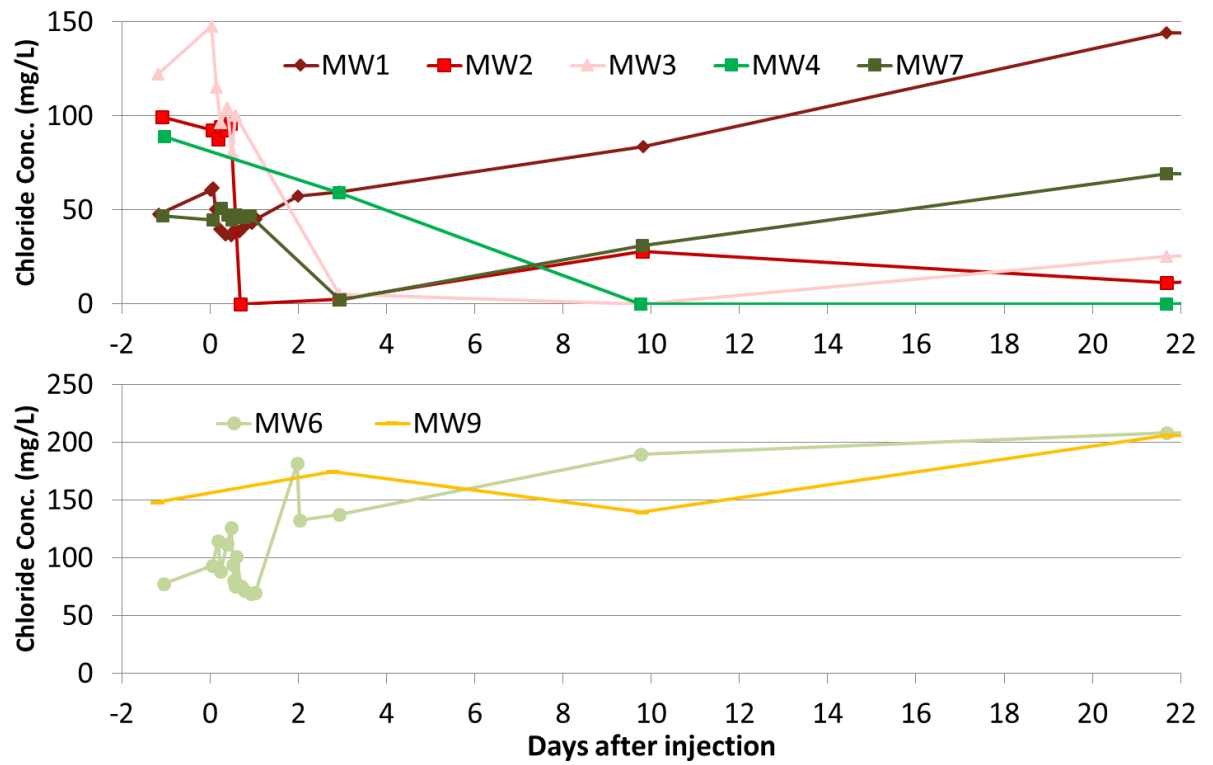
b.)



c.)



d.)



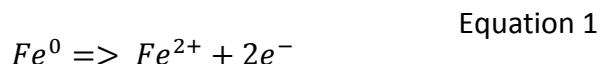
9.1 Background

This section provides detailed information for the quantification of electron equivalents, either evolved or consumed, due to the injection of nZVI. Calculations are based on the equivalents of electrons required for dechlorination.

Since each mole of cVOC transformed requires two moles of electron reducing equivalents per chloride reduced, the independently measured cVOC and chloride concentrations provide independently derived estimates of products and reactants, respectively, involved in reductive dechlorination. Thus, an estimate of potential degradation can be inferred from a reducing equivalents balance based on the transformation of sampled cVOCs and compared to the reducing equivalents calculated from chloride evolved. Both estimates are independent of the reductive agent that dechlorinated the contaminant and result in a total estimate of the dechlorination that occurred. However, the chloride estimate is expected to be inherently higher than the cVOC based estimate as more reaction products are included in the analysis (eg. contribution of VC degradation to ethene, yielding chloride).

9.1.1 Electron Balance for the oxidation of nZVI

Electrons transferred during the oxidation of nZVI are utilized for the reduction of chlorinated solvents. The half Reaction for nZVI oxidation is:



$$[Fe^0] = [Fe] \times \text{ZVI content}$$

Equation 2

Assuming all zero valent iron (Fe^0) is oxidized to ferrous iron (Fe^{2+}), from equation 2;

$$e^- = 2[Fe^0]$$

Equation 3

Example Calculation, For 1 Liter of nZVI slurry based on measured Fe^0 (Kocur et al. 2014)

$$[Fe^0] = \left[1 \frac{g}{L} Fe \right] \times \frac{mol}{55.8 g} \times 0.554 \text{ (ZVI content)} = 0.009925 \text{ mol/L}$$

$$e^- = 2[0.009925 \text{ mol/L}] = 0.01985 \frac{mol}{L} \text{ or } 19.85 \text{ mM}$$

<i>Liters</i>	<i>Fe^0</i>	<i>e^-</i>
<i>1</i>	<i>0.0099 mol</i>	<i>0.0198 mol</i>
<i>700</i>	<i>6.94 mol</i>	<i>13.89 mol</i>

9.1.2 Electron balance for aqueous cVOC Sample data

Assumptions: For the electron equivalent based on VOC concentrations it is assumed that the compounds originally started as a source most oxidized compound (PCE; 1,1,1,2 TeCA; 1,1,2,2 TeCA; and carbon tetrachloride were known to be the source compounds), and each reaction product can be evaluated based on the number of electrons that would be consumed in reducing these parent compounds to the measured dechlorination products. For example, the conversion of PCE to cis-DCE and VC uses 4 and 6 electrons respectively.

To calculate the molar concentration of electron reducing equivalents required to reduce source compounds to daughter products the concentrations of the daughter products are required. Summing the product of each daughter compound concentration [cVOC] and the number of electrons required for the reduction of a parent compound to that daughter product gives $e^-_{req.}$ which can then be related to the concentration of electrons in each sample (e^-_{sample}).

$$(e^-_{sample}) = \sum_{All\ compounds} e^-_{req.} \times [cVOC] \quad \text{Equation 4}$$

The electron reducing equivalent concentrations at each well are evaluated using equation 5 by comparing the total electron reducing equivalent concentrations at two different sample times. This estimate represents the total reducing equivalents concentration (e^-_{well}) associated with transformation of the selected source compounds to various daughter products, represented as a concentration.

$$(e^-_{well}) = e^-_{sample} - e^-_{background} \quad \text{Equation 5}$$

e^-_{well} is the concentration of electrons that were required to reduce the parent compounds to daughter compounds over the period evaluated at each well. This provides a measure of the reducing equivalents consumed in the reduction of the source compounds to various daughter

products. This does not distinguish between reduction pathways. Note: since ethane, ethene, and methane concentrations were not measured, the transformation of daughter compounds to these compounds is not included in this estimate. Therefore it is likely an underestimate.

Example Calculation, for MW1, is provided in Table S1, the sample calculation below shows the calculation for MW1 samples taken on Day -1.2 (the background sample) and Day 3. This results in the total reducing equivalent of 0.002 mmol/L (or mM) 3 days following the injection.

$$(e^-_{\text{background sample (-1.2 days)}}) = \sum^{\text{All compounds}} e^-_{\text{req.}} \times [\text{cVOC}] = 0.0818 \text{ mmol/L}$$

$$(e^-_{\text{Day 3 sample}}) = \sum^{\text{All compounds}} e^-_{\text{req.}} \times [\text{cVOC}] = 0.0838 \text{ mmol/L}$$

Using these example values in table S1 and the values calculated (e^- samples), the total reducing equivalents of transformation in MW1 is estimated by the difference of the values summed in the last column compared to the background column. It should be noted that in some cases the total reducing equivalents are negative due to the fact that the sum of all cVOCs in the samples are higher after injection.

$$(e^-_{\text{MW1}}) = e^-_{\text{Day 3 sample}} - e^-_{\text{background sample}} = 0.0015 \text{ mmol/L}$$

Appendix C. 3: Example Calculation of electron balance for aqueous cVOCs at Monitoring Well 1.

Conc (mM)	PCE	TCE	Cis 1,2 DCE	Trans 1,2 DCE	1,1 DCE	VC	1,1,2,2-TeCA	1,1,1,2-TeCA	1,1,1-TCA	1,1,2-TCA	CF	CCl4	1,2 DCA	1,1 DCA	e- Sample
electron equivalents per mole	0	2	4	4	4	6	0	0	2	2	2	0	4		mM
Time after Inj.															
-1.2 days	0.00245	0.00776	0.01335	0.00000	0.00000	0.00072	0.00012	0.00008	0.00067	0.00038	0.00265	0.00017	0.00000	0.00027	0.081
1.0 days	0.00503	0.00492	0.00693	0.00022	0.00000	0.00098	0.00013	0.00007	0.00051	0.00035	0.00185	0.00071	0.00000	0.00080	0.052
2.0 days	0.00086	0.00708	0.01201	0.00021	0.00000	0.00078	0.00000	0.00006	0.00055	0.00018	0.00238	0.00005	0.00000	0.00047	0.075
2.9 days	0.00060	0.00547	0.01467	0.00018	0.00000	0.00088	0.00000	0.00006	0.00055	0.00019	0.00219	0.00000	0.00000	0.00044	0.083
9.8 days	0.00017	0.00180	0.02079	0.00022	0.00000	0.00206	0.00000	0.00006	0.00051	0.00012	0.00161	0.00000	0.00000	0.00046	0.106
21.7 days	0.00060	0.00072	0.04259	0.00036	0.00000	0.01207	0.00000	0.00006	0.00026	0.00000	0.00013	0.00000	0.00000	0.00077	0.249

9.1.3 Electron balance for chloride ion evolution

In this analysis it is assumed that the increases in concentrations of chloride is due to cVOC dechlorination.

To calculate the electrons required to produce observed chloride concentrations in each well ($e^-_{\text{well-cl}}$) the difference between the chloride in the sample, at a given sampling time, and the chloride concentration, in the background sample for that well, is required.

$$\Delta Cl_{\text{well}}^- = [Cl_{\text{sample}}^-] - [Cl_{\text{background}}^-] \quad \text{Equation 6}$$

This chloride concentration is then converted to a concentration of electrons assuming $2e^-$ are required for each Cl^- in solution.

$$e^-_{\text{well-cl}} = \frac{\Delta Cl_{\text{well}}^-}{35.45 \frac{\text{mmol}}{\text{mg}}} \times \frac{2e^-}{Cl^-} \quad \text{Equation 7}$$

$e^-_{\text{well-cl}}$ is the concentration of electrons that were required to reduce the parent compounds, producing the chloride concentrations measured over the period evaluated at each well.

Example Calculation for MW1 in Table S2

Using MW1 as an example in Table S2, the difference in chloride concentrations compared to the background sample are evaluated for MW1 3 days after injection.

$$\Delta Cl_{\text{MW1-3days}}^- = [Cl_{\text{MW1-3 days sample}}^-] - [Cl_{\text{MW1-background sample}}^-] = 12.12 \text{ mmol/L}$$

From Equation 7:

$$e_{MW1-Cl}^- = \frac{12.12 \text{ mg } Cl^- / L}{35.45 \frac{\text{mmol}}{\text{mg}}} \times \frac{2e^-}{Cl^-} = 0.684 \text{ mmol/L}$$

Appendix C. 4: Example Calculation of electron balance for Chloride concentrations at MW1

Days after injection	Chloride Conc.	ΔCl_{MW1} (Sample-b/g)		
Days	mg/L	mg/L		
-1 (b/g)	47.5	0.00		
0	60.3	12.7		
1	45.2	-2.2		e^-_{MW1-Cl}
2	57.3	9.7		mmol/L
3	59.6	12.1	3 days	0.68
10	83.7	36.2		
21	144.1	96.5		

9.1.4 Electron Balance based on Microbial yield.

Metabolic dechlorination from microbial species (e.g., *Dehalococcoides spp. (dhc)*) will result in the reduction of a chlorinated solvent or hydrocarbon. Microbial reductive dechlorination of chlorinated solvents will yield reduced chlorinated products as well as biomass associated with the replication of the organism. This yield can be expressed as:

$$\begin{aligned} \text{Yield} \left(\frac{16S \text{ rRNA gene copies}}{\text{mmol } Cl \text{ released}} \right) &= \frac{\Delta X}{\Delta S} \\ &= \frac{\Delta \text{Organisms} \left(\frac{16S \text{ rRNA gene copies}}{L} \right)}{\Delta \text{Products} \left(\frac{\text{mmol } Cl \text{ released}}{L} \right)} \end{aligned} \quad \text{Equation 8}$$

Where Yield is a literature value that is experimentally determined for each specific microorganism (*dhc* in this case) metabolizing a specific chlorinated compound. ΔX is the change in the number of copies of the 16S rRNA gene on a volumetric basis (copies/L), and ΔS is the change in the metabolic products that are produced from the metabolic growth of the

specific organism on a volumetric basis (mmol Cl⁻/L). In this case chloride ions from dechlorination can be converted to electrons (Cl⁻ = 2 e⁻).

The electron balance can be calculated to get ΔS by comparing the gene copies for two *dhc* population samples from a well at two different sampling events and assuming a literature value for the yield from Loeffler (2013).

Example Calculation for the Yield of dhc (At MW1)

Yield for dhc = Yield = 1.67 x 10⁸ copies/μmol Cl⁻ taken from (Löffler et al. 2013)

Gene Copies of dhc per Liter in background sample = X_{background} = 7.3x10⁶ copies/L

Gene Copies of dhc per Liter in sample at 2 days = X_{2 days} = 6.1x10⁷ copies/L

Therefore ΔX = 5.3x10⁷ copies/L

Assuming a yield of 1.67x10⁸ copies/ μmol of Cl⁻ released, ΔS is isolated from equation 8:

$$\Delta S = \frac{\Delta X}{Yield} = \frac{5.3 \times 10^7 \frac{\text{copies}}{L}}{1.67 \times 10^8 \left(\frac{\text{copies}}{\mu\text{mol Cl}^-} \right)} = 0.32 \times \frac{2 \text{ mmol e}^-}{1000 \mu\text{mol Cl}^-} =$$

$$\Rightarrow 0.00064 \text{ mmol } \frac{\text{e}^-}{L} \text{ of electron reducing equivalents}$$

Appendix C. 5: Microbial electron reducing equivalents based on the yield of microorganism

	$X_{b/g}$	$X_{2 \text{ Days}}$	ΔX	Yield	ΔS	e^- / L
	copies/L	copies/L		copies/umol Cl released	umol Cl released/L	mmol/L
	b/g sample	2 day sample				
MW1	7.3E+06	6.1E+07	5.3E+07	1.67E+08	0.3196	6.4E-04
MW2	3.5E+06	4.8E+08	4.7E+08	1.67E+08	2.8296	5.7E-03
MW4	2.2E+06	2.9E+04	-2.1E+06	1.67E+08	-0.0127	-2.5E-05
MW5	1.4E+06	3.0E+06	1.6E+06	1.67E+08	0.0095	1.9E-05
MW6^a	6.8E+06	2.9E+07	2.2E+07	1.67E+08	0.1327	2.7E-04
MW9	1.3E+07	4.7E+06	-8.1E+06	1.67E+08	-0.0486	-9.7E-05
INJW	1.4E+07	5.0E+06	-8.9E+06	1.67E+08	-0.0531	-1.1E-04
	^a Average value is used as actual value was not measured					

Appendix C. 6: Raw data from analytical analysis.

Date	Time (Inj. Zeroed)	Sample	Chloride	1,1-DCE	DCM	Trans 1,2- DCE	1,1- DCA	Cis- 1,2- DCE	CF	1,1,1- TCA	CCl4	1,2- DCA	TCE	1,1,2- TCA	PCE	1,1,1,2- TeCA	1,1,2,2 TeCA	VC	DKC	VCA
	Days	Well	mg/L	mg/L	mg/L	mg/L	mg/L	mg/L	mg/L	mg/L	mg/L	mg/L	mg/L	mg/L	mg/L	mg/L	mg/L	mg/L	mg/L	copies/L
Nov 29.10	-1.2	MW1	47.5	0.000	0.000	0.000	0.027	1.294	0.317	0.089	0.026	0.000	1.020	0.051	0.407	0.014	0.020	0.045	7.32E+06	4.69E+05
Nov 29.10	-1.1	MW2	99.7	0.000	0.000	0.000	0.029	0.565	0.158	0.062	0.010	0.000	0.660	0.000	0.333	0.008	0.000	0.038	3.46E+06	9.43E+05
Nov 29.10	-1.0	MW4	89.1	0.000	0.000	0.000	0.018	0.129	0.162	0.075	0.043	0.000	0.956	0.008	1.414	0.014	0.000	0.012	2.15E+06	2.27E+05
Nov 29.10	-1.0	MW5	64.5	0.000	0.000	0.000	0.014	0.086	1.013	0.164	0.063	0.000	0.406	0.000	0.594	0.009	0.022	0.104	1.39E+06	1.02E+05
Nov 29.10	-1.1	MW6	77.9	0.000	0.000	0.000	0.045	2.415	0.283	0.095	0.017	0.000	1.269	0.171	0.016	0.014	0.020	0.174	1.28E+07	1.06E+06
Nov 29.10	-1.2	MW9	148.5	0.000	0.000	0.000	0.041	0.062	2.346	0.345	0.092	0.000	0.931	0.043	0.031	0.012	0.031	0.279	1.28E+07	1.06E+06
Dec 1.10	0.9	MW4	191.3	0.000	0.000	0.000	0.060	0.101	3.922	0.287	0.086	0.114	0.000	1.167	0.000	0.481	0.009	0.020	0.923	
Dec 1.10	0.9	MW4	66.4	0.000	0.000	0.000	0.021	0.057	0.305	0.281	0.085	0.139	0.000	0.731	0.070	1.451	0.019	0.000	0.036	
Dec 1.10	0.9	MW6	68.8	0.000	0.000	0.000	0.039	0.044	1.391	0.311	0.105	0.112	0.000	1.134	0.159	0.032	0.017	0.020	0.129	
Dec 1.10	0.9	MW5	55.1	0.000	0.000	0.000	0.101	1.015	0.180	0.066	0.100	0.000	0.495	0.024	0.746	0.010	0.023	0.111		
Dec 1.10	1.0	MW1	42.8	0.000	0.000	0.000	0.021	0.079	0.672	0.221	0.068	0.109	0.000	0.646	0.047	0.834	0.012	0.022	0.061	
Dec 2.10	1.8	MW2		0.000	0.000	0.000	0.000	0.000	0.000	0.000	0.000	0.000	0.000	0.000	0.000	0.000	0.000	0.000	0.000	
Dec 2.10	2.0	MW4	75.7	0.000	0.000	0.000	0.028	0.034	0.471	0.444	0.094	0.051	0.000	0.932	0.165	1.353	0.024	0.021	0.040	4.76E+08
Dec 2.10	2.0	MW5	53.5	0.000	0.000	0.000	0.000	0.084	1.094	0.159	0.058	0.006	0.000	0.369	0.022	0.342	0.010	0.022	0.088	2.89E+04
Dec 2.10	2.0	MW6	181.6	0.000	0.000	0.000	0.084	1.134	4.947	0.188	0.086	0.000	0.000	0.384	0.053	0.012	0.008	0.000	0.835	2.90E+07
Dec 2.10	2.0	MW1	57.3	0.000	0.000	0.000	0.047	1.164	0.284	0.074	0.007	0.000	0.000	0.930	0.024	0.443	0.010	0.000	0.049	6.07E+07
Dec 2.10	2.0	MW4		0.000	0.000	0.000	0.000	0.000	0.000	0.000	0.000	0.000	0.000	0.000	0.000	0.000	0.010	0.000	0.055	6.89E+05
Dec 2.10	2.0	MW9	402.8	0.000	0.000	0.000	0.045	0.053	1.743	0.354	0.088	0.018	0.000	1.084	0.000	0.613	0.010	0.000	0.000	
Dec 3.10	2.9	MW1	59.7	0.000	0.000	0.000	0.017	0.044	1.432	0.262	0.073	0.000	0.000	0.719	0.026	0.100	0.010	0.000	0.010	
Dec 3.10	2.9	MW2	2.7	0.000	0.000	0.000	0.000	0.000	0.141	0.027	0.000	0.000	0.000	0.249	0.000	0.184	0.000	0.000	0.000	
Dec 3.10	2.9	MW4	59.0	0.000	0.000	0.000	0.016	0.117	0.129	0.064	0.034	0.000	0.000	0.360	0.012	0.529	0.010	0.022	0.066	
Dec 3.10	2.9	MW5	50.1	0.000	0.000	0.000	0.059	0.778	0.141	0.057	0.000	0.000	0.000	0.360	0.000	0.000	0.000	0.000	0.000	
Dec 3.10	2.9	MW6	137.8	0.000	0.000	0.000	0.084	0.127	4.747	0.146	0.084	0.000	0.000	0.200	0.069	0.000	0.010	0.000	0.782	
Dec 3.10	2.9	MW9	174.9	0.000	0.000	0.000	0.040	0.055	1.928	0.320	0.087	0.015	0.000	1.066	0.000	0.519	0.010	0.000	0.305	
Dec 10.10	9.8	MW4	0.0	0.000	0.000	0.000	0.032	0.036	0.428	0.443	0.093	0.055	0.000	0.917	0.134	1.408	0.021	0.000	0.046	
Dec 10.10	9.8	MW6	189.9	0.000	0.000	0.000	0.130	0.147	7.795	0.321	0.096	0.000	0.000	0.313	0.061	0.027	0.010	0.000	1.772	
Dec 10.10	9.8	MW5	80.2	0.000	0.000	0.000	0.015	0.096	1.333	0.168	0.059	0.000	0.000	0.394	0.029	0.374	0.010	0.000	0.143	
Dec 10.10	9.8	MW9	139.4	0.000	0.000	0.000	0.045	0.061	2.227	0.331	0.087	0.021	0.000	1.099	0.000	0.485	0.010	0.000	0.345	
Dec 10.10	9.8	MW2	28.1	0.000	0.000	0.000	0.023	0.373	0.046	0.042	0.000	0.000	0.000	0.131	0.000	0.248	0.000	0.000	0.026	
Dec 10.10	9.8	MW1	85.7	0.000	0.000	0.000	0.021	0.046	2.015	0.192	0.068	0.000	0.000	0.236	0.016	0.029	0.010	0.000	0.129	
Dec 22.10	21.7	MW1	144.1	0.000	0.000	0.000	0.035	0.076	4.127	0.016	0.035	0.000	0.000	0.095	0.000	0.099	0.010	0.000	0.755	
Dec 22.10	21.7	MW2	11.1	0.000	0.000	0.000	0.018	0.819	0.051	0.000	0.000	0.000	0.000	0.531	0.000	0.101	0.000	0.000	0.026	
Dec 22.10	21.7	MW4	0.0	0.000	0.000	0.000	0.038	0.051	0.564	0.393	0.047	0.036	0.000	0.372	0.106	0.863	0.017	0.000	0.061	
Dec 22.10	21.7	MW5	92.7	0.000	0.000	0.000	0.018	0.143	1.777	0.104	0.023	0.000	0.000	0.107	0.025	0.398	0.010	0.000	0.223	
Dec 22.10	21.7	MW6	208.5	0.000	0.000	0.000	0.064	0.107	3.406	0.078	0.027	0.000	0.000	0.000	0.012	0.035	0.010	0.000	2.401	
Dec 22.10	21.7	MW9	205.7	0.000	0.000	0.000	0.042	0.074	2.684	0.181	0.035	0.010	0.000	0.808	0.000	0.387	0.010	0.000	0.666	

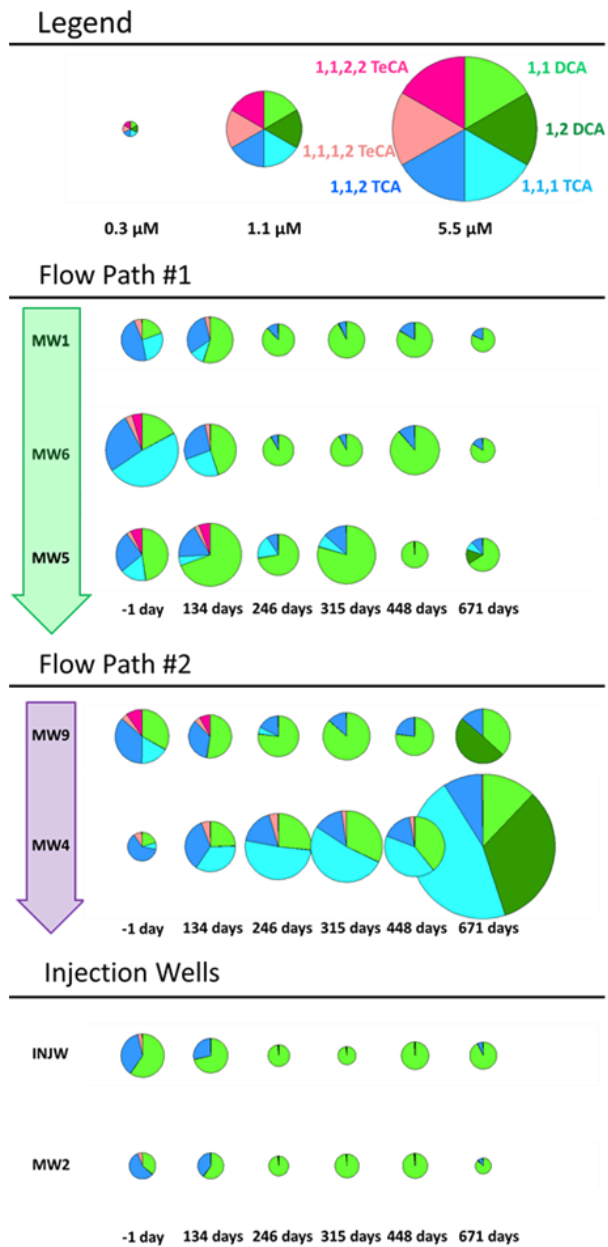
9.2 References

Löffler, F. E., J. Yan, K. M. Ritalahti, L. Adrian, E. A. Edwards, K. T. Konstantinidis, J. A. Müller, H. Fullerton, S. H. Zinder and A. M. Spormann (2013). "Dehalococcoides mccartyi gen. nov., sp. nov., obligately organohalide-respiring anaerobic bacteria relevant to halogen cycling and bioremediation, belong to a novel bacterial class, Dehalococcoidia classis nov., order Dehalococcoidales ord. nov. and family Dehalococcoidaceae fam. nov., within the phylum Chloroflexi." *International Journal of Systematic and Evolutionary Microbiology* 63(Pt 2): 625-635.

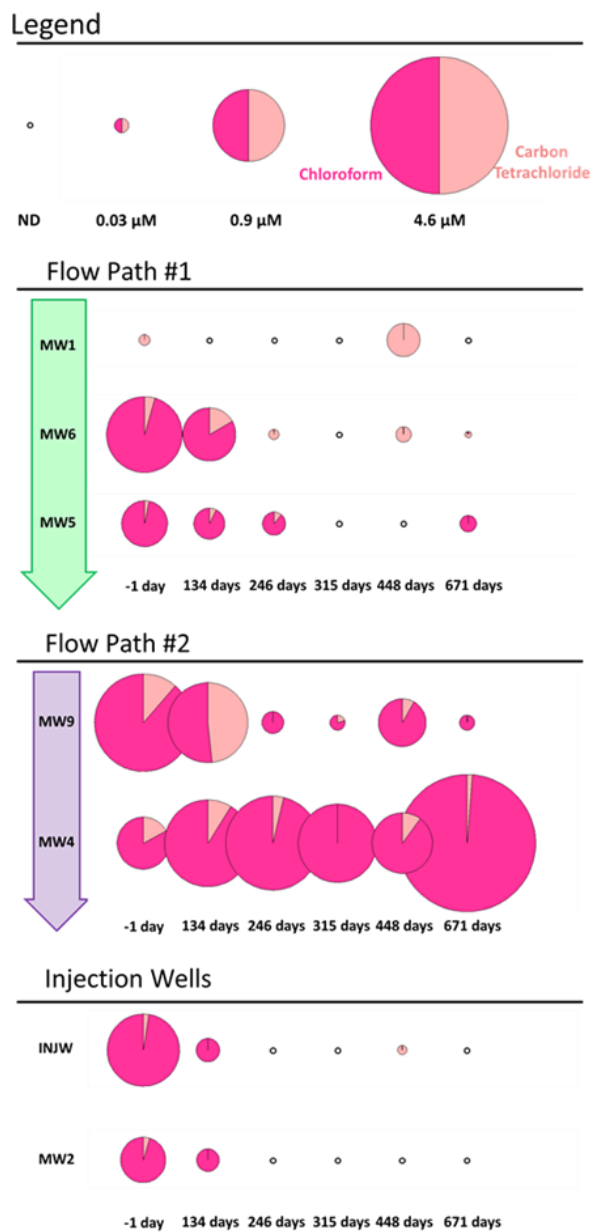
10 Appendix D: Supplemental Information for Chapter 5: Long Term Dechlorination Following nZVI/CMC Injection and Impact on Microbial Communities, Including Organohalide-Respiring Microorganisms

Appendix D. 1: Bubble Pie charts similar to the Chlorinated Ethenes in Figure 1, showing the Chlorinated Ethanes and Methanes. Although these cVOCs are an order of magnitude lower than the Chlorinated Ethenes, they show distinct patterns of degradation over the monitoring period, and show the potential inhibition due to high concentrations of chloroform in MW4. MW6 provides a good comparison to MW4 as both contain high CF concentrations prior to injection. In MW6, CF concentrations declined and were accompanied by declining concentrations of all cVOCs, whereas in MW4 there were minimal changes in cVOCs overall, apart from the increased inhibitor concentrations (CF and 1,1,1 TCA).

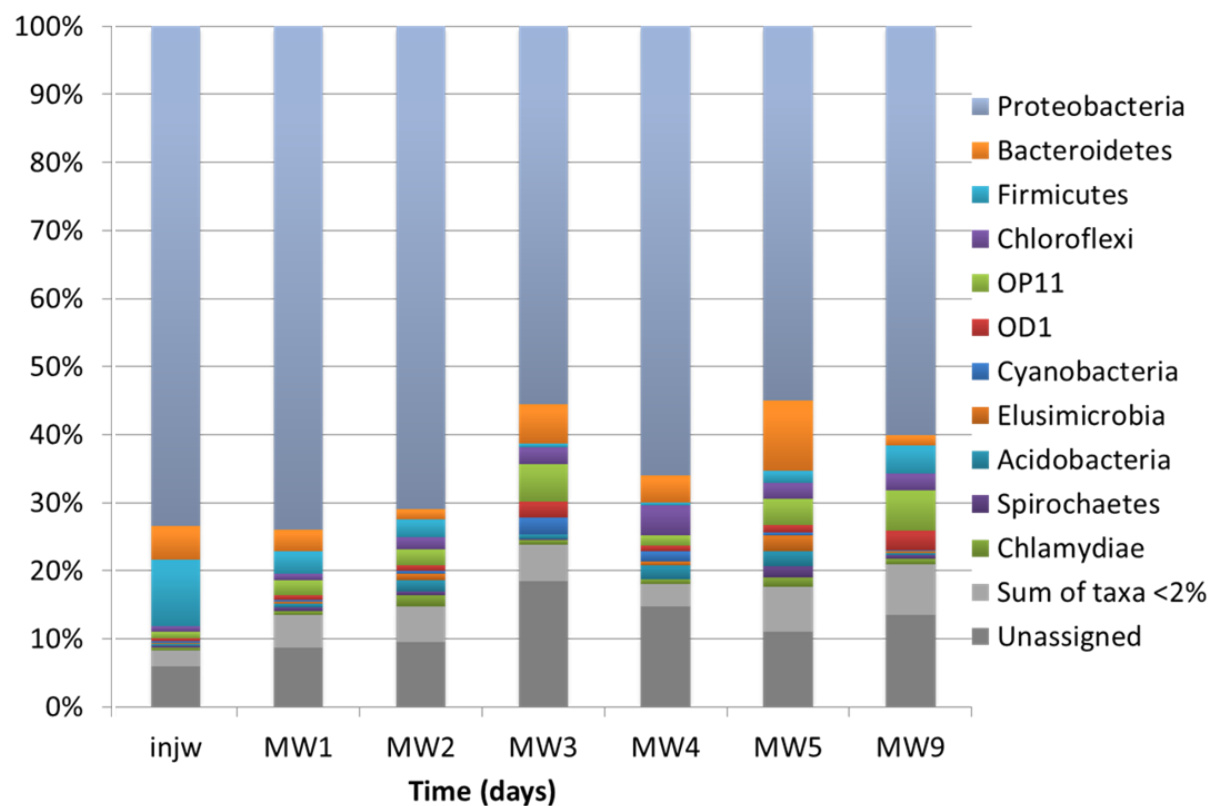
a.



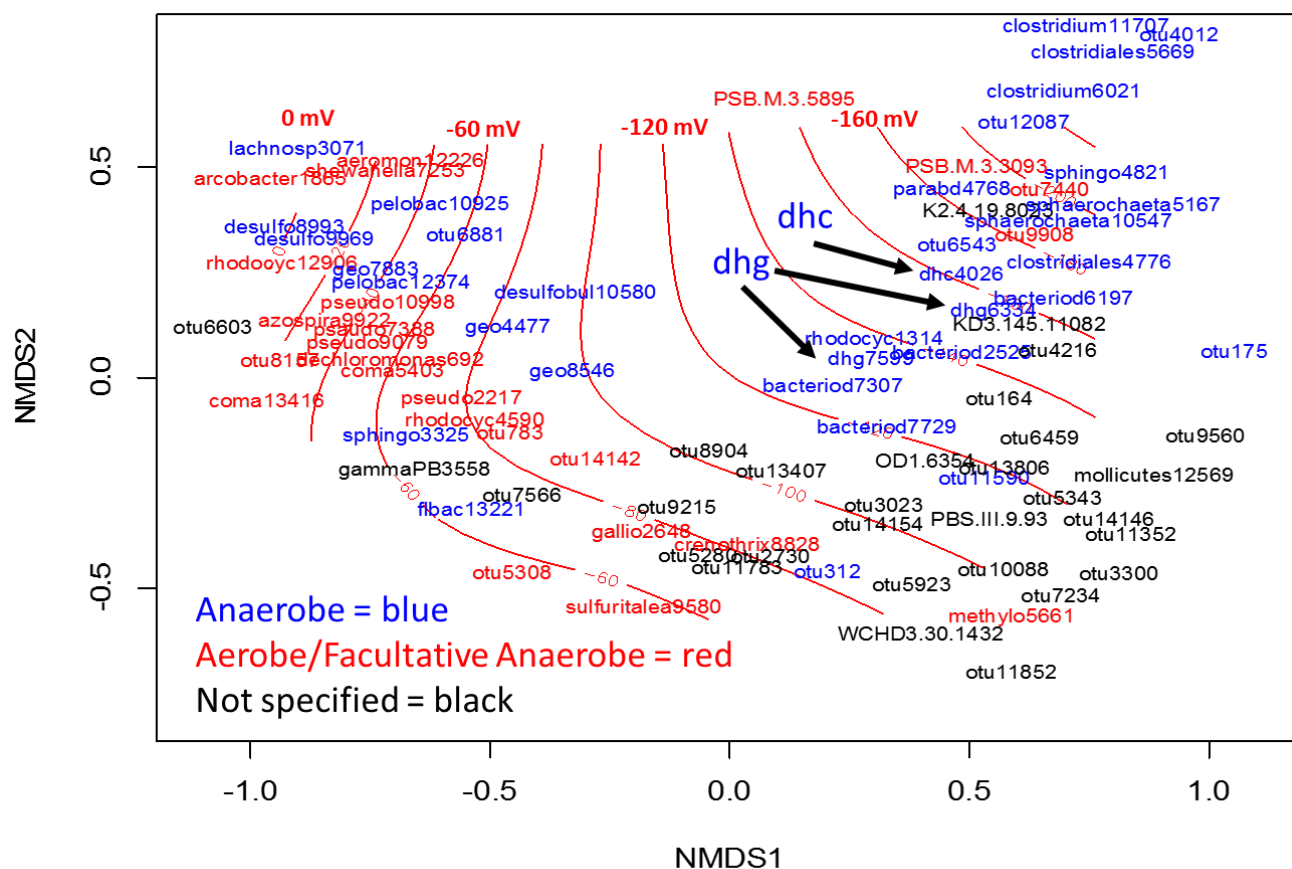
b.



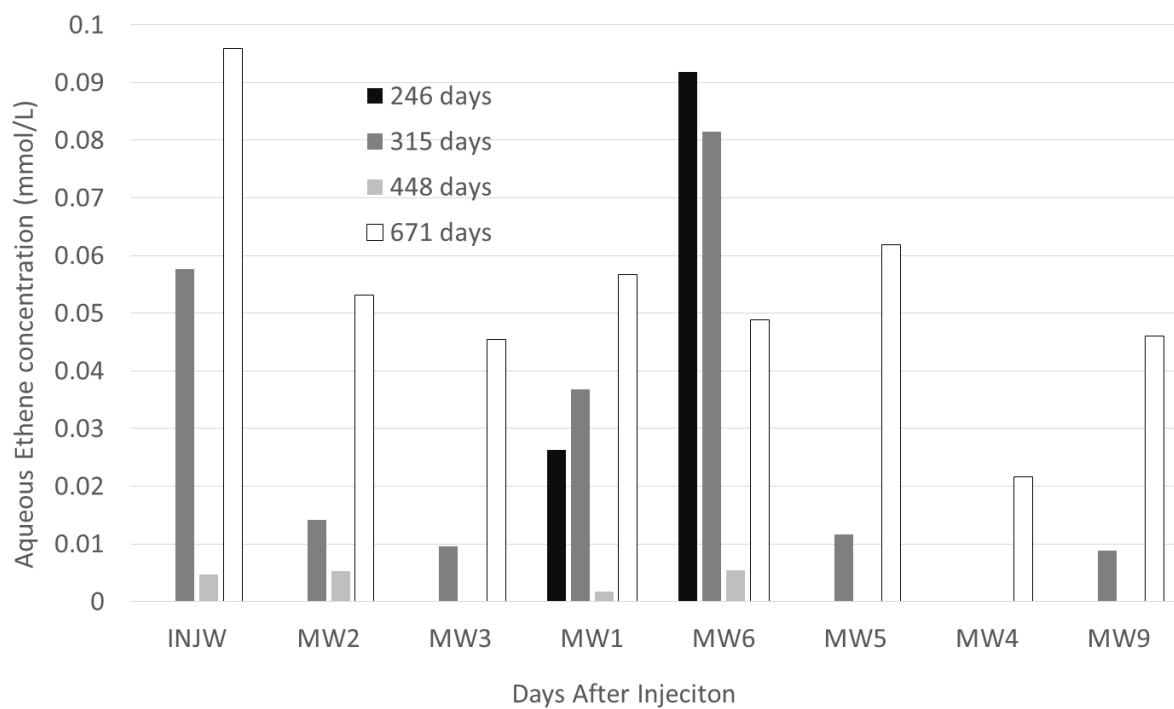
Appendix D. 2: Amplicon pyrosequencing data in background monitoring points. Results are grouped by phylum showing that the microbial communities are similar throughout the site prior to injection. A high percentage of community is identified from Green genes database.



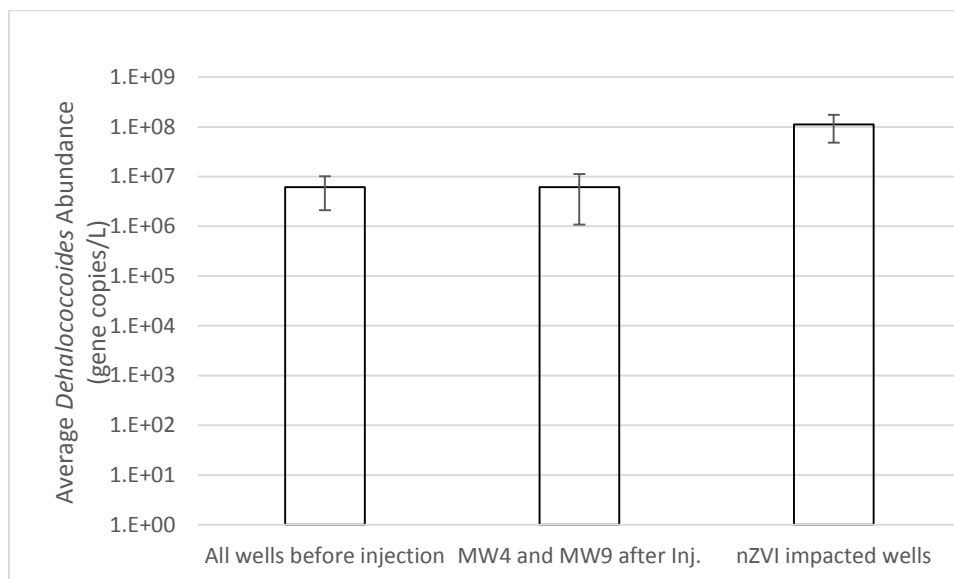
Appendix D. 3: High resolution version of Figure 5d showing ordination of species and ORP contours.



Appendix D. 4: Ethene Data collected following injection. Downgradient and injection wells have the highest Ethene concentrations one year after injection. Ethene was not analyzed prior to 246 days.



Appendix D. 5: Statistical analysis of the mean for *Dehalococcoides* abundance in background wells, non-impacted wells, and nZVI impacted wells.



11 Acronyms

ZVI	- Zero valent Iron
CMC	- Carboxy-methyl-cellulose polymer
nZVI	- Nanoscale zero valent Iron
NAPL	- Non-aqueous phase liquid
MW	- Monitoring well
INJW	- Injection well
ORP	- Oxidation reduction potential
cVOC	- Chlorinated volatile organic compound
PCE	- Perchloroethylene
TCE	- Trichloroethylene
Cis-DCE	- Cis-isomer of dichloroethene
VC	- Vinyl chloride
NUC	- North utility corridor
qPCR	- Quantitative polymerase chain reaction
DNA	- Deoxyribonucleic acid
<i>dhc</i>	- <i>Dehalococcoides</i>
OTU	- Operational taxonomic unit
<i>vcrA</i>	- <i>Vinyl chloride reductase gene</i>

TOC	Total organic carbon
TEM	Transmission electron microscopy
EDS	Energy dispersive x-ray spectroscopy
DLS	Dynamic Light Scattering

Vitae

Name: Christopher M.D. Kocur

Post-secondary Education and Degrees: The University of Western Ontario
London, Ontario, Canada
2010-2015 Ph.D.

The University of Western Ontario
London, Ontario, Canada
2007-2009 M.E.Sc.

The University of Western Ontario
London, Ontario, Canada
2003-2007 B.E.Sc.

Honours and Awards: Canadian Foundation for Geotechnique
Michael Bozozuk National Graduate Scholarship
2015

Natural Science and Engineering Research Council
Industrial Post-Graduate Scholarship 2
2010-2014

L.G. Sonderman Award
Geotechnical Research Center
2011

Walkerton Clean Water Center
Graduate Scholarship
2007-2008

Related Work Experience Staff Consultant
CH2M HILL Canada Ltd – Kitchener Office
May 2010 – April 2014

Teaching Assistant
Dept. of Civil & Environmental Engineering
Jan 2007 – December 2013

Publications:

Kocur, C.M.D., Lomheim, L, Boparai, H.K., Chowdhury, A.I.A., Weber, K.P., Austrins L.M., Edwards, E.A., Sleep, B.E., O'Carroll D.M. **Contributions of Abiotic and Biotic Dechlorination Following Carboxymethyl Cellulose Stabilized Nanoscale Zero Valent Iron Injection.** *Enviro. Sci. Technol.*, 2015 doi: 10.1021/acs.est.5b00719

Kocur, C.M., Chowdhury, A.I., Sakulchaicharoen, N., Boparai, H.K., Weber, K.P., Sharma, P., Krol, M., Austrins, L., Peace, C., Sleep, B.E., O'Carroll, D.M. **Characterization of nZVI in a field scale test** *Environ. Sci. Technol.*, 2014, 48 (5), pp 2862–2869 doi:10.1021/es4044209

Kocur, Chris M., O'Carroll, Denis M., Sleep, Brent E., **Impact of nZVI stability on mobility in porous media**, *Journal of Contaminant Hydrology* (2013), 145. 17-25
doi:10.1016/j.jconhyd.2012.11.001

O'Carroll D., Sleep B., Krol M., Boparai H., Kocur C. **Nanoscale zero valent iron and bimetallic particles for contaminated site remediation.** *Adv. Water Resources* (2013) 51, 104-122
doi:10.1016/j.advwatres.2012.02.005

Krol, M.M., Oleniuk, A.J., Kocur, C.M., Sleep, B.E., Bennett, P., Xiong, Z., O'Carroll, D.M. (2013) **A Field-Validated Model for In Situ Transport of Polymer-Stabilized nZVI and Implications for Subsurface Injection.** *Environ. Sci. Technol.*, 47 (13) 7332-7340. doi: 10.1021/es3041412.

Invited Talks

Kocur, C.M. O'Carroll, D.M. (2014) **Pilot Scale Demonstration of a Coupled Abiotic and Biotic Remediation using nZVI.** *In the proceedings of the 2014 – Contaminated Site Management: Sustainable Remediation & Management of Soil, Sediment, and Water Conference.* San Diego, CA, Nov 17-20

Kocur, C.M (2011) **Nanometal Technologies for Subsurface Remediation.** *Manitoba Environmental Industry Association – Remediation Conference.* Feb 16 Winnipeg, Man.

Media Appearances

“The Nano Revolution: Will Nano Save the Planet?” *The Nature of Things with David Suzuki.* CBC-TV, Oct 27.2011